Advances in the Synthesis and Application of Iridium(I) Complexes for Use in Hydrogen Isotope Exchange

Thesis submitted to the University of Strathclyde in fulfilment of the requirements for the degree of Doctor of Philosophy

By

Alison R. Cochrane

Department of Pure and Applied Chemistry

University of Strathclyde

Thomas Graham Building

295 Cathedral Street

Glasgow

G1 1XL

August 2012

Declaration of Copyright

Acknowledgements

First and foremost I would like to thank my supervisor, Prof. Billy Kerr. His patience, guidance and encouragement over the past five years have been invaluable. His expertise in organic chemistry come second only to his knowledge of fine wines, and I now leave the group knowing never to order a German chardonnay!

I would also like to thank my industrial supervisor, Göran Nilsson, for his continued interest in the project, and for always sending chemicals when requested. The computational work within this thesis would not have been possible without the help of Dr Tell Tuttle and Dr Bhaskar Mondal, and for this I am truly grateful. I am also indebted to Dr Alan Kennedy for his efforts in resolving the crystal structures.

I would not have reached the end of my PhD studies had it not been for the completely ridiculous yet highly amusing lab banter provided by the Kerr Group members, past and present: Steph, Marek, Chief, L-Patz, Linsey, Tina, Natalie, Malcolm, Rachael, Sharon, Kat, Kevin, Martin and Scott. Special thanks must go to Calum and Marc, my fumehood buddies and fellow Team Iridium members, and also to Goldie for our many Friday nights at Oran Mor (just one more skittle bomb?!).

Finally I would like to thank my parents, Sandra and Iain, and my sister, Lynne. Their continued love and support over the past years has been tremendous, and I would not be where I am today had it not been for them.

Summary

Investigations into the application of catalysts of the type $[Ir(COD)(PR_3)(IMes)]PF_6$ in the field of hydrogen isotope exchange have been undertaken. In particular, the use of alternative solvents has been examined, resulting in the identification of reaction media considered more industrially acceptable than those currently utilised in isotopic labelling processes. Following a series of optimisation studies, the newly developed conditions for H-D exchange were applied to a range of substrates containing a variety of functional groups. In the majority of instances, high levels of deuteration were achieved in reactions employing low catalyst loadings and short reaction times.

With regards to the iridium complexes themselves, focus has centred on the introduction of alternative NHC ligands, leading to the synthesis of six novel Ir(I) catalysts. These complexes have been employed in hydrogen isotope exchange reactions, demonstrating high activity in the isotopic labelling of numerous substrates. As a result of such explorations, increased levels of selectivity have been achieved in compounds offering multiple sites of labelling, with catalysts displaying a greater preference for exchange *via* a 5-mmi over the less energetically favourable 6-mmi. In addition, a catalyst capable of facilitating higher levels of isotope incorporation adjacent to a sulfonamide moiety has been accomplished.

A series of DFT studies have also been undertaken. The calculation of solvent binding energies to the iridium complex has revealed a broad correlation between the strength with which solvent molecules coordinate to the metal centre, and the degree of isotope incorporation observed. Further theoretical investigations were performed regarding our novel Ir(I) complexes bearing alternative NHC ligands. More specifically, computational experiments have identified the relative energies of the key processes which occur within the catalytic cycle.

Abbreviations

°C	Degrees Celsius
$\%V_{bur}$	Percent Buried Volume
Ac	Acetyl
Ad	Adamantyl
ADMET	Adsorption, Distribution, Metabolism, Excretion and Toxicology
Ar	Aryl
Atm.	Atmosphere
BARF	Tetrakis[3,5-bis(trifluoromethyl)phenyl]borate
BMI	1-Butyl-3-methylimidazolium
Bn	Benzyl
cm	Centimetre
COD	Cycloocta-1,5-diene
COX	Cyclooxygenase
CNS	Central Nervous System
Cp*	$C_5(CH_3)_5$
Cy	Cyclohexyl
DCM	Dichloromethane
DMF	Dimethylformamide
DMSO	Dimethyl Sulfoxide
DNA	Deoxyribonucleic Acid
Dppe	1,2-Bis(diphenylphosphino)ethane
Et	Ethyl
eq.	Equivalents
FDA	Food and Drugs Administration
FTIR	Fourier Transform Infrared
g	Grammes
h	Hours
HIE	Hydrogen Isotope Exchange
Hz	Hertz
IAd	1,3-Bis(adamantyl)imidazol-2-ylidene
ICy	1,3-Bis(cyclohexyl)imidazol-2-ylidene

IMe	1,3-Dimethylimidazol-2-ylidene
IMes	1,3-Bis(2,4,6-trimethylphenyl)imidazol-2-ylidene
IPr	1,3-Bis(2,6-diisopropylphenyl)imidazol-2-ylidene
^{i}Pr	*iso*-Propyl
IR	Infrared
J	Coupling Constant
K	Kelvin
kcal	Kilocalories
KIE	Kinetic Isotope Effect
L	Ligand
M	Molar
Me	Methyl
Mes	Mesityl
mg	Milligrammes
MHz	Megahertz
ml	Millilitres
mmi	Membered Metallacyclic Intermediate
mmol	Millimoles
mol	Moles
m.p.	Melting Point
^{n}Bu	*n*-Butyl
NCE	New Chemical Entity
NHC	*N*-Heterocyclic Carbene
NMR	Nuclear Magnetic Resonance br s – broad singlet s – singlet d – doublet dd – doublet of doublets t – triplet m – multiplet
p	*para*
Ph	Phenyl
PKIE	Primary Kinetic Isotope Effect
ppm	Parts Per Million

psi	Pounds Per Square Inch
py	Pyridine
r.t.	Room Temperature
SIMes	1,3-Bis(2,4,6-trimethylphenyl)imidazolidine-2-ylidene
SIPr	1,3-Bis(2,6-diisopropylphenyl)imidazolidine-2-ylidene
SKIE	Secondary Kinetic Isotope Effect
^{t}Bu	*tert*-Butyl
Temp.	Temperature
TEP	Tolman Electronic Parameters
tert	Tertiary
TLC	Thin Layer Chromatography
THF	Tetrahydrofuran
UV	Ultraviolet

Contents

1 Introduction

1.1 Isotopic Labelling

With the continued emergence of new diseases and novel strains of existing viruses, there remains constant pressure on the world's pharmaceutical companies to provide effective vaccines and treatments. Drug development is an extremely long and costly process; a recent report in 2010 estimated the development of a single drug to cost in excess of $1 billion,[1] while the process itself can take as long as 15 years. Perhaps even more alarming is the fact that of every ten thousand compounds synthesised, only one will complete the demanding journey from the chemical laboratory to become available to the public as a marketed drug.[2] Indeed, in 2010 the US Food and Drugs Administration (FDA) approved only 21 new drugs, while the equivalent levels in 2008 and 2009 were not substantially higher at 24 and 25, respectively.[3]

The majority of new chemical entities (NCEs) fail in clinical trials as a result of poor pharmacokinetics. Specific requirements exist with respect to the performance of drug candidates in adsorption, distribution, metabolism, excretion and toxicology (ADMET) studies; failure to comply with such safety constraints results in the withdrawal of any unsuccessful compounds. With attrition rates at such an elevated level, there is a clear drive for pharmaceutical companies to recognise failing attributes of potential drug candidates at an earlier stage. It is suggested that if such predictions were increased by only 10%, a saving in drug development costs of $100 million per drug could be achievable.[4] By incorporating a tracer into a prospective drug molecule, access to vital information regarding its breakdown and pharmacodynamics can be attained, thus highlighting any undesirable interactions which may occur. One method which enables such a feat is isotopic labelling.

Isotopes are atoms of the same element which possess different mass numbers, resulting from a difference in the number of neutrons present in the atom's core.[5] With identical electronic configurations, isotopes display nearly identical chemical behaviour. The main exception to this is illustrated in their speed of reaction, as lighter isotopes are known to react somewhat more quickly than their heavier analogues. Such an effect is particularly evident for hydrogen and deuterium, as the latter has twice the mass of the former. Significant differences in the stability of isotopes are also apparent due to their different neutron/proton ratios. The higher the ratio, the less stable the nucleus, hence the increased probability of the isotope undergoing nuclear decay. Such isotopes are termed radioisotopes, examples of which include ^{14}C, ^{235}U and ^{3}H. Conversely, isotopes which have lower neutron/proton ratios, such as ^{15}N, ^{13}C and ^{2}H, are not subject to nuclear decay, hence they are referred to as stable isotopes. The utilisation of stable isotopes as metabolic tracers predates the use of radioactive isotopes by approximately twenty years; however only within the past three decades has their employment over their decaying counterparts resurged.[6] One of the main advantages offered by stable isotopes is their nonradioactive nature, presenting little or no danger to human subjects. An additional benefit is their ease of detection, achieved through the use of simple analytical techniques such as mass spectrometry and infrared (IR) spectroscopy.

Radioactive and stable isotopes of both carbon and hydrogen are commonly employed as tracers in metabolic studies. Accordingly, a number of methods have been investigated which enable their incorporation into candidate drug molecules. The preparation of ^{13}C- or ^{14}C-labelled molecules often involves the use of a starting material which already has the label in position. While a considerable advantage is the specific insertion of the isotope, difficulties in the ensuing synthesis of the target molecule are frequently encountered, typically resulting in the requirement of additional synthetic steps. In contrast, the incorporation of deuterium and tritium, ^{2}H and ^{3}H respectively, generally occurs at the end of a synthesis, when the desired molecule has been completely constructed. Such a process is of significant benefit to pharmaceutical companies, enabling the preparation of compounds containing high levels of complexity, such as the AstraZeneca substrate nedocromil sodium **1** (**Figure 1**),[7] without complications arising from the presence of an isotope.

Figure 1

^{2}H or ^{3}H incorporation is achieved via a number of techniques, of which *ortho*-lithiation was previously the most common. A number of limitations are associated with such a procedure however; in particular, competition reactions such as metal-halogen exchange and elimination reactions often arise. A more mild and reliable method for the introduction of deuterium or tritium into a molecule is provided by transition metal-catalysed hydrogen isotope exchange (HIE).

1.2 Transition Metal-catalysed Hydrogen Isotope Exchange

Over recent years, a number of transition metal complexes have demonstrated efficiency in hydrogen isotope exchange reactions.[8] One of the first examples of HIE by means of homogeneous catalysis was reported in 1967 by Garnett and Hodges.[9] Under carefully controlled acidic conditions and in the presence of deuterated water, platinum(II) salts, such as K_2PtCl_4, were employed in a simple one-step procedure to label a number of aromatic compounds (**Scheme 1**). While the substrate scope of this system was limited, and the regioselectivity of exchange and levels of incorporation achieved were poor, the initial results obtained clearly demonstrated the potential which existed within this area of research.

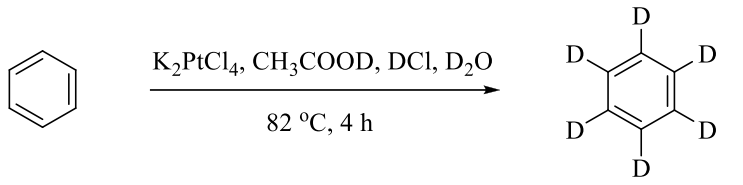

3 **4**

10.7% deuteration

Scheme 1

Following on from this discovery, Garnett proceeded to examine the efficiency of alternative catalysts within this field, namely complexes of iridium[10] and rhodium.[11] In the case of the former, the isotopic labelling of benzene facilitated by sodium chloroiridite, Na_3IrCl_6, was found to proceed to improved levels of 63% deuteration (**Scheme 2**).[10] Additional substrates investigated included a range of alkylbenzenes, demonstrating the potential to also incorporate deuterium into the α-methylene positions of such compounds.

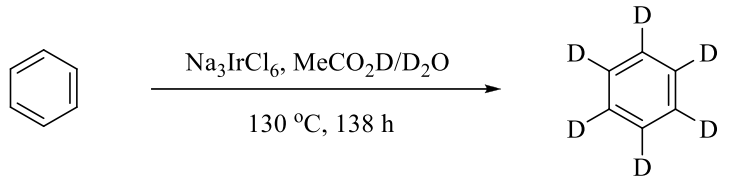

3 **4**

63% deuteration

Scheme 2

The rhodium species under consideration, $RhCl_3$, was also found to facilitate the exchange of hydrogen for deuterium in aromatic compounds, albeit at a slower rate than that observed with the previously described Ir complex.[11] Once again, deuteration in the alkyl groups of substrates such as toluene was detected, with no particular positions in the aromatic ring being labelled preferentially (**Scheme 3**).

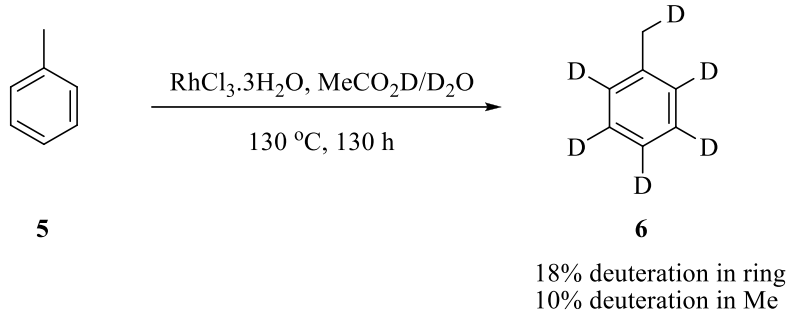

5 **6**

18% deuteration in ring
10% deuteration in Me

Scheme 3

Some years later, investigations by Lockley illustrated that high levels of regioselectivity could, indeed, be achieved in H-D exchange reactions catalysed by rhodium trichloride.[12] Through the introduction of a carboxyl moiety, incorporation of deuterium now took place almost exclusively at positions β to the functional group (**Scheme 4**).

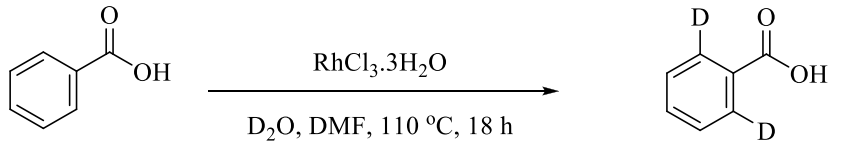

7 **8**

95% deuteration

Scheme 4

In a subsequent publication Lockley suggested that, akin to the proposed mechanism of *ortho*-lithiation, the high levels of regioselectivity observed were a result of an initial coordination between the lone pair of electrons of the substrate carboxyl group and the catalyst metal centre.[13] H-D exchange at the neighbouring *ortho*-positions of the substrate would therefore be greatly favoured over the corresponding reaction at the remote *meta*- or *para*-positions. Further postulation included the involvement of a cyclometallation process giving **9**, as depicted in **Scheme 5**.

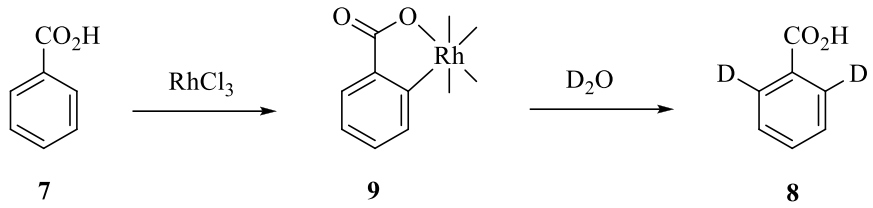

7 **9** **8**

Scheme 5

The regioselective deuteration of aromatic amides and amines was also explored, expanding the range of functional groups capable of directing isotopic labelling. In addition, Lockley investigated the directing capabilities of anilides.[14] A variety of substituted acetanilides were examined and, in general, HIE reactions proceeded to deliver high levels of deuterium incorporation in the expected *ortho*-position (**Scheme 6**).

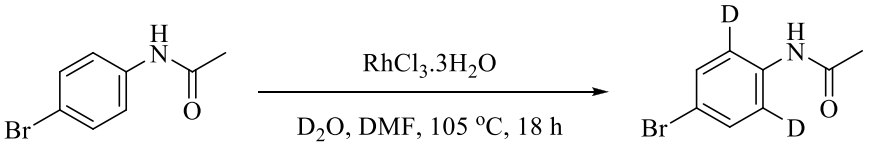

10 **11**

92% deuteration

Scheme 6

In comparison to the previous results obtained, which involved coordination of the Lewis basic oxygen to the metal centre furnishing a 5-membered metallacyclic intermediate (5-mmi) **12**, the directing capability of the anilide moiety demonstrated the potential to promote deuterium substitution in a C-H bond positioned 5 atoms away from the coordinating group. Unearthing the existence of such a 6-membered metallacyclic intermediate (6-mmi) **13** (**Figure 2**) thereby greatly broadened the scope of substrates which could, in theory, be labelled under these transition metal-catalysed conditions.

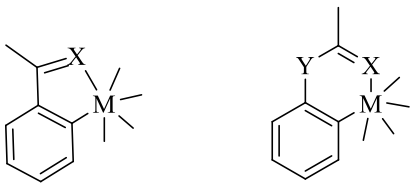

12 5-mmi **13** 6-mmi

Figure 2

Indeed, further investigations into the use of $RhCl_3$ as an efficient H-D exchange mediator involved the labelling of various drug molecules containing a number of functional groups, such as carboxylic acids, amides, amines, anilides, and heterocycles (**Scheme 7**).[15] While the majority of compounds were delivered with high degrees of deuterium incorporation, and in a regioselective manner, the requirement of relatively high catalyst loadings remained a considerable weakness of this technique.

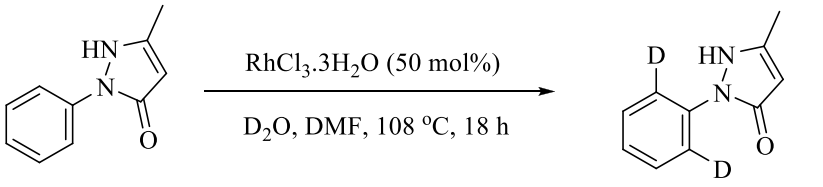

14 **15** 95% deuteration

Scheme 7

In 1992, Heys reported preliminary results regarding the use of $[IrH_2(Me_2CO)_2(PPh_3)_2]BF_4$ **16** in hydrogen isotope exchange reactions.[16] Complex **16** had previously been utilised in C-H activation studies published by Crabtree, however such explorations were focused on the oxidative addition step of such a process, rather than determining the efficiency of complex **16** in HIE reactions.[17] Indeed, the only substrates shown by Crabtree *et al*. to undergo isotopic labelling facilitated by this cationic iridium species were caffeine **17** and 8-methylquinoline **18** (**Figure 3**).

17 **18**

Figure 3

Pleasingly, the studies by Heys revealed that complex **16** delivered good levels of deuterium incorporation over a wide range of substrates (**Scheme 8**).[16] Consistent with Lockley's observations, exchange occurred almost exclusively in the C-H bond positioned *ortho* to the coordinating functional group, reinforcing the proposal of a mechanism involving a 5-mmi. In contrast, Heys' protocol exhibited distinct advantages over the previous conditions employing $RhCl_3$, such as a greatly reduced catalyst loading of approximately 2 mol%, and the replacement of D_2O with deuterium gas as the isotope source.

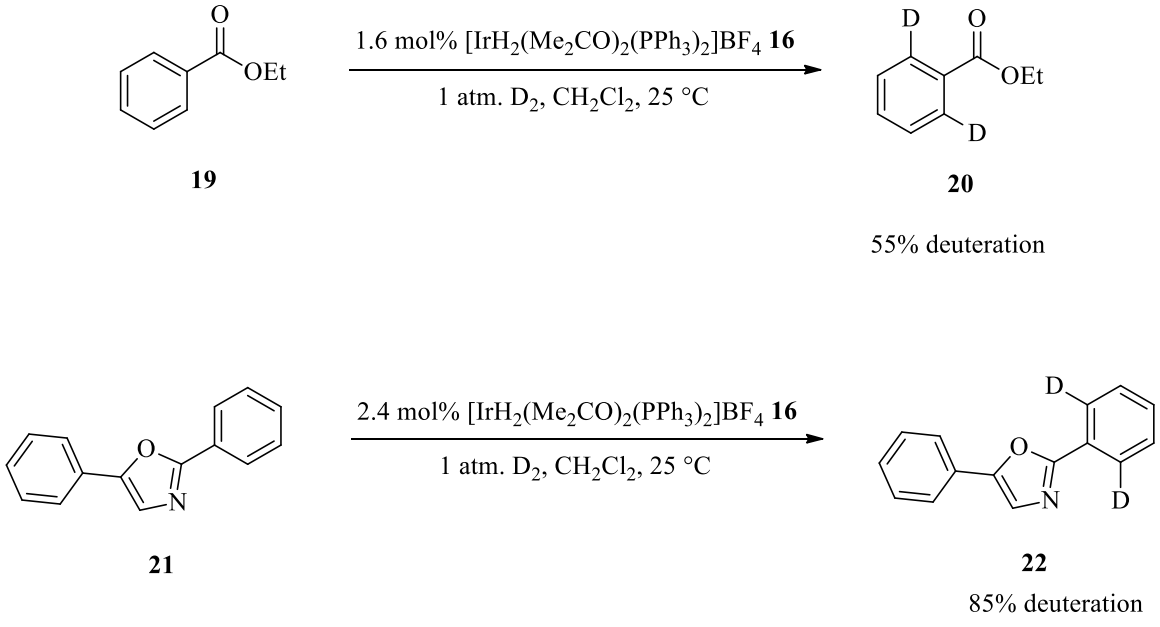

Scheme 8

A second iridium catalyst shown to be effective in the same area of research was [Ir(COD)(PCy_3)(py)]PF_6 **23**, more commonly known as Crabtree's catalyst.[18] Studies by Hesk revealed that, at a catalyst loading of 5 mol%, this commercially available complex could facilitate high levels of H-D exchange in substituted acetanilides, again in a highly regioselective manner (**Scheme 9**).[19]

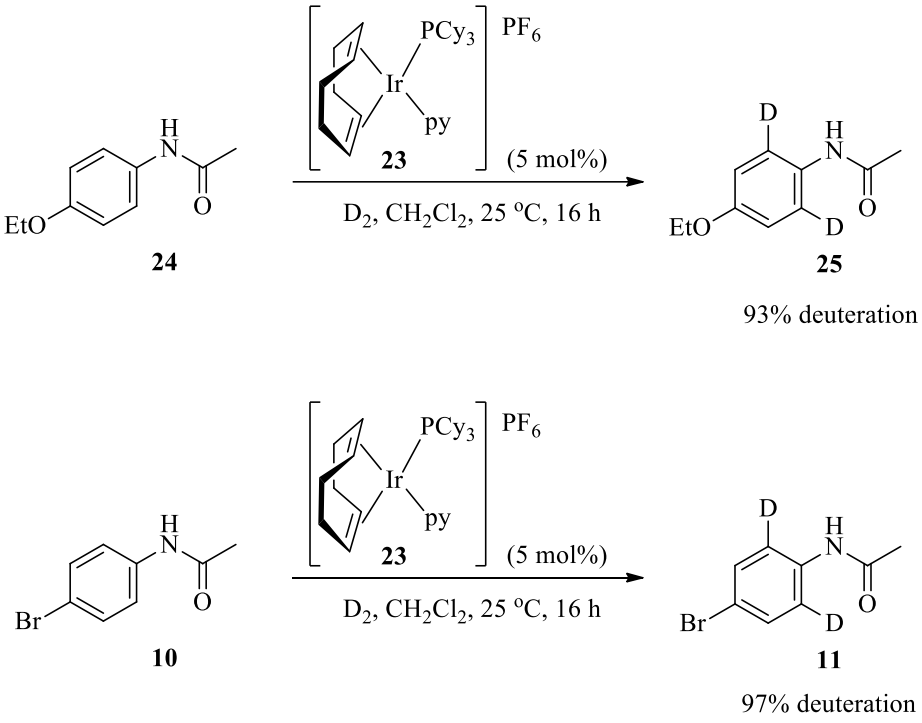

Scheme 9

Encouraged by Hesk's findings, Heys subsequently reported further results regarding the use of iridium complexes in HIE reactions.[20] Initial results obtained revealed [Ir(COD)(PPh_3)$_2$]BF_4 **26** to facilitate H-D exchange more efficiently than the earlier reported pre-reduced complex **16**. Such a discovery instigated a series of investigations into isotopic labelling procedures utilising commercially available pre-catalysts of the type [Ir(COD)(L)$_2$]X. In particular, the use of complexes **26** and **27** was examined (**Figure 4**).

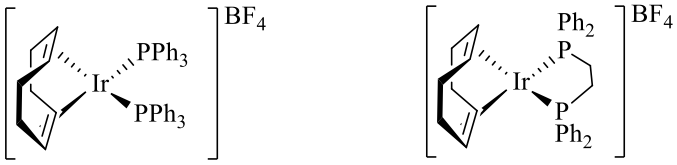

26 **27**

Figure 4

While complex **27**, bearing the bidentate ligand 1,2-bis(diphenylphosphino)ethane (dppe), displayed activity in the labelling of substrates *via* either a 5-mmi or a 6-mmi, catalysts such as **26**, containing monodentate phosphines, demonstrated selectivity for H-D exchange proceeding *via* a 5-mmi (**Table 1**). High levels of incorporation could, indeed, be achieved in positions five bonds away from the coordinating heteroatom (i.e. *via* a 6-mmi) in the presence of the latter complex, **26**, however such a degree of deuteration was only observed in cases employing catalyst loadings in excess of 50 mol%.

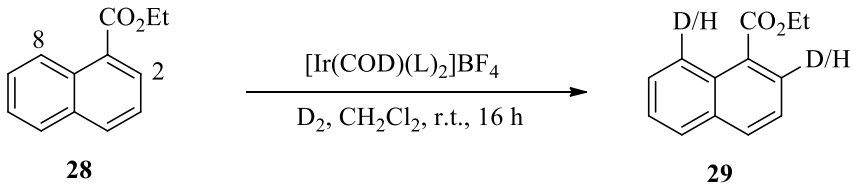

28 **29**

Scheme 10

Complex	Loading (mol%)	(Mol D) mol^{-1} at C2	(Mol D) mol^{-1} at C8
26	2.2	0.90	-
27	2.5	0.54	0.35

Table 1

Heys deduced that the differences in labelling capabilities of the mono- and bidentate phosphine complexes arose as a result of the steric congestion present around each of the

metal centres. While monodentate phosphine ligands such as PPh_3 occupy a *trans*-orientation **30**, bidentate ligands such as dppe remain in a *cis*-arrangement **31**, increasing the coordination sphere in the vicinity of the substrate C-H bond at which substitution would occur (**Figure 5**). In such a situation, the accommodation of the larger and less planar 6-mmi ring system would be significantly more feasible.

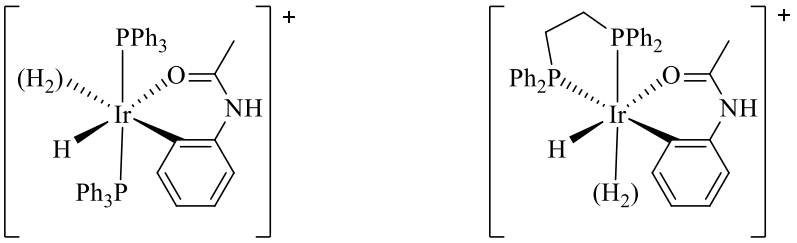

30 **31**

Figure 5

Heys' explanation for the observations described above centred on the proposed catalytic cycle by which HIE is believed to occur (**Scheme 11**). Complexes such as **26** are pre-catalysts, and must undergo an initial activation process to access the catalytically active Ir(I) species. Such an activation is achieved through exposure of **26** to deuterium gas, facilitating the removal of the COD ligand as d_4-cyclooctane. The resulting coordinatively unsaturated Ir(I) **32** is stabilised by ligands "S" which may be solvent molecules or other loosely bound species, such as dihydrogen or substrate molecules. Coordination of the substrate to the metal centre through the lone pair of electrons on the heteroatom leads to the displacement of S, and subsequent oxidative insertion of Ir into the aromatic C-H bond positioned *ortho* to the functional group furnishes Ir(III) species **35**. The exchange of hydrogen and deuterium then occurs in a process known as fluxionality, a step key to the overall mechanistic pathway. As a consequence of such an exchange, deuterium is situated *cis* to the Ir-C bond, an arrangement required for the ensuing reductive elimination process. With incorporation of the isotope into the *ortho*-position of the substrate aryl ring, dissociation of the labelled compound **38** regenerates the original coordinatively unsaturated Ir(I) species **32**, enabling continuation of the catalytic cycle.

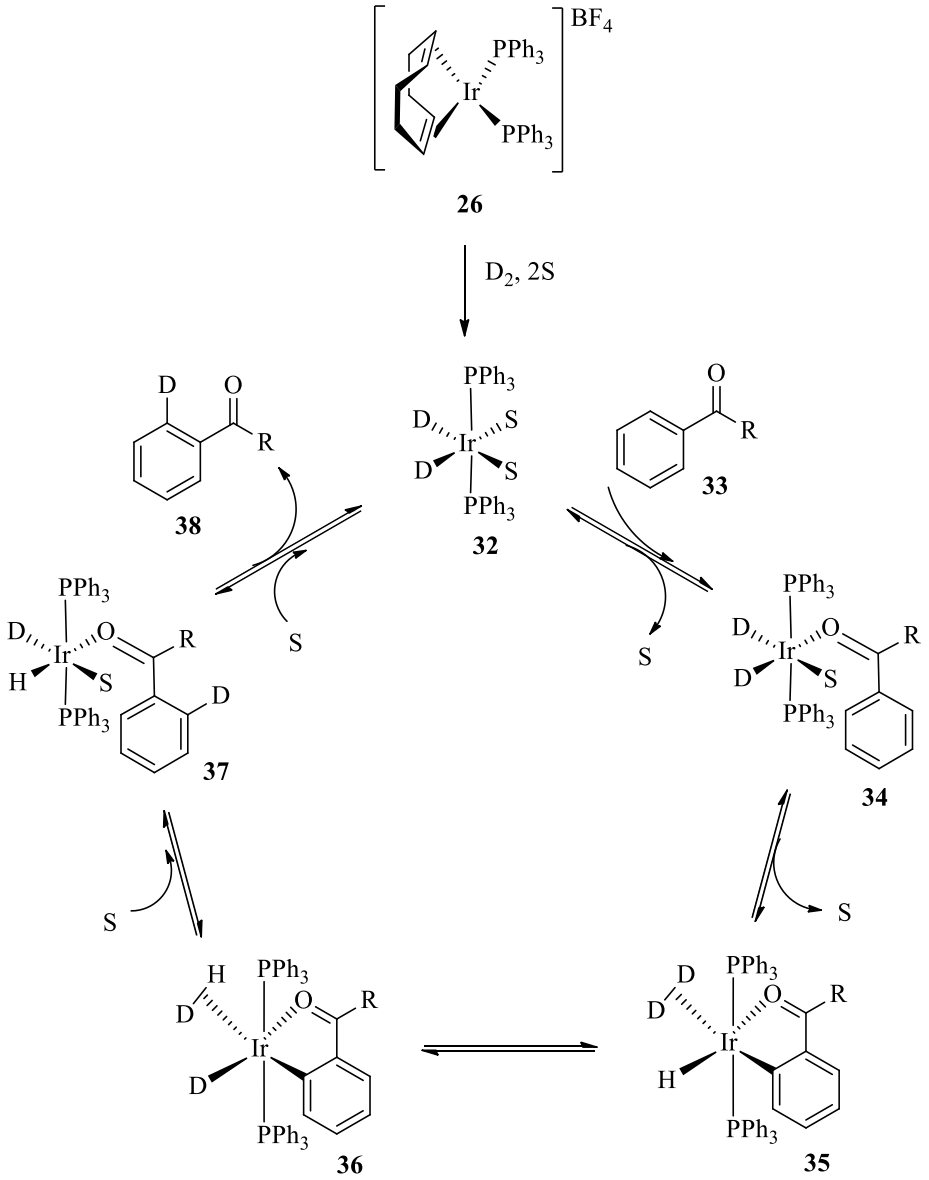

Scheme 11

In 2001, individual reports from Salter[21] and Herbert[22] described complementary investigations regarding the *in situ* preparation of catalysts of the type $[Ir(COD)(L)_2]X$. By eliminating the need to produce and isolate individual complexes, the reactivity of numerous potential catalysts could be explored in a rapid and efficient manner. Of the complexes screened, those containing tertiary phosphine ligands delivered the highest levels of deuterium incorporation over a wide range of substrates (**Scheme 12**, **Table 2**). Furthermore,

the levels of isotopic labelling achieved were comparable to those obtained in reactions employing the isolated complexes.

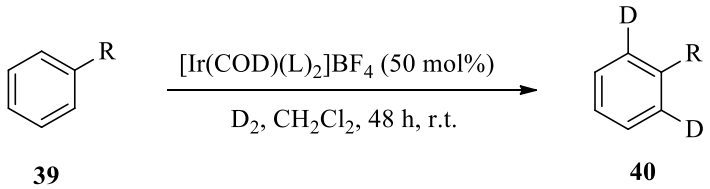

39 **40**

Scheme 12

R	L	% D with Complex Formed *in situ*	% D with Isolated Complex
$COCH_3$	PPh_3	80	90
$CONMe_2$	PPh_2Me	80	75
NHAc	PPh_2Me	80	80
2-Pyridinyl	PPh_3	70	90

Table 2

In an effort to determine any potential relationships between specific complexes and substrate selectivities, Herbert and co-workers embarked on a series of optimisation studies.[23] In particular, the ratio of phosphine ligands to iridium was examined, as it was proposed that different catalytic activity may be observed in complexes containing different stoichiometries of phosphine ligands (**Scheme 13**).

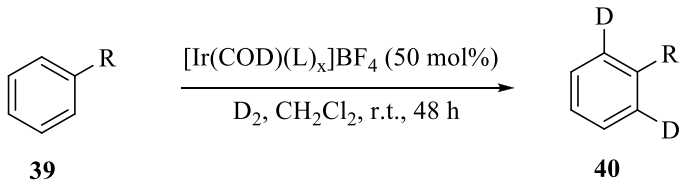

39 **40**

Scheme 13

R	L	X	% Deuteration
$COCH_3$	PPh_3	1	75
$COCH_3$	PPh_3	2	80
$COCH_3$	PPh_3	3	100
1-pyrazolyl	PPh_2Me	1	30
1-pyrazolyl	PPh_2Me	2	40
1-pyrazolyl	PPh_2Me	3	10

Table 3

As the results shown in **Table 3** illustrate, no such correlation was detected. Having stated this, it was postulated that slight modifications with respect to the electronic properties of the phosphine ligands employed may enable further optimisation of exchange within specific substrates. For example, the labelling of 2-phenylpyridine **41** proceeded with high levels of deuterium incorporation in the presence of electron-poor phosphine ligands, but failed to deliver any of the isotopically enriched product **42** when complexes bearing the more electron-rich PCy_3 were employed (**Scheme 14**, **Table 4**).

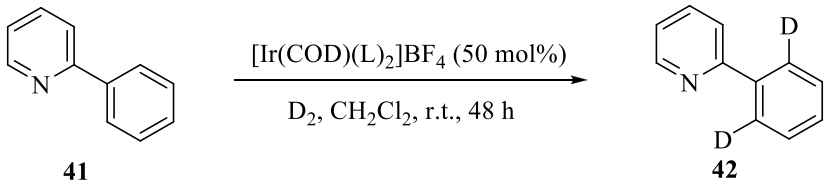

41 **42**

Scheme 14

L	% Deuteration
$P(C_6H_5)_3$	70
PCy_3	0

Table 4

1.3 Crabtree's Catalyst

Although initial studies by Hesk had revealed Crabtree's catalyst **23** to be effective in the regioselective isotopic labelling of substrates such as substituted acetophenones, benzophenones and acetanilides,[19] there existed a significant period of time in which further explorations with this commercially available complex in HIE reactions lay dormant. It was not until 2001 that attention returned to the use of complex **23** in H-D exchange reactions, with more extensive investigations into the scope and limitations of Crabtree's catalyst in this area of research reported by Herbert and co-workers.[24] Comparison of the results obtained in the deuteration of a range of aromatic substrates revealed a number of trends to be apparent (**Scheme 15**, **Table 5**). Firstly, the labelling of benzamides proceeded more efficiently than that of ethyl benzoates, a feature which is almost certainly a consequence of the electron-donating ability of the coordinating substituent. In addition, the deuteration of *N*-alkyl substituted benzamides did not appear to be affected by the steric bulk present on the amide nitrogen. Indeed, similar levels of isotope incorporation were observed in the labelling of *N*,*N*-dimethylbenzamide and *N*,*N*-diisopropylbenzamide, with both substrates labelled to a higher degree than benzamide itself (Entries 1, 2 and 3). While the electronic nature of aryl substituents did not appear to influence the levels of deuteration observed in benzamides, exemplified by the comparable degree of exchange detected in *p*-methoxybenzamide and *p*-nitrobenzamide (Entries 4 and 5), electron-rich ethyl benzoates were labelled more efficiently than their electron-poor counterparts (Entries 6 and 7). Such a difference further demonstrated the relationship between the coordinating ability of the substrate and the level of D incorporation achieved.

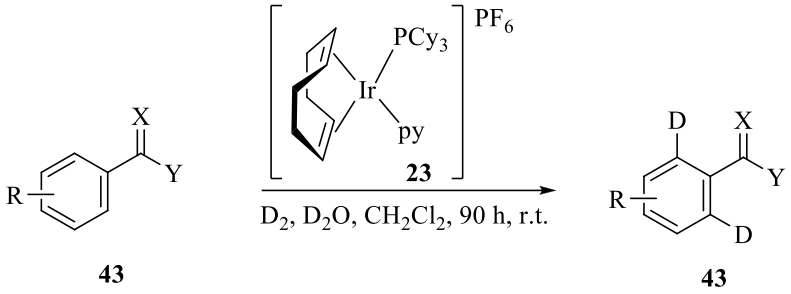

Scheme 15

Entry	X	Y	R	Catalyst Loading (mol%)	% Deuteration
1	O	NH_2	H	110	65
2	O	NMe_2	H	110	80
3	O	N^iPr_2	H	100	90
4	O	NMe_2	4-OMe	100	80
5	O	NMe_2	4-NO_2	100	80
6	O	OEt	4-OMe	130	85
7	O	OEt	4-NO_2	120	20

Table 5

Further experiments included investigating the effect on incorporation levels which arose as a result of increasing the distance between the coordinating functional group and the C-H bond undergoing activation. Three substrates were examined, namely 1-indanone, tetralone and benzosuberone (**Scheme 16**). As revealed by the values displayed below in **Table 6**, guiding the directing heteroatom towards the position at which exchange occurs increases the degree of deuteration achieved.

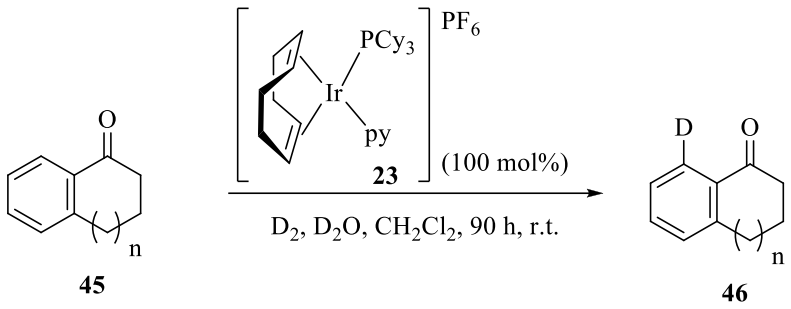

Scheme 16

Substrate	*n*	% Deuteration
1-Indanone	0	31
1-Tetralone	1	68
1-Benzosuberone	2	76

Table 6

Although originally developed for use in the field of olefin hydrogenation,[18] complex **23** was, until recently, the most frequently utilised transition metal catalyst for hydrogen isotope exchange reactions. As demonstrated by numerous examples given to this point, H-D exchange reactions facilitated by Crabtree's catalyst often require (super-)stoichiometric quantities of the complex to achieve high levels of deuterium incorporation.[24] Another significant limitation of complex **23** is its tendency to deactivate. In hydrogenation experiments, this deactivation occurs either at higher temperature, or following either the complete consumption of mono- or disubstituted olefins, or after short periods of time in the presence of more hindered tri- and tetrasubstituted olefins. Such a disablement arises through the formation of inactive hydride-bridged iridium clusters,[18] an example of which is shown in **Figure 6**.

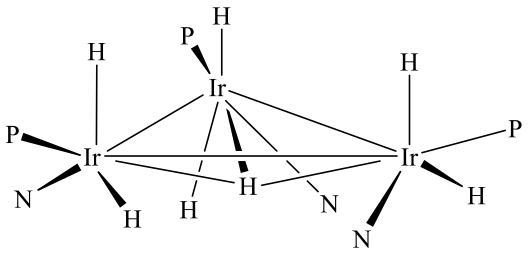

47

Figure 6

1.4 Analogues of Crabtree's Catalyst

Inspired by the high reactivity of Crabtree's catalyst but aware of its limitations, Nolan investigated the effect of modifying the ligands present around the iridium centre, and applied the resulting complex to the hydrogenation of simple olefins.[25] Previous reports had revealed that the replacement of bulky phosphines with sterically encumbered *N*-heterocyclic carbenes (NHCs) such as 1,3-bis(2,4,6-trimethylphenyl)imidazol-2-ylidene (IMes) **48** and 1,3-bis(2,6-diisopropylphenyl)imidazol-2-ylidene (IPr) **49** led to increased catalyst performance in a range of processes including olefin metathesis,[26] hydroformylation[27] and C-C bond formation reactions.[28] Nolan and co-workers therefore envisaged that the exchange of the tricyclohexylphosphine ligand of Crabtree's catalyst with the bulky, saturated 1,3-dimesityl-4,5-dihydroimidazol-2-ylidene (SIMes) **50** could produce a more active and more thermally stable catalyst in comparison to the parent compound.

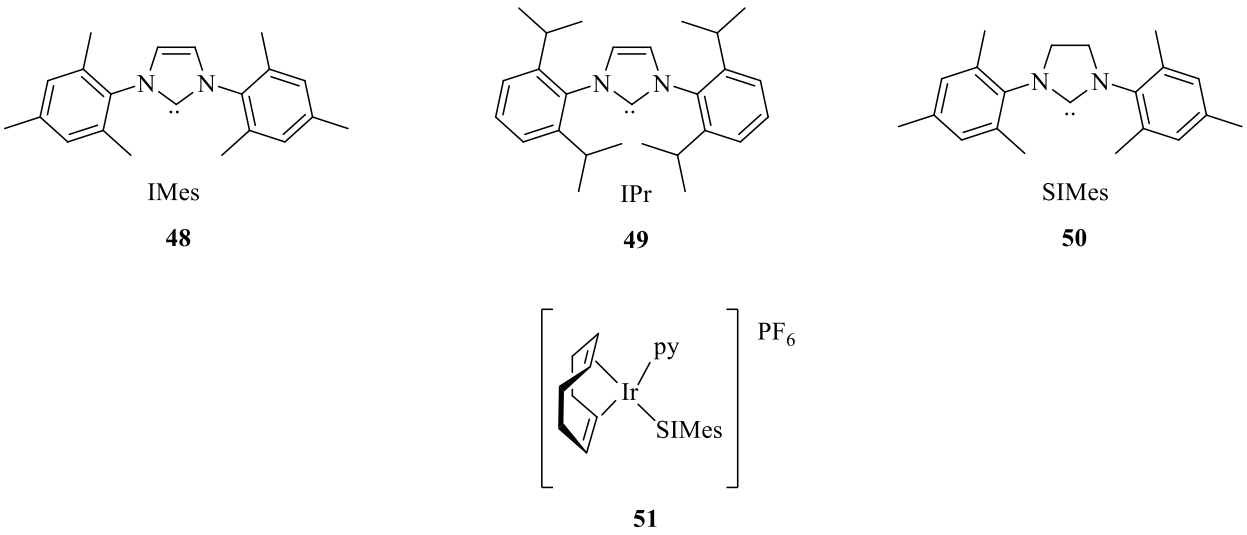

Figure 7

Investigations into the catalytic hydrogenation of simple olefins facilitated by complex **51** revealed that, under ambient conditions, the NHC-containing complex displayed a lower efficiency than that exhibited by Crabtree's catalyst (**Scheme 17**, **Table 7**, Entries 1 and 2). In contrast, reactions performed at the higher temperature of 50 °C and under an increased pressure of 60 psi exposed Nolan's complex as the superior catalyst, indicating such a species possesses a greater thermal tolerance than complex **23** (Entries 3 and 4).

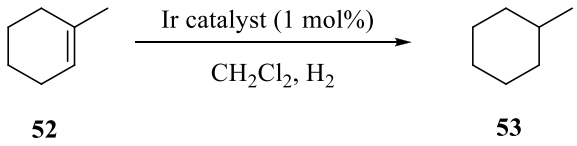

Scheme 17

Entry	Complex	Time (h)	Temp. (°C)	Pressure (psi)	Yield (%)
1	**23**	2	25	15	65
2	**51**	3.5	25	15	42
3	**23**	7	50	60	34
4	**51**	7	50	60	100

Table 7

Despite its lower efficiency when employed in reactions performed at room temperature, the higher thermal stability demonstrated by complex **51** was an attractive element and, consequently, acquired the attention of researchers within our own laboratory.[29] Having displayed only a slightly lower activity than that of Crabtree's catalyst in the field of olefin hydrogenation,[25] it was proposed that complex **51** may also facilitate efficient H-D exchange in the area of isotopic labelling. Indeed, initial results obtained in the deuteration of simple substrates such as acetophenone **54** and benzophenone **57** were extremely pleasing, revealing complex **51** to label such compounds to a degree equivalent to that achieved using Crabtree's catalyst (**Scheme 18**, **Table 8**).

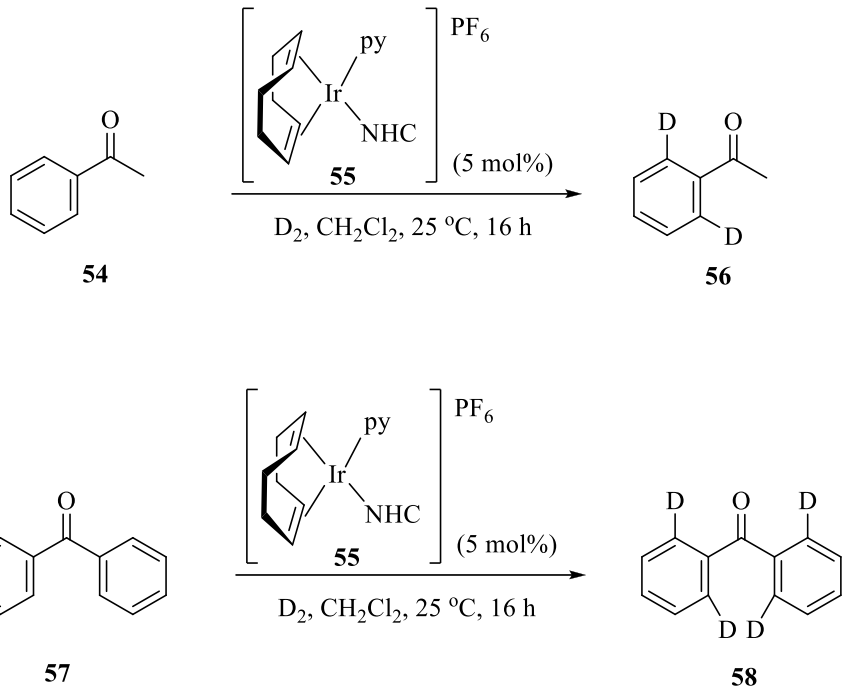

Scheme 18

Substrate \ NHC	% Deuteration			Deuteration using Crabtree's
	IMes **48**	IPr **49**	SIMes **50**	
Acetophenone	89	81	94	95
Benzophenone	68	82	94	95

Table 8

Further investigations included the deuteration of alternative substrates with complexes of the type [Ir(COD)(NHC)(py)]PF_6.[29] While the isotopic labelling of a range of compounds proceeded to deliver high levels of deuterium incorporation, the degree of H-D exchange observed in more demanding substrates such as benzamide **59** and benzenesulfonamide **61** was considerably lower (**Scheme 19**).

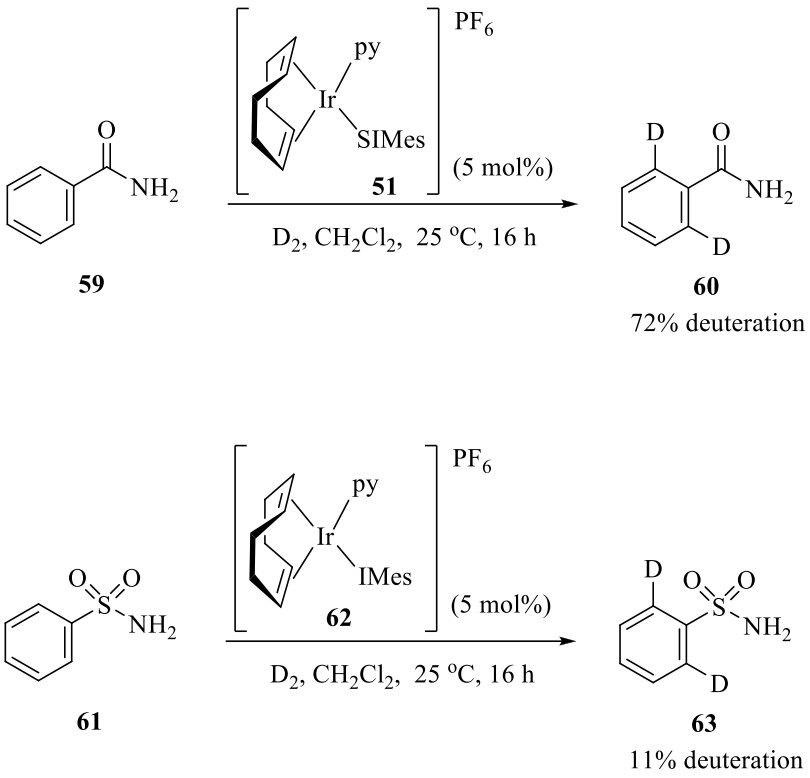

Scheme 19

Shortly after Nolan and co-workers published their findings regarding the preparation of complex **51** and its subsequent employment in the hydrogenation of olefins, an alternative modification to Crabtree's catalyst was reported by Buriak.[30] As opposed to substituting the tricyclohexylphosphine ligand with an NHC, analogous to the work of Nolan, Buriak exchanged the pyridine ligand, thus creating complexes of the type $[Ir(COD)(PR_3)(NHC)]PF_6$ (**Figure 8**). More specifically, two different NHC ligands were investigated; the more stable, sterically encumbered 1,3-bis(2,4,6-trimethylphenyl)imidazol-2-ylidene (IMes) **48**, and the somewhat less stable and smaller 1,3-dimethylimidazol-2-ylidene (IMe) **64**.

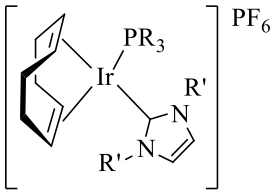

65 R = PPh_3 R' = IMe
66 R = PCy_3 R' = IMe
67 R = P^nBu_3 R' = IMe
68 R = P^nBu_3 R' = IMes

IMe
64

Figure 8

The application of such complexes in olefin hydrogenation revealed a similar reactivity to that of Crabtree's catalyst. In addition, the efficiency of those complexes bearing a mixed NHC/phosphine ligand set in the coordination sphere around the metal centre surpassed that of complexes containing a pyridine/NHC combination. Further examination of the reaction outcomes showed that for unhindered olefins, complexes incorporating the larger IMes ligand were more effective, whilst the hydrogenation of tri- or tetrasubstituted olefins proceeded at a greater rate when catalysts bearing the slighter IMe ligand were employed (**Scheme 20**, **Table 9**).

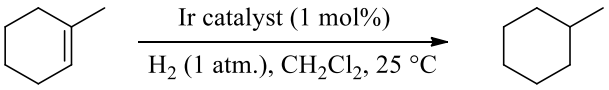

52 **53**

Scheme 20

Entry	Complex	Time (min)	Conversion (%)
1	**23**	16	99
2	**67**	21	100
3	**68**	180	100

Table 9

In a more recent publication, Buriak extended the scope of catalysts which displayed efficiency in olefin hydrogenation, identifying the optimum complex **69**, which pairs the

small tri-*n*-butylphosphine with the bulky, saturated NHC, SIMes (**Figure 9**).[31] Furthermore, substitution of the hexafluorophosphate counterion with the significantly larger, non-coordinating tetrakis[3,5-bis(trifluoromethyl)phenyl]borate (BARF) anion **70** was found to greatly increase both the activity and stability of the resulting complex (**Scheme 21**, **Table 10**, Entries 1 and 2). Indeed, even the efficiency of Crabtree's catalyst was slightly improved upon the integration of such a counter anion (Entries 3 and 4).

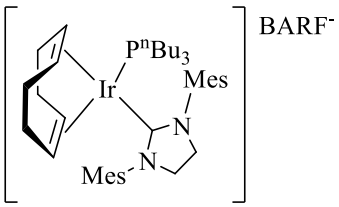

69

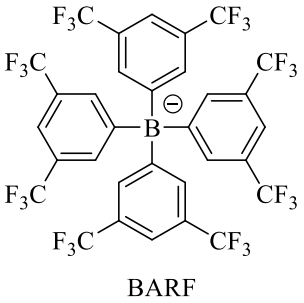

70

Figure 9

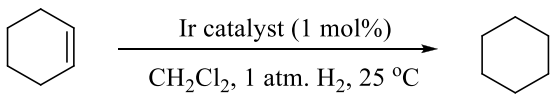

71 **72**

Scheme 21

Entry	Catalyst	Time (min)	% Conversion
1	[Ir(COD)(P^{n}Bu$_3$)(SIMes)]PF$_6$	24	100
2	[Ir(COD)(P^{n}Bu$_3$)(SIMes)]BARF	17	100
3	[Ir(COD)(PCy$_3$)(py)]PF$_6$	9	100
4	[Ir(COD)(PCy$_3$)(py)]BARF	7	100

Table 10

As described previously, the deactivation through the formation of hydride-bridged iridium clusters is a significant drawback of Crabtree's catalyst (*vide supra*). Buriak proposed that in non-polar solvents such as DCM, the PF_6 counter ion would coordinate to the cationic iridium complexes to a substantial degree. Substituting this anion for the non-polar BARF **70** would potentially alleviate such coordination, however, due to its large steric bulk, the latter counter ion may also hinder the amalgamation of catalyst monomers, preventing the formation of the undesired inactive Ir dimers and trimers.

Having achieved success in the application of Nolan's complex **51** in the field of hydrogen isotope exchange, attention in the Kerr group turned to the mixed phosphine/NHC iridium catalysts as detailed by Buriak.[32] As complex **67** had previously been uncovered as a highly efficient hydrogenation catalyst, it was envisaged that its performance in isotopic labelling reactions may be equally impressive. Investigations into such an area focused on the deuteration of acetophenone **54** and acetanilide **73**, however no D incorporation was observed in either case (**Scheme 22**).

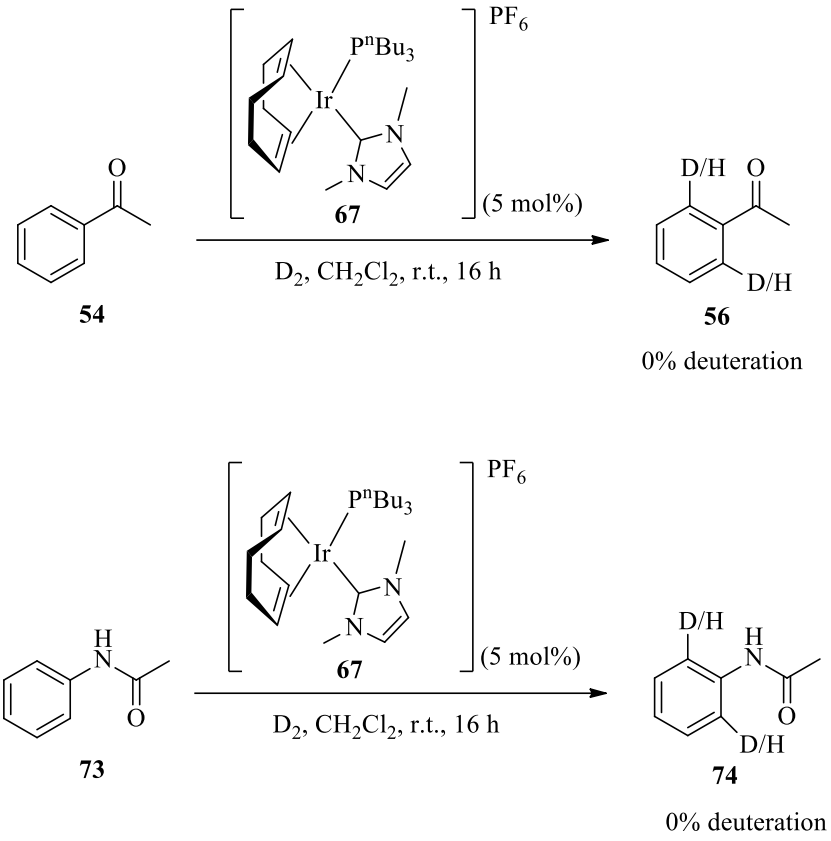

Scheme 22

Although these initial results were disappointing, it was proposed that alternative complexes of the type $[Ir(COD)(PR_3)(NHC)]PF_6$ may serve as active catalysts in HIE reactions, in particular those which contained more sterically encumbered ligands. The synthetic route employed in the preparation of complex **67** is based on a procedure previously reported by Herrmann and Köcher, which utilises an *in-situ* deprotonation of the imidazolium salt.[33] In contrast, the synthesis of complex **68** bearing the significantly larger IMes NHC requires formation of the free carbene prior to its reaction with $[Ir(COD)Cl]_2$.[30] Despite identifying the necessity of such a modification, Buriak was unable to prepare complexes pairing a bulky phosphine alongside the sterically encumbered IMes ligand; a failure attributed to the large size of the NHC, which presumably hinders coordination of the incoming phosphine to the iridium centre.

As the synthetic procedures employed by Buriak had failed to deliver such complexes, focus within our laboratory centred on the careful manipulation of such methods.[32] Pleasingly, key modifications to the preparative route such as the use of a non-polar solvent in the first step led to the successful production of complexes **75**, **76** and **68** (**Figure 10**). Furthermore, this newly developed procedure eliminated the necessity to preform the free carbene, thereby circumventing the requirement of a glovebox, and greatly increasing the practical accessibility of these complexes.

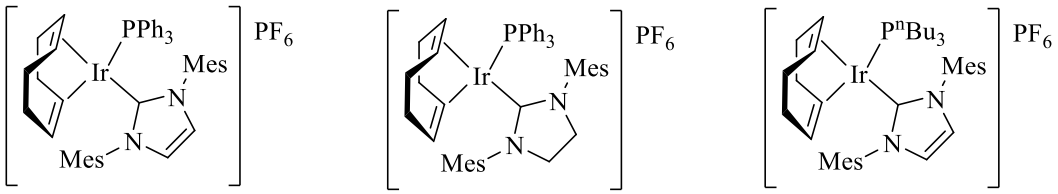

75 **76** **68**

Figure 10

With the desired complexes in hand, investigations into their performance in hydrogen isotope exchange reactions commenced. Under the standard conditions employed within our laboratory, labelling the simple substrate acetophenone **54** with 5 mol% of the Ir(I) complex over a reaction time of 16 hours, excellent levels of deuterium incorporation were delivered in each case (**Scheme 23**, **Table 11**).[32]

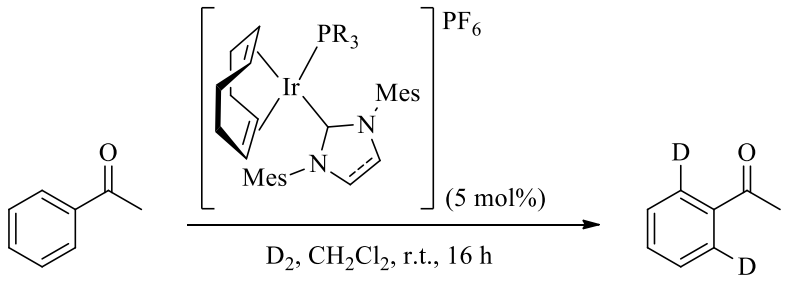

54 **56**

Scheme 23

Complex	PR_3	NHC	% Deuteration
68	P^nBu_3	IMes	98
75	PPh_3	IMes	98
76	PPh_3	SIMes	99

Table 11

Further examination of these newly developed complexes in the field of HIE revealed their ability to label a variety of substrates, with extremely high levels of deuteration observed in the majority of instances. More specifically, excellent isotope incorporations were achieved in compounds containing a selection of functional groups including amides, anilides and heterocycles (**Scheme 24**).

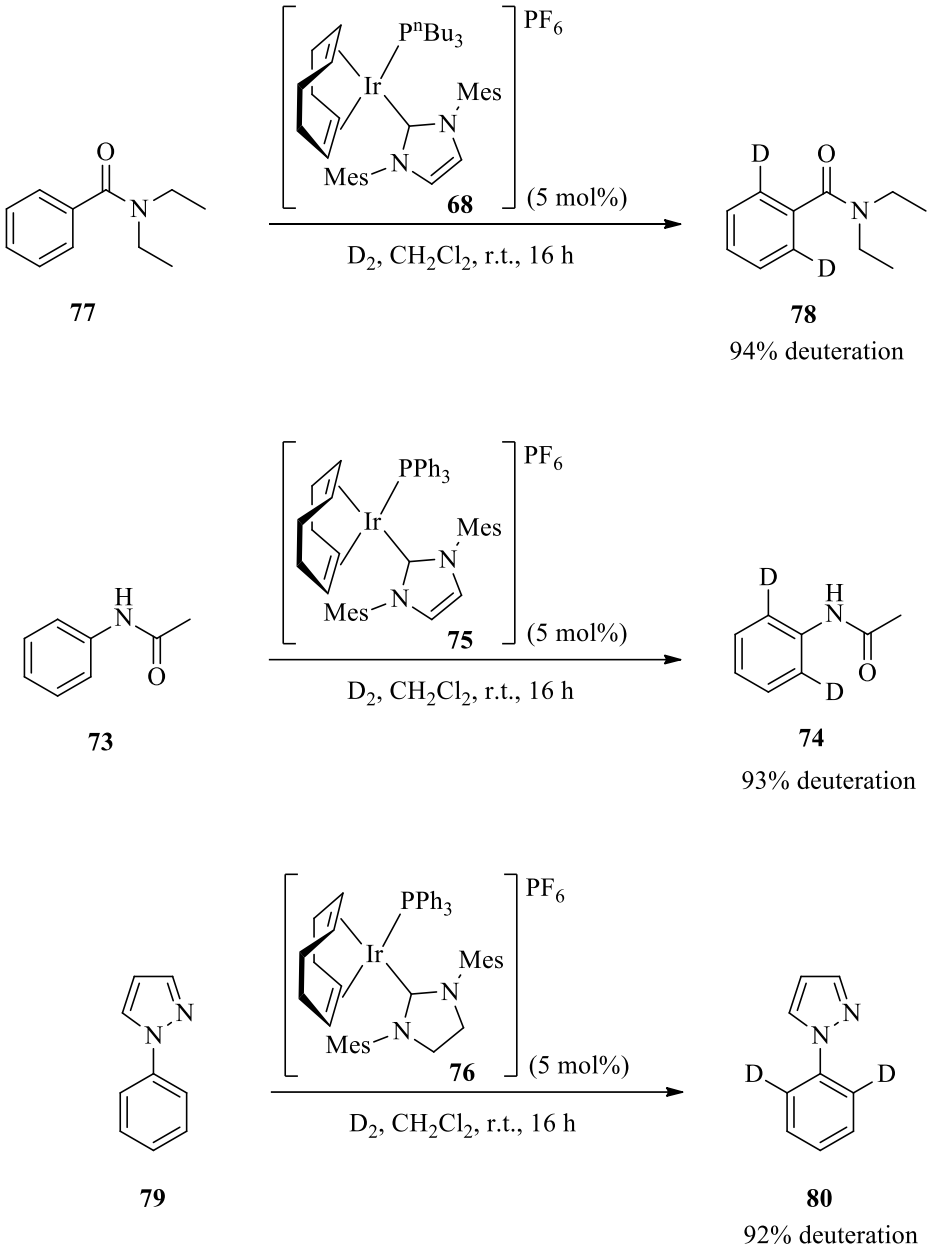

Scheme 24

In view of the remarkable activity displayed by complex **75** to this point, it was predicted that such high levels of deuterium incorporation could be maintained in reactions employing lower quantities of the catalyst over shorter time periods. Indeed, a brief optimisation study revealed that a catalyst loading of just 0.5 mol% and reaction time of 2 hours is sufficient to label acetophenone **54** to an excellent 95% deuteration (**Scheme 25**).[32]

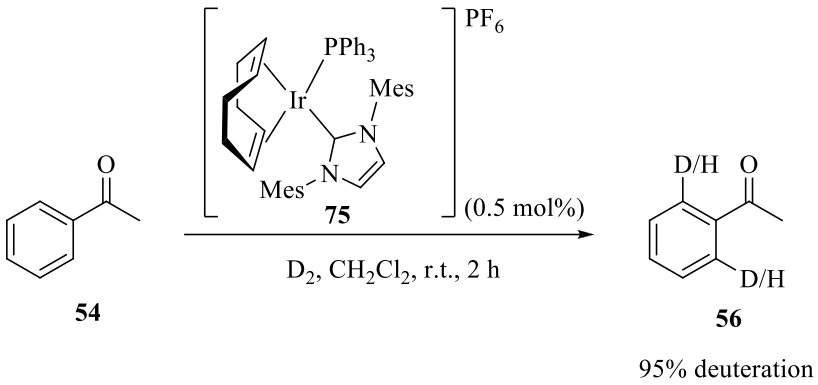

Scheme 25

Careful analysis of the results obtained thus far regarding the use of complexes of the type $[Ir(COD)(PR_3)(NHC)]PF_6$ in HIE reactions revealed that catalysts bearing the unsaturated IMes ligand displayed higher efficiency in the labelling of a wider range of substrates than that achieved by their saturated analogues.[32] In addition, complex **75** containing the larger triphenylphosphine ligand showed superior activity over complex **68**. It was therefore proposed that maintaining the IMes ligand and simply altering the phosphine ligand may give rise to significant differences in catalyst performance, or even a range of effective HIE catalysts.

Explorations into such an area began with the variation of the steric properties of the phosphine moiety.[34,35] To enable an accurate comparison, the electronic properties of the phosphines could not be modified by any substantial degree. With similar electronic parameters to triphenylphosphine but significantly different sterics (**Table 12**),[36] tribenzylphosphine and dimethylphenylphosphine offered an attractive starting point for this investigation.[34,35]

Phosphine	Cone Angle (°)
$P(CH_2Ph)_3$	165
PPh_3	145
PMe_2Ph	122

Table 12

81 **82**

Figure 11

Complexes **81** and **82** shown in **Figure 11** were thus synthesised and applied to H-D exchange reactions. Pleasingly, the initial results obtained in the deuteration of acetophenone **54** demonstrated the activity of these novel complexes to be comparable to that of complex **75** (**Scheme 26**, **Table 13**).[34,35]

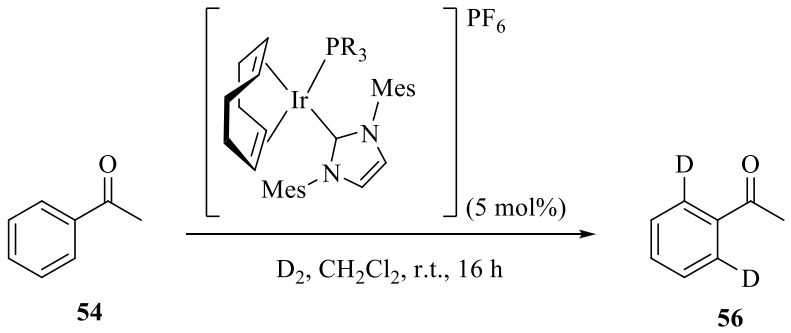

54 **56**

Scheme 26

Catalyst	PR_3	% Deuteration
75	PPh_3	97
81	$P(CH_2Ph)_3$	98
82	PMe_2Ph	98

Table 13

In an analogous manner to investigations carried out with complex **75**, rate and activity studies for the use of complexes **81** and **82** were undertaken (**Scheme 27**, **Table 14**).[34,35] Such explorations revealed that both complexes could be employed in HIE reactions at exceedingly low catalyst loadings, delivering levels of isotope incorporation as high as those detailed in **Table 13**, within considerably reduced reaction times.

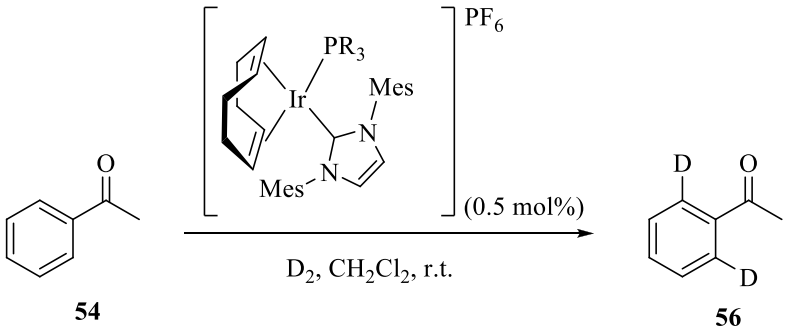

Scheme 27

Complex	PR_3	Time (h)	% Deuteration
81	$P(CH_2Ph)_3$	1	97
82	PMe_2Ph	1.5	97

Table 14

Further investigations regarding the isotopic labelling of alternative substrates with complexes **75**, **81** and **82** reinforced the remarkable activity displayed by complexes of this type. Of particular interest was the degree of selectivity exhibited in the deuteration of

benzanilide **83** by complex **82**. Substrate **83** offers two sites at which labelling can occur, through both a 5- and a 6-mmi, in positions *a* and *b*, respectively (**Scheme 28**). At a catalyst loading of 5 mol%, complex **82** delivers the isotopically-enriched product **84** with equally excellent incorporations achieved in both positions. However, in the presence of a significantly reduced quantity of complex **82**, H-D exchange at position *a* remains at a high level, while that observed at position *b* is drastically reduced (**Table 15**).[34,35]

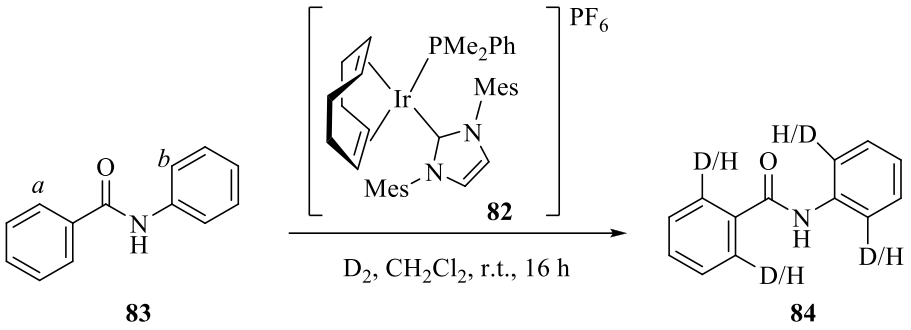

Scheme 28

Catalyst Loading (mol%)	% Deuteration	
	a	*b*
5	95	93
0.5	94	2

Table 15

Following investigations regarding the steric properties of phosphine ligands, focus within the Kerr group turned to the examination of the ligands' electronic properties.[34] With similar cone angles of 132°, 136° and 130°, respectively, P^nBu_3, $PMePh_2$ and $P(O^iPr)_3$ appeared ideal candidates due to their significant differences in electronic parameters.[36] The novel complexes **85** and **86** (**Figure 12**) were therefore prepared and their performance in hydrogen isotope exchange reactions investigated and compared to that of complex **68**.[34]

85 **86**

Figure 12

Pleasingly, high levels of deuterium incorporation were achieved in the isotopic labelling of numerous substrates bearing various functional groups such as ketones, amides and heterocycles (**Scheme 29**, **Table 16**).

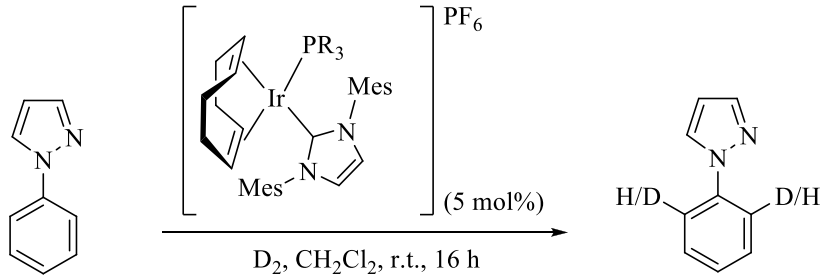

79 **80**

Scheme 29

Enrty	Complex	PR_3	% Deuteration
1	**68**	P^nBu_3	93
2	**85**	$PMePh_2$	94
3	**86**	$P(O^iPr)_3$	98

Table 16

The results obtained in such studies did not, however, reveal any distinct relationships between the electronic properties of the phosphine ligand present on the metal centre and the activity of the overall complex. Having stated this, it became apparent that with certain

substrates, higher degrees of deuterium incorporation were achievable if specific catalysts were employed in the reaction as opposed to others. For example, the isotopic labelling of 2-phenylpyridine **41** facilitated by complex **68** proceeded to a moderate level of 58% D incorporation (**Table 17**, Entry 1) while, in contrast, the use of complex **86** delivered the desired compound **42** with an excellent 96% deuteration (Entry 3). Such a significant difference in the extent of labelling is consistent with observations made previously by Herbert,[24] indicating this particular substrate prefers to coordinate to a more electron-deficient metal centre than to a complex rich in electron density.

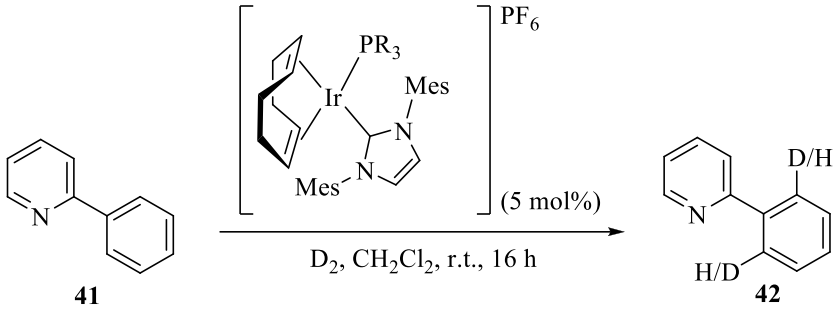

Scheme 30

Entry	Catalyst	PR_3	% Deuteration
1	**68**	P^nBu_3	58
2	**85**	$PMePh_2$	92
3	**86**	$P(O^iPr)_3$	96

Table 17

1.5 Hydrogen Isotope Exchange in Alternative Reaction Media

As discussed earlier, Crabtree's catalyst **23** was originally developed for use in olefin hydrogenation reactions.[18] During investigations which ultimately led to the birth of complex **23**, it was proposed that a key feature of an efficient homogeneous hydrogenation catalyst

would be the free availability of active sites on the metal centre itself. As competition for such active sites may occur between substrate and coordinating solvent molecules, it was reasoned that the efficacy of the cationic iridium complexes under examination may be improved by performing the reactions in a non-coordinating solvent. Experiments were therefore carried out in reaction media such as benzene, toluene, and hexane. However, in each instance the formation of catalytically inactive precipitates was observed. As such species were found to dissolve only in dichloromethane (DCM), this solvent was employed in hydrogenation reactions and was found to deliver the desired results.

Since this discovery, DCM has been the solvent of choice for reactions catalysed by Crabtree's complex and, indeed, many other hydrogenation and hydrogen isotope exchange catalysts (*vide supra*). However, there do exist a number of concerns regarding the use of such a reaction medium, the most significant being its suspected carcinogenicity.[37] Other hazards associated with DCM include its high vaporisability as upon inhalation it can induce asphyxiation, as well as its potential to act as a skin irritant, CNS depressant, and DNA mutagen.

In view of these issues, it would be extremely favourable to reduce the volume of DCM used in industrial applications. Indeed, the most recently published GlaxoSmithKline Solvent Selection Guide identifies DCM as a solvent with which there are "major issues".[38] In addition, the identification of suitable replacements for DCM in medicinal chemistry research would be beneficial due to the low solubility of numerous potential drug candidates in this reaction medium. Several research groups have therefore examined the application of solvents other than DCM in the field of hydrogen isotope exchange.

As described earlier, the first examples of H-D exchange facilitated by Crabtree's catalyst were reported by Hesk and co-workers.[19] While the majority of investigations were performed using DCM as the reaction solvent, these initial studies also included a brief exploration of alternative reaction media due to the poor solubility of certain substrates in

DCM (**Scheme 31**). As illustrated by the results in **Table 18**, the isotopic labelling of acetanilide **73** did not proceed in either acetone, dimethylformamide (DMF) or dioxane. Further inspection of alternative reaction media included the application of co-solvents, whereby a small volume of a more polar solvent was added to DCM. While small volumes of acetone were tolerated, the labelling achieved in a MeOH/DCM mixture was significantly reduced, with no desired isotopically-enriched product delivered in the presence of DMF (Entry 8).

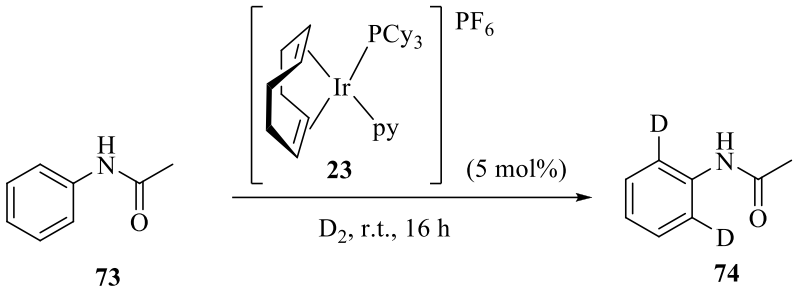

Scheme 31

Solvent	d0	d1	d2
CH_2Cl_2	0	7	93
Acetone	100	-	-
DMF	100	-	-
Dioxane	100	-	-
5% Acetone in CH_2Cl_2	4	19	77
10% Acetone in CH_2Cl_2	6	31	63
5% MeOH in CH_2Cl_2	14	46	40
5% DMF in CH_2Cl_2	100	-	-

Table 18

Further efforts to determine the isotopic labelling capabilities of Crabtree's catalyst were conducted by Herbert and co-workers.[24] Once again, the majority of investigations were

performed using DCM as the reaction solvent, however a short comparison study was carried out to examine the degree of deuterium incorporation obtained in reactions employing the more polar methanol as the reaction medium. As illustrated in **Table 19**, H-D exchange was observed in a number of substrates, albeit at somewhat reduced levels.

Substrate	% Deuteration (DCM)[a]	% Deuteration (MeOH)[a]
Benzamide	64	17
Ethyl benzoate	20	0
N-Phenylpyrazine	74	33

[a] 100 mol% Crabtree's catalyst, **23**

Table 19

An alternative approach to solving issues regarding substrate solubility was reported in 2003.[39] As opposed to examining typical organic solvents as potential replacements of DCM, Salter investigated HIE reactions employing ionic liquids as suitable reaction media. The labelling of various substrates known to be poorly soluble in DCM was carried out, including that of paracetamol **87** (**Scheme 32**). Comparison between reactions run in DCM and the commercially available 1-butyl-3-methylimidazolium hexafluorophosphate [BMI][PF_6] revealed that a significantly higher degree of H-D exchange was achieved in the latter solvent, undoubtedly due to the increased solubility of compound **87** (**Table 20**).

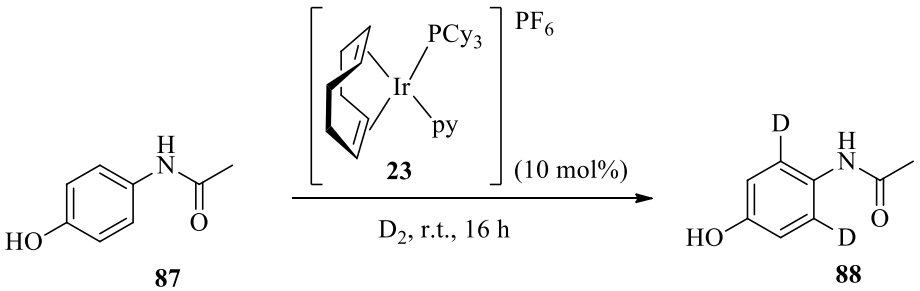

Scheme 32

Solvent	% Deuteration
DCM	8
[BMI][PF_6]	59

Table 20

More recently, Schou demonstrated the enhanced efficiency which could be achieved in HIE reactions catalysed by rhodium black, by employing Crabtree's catalyst as an additive.[40] The examination of a number of substrates revealed that, in general, higher deuterium incorporations could be attained in reactions facilitated by the Rh/Ir mixture when compared to the levels of deuteration observed in the presence of the heterogeneous catalyst alone. Of particular interest was the isotopic labelling of 4-amino-pyrimidine-5-carboxylic acid **89**. While reactions employing Rh black or Crabtree's catalyst individually failed to deliver the desired isotopically labelled product, a mixture of the two catalysts furnished compound **90** with a 60% deuteration (**Scheme 33**), albeit with a significantly elevated (combined) catalyst loading.

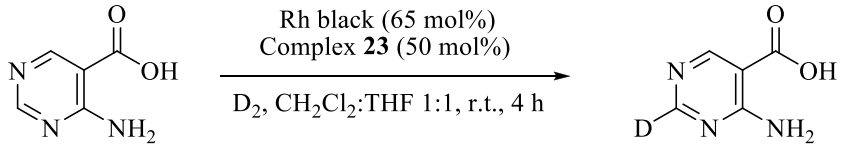

89 → **90** (60% deuteration)

Scheme 33

As illustrated in the above scheme, reactions catalysed by the Rh/Ir combination were typically performed in a 1:1 DCM:THF solvent mixture. To determine how robust the system under consideration was, the labelling of substrate **91** was performed in a variety of solvents (**Scheme 34**). Good to excellent deuterium incorporations were achieved in solvents such as EtOAc and THF alone, while no isotopic labelling was detected in Et_2O (**Table 21**). The

latter outcome is proposed to be due to the poor solubility of compound **91** in this solvent, rather than as a result of any interference such as poisoning of the catalyst.

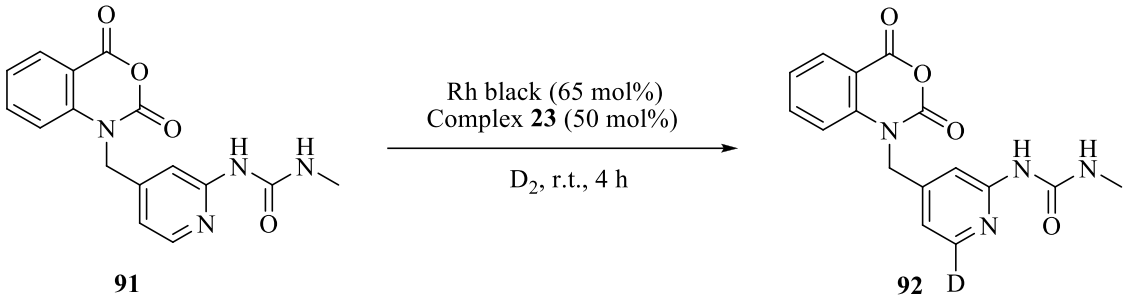

Scheme 34

Solvent	% Deuteration
THF:DCM (1:1)	93
DCM	60
THF	89
EtOAc	84
Et_2O	0

Table 21

1.6 Phosphines as Ligands

As demonstrated, the properties of transition metal complexes can be manipulated with a degree of simplicity through the use of phosphine ligands. Such a feature is extremely attractive to synthetic chemists, hence the frequent appearance of phosphines in organometallic species. By altering the R groups present on tertiary phosphines, both the steric and electronic properties of the ligands can be controlled in a systematic and predictable manner, creating the desired effect in terms of both electron density on, and steric bulk around, the metal centre. The bonding between phosphines and a metal is comprised of two elements.[41] The first, a σ bond, is formed from donation of the lone pair of electrons on

the central phosphorus atom to the metal; more specifically, from a filled sp^3 orbital on the phosphorus into empty d-orbitals of the metal (**Figure 13**, **93**). As π-acceptors, phosphines can also participate in backbonding, accepting electron density from filled metal d-orbitals into the σ* orbital of the P-R bond, as depicted by **94**. Although such an acceptance will result in a lengthening of the P-R bond, any obvious extension is concealed by the simultaneous shortening of the same bond, caused by donation of the phosphorus lone pair to the metal.

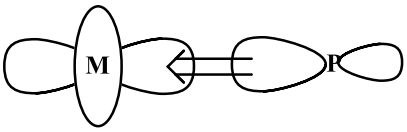

93

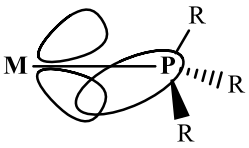

94

Figure 13

In 1977, Tolman introduced the cone angle, a concept now widely recognised as a method of quantifying the steric influence imparted by phosphine ligands.[36] By measuring the angle of a cylindrical cone, the apex of which accommodates the metal and extends outwards to enclose the outermost atoms of the substituents, an indication of the steric bulk associated with each ligand could be determined (**Figure 14**).

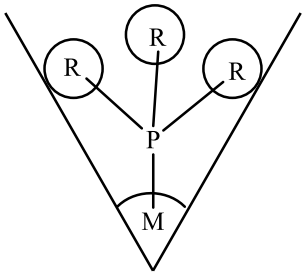

Figure 14

By altering the R groups present on the central phosphorus atom, the size of the ligand can be modified which, in turn, enables fine tuning of the reactivity of the resulting metal complex. For example, by employing more sterically demanding ligands, access to the metal centre can be restricted, thus preventing coordination of additional ligands. Furthermore, knowledge of the steric bulk surrounding a metal centre enables a better understanding regarding not only the coordination of additional ligands, but also the dissociation of ligands already attached to the metal. The cone angles for selected phosphines are shown below in **Table 22**.

Phosphine	Cone Angle (°)
PMe_3	118
$P(O^iPr)_3$	130
PEt_3	132
$PMePh_2$	136
PPh_3	145

Table 22

In addition to examining the steric effects associated with phosphine ligands, Tolman also quantified their electronic parameters. Such explorations involved the measurement of carbonyl stretching frequencies in complexes of the type $Ni(CO)_3L$, where L = tertiary phosphine. As the electron-donating capabilities of the substituents on the phosphorus increase, σ-donation from the phosphine ligand is enhanced, hence more electron density is pushed onto the metal centre. As poor π-acceptors, electron-rich phosphines do not readily accept electron density from filled metal d-orbitals. Instead, an increase in backbonding occurs between the metal and the carbonyl ligands, raising the electron density present in the π*-antibonding orbital of the C-O bond. Such an increase causes a weakening of the C-O bond, resulting in a lower stretching frequency as observed by infrared spectroscopy. As shown in **Table 23**, altering the phosphine substituents from phenyl to methyl causes a decrease in CO stretching frequency of approximately 5 cm^{-1}. A further reduction is observed in the presence of *iso*-propyl groups, with the most strongly electron-donating phosphine, PCy_3, giving rise to the lowest carbonyl stretching frequency of 2056.4 cm^{-1}.

Phosphine	ν_{CO} cm^{-1}
PPh_3	2068.9
PMe_3	2064.1
$P(^iPr)_3$	2059.2
PCy_3	2056.4

Table 23

1.7 *N*-Heterocyclic Carbenes as Ligands

The first reports of *N*-heterocyclic carbenes in organometallic complexes emerged in 1968, when Wanzlick[42] and Öfele[43] detailed the preparation of mercury-NHC **95** and chromium-NHC **96** complexes, respectively (**Figure 15**). Since this time, the use of such ligands has increased significantly, and there now exist numerous examples of transition metal-NHC complexes which are capable of facilitating a range of processes.[44]

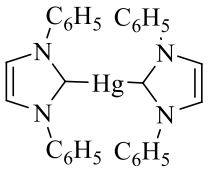

95

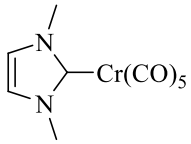

96

Figure 15

In many instances, NHCs have been identified as attractive alternative ligands to phosphines, due to their enhanced stability, strong σ-donating abilities, and poor π-accepting capabilities, as well as the relative ease with which their complexes can be prepared.[45] Indeed, work by Nolan has revealed that in ruthenium complexes of the type Cp*Ru(L)Cl, NHC ligands bind to the metal centre by approximately 5 kcal mol^{-1} more strongly than the significantly electron-donating tricyclohexylphosphine ligand.[26] Such a difference in binding strength

offers great advantages, such as the reduced probability of ligand dissociation, enabling lower quantities of ligand to be employed in catalytic reactions.[46]

As mentioned, transition metal complexes bearing NHC ligands have displayed high efficiency in a number of metal-mediated reactions, including Pd-catalysed cross-coupling reactions, such as the Suzuki-Miyaura reaction[47] and the Heck reaction,[48] as well as within hydrogenations[28] and olefin metathesis.[49] Perhaps one of the most well documented transition metal complexes containing an NHC ligand as a phosphine replacement is Grubbs second generation catalyst, developed for use in ring closing metathesis reactions.[50] Substitution of one of the tertiary phosphine ligands present in the first generation complex **97** with the saturated NHC ligand SIMes produced a highly active species **98**, the reactivity of which surpassed that of **97**.

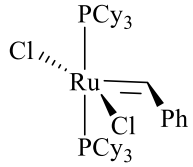

97

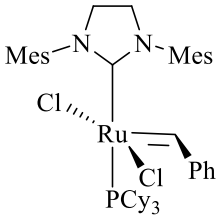

98

Figure 16

Despite the stability of their metal complexes, the preparation, handling and storage of NHCs themselves require stringent conditions, as the free carbenes are not generally stable to air or moisture. Having stated this, in 1991 Arduengo reported the synthesis and structural characterisation of the first crystalline carbene.[51] The preparation of 1,3-bis(1-adamantyl)imidazol-2-ylidene **100** was achieved through deprotonation of the corresponding imidazolium salt **99** by sodium hydride in the presence of catalytic quantities of DMSO (**Scheme 35**). Alternatively, KO^{t}Bu could be employed, delivering the free carbene in high yields.

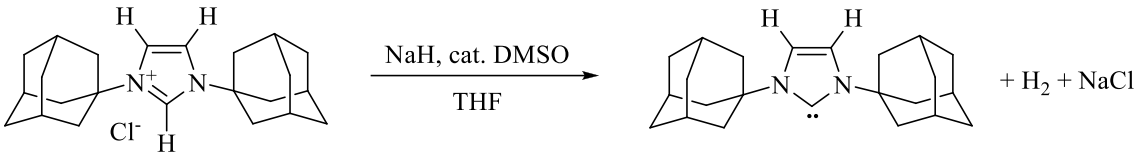

99 **100**

Scheme 35

The stability of carbene **100** is attributed to a combination of the steric hindrance presented by the bulky adamantyl substituents, and the electronic properties of the 5-membered heterocycle. As singlet carbenes, NHCs contain a pair of non-bonding electrons which occupy an sp^2 orbital in the plane of the ring (**Figure 17**). Such a coupling results in a vacant p orbital on the carbene carbon into which electron density from the neighbouring nitrogen atoms can be donated. In conjunction with the unsaturated backbone, a pseudo aromatic system with 6 π-electrons is thus created. Further stabilisation of the lone pair of electrons in the sp^2 orbital results from the σ-withdrawal by the heteroatoms adjacent to the carbenic carbon.[51,52]

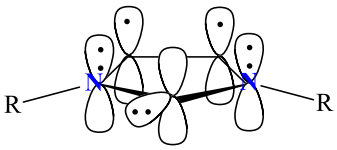

Figure 17

In an analogous technique to that utilised by Tolman,[36] the electronic properties of NHC ligands have been determined by measuring the IR stretching frequencies of C=O bonds in complexes of the type $M(NHC)(CO)_xL$. Originally investigated utilising Ni complexes,[53] the electronic nature of NHC ligands has since been uncovered in complexes containing a range of metals, however, this discussion will centre only on the values established using iridium complexes.[46]

The carbonyl stretching frequencies for numerous compounds of the form [(L)Ir(CO)$_2$Cl] have been determined, enabling a direct comparison to be made between the electron-donating properties of tertiary phosphines and *N*-heterocyclic carbenes. As indicated by the values listed in **Table 24**, the most weakly donating NHC ligand 1,3-bis(2,6-diisopropylphenyl)imidazolidine-2-ylidene (SIPr) **101**, is significantly more donating than the most electron-rich phosphine, PCy$_3$. Furthermore, while the differences in phosphine electronic parameters are quite large, those between NHC ligands are really relatively small. As expected, alkyl substituted NHCs give rise to shorter stretching frequencies than aryl containing ligands, with the most strongly donating NHC bearing adamantyl substituents. It was also found that saturated NHCs are slightly less donating than their unsaturated equivalents, a feature which had been previously observed in NHC-containing Ni complexes.[53]

L	ν_{CO} (cm^{-1})	TEP (cm^{-1})
PPh$_3$	2043.5	2068.9
PMe$_2$Ph	2044.0	2067.0
PCy$_3$	2028.0	2056.4
SIPr	2024.9	2052.2
SIMes	2024.6	2051.5
IPr	2023.9	2051.5
IMes	2023.1	2050.7
ICy	2023.0	2049.6
IAd	2021.6	2049.5

Table 24

As the electronic properties of numerous phosphine and NHC species have been studied by both of the previously described methods, their respective values have been plotted in a manner presented in **Figure 18**. Consequently, the calculation of the resultant linear regression equation has revealed a linear correlation between the average ν_{CO} values for complexes of the type [(L)Ir(CO)$_2$Cl] and their recorded Tolman electronic parameter (TEP)

coefficients. It is therefore proposed that the TEPs for new NHC ligands could be determined by extrapolation of their Ir complex ν_{CO} measurements, eliminating the need for additional experiments including the synthesis and carbonyl stretching frequency determination of $Ni(CO)_3(NHC)$ complexes.

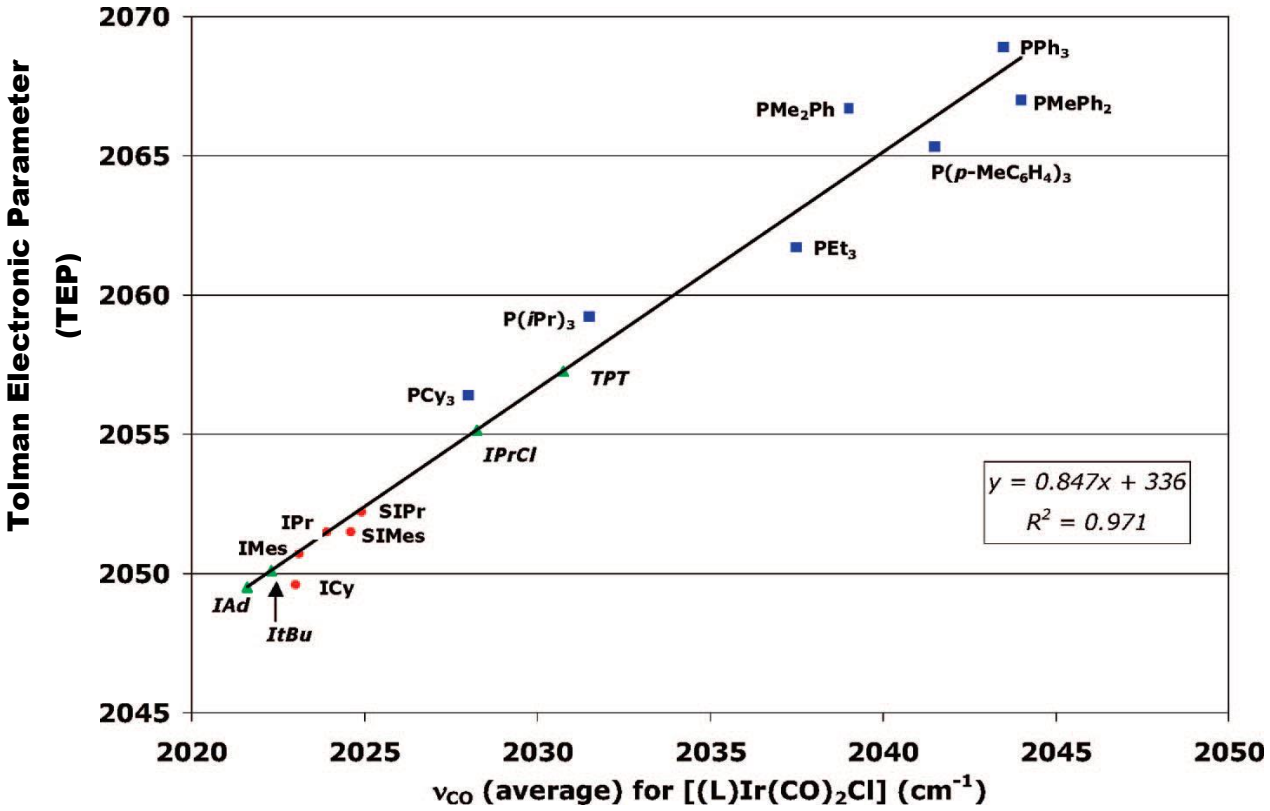

Figure 18 – Correlation of average ν_{CO} values for $[(L)Ir(CO)_2Cl]$ complexes with Tolman electronic parameters[46]

While the electronic parameters of NHCs have been determined in a similar method to that employed for phosphine ligands, the steric influence of the former ligands has been quantified using an alternative approach to the phosphine cone angle. Studies by Nolan and Cavallo have introduced the concept of percent buried volume ($\%V_{bur}$), a technique which measures the volume of a sphere, the core of which hosts the metal centre, and which is occupied by the substituents of the NHC ligand (**Figure 19**).[54] The larger the ligand, the greater the volume of the sphere which is buried by the coordinated atoms, hence the larger

the $\%V_{bur}$. The reported values are calculated from X-ray crystallography data, employing a radius of 3 Å, and positioning the coordinating atom at two distances away from the metal centre, 2.00 Å and 2.28 Å, which relate to the average distances between the metal and NHC and PR_3 ligands, respectively, in the Ni complexes originally studied in the determination of the phosphine cone angle.[36]

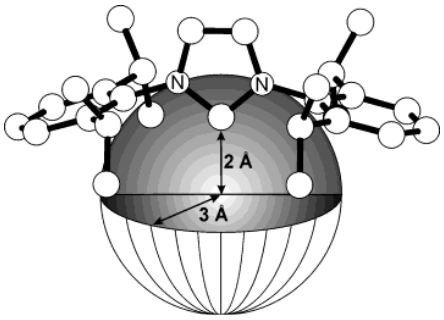

Figure 19

The steric bulk of various NHC ligands have been quantified using this technique, in complexes containing various metals such as ruthenium, rhodium, iridium, gold, silver, and palladium.[54b] In general, comparable values for $\%V_{bur}$ are obtained for NHC ligands in complexes of different metals, however some significant differences have been observed. For example, in complexes of the type [(NHC)AuCl], SIPr **101** is found to have a larger $\%V_{bur}$ value than its unsaturated analogue IPr **49** (**Figure 20**). In the corresponding Ag and Cu complexes, however, the opposite is true (**Table 25**). In addition, it became apparent that the values attained for ligands such as IMes **48** and SIMes **50** were dependent on the coordination number of the metal. For example, in linear complexes of the form (IMes)MX, the quoted $\%V_{bur}$ values for IMes are generally below 36%, whereas in tetra- and pentacoordinated complexes, the maximum observed $\%V_{bur}$ is 33%. Such a variation indicates a certain degree of flexibility within the mesityl-based NHCs to minimise the crowding around the metal centre.

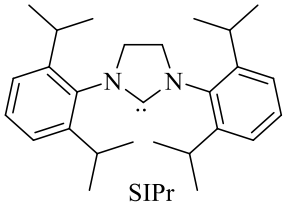

SIPr

101

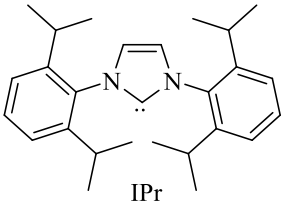

IPr

49

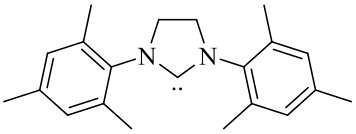

SIMes

50

Figure 20

NHC	$\%V_{bur}$ (Cu)	$\%V_{bur}$ (Ag)	$\%V_{bur}$ (Au)
SIMes	36.9	36.1	36.9
IPr	47.6	46.5	44.5
SIPr	46.4	44.5	47.0

Table 25

In view of these findings, this discussion will focus on the iridium complex, [(NHC)Ir$(CO)_2$Cl], previously utilised in studies to determine the electronic parameters of NHC ligands.[46] Of the NHCs examined, those bearing adamantyl or *tert*-butyl groups gave rise to the highest percent buried volumes (**Table 26**, Entries 1 and 2). As expected, ligands containing the bulkier 2,6-diisopropyl substituents were found to have larger $\%V_{bur}$ values than those which included mesityl groups, with the smallest NHC ligand revealed as the aliphatic ICy ligand (Entry 7). In addition, comparison of ligands containing a saturated or unsaturated backbone revealed those possessing the latter attribute to be slightly smaller than their saturated analogues (Entries 3 and 4, and Entries 5 and 6).

Entry	Complex	$\%V_{bur}$ at Ir-C^{NHC} distance (Å)	
		2.00	2.28
1	[(I^tBu)$Ir(CO)_2Cl$]	33	28
2	[(IAd)$Ir(CO)_2Cl$]	33	27
3	[(SIPr)$Ir(CO)_2Cl$]	29	23
4	[(IPr)$Ir(CO)_2Cl$]	26	20
5	[(SIMes)$Ir(CO)_2Cl$]	27	21
6	[(IMes)$Ir(CO)_2Cl$]	26	20
7	[(ICy)$Ir(CO)_2Cl$]	23	19

Table 26

2 Proposed Work

As discussed, research within our laboratory has focused on hydrogen isotope exchange reactions employing novel and highly active catalysts of the type $[Ir(COD)(PR_3)(IMes)]PF_6$. More specifically, complexes bearing the sterically distinct tribenzylphosphine, triphenylphosphine, and dimethylphenylphosphine have been synthesised and applied to the labelling of a number of substrates. As shown below (**Scheme 36**), reactions carried out under the standard protocol require only minimal amounts of catalyst to deliver excellent levels of incorporation, in short reaction times.[35]

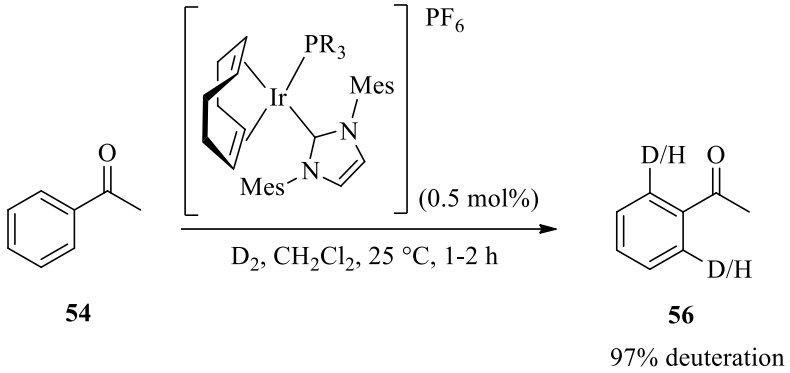

Scheme 36

For the reasons outlined previously, a drawback to this system exists in the use of a chlorinated, and industrially less acceptable solvent. As described, DCM is also relatively non-polar, presenting difficulties with respect to the solubility of more drug-like molecules which invariably contain polar functional groups. One of the initial objectives of this research project is, therefore, to investigate the application of alternative solvents in these labelling reactions. The use of a more polar and non-halogenated, hence more environmentally benign, reaction medium would greatly benefit pharmaceutical applications; however, such a modification would only be deemed advantageous if the efficiency of the catalytic system was maintained.

With respect to the Ir(I) complexes themselves, previous work within our laboratory has focused on the alteration of the phosphine ligands.[34,35] Indeed, both the steric and electronic properties of such ligands have been investigated, and their effects on catalyst reactivity studied. In contrast, no studies regarding the NHC ligands have been performed. An additional objective of this research project is therefore to synthesise novel complexes bearing different NHC ligands, and to determine any relationships observed regarding the different steric and electronic properties of such ligands and their performance in HIE reactions. The use of computational experiments may also enable comparisons to be drawn between the activity of novel Ir(I) complexes and the previously reported IMes-containing catalysts. Of particular interest would be the calculation of the relative energies of the key processes within the HIE mechanistic cycle, which may underpin any differences displayed by complexes bearing alternative NHC ligands.

Four imidazolium salts, together with the isolated Arduengo's carbene **100**,[51] were available within our laboratory (**Figure 21**). These instantly accessible ligands differ substantially with respect to both their steric environments and electronic parameters, and so provide a good initial starting point for this exploration.

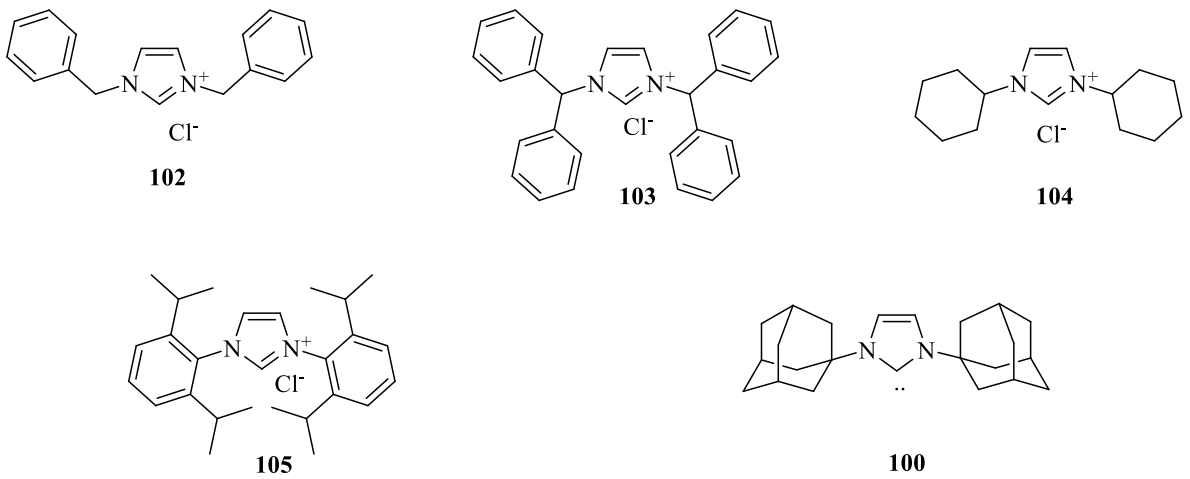

Figure 21

3 Results and Discussion

3.1 Preparation of Iridium(I) Complexes

Prior to any further investigation regarding the use of our catalysts in hydrogen isotope exchange reactions, it was first required to perfect the technique of synthesising the previously developed complexes.

The preparation of such catalysts is outlined below in **Scheme 37**.[35] Upon treatment of a solution of $[Ir(COD)Cl]_2$ **106** in benzene with NaOEt, a red to yellow colour change is observed. After stirring for a short time, the imidazolium salt **107** is added, enabling formation of the stable Ir(COD)(IMes)Cl intermediate **108**. Addition of silver hexafluorophosphate results in the formation of a dark precipitate, verifying abstraction of the halide anion. Following filtration through celite under an inert atmosphere, the penultimate step of the synthesis involves addition of the phosphine, causing a distinct orange to red colour change. Finally, recrystallisation techniques are employed to isolate the desired complex **109**.

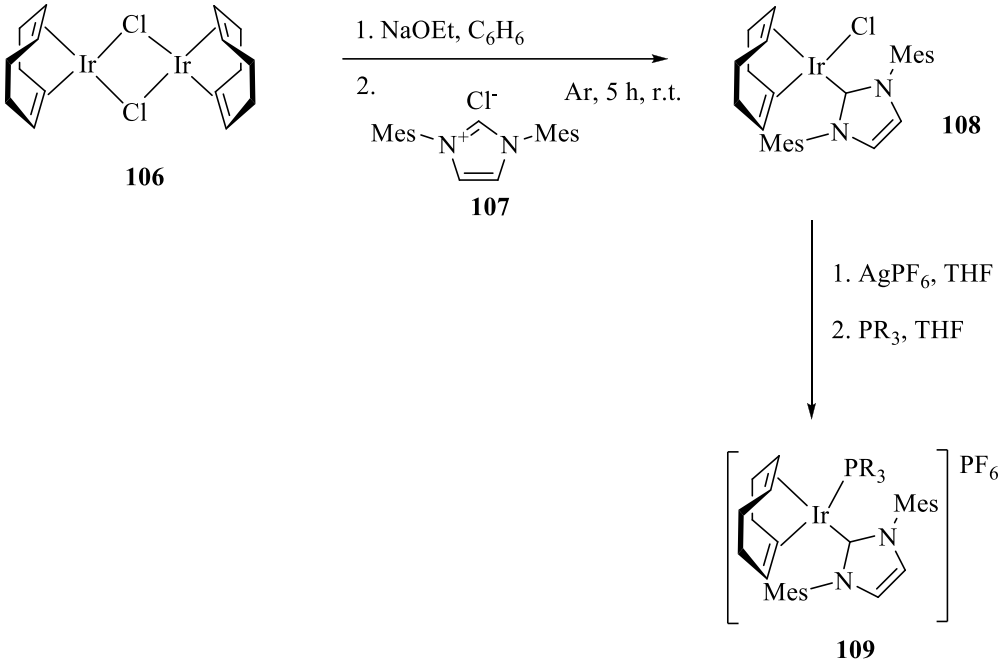

Scheme 37

Following this procedure, the first catalyst synthesised was complex **75**, bearing the sterically encumbered IMes NHC ligand, and triphenylphosphine (**Figure 22**). While initial yields achieved were low, subsequent attempts at the preparation of complex **75** led to higher and more consistent yields being obtained; the highest yield of 57% was comparable with those previously attained within our laboratory (**Table 27**).[35]

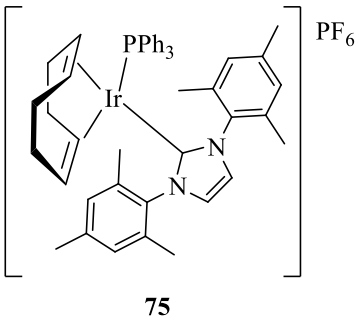

Figure 22

Run	Yield of **75** (%)
1	33
2	47
3	51
4	56
5	57

Table 27 - Preparation of complex **75** using reaction sequence of **Scheme 37**

Satisfied that complex **75** could now be prepared without difficulty, attention turned to the synthesis of complex **81**, containing the slightly more bulky tribenzylphosphine (**Figure 23**). As had been observed previously, repeated attempts at this synthesis saw a steady increase in the yields obtained (**Table 28**). Pleasingly, the greatest yield achieved of 63% (Entry 4) is slightly higher than had been attained within our group thus far.[35]

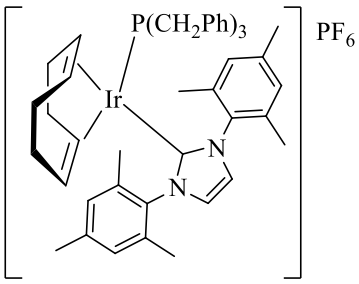

81

Figure 23

Run	Yield of **81** (%)
1	32
2	44
3	57
4	63
5	60

Table 28 - Preparation of complex **81** using reaction sequence of **Scheme 37**

Finally, the last known catalyst of this series, complex **82**, which incorporates dimethylphenylphosphine in conjunction with IMes, was prepared and isolated (**Figure 24**). Again, this synthesis was repeated until satisfactory yields were obtained (**Table 29**).

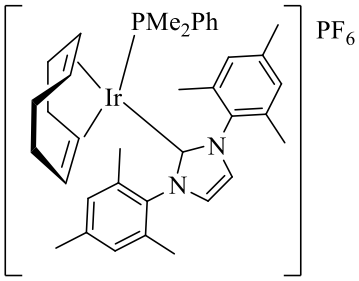

82

Figure 24

Run	Yield of **81** (%)
1	22
2	32
3	43
4	48
5	56

Table 29 - Preparation of complex **82** using reaction sequence of **Scheme 37**

3.2 Preparation of Substrates

With the required Ir(I) catalysts in hand, attention turned to the synthesis of a number of substrates which would be employed in the forthcoming isotopic labelling studies. Previous work within this area of research had included the labelling of a selection of amides, chosen to determine the effect of increasing alkyl substitution on the nitrogen atom.[34] As H-D exchange is possible within the *N*-methyl groups, as well as in the expected *ortho*-positions on the aromatic ring, it was proposed that the presence of an additional methyl group in the

para-position would enable a more accurate analysis of labelling levels with respect to the integration of the ^{1}H NMR spectrum. Thus, as shown in **Scheme 38**, *N*,*N*,4-trimethylbenzamide **111** was prepared from *p*-toluoyl chloride **110** and dimethylamine, and isolated in a high 99% yield.

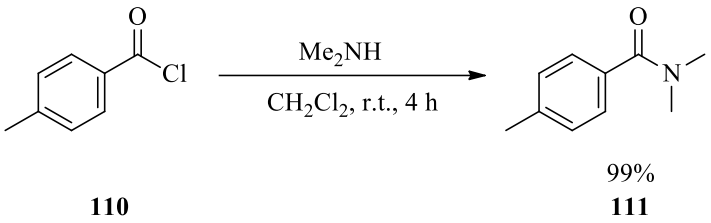

110 **111**

Scheme 38

The next substrate, *N*-ethyl-*N*,4-dimethylbenzamide **112** was prepared in a similar manner, from *p*-toluoyl chloride **110** and ethylmethylamine. Pleasingly, compound **112** was isolated in an excellent 98% yield (**Scheme 39**).

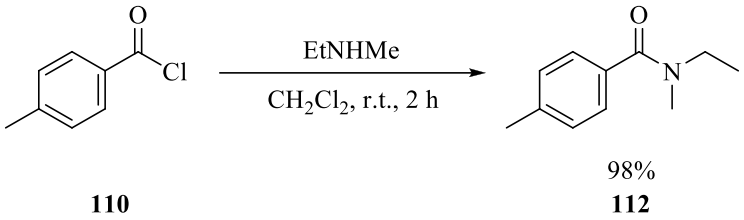

110 **112**

Scheme 39

The final substrate required for the HIE studies was *N*,*N*-diethyl-4-methylbenzamide **113**. Again, the reaction between *p*-toluoyl chloride **110** and diethylamine delivered compound **113** in a respectable 83% yield (**Scheme 40**).

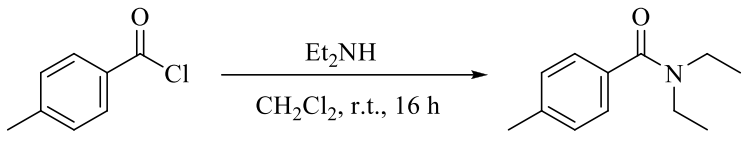

110 **113**

Scheme 40

3.3 Application of Iridium(I) Complexes in Hydrogen Isotope Exchange

Having successfully prepared the required Ir(I) complexes together with the necessary substrates, focus turned to the application of the catalysts in hydrogen isotope exchange reactions. To assess the performance of each complex, a number of test reactions were carried out, employing minimum catalyst loadings and reaction times, as had been determined by previous researchers within our laboratory.[35] Pleasingly, under these conditions, the excellent D incorporations expected with each complex were achieved (**Scheme 41**, **Table 30**).

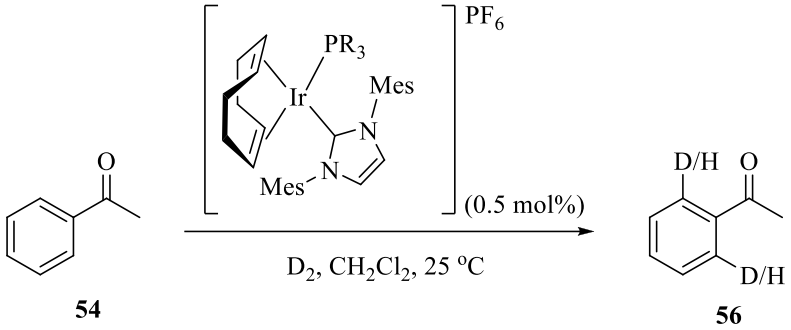

54 **56**

Scheme 41

Entry	Complex	Time (h)	% Deuteration	
			Run 1	Run 2
1	**75**	2	97	96
2	**81**	1	97	97
3	**82**	1.5	97	97

Table 30

3.3.1 Solvent Investigations

Satisfied with the performance of each of the prepared complexes in DCM, investigations began to identify alternative solvents in which hydrogen isotope exchange reactions could be performed efficiently. As mentioned previously, there exist certain requirements regarding the properties of different reaction media, namely environmental factors, as well as the ability to dissolve more polar substrates. Based on this, a number of solvents were examined ranging from non-polar toluene, to the significantly more polar acetone. The initial results obtained from this study, which involved the labelling of acetophenone by complex **75** under the standard deuteration conditions, are illustrated below (**Scheme 42**, **Table 31**).

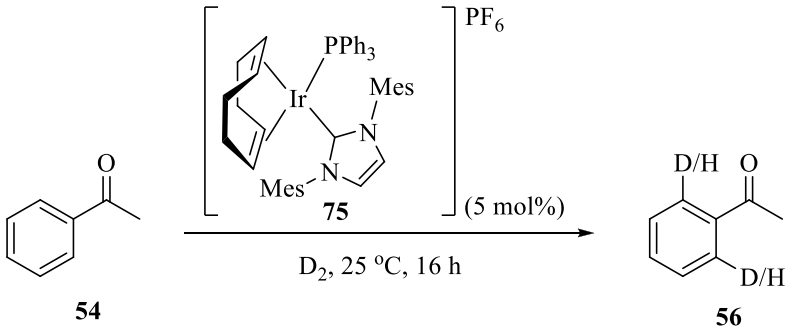

Scheme 42

Entry	Solvent	% Deuteration	
		Run 1	Run 2
1	Toluene	57	44
2	Et_2O	93	94
3	^tBuOMe	90	92
4	Acetone	41	45
5	THF	38	48
6	2-MeTHF	95	94

Table 31

Unfortunately, the first HIE reactions employing toluene as the solvent resulted in relatively low incorporations of approximately 50% (Entry 1). It is proposed that such reduced levels of D incorporation are due to the poor solubility of complex **75** in this non-polar solvent. In contrast, the results obtained with diethyl ether were significantly more encouraging (Entry 2), delivering levels of isotope exchange which are comparable to those achieved in DCM. Similar incorporations were attained in reactions utilising *tert*-butyl methyl ether (Entry 3). The use of acetone and THF as solvents produced only moderate degrees of deuteration, undoubtedly due to their strong coordinating natures. Indeed, previous work carried out within our laboratory has identified THF as a suitable poison for our Ir(I) complexes in the selective hydrogenation of alkynes.[55] In contrast, moving to 2-MeTHF had a positive effect; a slight increase in the steric bulk compared to THF is clearly sufficient to reduce the coordinating capabilities of the solvent molecule, enabling excellent levels of H-D exchange to occur.

3.3.1.1 DFT Studies

Importantly at this stage, and in attempts to provide further insight into the results described above, a series of DFT calculations were undertaken in collaboration with Dr Tell Tuttle and Dr Bhaskar Mondal at the University of Strathclyde, examining the binding energies associated with each solvent investigated. In accordance with the reaction mechanism of

hydrogen isotope exchange as proposed by Heys (**Scheme 11**, p.12),[20] it was postulated that the strength of binding between the free solvent molecule and the iridium centre would play a significant role in the reaction energetics, and may impede coordination of the incoming substrate. It should be noted from the outset that to reduce the cost of the computational experiments, the triphenylphosphine ligand present in complex **75** was replaced with the significantly smaller trimethylphosphine. Previous theoretical calculations carried out within this area of research had also successfully included the employment of the smaller phosphine ligand.[34] In these previous experiments it was observed that reactions performed using the smaller phosphine produced comparable values to those obtained in analogous calculations which employed the parent complex **75**.

As depicted in Heys' postulated reaction mechanism (**Scheme 11**, p.12), two solvent molecules are envisaged to bind to the coordinatively unsaturated Ir species formed following activation of the complex through the loss of d_4-cyclooctadiene.[20] Based on this assumption, the theoretical calculations performed involved analysis of structures in which the two solvent molecules approach the metal centre in the equatorial plane, opposite the positions occupied by the deuterium ligands. The optimised structures illustrating the binding of each of the different solvents are depicted in **Figure 25**.

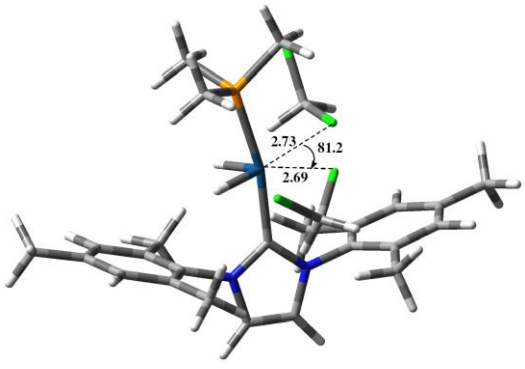

$Ir(D_2)(IMes)(PMe_3)(DCM)_2$

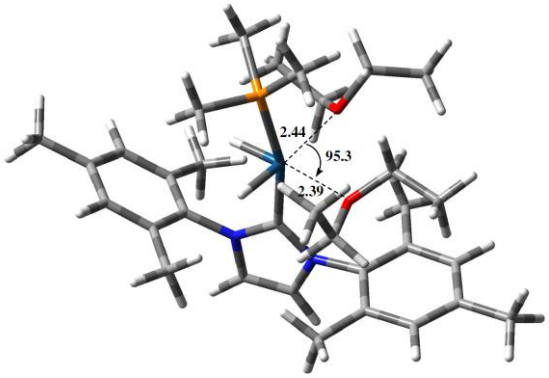

$Ir(D_2)(IMes)(PMe_3)(Et_2O)_2$

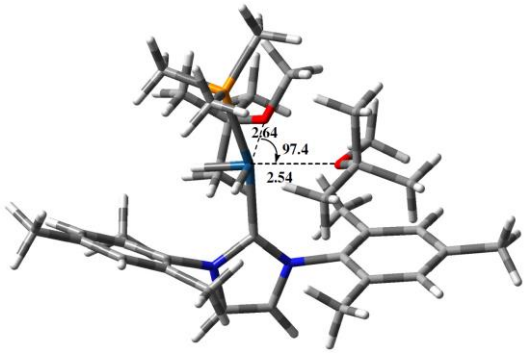

$Ir(D_2)(IMes)(PMe_3)(^tBuOMe)_2$

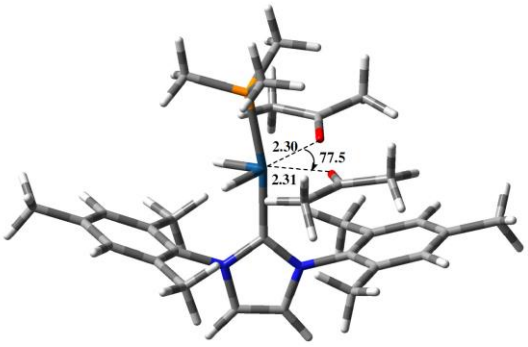

$Ir(D_2)(IMes)(PMe_3)(acetone)_2$

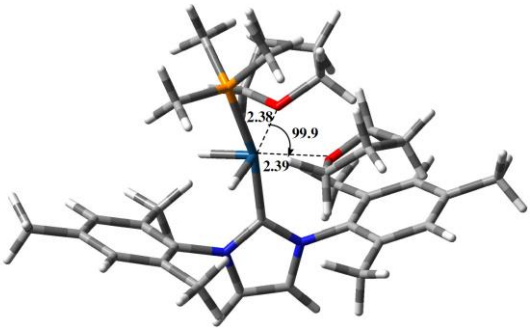

$Ir(D_2)(IMes)(PMe_3)(THF)_2$

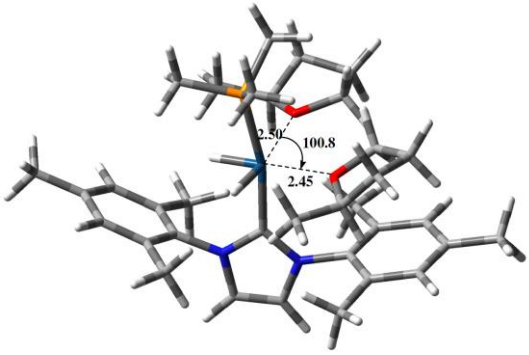

$Ir(D_2)(IMes)(PMe_3)(2\text{-}MeTHF)_2$

Figure 25 – Optimised structures for bi-solvent complexes computed using the M06 level of theory

As discussed previously, the moderate levels of deuteration attained in HIE reactions conducted in toluene were thought to be a result of the poor solubility of the Ir complex in this solvent, therefore the aromatic reaction medium was not included in the solvent binding energy calculations. The remaining five solvents described in this investigation were examined in the theoretical model in which the explicit binding energies were calculated for the above structures with respect to the solvent-free structures. As displayed in **Table 32**, the binding energies were calculated in the gas phase as well as in solution. The explicit solvent binding energies (ΔE) were calculated using the following equation:

$$Ir(D_2)(PMe_3)(IMes) + 2S \rightleftharpoons Ir(D_2)(PMe_3)(IMes)(S)_2$$

$$\Delta E = E[Ir(D_2)(PMe_3)(IMes)(S)_2] - E[Ir(D_2)(PMe_3)(IMes)] - 2E[S]$$

The effect of solvent polarisation was also determined, by treating each solvent-containing complex in the relevant reaction medium e.g. $Ir(D_2)(PMe_3)(IMes)(acetone)_2$ was treated in an acetone solvent environment. Due to the limitations of the program used, ^{t}BuOMe and 2-MeTHF could not be included in the solvation model. Having stated this, comparison of the results illustrated below does reveal a distinct trend in the values obtained, implying that no additional information would be gained from the presence of such additional solution phase figures.

Entry	Solvent	Complex	Binding Energy (kcal/mol)	
			Gas Phase	Solvent
1	DCM	$Ir(D)_2(IMes)(PMe_3)(DCM)_2$	-16.19	-11.46
2	Et_2O	$Ir(D)_2(IMes)(PMe_3)(Et_2O)_2$	-31.56	-26.97
3	^{t}BuOMe	$Ir(D)_2(IMes)(PMe_3)(^t BuOMe)_2$	-23.87	-
4	Acetone	$Ir(D)_2(IMes)(PMe_3)(acetone)_2$	-43.10	-35.72
5	THF	$Ir(D)_2(IMes)(PMe_3)(THF)_2$	-40.56	-34.61
6	2-MeTHF	$Ir(D)_2(IMes)(PMe_3)(2\text{-}MeTHF)_2$	-37.29	-

Table 32 – Binding energies of bi-solvated complexes, calculated using the equation shown previously (p.62)

From the results shown it can be concluded that, as expected, DCM molecules bind least strongly to the metal centre (Entry 1). Surprisingly, the most weakly coordinating of the ethereal reaction media was found to be ^{t}BuOMe (Entry 3), followed by Et_2O (Entry 2), 2-MeTHF (Entry 6) and finally THF (Entry 5). The most strongly bound solvent was identified as acetone (Entry 4). While the difference between the binding energies of acetone (and THF) and 2-MeTHF does not align with the large difference between the levels of H-D exchange observed in reactions performed in each of these solvents, it should be noted that a

broad correlation exists between the current theoretical findings and our previous experimental results. It is therefore proposed that the relationship between solvent binding strength and the degree of isotopic labelling observed does not progress in a linear fashion, but may in fact reach an upper limit at which point solvent coordination impedes subsequent catalysis.

As well as examining the strength of binding between the individual solvent molecules and the iridium centre, the influence imparted by each solvent on the coordination of the substrate was investigated. Such a process results in the replacement of one solvent molecule, hence comparison of the binding energies of the substrate to the mono-solvent complex would reveal which systems are stabilised to the greatest degree as a result of this substitution. Based on all of this, the binding energies of acetophenone to the solvent-bound Ir complexes are displayed in **Table 33**.

Entry	Solvent	Complex	Binding Energy (kcal/mol)	
			Gas Phase	Solvent
1	DCM	$Ir(D)_2(IMes)(PMe_3)(DCM)(PhCOMe)$	-14.03	-10.31
2	Et_2O	$Ir(D)_2(IMes)(PMe_3)(Et_2O)(PhCOMe)$	-6.35	-4.58
3	^tBuOMe	$Ir(D)_2(IMes)(PMe_3)(^tBuOMe)(PhCOMe)$	-11.85	-
4	Acetone	$Ir(D)_2(IMes)(PMe_3)(acetone)(PhCOMe)$	0.74	2.47
5	THF	$Ir(D)_2(IMes)(PMe_3)(THF)(PhCOMe)$	-2.13	-0.27
6	2-MeTHF	$Ir(D)_2(IMes)(PMe_3)(2\text{-}MeTHF)\ (PhCOMe)$	-4.30	-

Table 33 – Calculated binding energies for mono-solvated complexes containing one substrate ligand

Comparison of the values displayed above reveal that the binding energy of acetophenone to the solvent-bound Ir complexes follows the reverse order to that observed previously in the

solvent binding energy calculations. More specifically, the system stabilised to the greatest degree by replacement of a solvent molecule with one of a substrate is that containing DCM (Entry 1), followed relatively closely by ^{t}BuOMe (Entry 3), then Et_2O (Entry 2). A difference of approximately 2 kcal/mol was calculated in the binding of acetophenone to complexes including THF and 2-MeTHF, with the latter system displaying a lower energy of -4.30 kcal/mol (Entries 5 and 6). Unsurprisingly, the complex containing the most strongly coordinating solvent, acetone, is actually destabilised upon replacement of a solvent molecule with one of acetophenone (Entry 4). Such a value indicates a clear preference for the solvent molecule to remain bound to the metal centre rather than its substitution by a substrate, resulting in low levels of isotope incorporation in HIE reactions performed in this reaction medium. Once again, the order of stabilisation of complexes in which a solvent molecule is replaced by one of a substrate broadly correlates with that revealed by our practical experimental results. It should therefore be reiterated that the binding strengths of solvent molecules such as THF and acetone may lie outwith the acceptable range of values which are deemed favourable for the process of hydrogen isotope exchange to proceed without incident.

Based on the results obtained thus far, three of the solvents examined were selected for further investigation. Due to the poor results obtained with toluene, acetone, and THF, focus on these reaction media was abandoned, leaving diethyl ether, *tert*-butyl methyl ether and 2-methyltetrahydrofuran as potential replacements of DCM. It should be noted at this point that, as with every organic solvent, limitations do exist with the three reaction media chosen for the following studies. Having stated this, such limitations are deemed to be less significant than those associated with DCM. Indeed, two of the world's largest pharmaceutical companies, GlaxoSmithKline and Pfizer, have termed ^{t}BuOMe and 2-MeTHF as "usable solvents", in comparison to the "undesirable" classification given to DCM.[38,56] In addition, 2-MeTHF has been highlighted as a potential replacement of DCM in other areas of chemistry due to its high polarity but low miscibility with water.[57]

As discussed earlier, previous work within our laboratory has illustrated the remarkable catalytic activity of our iridium(I) complexes.[35] Under the current conditions employing DCM as the solvent, excellent levels of D incorporation are achieved using catalyst loadings

as low as 0.5 mol%, and short reaction times of between 1 and 2 hours. The next logical step in our current investigations was, therefore, to determine if such an efficient catalytic procedure could be retained in systems utilising alternative solvents.

3.3.2 Rate and Activity Studies

The first solvent to be examined further was diethyl ether. Initial investigations commenced with a time study employing the simple substrate acetophenone **54**, and 5 mol% of [Ir(COD)(PBn_3)(IMes)]PF_6, complex **81** (**Scheme 43**). As shown in **Table 34**, shortening the reaction time from 16 hours to 1 hour had no detrimental effect on the extent of D incorporation obtained (Entries 1 and 3). When the reaction time was further reduced to 30 minutes however, only a moderate level of isotope labelling was observed (Entry 4).

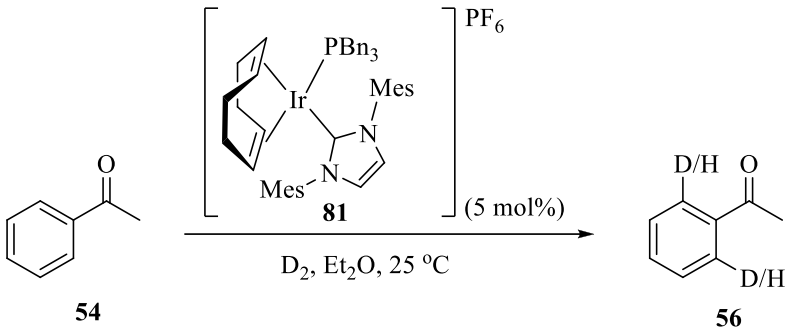

Scheme 43

Entry	Time (h)	% Deuteration	
		Run 1	Run 2
1	16	93	94
2	2	96	95
3	1	94	92
4	0.5	63	65

Table 34

Having established the optimum reaction time for the labelling of acetophenone **54** with complex **81**, attention turned to the amount of catalyst required (**Scheme 44**, **Table 35**). Pleasingly, excellent levels of isotope incorporation were maintained when the catalyst loading was reduced from 5 mol% to 3 mol% (Entry 1). However, decreasing the quantity of complex **81** further to 1 mol% resulted in only moderate levels of labelling of around 70% D (Entry 2).

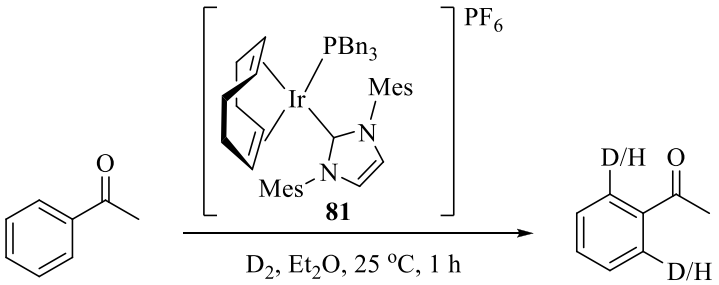

54 **56**

Scheme 44

Entry	Catalyst Loading (mol%)	% Deuteration	
		Run 1	Run 2
1	3	96	97
2	1	72	67

Table 35

With the optimum conditions in hand for the use of complex **81** in HIE reactions performed in Et_2O, focus turned to systems employing complex **75**, $[Ir(COD)(PPh_3)(IMes)]PF_6$, in the same solvent. As before, investigations began with a time study, utilising 5 mol% of the catalyst (**Scheme 45**). Once again, the initial results were extremely encouraging as the level of isotope exchange achieved after 1 hour was equivalent to that observed after a much longer reaction time of 16 hours (**Table 36**, Entries 1 and 3). Although decreasing the reaction period further to 30 minutes did result in a slight reduction in labelling, the extent of

deuteration attained remained at a good level, with the isotopically-enriched product delivered in a good 84% D loading (Entry 4).

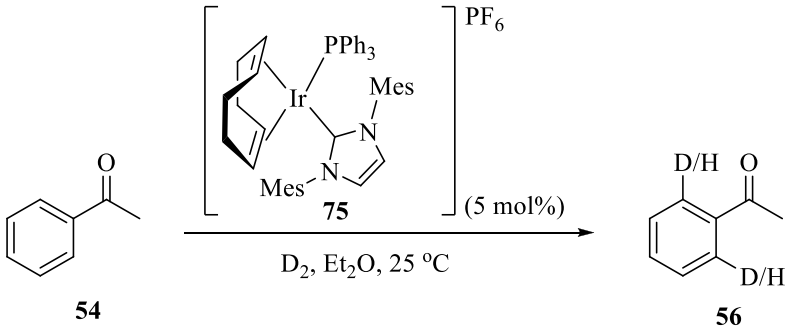

54 56

Scheme 45

Entry	Time (h)	% Deuteration	
		Run 1	Run 2
1	16	93	94
2	2	94	94
3	1	94	93
4	0.5	84	84

Table 36

Further studies regarding the use of complex **75** in Et_2O centred on the quantity of catalyst required in the labelling reactions. Employing a catalyst loading of 3 mol% over 1 hour resulted in a somewhat lower level of H-D exchange, with up to a moderate 77% deuteration being obtained (**Table 37**, Entry 1). Pleasingly, extending the reaction time to 2 hours proved extremely advantageous, increasing the levels of labelling achieved to an excellent 92% (Entry 2).

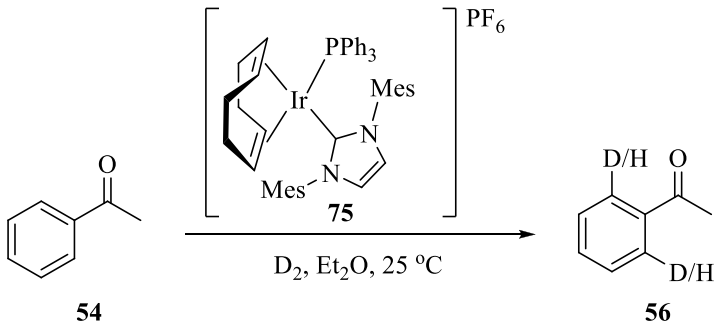

Scheme 46

Entry	Catalyst Loading (mol%)	Time (h)	% Deuteration	
			Run 1	Run 2
1	3	1	77	72
2	3	2	92	90

Table 37

The final complex to be investigated in isotope labelling experiments performed in Et_2O was [Ir(COD)(PMe_2Ph)(IMes)]PF_6 **82** (**Scheme 47**). As shown below in **Table 38**, optimisation of the reaction time revealed that excellent deuterium incorporation could be achieved in reactions run for periods as short as 30 minutes (Entry 4).

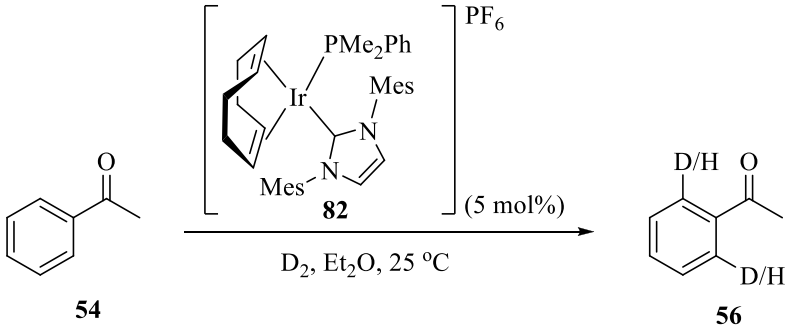

Scheme 47

Entry	Time (h)	% Deuteration	
		Run 1	Run 2
1	16	94	95
2	2	97	96
3	1	96	96
4	0.5	98	97

Table 38

The next step in the optimisation process involved examining the amount of complex **82** required to afford acceptable levels of isotopic labelling over the selected 30 minute reaction time. As shown below (**Scheme 48**, **Table 39**), a short catalyst loading study revealed that a reduced level of 3 mol% of complex **82** was sufficient to deliver an excellent 98% incorporation (Entry 1). Decreasing the catalyst loading further to 1 mol% proved to be unfavourable however, resulting in a relatively low deuteration level of 34% (Entry 2). Having stated this, increasing the reaction time to 1 hour at this low catalyst loading delivered the isotopically-enriched product in a maximum of 88% D incorporation. To further promote the degree of labelling at this pleasingly low catalyst loading, the reaction time was extended to 2 hours, furnishing compound **56** with an excellent deuterium loading of 96% (Entry 4).

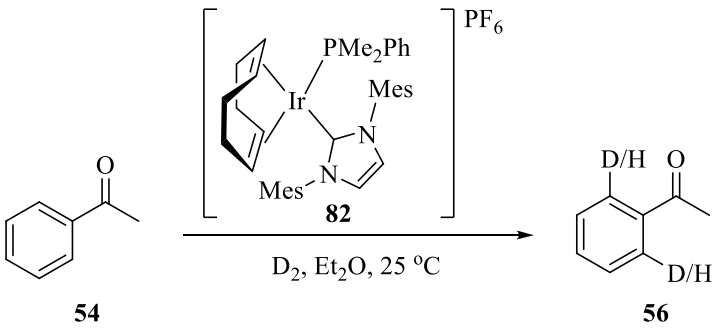

Scheme 48

Entry	Catalyst Loading (mol%)	Time (h)	% Deuteration	
			Run 1	Run 2
1	3	0.5	98	92
2	1	0.5	34	34
3	1	1	80	88
4	1	2	96	90

Table 39

The next solvent to be examined in this area of research was ^{t}BuOMe. In a manner analogous to studies performed in Et_2O, the first catalyst to be examined was complex **81**, operating at a catalyst loading of 5 mol% over different reaction times (**Scheme 49**, **Table 40**). Reducing the reaction period from 16 hours to 2 hours did not result in any decrease in the level of labelling observed, however a reduction in D incorporation to approximately 58% was detected in reactions run for 1 hour (Entry 3).

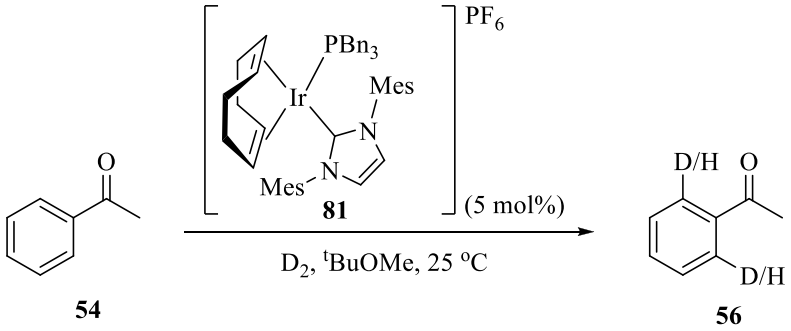

Scheme 49

Entry	Time (h)	% Deuteration	
		Run 1	Run 2
1	16	92	97
2	2	94	90
3	1	63	52

Table 40

In an attempt to lower the amount of catalyst required in HIE reactions performed in ^{t}BuOMe, a short catalyst loading study was undertaken. As the results in **Table 41** illustrate, reducing the quantity of complex present to 3 mol% delivered the isotopically-enriched product **56** in up to a good 87% deuteration (Entry 1). However, extending the reaction time further to 3 hours offered no significant improvement, with a maximum of 90% D loading achieved. In view of these findings, the optimum conditions for the use of complex **81** in ^{t}BuOMe were selected as a catalyst loading of 5 mol% and a reaction time of 2 hours (**Table 40**, Entry 2).

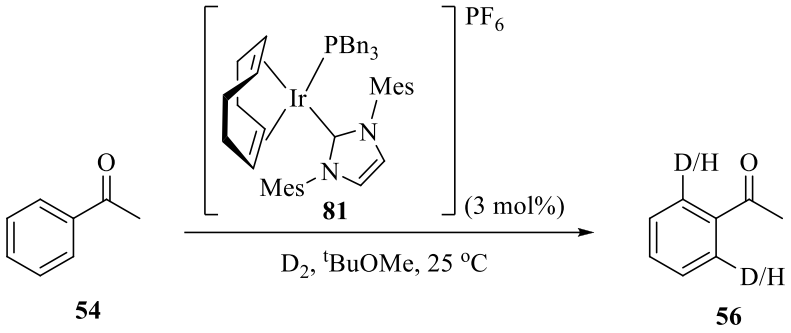

Scheme 50

Entry	Time (h)	% Deuteration	
		Run 1	Run 2
1	2	79	87
2	3	90	85

Table 41

Efforts to further probe the potential use of ^{t}BuOMe as a replacement for DCM involved a time study utilising complex **75** (**Scheme 51**, **Table 42**). As had been observed in earlier reactions employing complex **81**, reactions run for periods shorter than 2 hours delivered only moderate levels of between 55 and 78% D incorporation (Entries 3 and 4).

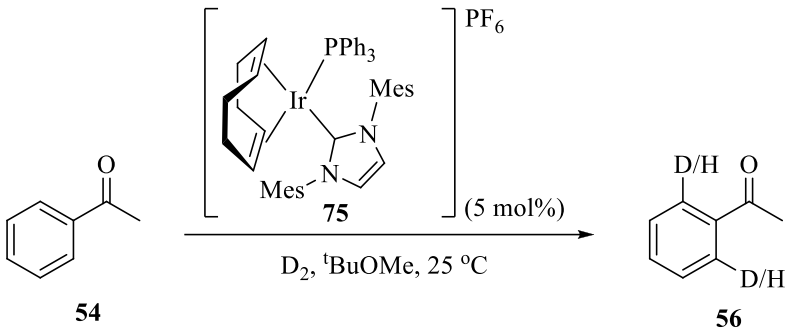

Scheme 51

Entry	Time (h)	% Deuteration	
		Run 1	Run 2
1	16	90	92
2	2	89	91
3	1	78	76
4	0.5	63	55

Table 42

Unfortunately, the high levels of isotope labelling achieved with 5 mol% of complex **75** over 2 hours were not maintained in reactions employing a reduced catalyst loading of 3 mol%, furnishing compound **56** only in up to a 75% deuteration (**Scheme 52**, **Table 43**). As determined previously, the optimum conditions for the use of complex **81** in ^{t}BuOMe employ a catalyst loading of 5 mol%, and a reaction time of 2 hours. Complex **75** is known to react at a rate slightly lower than that of its tribenzylphosphine analogue.[35] It was proposed that to obtain an acceptable degree of labelling, the use of a reduced catalyst loading would require a much extended reaction time. Therefore, the most favourable system for H-D exchange with complex **75** in ^{t}BuOMe was determined to employ identical conditions as those found for complex **81** (5 mol% catalyst loading over a 2 hour reaction time).

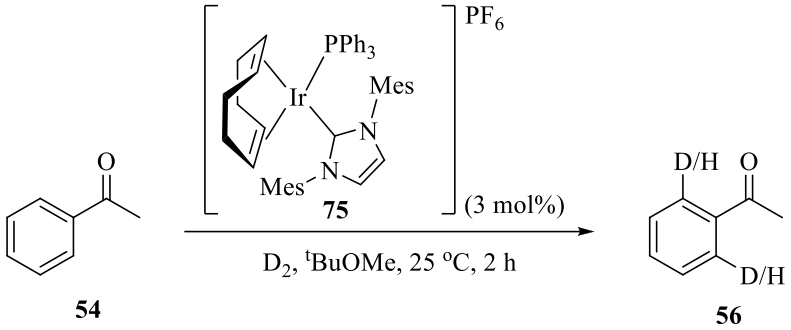

Scheme 52

Entry	% Deuteration	
	Run 1	Run 2
1	66	75

Table 43

Following completion of the studies for both complexes **81** and **75** in ^{t}BuOMe, attention turned to the use of complex **82** in the same reaction medium. In a manner similar to previous investigations carried out, efforts began with a short time study (**Scheme 53**).

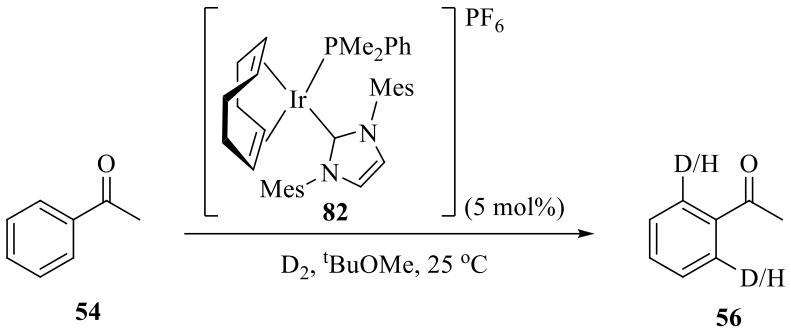

Scheme 53

Entry	Time (h)	% Deuteration	
		Run 1	Run 2
1	16	90	88
2	2	93	86
3	1	96	94
4	0.5	80	76

Table 44

As shown above in **Table 44**, excellent levels of deuterium incorporation were achieved after as little time as 1 hour (Entry 3). Although extremely pleasing, this result was based on a catalyst loading of 5 mol%. It was therefore envisaged that such high levels of labelling could be retained using lowered amounts of complex **82**. Indeed, it was found that employing a reduced catalyst loading of 3 mol% resulted in levels of H-D exchange equivalent to those obtained at the slightly higher loading of 5 mol% (**Table 45**, Entry 1). Unfortunately, attempts to further decrease the quantity of catalyst required in this system were unsuccessful; the labelling of **54** with only 1 mol% of complex **82** yielding up to a moderate 72% incorporation (Entry 2).

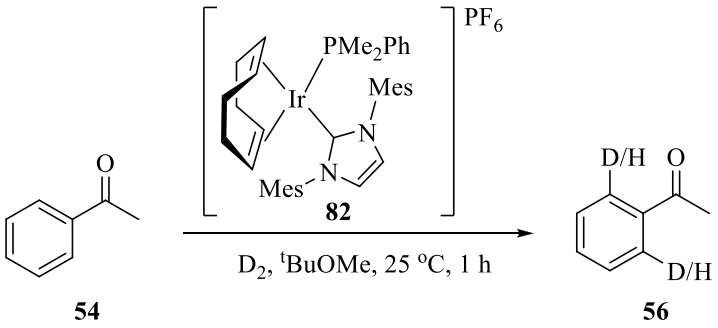

Scheme 54

Entry	Catalyst Loading (mol%)	% Deuteration	
		Run 1	Run 2
1	3	94	86
2	1	68	72

Table 45

The final solvent to be further investigated as a suitable replacement for DCM in HIE reactions was 2-MeTHF. From the outset, extremely encouraging results were obtained; a time study using 5 mol% of complex **81** revealed that the reaction had essentially reached completion after only 30 minutes (**Scheme 55**, **Table 46**).

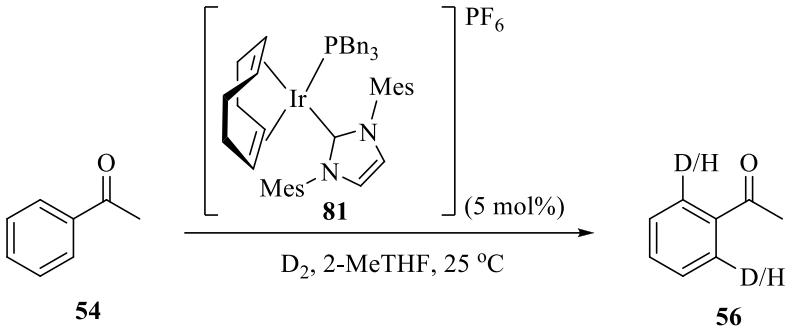

Scheme 55

Entry	Time (h)	% Deuteration	
		Run 1	Run 2
1	16	97	92
2	2	97	95
3	1	95	92
4	0.5	94	91

Table 46

The reactivity of complex **81** in 2-MeTHF was further examined by means of a catalyst loading study. As shown in **Table 47**, a significant decrease in deuterium incorporation was

observed in systems run for the selected 30 minute reaction period in the presence of 3 mol% of the Ir(I) catalyst. As extending the reaction time had been advantageous in previous investigations, it was proposed that a similar effect could be produced here. Indeed, performing the reaction for a slightly longer time of 1 hour proved to be highly successful; the use of the lower 3 mol% catalyst loading and short reaction time delivered an excellent 96% deuteration (Entry 2).

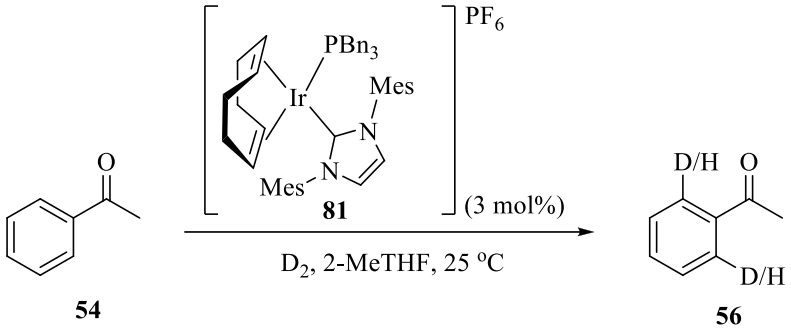

Scheme 56

Entry	Time (h)	% Deuteration	
		Run 1	Run 2
1	0.5	55	59
2	1	96	90

Table 47

With the optimum conditions for the use of complex **81** in 2-MeTHF in hand, focus turned to the employment of complex **75** in the same solvent (**Scheme 57**, **Table 48**). As previous results had shown complex **75** to display a slight decrease in reactivity in comparison to complex **81**, from the results shown in **Table 48** an optimum reaction time of 2 hours was selected for use in further investigations.

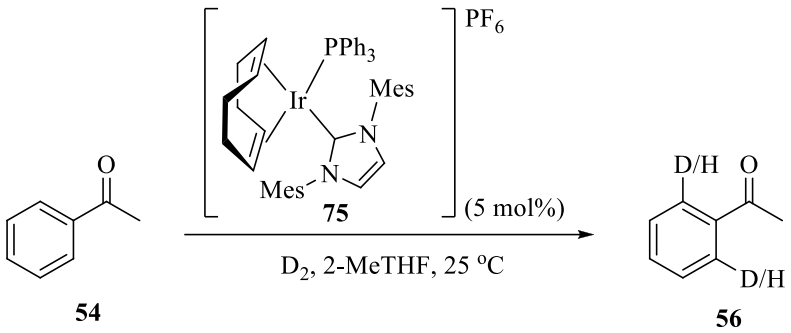

Scheme 57

Entry	Time (h)	% Deuteration	
		Run 1	Run 2
1	16	95	94
2	2	97	96
3	1	91	94
4	0.5	76	63

Table 48

Based on these outcomes, a catalyst loading study was initiated (**Scheme 58**). As displayed in **Table 49**, excellent levels of incorporation were retained when the amount of complex **75** employed in the reaction was decreased to 3 mol% (Entry 1). Perhaps unsurprisingly, reducing the catalyst loading further to 1 mol% resulted in only poor levels of labelling (Entry 2).

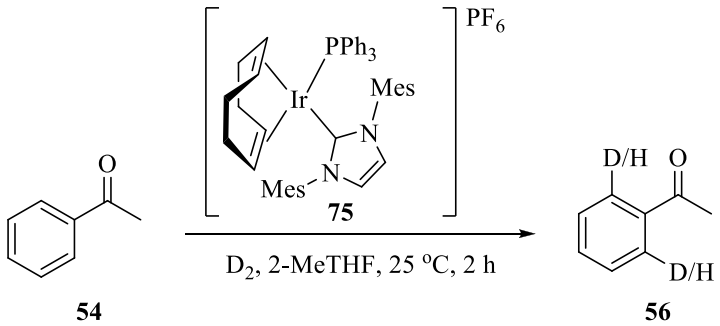

Scheme 58

Entry	Catalyst Loading (mol%)	% Deuteration	
		Run 1	Run 2
1	3	95	88
2	1	26	20

Table 49

The final investigations to be carried out regarding the labelling of acetophenone **54** in alternative reaction media involved the use of complex **82** in 2-MeTHF. Once again, explorations were instigated with a reaction time study (**Scheme 59**).

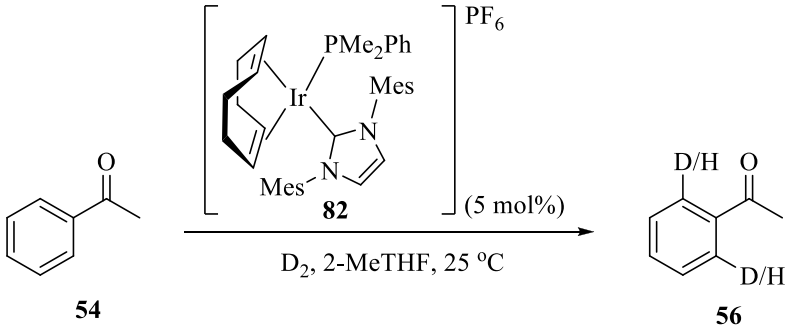

Scheme 59

Entry	Time (h)	% Deuteration	
		Run 1	Run 2
1	16	98	98
2	1	96	98
3	0.5	96	90

Table 50

As the results above in **Table 50** illustrate, excellent incorporations were achieved after only 30 minutes (Entry 3). As such high labelling was attained after an extremely short period of time, it was anticipated that the amount of catalyst employed in the reaction could be reduced, without causing a substantial decrease in the overall efficiency of the system. A brief catalyst loading study was therefore carried out (**Scheme 60**).

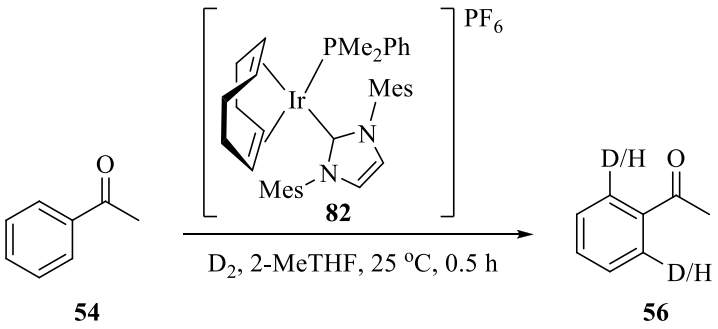

Scheme 60

Entry	Catalyst Loading (mol%)	% Deuteration	
		Run 1	Run 2
1	3	98	95
2	1	33	37

Table 51

Pleasingly, such high degrees of H-D exchange were retained upon lowering the catalyst loading to 3 mol% (**Table 51**, Entry 1). In an attempt to optimize the conditions further, the reaction was performed with just 1 mol% of complex **82**, however a significant deterioration in the degree of deuteration to just 37% was detected (Entry 2).

The results obtained to this point were extremely encouraging, demonstrating the high activity of our iridium(I) complexes in hydrogen isotope exchange reactions performed in reaction media deemed significantly more industrially acceptable than DCM. In the majority of instances, excellent levels of deuterium incorporation can be achieved in systems which employ low catalyst loadings (in some cases as low as 1 mol%), and short reaction times of between 30 minutes and 2 hours. In this regard, the optimised protocols for use with the acetophenone test substrate are shown in **Table 52**. Indeed, the relative ordering of reactivity of each solvent broadly aligns with that observed previously in our initial test reactions with acetophenone in various solvents (**Table 30**).

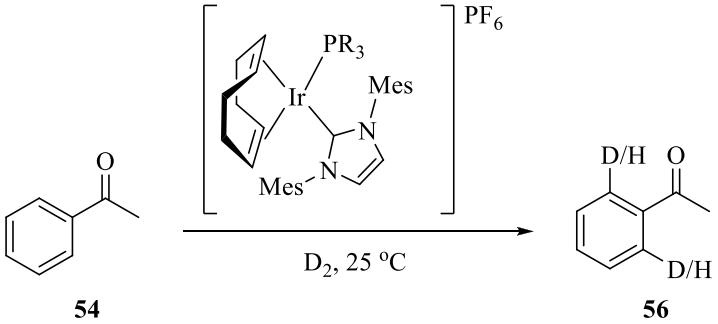

54 **56**

Scheme 61

Solvent	PR_3	Catalyst Loading (mol%)	Time (h)	% Deuteration
Et_2O	PBn_3	3	1	97
	PPh_3	3	2	92
	PMe_2Ph	1	2	96
^tBuOMe	PBn_3	5	2	94
	PPh_3	5	2	91
	PMe_2Ph	3	1	94
2-MeTHF	PBn_3	3	1	96
	PPh_3	3	2	95
	PMe_2Ph	3	0.5	98

Table 52

In order to establish the efficiency of these newly developed optimum conditions employing Ir(I) complexes in solvents identified as suitable replacements for DCM, labelling reactions involving different substrates were performed. The first compound examined was benzophenone **57** which, in a manner similar to acetophenone, is labelled *via* a 5-mmi. However, in this instance, there are four possible sites of labelling as opposed to two. Previous results obtained within our research group revealed that in reactions employing this substrate in DCM, at a catalyst loading of 5 mol% and a reaction time of 16 hours, isotope incorporations of 95% are attainable with each of our routinely used Ir(I) complexes.[35] The recently identified conditions for the use of complexes **75**, **81** and **82** in Et_2O were therefore applied to the labelling of benzophenone **57** (**Scheme 62**). As the results in **Table 53**

illustrate, high to excellent levels of H-D exchange were obtained with each catalyst. Of particular success was the extent of labelling achieved with complex **82**, delivering levels of isotope incorporation comparable to those attained in DCM, but at a significantly lower catalyst loading and over a shorter reaction time (Entry 3).

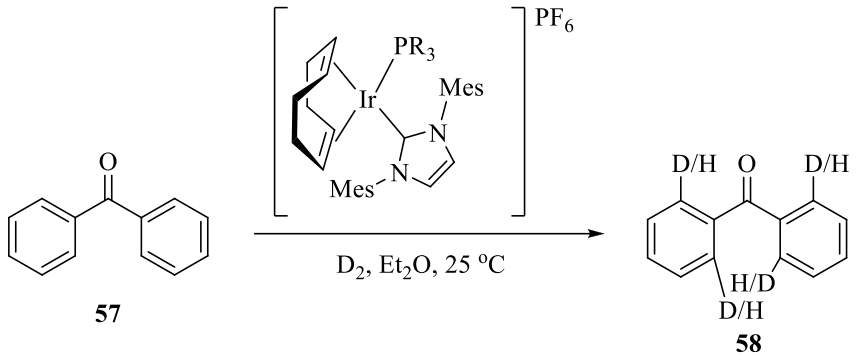

57 **58**

Scheme 62

Entry	Complex	PR_3	Catalyst Loading (mol%)	Time (h)	% Deuteration	
					Run 1	Run 2
1	**81**	PBn_3	3	1	83	76
2	**75**	PPh_3	3	2	87	85
3	**82**	PMe_2Ph	1	2	94	94

Table 53

The labelling of substrate **57** was also carried out in ^{t}BuOMe (**Scheme 63**). Of the three solvents identified as suitable replacements for DCM, ^{t}BuOMe was revealed to require slightly higher catalyst loadings and longer reaction times to promote HIE to the same degree as that obtainable in Et_2O and 2-MeTHF. Even at these elevated levels, only moderate to good deuteration efficiencies were observed in the labelling of benzophenone **57** (**Table 54**, Entries 1, 2 and 3). Accordingly, it was proposed that the moderate levels of incorporation detected in the reaction employing complex **82** may be a result of the lower quantity of catalyst present in this system. In an attempt to promote the labelling of substrate **57** by complex **82** further, the reaction was repeated utilising a higher catalyst loading of 5 mol% and an extended reaction time of 16 hours. Pleasingly, the degree of H-D exchange observed

was somewhat improved, delivering compound **58** with up to a high 92% deuterium loading (Entry 4).

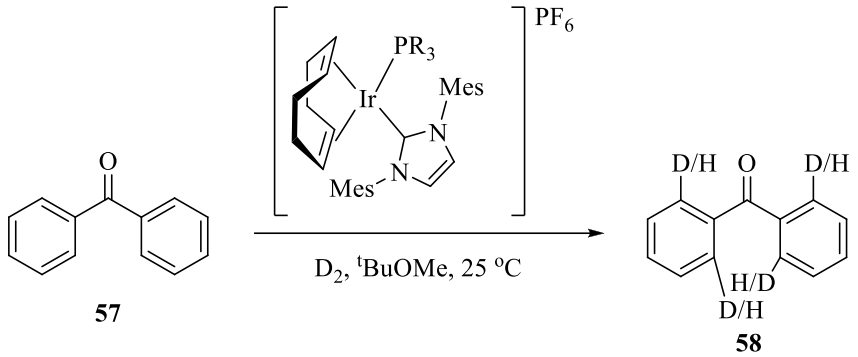

57 **58**

Scheme 63

Entry	Complex	PR_3	Catalyst Loading (mol%)	Time (h)	% Deuteration	
					Run 1	Run 2
1	**81**	PBn_3	5	2	68	66
2	**75**	PPh_3	5	2	72	81
3	**82**	PMe_2Ph	3	1	72	68
4	**82**	PMe_2Ph	5	16	92	88

Table 54

Investigations into the labelling of benzophenone **57** in alternative solvents to DCM were completed by examining the extent of isotope incorporation which could be achieved in reactions performed in 2-MeTHF (**Scheme 64**). Once again, moderate levels of deuteration were obtained in systems facilitated by complexes **81** and **75** (**Table 55**, Entries 1 and 2). In contrast, the shorter reaction time employed in reactions catalysed by complex **82** did not hinder the exchange process, delivering the desired compound **58** with a high D loading of 89% (Entry 3).

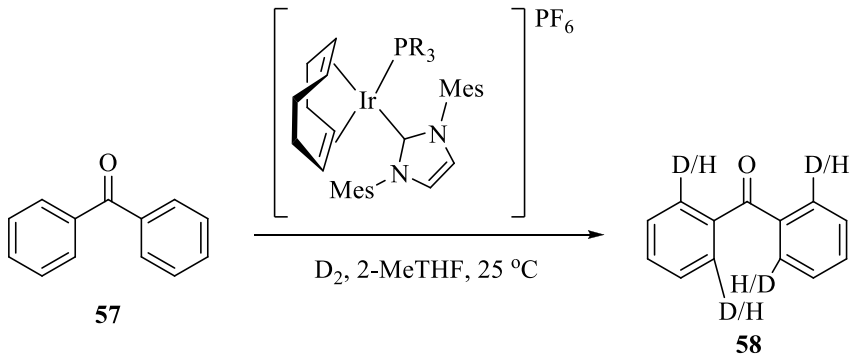

57 **58**

Scheme 64

Entry	Complex	PR_3	Catalyst Loading (mol%)	Time (h)	% Deuteration	
					Run 1	Run 2
1	**81**	PBn_3	3	1	76	73
2	**75**	PPh_3	3	2	70	72
3	**82**	PMe_2Ph	3	0.5	87	89

Table 55

Pleased with the results obtained for the labelling of benzophenone by each complex in Et_2O, ^tBuOMe and 2-MeTHF, attention turned to the next substrate to be examined in this programme, 2-phenylpyridine **41**. Previous work carried out within this field of study had shown that under the standard reaction conditions employing a 5 mol% catalyst loading and 16 hour reaction time in DCM, compound **41** could be isotopically labelled by complexes **75** and **82** to excellent levels of up to 98%.[35] However, the extent of deuteration delivered by complex **81** under the same reaction conditions was significantly lower, at only 38%. Upon repeating such an experiment it was discovered that the reliability of the original result was in question, and excellent levels of deuteration were indeed achievable under these conditions in DCM (**Scheme 65**).

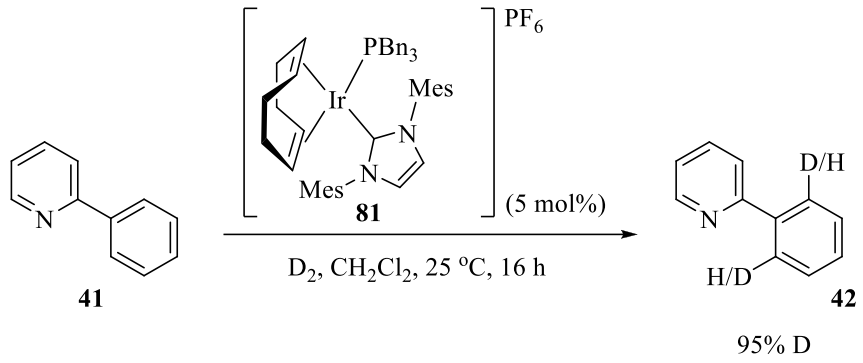

Scheme 65

Following from this fortunate discovery, focus returned to the application of Ir(I) catalysts in HIE reactions performed in alternative solvents. Initial results employing complexes **81** and **75** in Et_2O were extremely encouraging, furnishing results comparable to those obtained in DCM (**Table 56**, Entries 1 and 2). In contrast, under the optimum conditions developed, compound **41** was only labelled to a moderate 53% level of deuteration by complex **82**. It was suspected that these reduced levels of isotope incorporation were a result of the lower catalyst loading employed in the system. The liberated binding enthalpy for substrate **41** to the metal centre is known to be lower than that for other compounds investigated in this study (ΔH_{bind} for **41** = -7.9 kcal/mol at 298 K vs ΔH_{bind} for **54** = -11.3 kcal/mol at 298 K).[34] Therefore, with less catalyst present in the reaction, the probability of substrate **41** binding to the iridium compared with that of solvent coordination would be diminished. In an attempt to promote the levels of isotopic exchange, the reaction was repeated using a higher catalyst loading of 5 mol % and an extended reaction time of 16 hours. Unfortunately, no increase in the level of deuteration was observed (Entry 4).

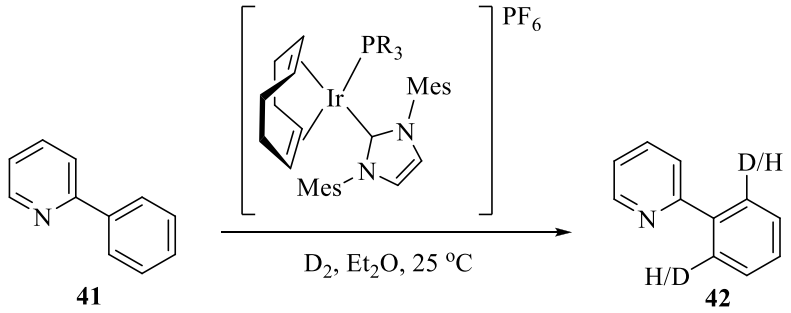

Scheme 66

Entry	Complex	PR_3	Catalyst Loading (mol%)	Time (h)	% Deuteration	
					Run 1	Run 2
1	**81**	PBn_3	3	1	96	95
2	**75**	PPh_3	3	2	96	94
3	**82**	PMe_2Ph	1	2	52	53
4	**82**	PMe_2Ph	5	16	55	57

Table 56

Results of a similar ilk were obtained in reactions performed in ^{t}BuOMe (**Scheme 67**, **Table 57**). Under the optimum conditions, H-D exchange in substrate **41** catalysed by complexes **81** and **75** proceeded to excellent levels of up to 97% D incorporation (Entries 1 and 2). The lower catalyst loading employed in reactions facilitated by complex **82** was found to impede deuteration of compound **41** however, delivering the desired product with a maximum of 10% D loading. Pleasingly, repeating this reaction with a higher quantity of complex **82** and an extended reaction time furnished isotope incorporations equivalent to those achieved with complexes **81** and **75** (Entry 4).

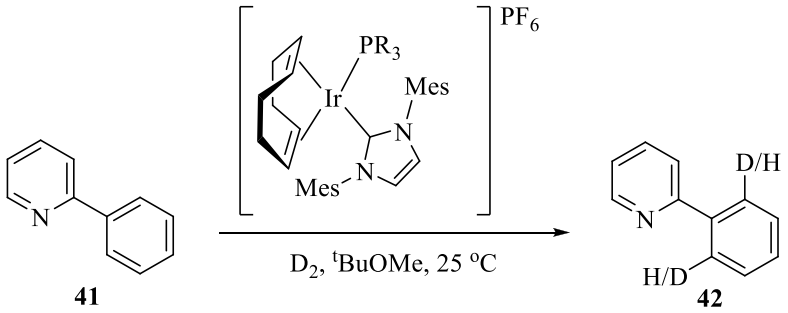

41 **42**

Scheme 67

Entry	Complex	PR_3	Catalyst Loading (mol%)	Time (h)	% Deuteration	
					Run 1	Run 2
1	**81**	PBn_3	5	2	97	92
2	**75**	PPh_3	5	2	91	90
3	**82**	PMe_2Ph	3	1	10	7
4	**82**	PMe_2Ph	5	16	95	93

Table 57

The labelling of substrate **41** by complexes **75**, **81** and **82** was also investigated in the third solvent utilised within this study, 2-MeTHF (**Scheme 68**). Once again, appreciably high levels of D incorporation were observed in the presence of complexes **81** and **75** (**Table 58**, Entries 1 and 2), while those detected in reactions catalysed by complex **82** led to only poor levels of H-D exchange of 5% (Entry 3). As increasing the catalyst loading and reaction time had proved favourable in previous instances, such conditions were applied to the deuteration of substrate **41** by complex **82**. Unfortunately, a significant enhancement in the degree of exchange was not attained, increasing the levels of D loading only to a maximum of 32% (Entry 4).

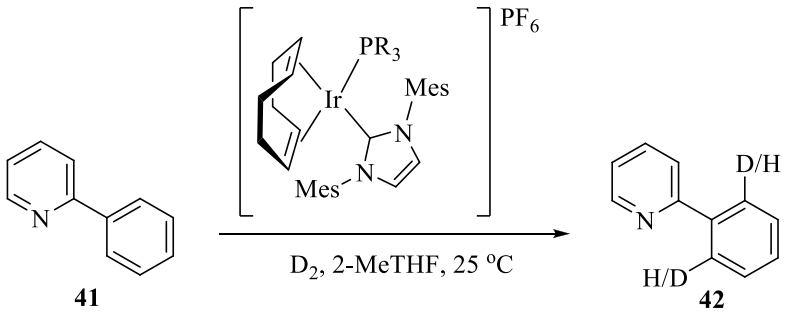

41 **42**

Scheme 68

Entry	Complex	PR_3	Catalyst Loading (mol%)	Time (h)	% Deuteration	
					Run 1	Run 2
1	**81**	PBn_3	3	1	88	96
2	**75**	PPh_3	3	2	91	97
3	**82**	PMe_2Ph	3	0.5	5	5
4	**82**	PMe_2Ph	5	16	32	24

Table 58

Of the three catalysts employed in this study, complex **82** contains the most electron-donating phosphine,[36] therefore the iridium core will possess more electron density in comparison with the centres of complexes **81** and **75**. As mentioned, 2-phenylpyridine **41** has a lower liberated binding enthalpy to the metal. In addition, this substrate is a relatively electron-deficient heterocycle, hence donation of electron density by compound **41** into the partially satisfied iridium core of complex **82** may be less effective. It may, therefore, be unsurprising that

lower levels of H-D exchange are observed in reactions facilitated by complex **82,** in contrast to the appreciably high degrees of isotope incorporation achieved in reactions catalysed by complexes **81** and **75**.

The next substrate to be examined in HIE reactions performed in alternative solvents was another heterocycle, *N*-phenylpyrazole **79**. In an analogous manner to previous investigations, the first reaction medium examined was Et_2O (**Scheme 69**). The results obtained under the optimum conditions developed for complexes **81** and **75** were extremely pleasing, delivering the desired product **80** with deuterium incorporations in the region of 95% (**Table 59**, Entries 1 and 2). The degree of deuteration achieved in reactions facilitated by complex **82** were slightly lower at approximately 70% (Entry 3), however this outcome is, again, likely to be a result of the lower quantity of catalyst present in the reaction.

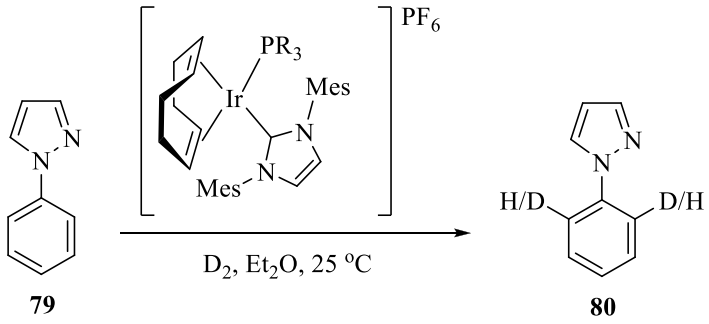

79 **80**

Scheme 69

Entry	Complex	PR_3	Catalyst Loading (mol%)	Time (h)	% Deuteration	
					Run 1	Run 2
1	**81**	PBn_3	3	1	94	92
2	**75**	PPh_3	3	2	95	94
3	**82**	PMe_2Ph	1	2	72	68

Table 59

In contrast to the results obtained in Et_2O, the highest levels of isotopic labelling detected in ^{t}BuOMe were achieved in reactions employing complex **82** (**Scheme 70**, **Table 60**). In this instance, a slight decrease in the steric bulk imparted by the phosphine ligand may be

advantageous, increasing accessibility of the substrate to the metal centre in the presence of the relatively large solvent molecules.

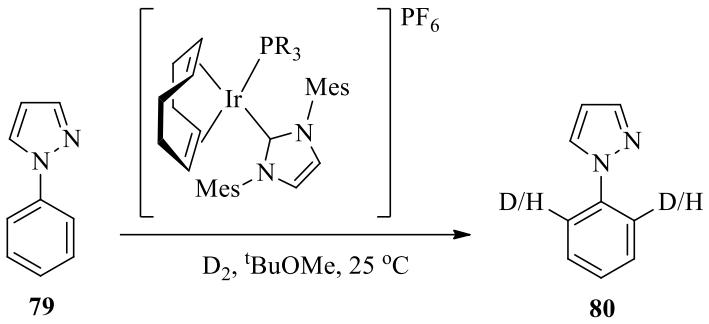

79 **80**

Scheme 70

Entry	Complex	PR_3	Catalyst Loading (mol%)	Time (h)	% Deuteration	
					Run 1	Run 2
1	**81**	PBn_3	5	2	82	82
2	**75**	PPh_3	5	2	83	84
3	**82**	PMe_2Ph	3	1	92	91

Table 60

Pleased with the levels of H-D exchange achieved in substrate **79** in Et_2O and ^tBuOMe, attention turned to the performance of the analogous reaction in 2-MeTHF (**Scheme 71**). Once again, the results obtained were extremely encouraging; in each case the isotopically-enriched product was furnished with excellent deuterium incorporations, up to a maximum of 97%.

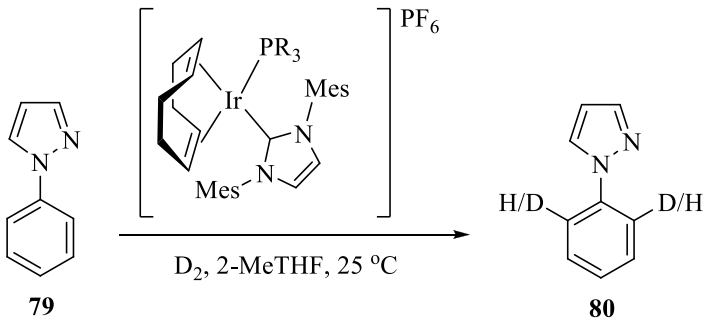

79 **80**

Scheme 71

Entry	Complex	PR_3	Catalyst Loading (mol%)	Time (h)	% Deuteration	
					Run 1	Run 2
1	**81**	PBn_3	3	1	94	92
2	**75**	PPh_3	3	2	89	96
3	**82**	PMe_2Ph	3	0.5	97	97

Table 61

The results obtained thus far clearly demonstrate the high activity of the iridium(I) complexes with regards to HIE reactions conducted in reaction media which are significantly more industrially acceptable than the commonly utilised DCM. At this stage in the investigation, the results obtained with each of the three catalysts were compared. In general, exchange reactions in which the triphenylphosphine catalyst **75** is employed require slightly longer reaction times to achieve a degree of labelling equivalent to that obtained with complexes **81** and **82**. When considering the activity of the latter complexes, it would initially appear that complex **82**, bearing the least sterically encumbered phosphine, displays superior activity in each of the three solvents. In each case, the optimum conditions include either a lower catalyst loading or shorter reaction time than those developed for the use of complex **81**. Having stated this, the labelling of 2-phenylpyridine **41** by complex **82** resulted in only poor to moderate incorporations, suggesting that the electronics of the substrate must be tuned carefully to complement those of the catalyst. In view of these findings, the tribenzylphosphine complex **81** was selected as the optimum catalyst for use in HIE reactions conducted in solvents identified as suitable replacements for DCM.

3.3.3 Labelling of Further Substrates Using $[Ir(COD)(PBn_3)(IMes)]PF_6$

To further explore the efficiency of complex **81** in HIE reactions performed in alternative reaction media, the substrate scope was expanded to include compounds which contain different functional groups capable of directing H-D exchange. The first substrate to be examined was benzamide **59** (**Scheme 72**). With no alkyl substitution on the nitrogen atom, deuterium incorporation is only possible within the aromatic ring (in the positions *ortho* to the amide functional group). The purity of this substrate is crucial to achieving reliable and

accurate results thus,[32,34] following the recrystallisation of compound **59**, a test reaction was carried out to ensure outcomes comparable to those obtained previously in our laboratory could be attained. Pleasingly, under the standard conditions of 5 mol% of complex **81** and a 16 hour reaction time, deuterium loadings slightly higher than the 79% D reported previously[35] were obtained (**Table 62**, Entry 1). In contrast, the labelling of substrate **59** in alternative solvents did not result in levels of incorporation comparable to those achieved in DCM. Having stated this, it should be noted that such reactions were carried out employing reduced catalyst loadings, and substantially shorter reaction times.

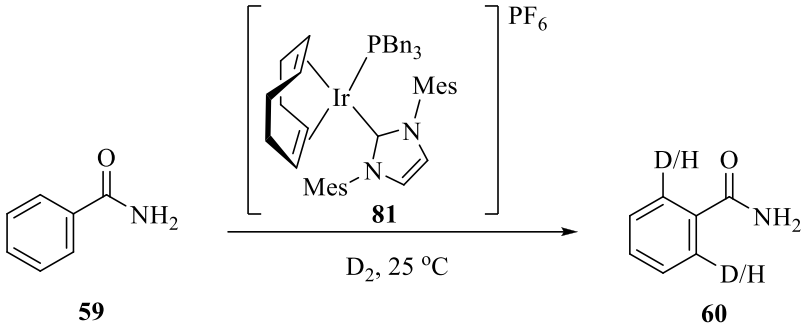

Scheme 72

Entry	Solvent	Catalyst Loading (mol%)	Time (h)	% Deuteration	
				Run 1	Run 2
1	DCM	5	16	86	92
2	Et_2O	3	1	28	24
3	^tBuOMe	5	2	38	43
4	2-MeTHF	3	1	64	64

Table 62

Using Et_2O, a relatively poor 28% deuteration was obtained (Entry 2), while only a slight increase in the levels of H-D exchange were achieved in reactions performed in ^tBuOMe (Entry 3). The use of 2-MeTHF, however, delivered the isotopically-enriched compound **60** in a good 64% level of deuteration. In an attempt to enhance the deuteration of substrate **59** in solvents other than DCM, the reactions were repeated employing a higher catalyst loading of 5 mol% and a longer reaction time of 16 hours (**Scheme 73**). Disappointingly, the use of these slightly more forcing reaction conditions did not result in any increase in the levels of deuterium incorporation detected in Et_2O (**Table 63**, Entry 1), while those obtained in ^tBuOMe were improved by only a small degree (Entry 2). Once again, reactions performed in 2-MeTHF proceeded to yield the highest levels of H-D exchange, furnishing compound **60** with levels of deuterium comparable to those achieved in DCM (Entry 3).

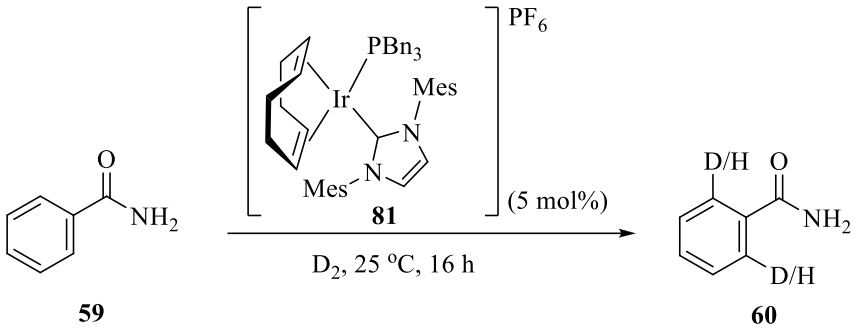

Scheme 73

Entry	Solvent	% Deuteration	
		Run 1	Run 2
1	Et_2O	27	29
2	^tBuOMe	57	49
3	2-MeTHF	89	79

Table 63

In contrast to substrate **59**, *N*,*N*,4-trimethylbenzamide **111** has four possible sites at which H-D exchange can occur; two positions on the aromatic ring *ortho* to the amide functional group, as well as in the two methyl substituents located on the nitrogen atom (**Scheme 74**). Previous work within our laboratory has demonstrated that, under the standard conditions of 5 mol% of complex **81** in DCM for 16 hours, substrate **111** is labelled to 91% in the *ortho*-positions, with an equivalent 93% incorporation in the *N*-methyl substituents.[34] Under the optimised conditions developed for HIE reactions in alternative solvents, exchange in the *ortho*-positions remains at a high level, however labelling in the methyl substituents is drastically reduced (**Table 64**). Such a difference is possibly a result of the shortened reaction times employed, suggesting that incorporation in the *N*Me groups occurs at a slower rate than that in the *ortho*-positions.

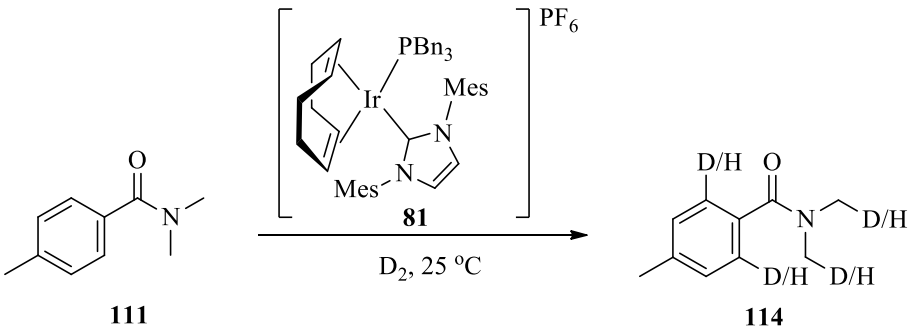

Scheme 74

Entry	Solvent	Catalyst Loading (mol%)	Time (h)	% Deuteration			
				Run 1		Run 2	
				ortho	*N*Me	*ortho*	*N*Me
1	Et_2O	3	1	81	13	83	13
2	^{t}BuOMe	5	2	96	18	93	24
3	2-MeTHF	3	1	95	22	94	24

Table 64

As expected, the labelling of *N*-ethyl-*N*,4-dimethylbenzamide **112** proceeded to deliver the isotopically-enriched compound **115** with deuterium atoms present in the *ortho*-positions of the aromatic ring, together with a lesser incorporation in the methyl substituent of the *N* atom (**Scheme 75**, **Table 65**). No incorporation in the *NEt* group was observed, indicating that the small increase in sterics between a methyl and ethyl group is sufficient to prevent deuterium incorporation in the two carbon chain. Such an outcome had been observed earlier in HIE studies performed in DCM, in which complex **81** labelled substrate **112** with a 95% incorporation on the aromatic ring, and a moderate 62% in the *N*-methyl substituent, with no exchange detected in the $-C_2H_5$ group.[34]

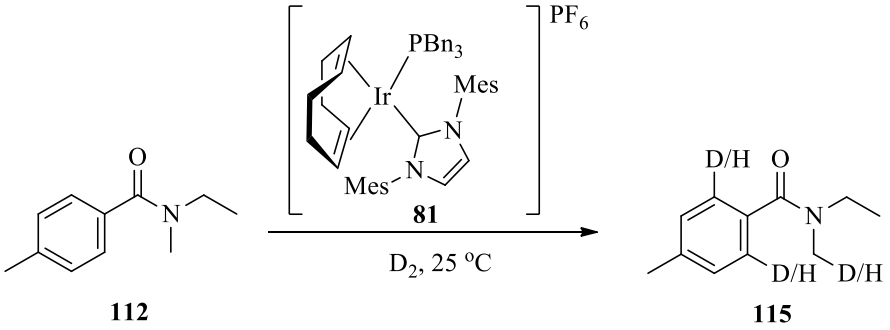

Scheme 75

Entry	Solvent	Catalyst Loading (mol%)	Time (h)	% Deuteration			
				Run 1		Run 2	
				ortho	NMe	*ortho*	NMe
1	Et_2O	3	1	91	22	88	21
2	^tBuOMe	5	2	95	31	95	30
3	2-MeTHF	3	1	91	17	85	13

Table 65

The next substrate examined within this series was *N*,*N*-diethyl-4-methylbenzamide **113**, bearing only ethyl substituents on the nitrogen atom of the amide. Previous results within our laboratory had demonstrated H-D exchange in compound **113** to occur only in the *ortho*-positions of the aromatic ring. Indeed, in DCM with 5 mol % of complex **81** over 16 hours, an excellent 97% incorporation was achieved.[35] Unfortunately, the deuteration of substrate **113** in other reaction media did not proceed to such high levels (**Table 66**). Using Et_2O and ^tBuOMe as solvents, incorporations of up to 56% and 47%, respectively, were obtained (Entries 1 and 2). On moving to 2-MeTHF, a marginal increase to 62% D loading was observed (Entry 3).

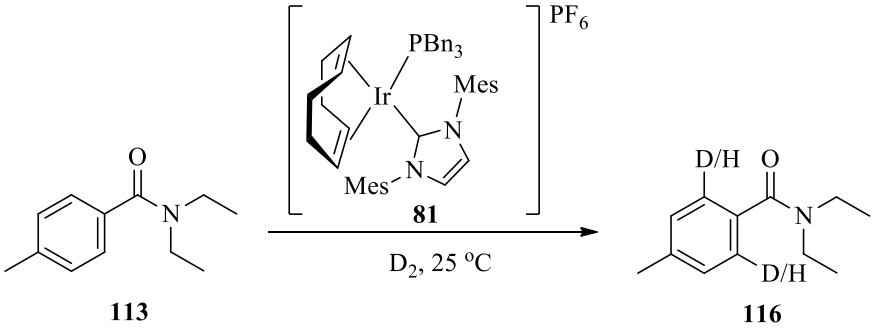

Scheme 76

Entry	Solvent	Catalyst Loading (mol%)	Time (h)	% Deuteration	
				Run 1	Run 2
1	Et_2O	3	1	51	56
2	^tBuOMe	5	2	47	46
3	2-MeTHF	3	1	62	61

Table 66

In an attempt to increase the levels of deuteration in substrate **113**, the above reactions were repeated in the presence of a greater quantity of catalyst and over an extended period of time

(**Scheme 77**). The application of these slightly more forcing conditions proved advantageous in reactions performed in Et_2O and 2-MeTHF, delivering the isotopically-enriched product **116** with more enhanced levels of deuteration than those detected previously (**Table 67**, Entries 1 and 3). Unfortunately, no significant improvement in the degree of labelling was attained in reactions run in ^tBuOMe (Entry 2).

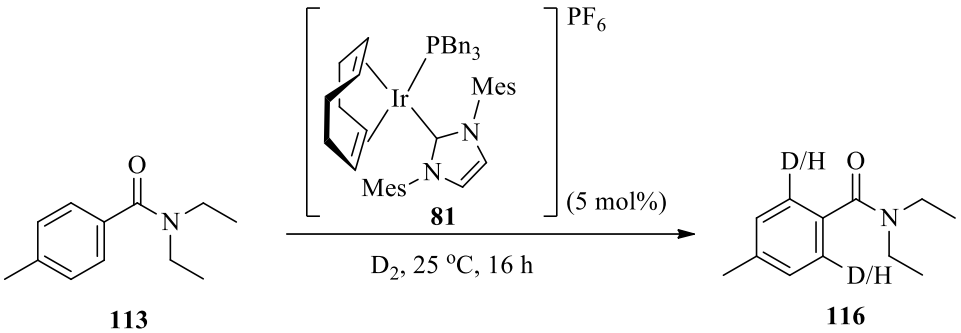

Scheme 77

Entry	Solvent	% Deuteration	
		Run 1	Run 2
1	Et_2O	71	74
2	^tBuOMe	53	54
3	2-MeTHF	85	78

Table 67

Having completed investigations regarding the use of amides which offer a selection of sites at which labelling could occur, attention returned to a substrate in which only one possible site of deuterium incorporation is possible. As depicted in **Scheme 78**, acetanilide **73** can be labelled only in the positions on the aromatic ring *ortho* to the directing amide functionality, and *via* a more challenging 6-mmi. As illustrated in **Table 68**, using the previously optimised

loading levels and reaction times, only moderate levels of deuteration were observed in each of the three solvents.

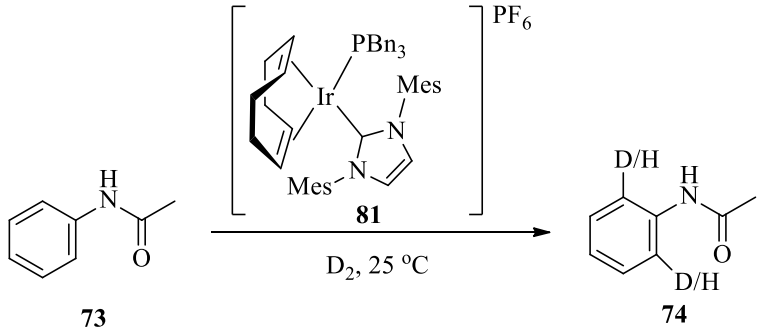

73 74

Scheme 78

Entry	Solvent	Catalyst Loading (mol%)	Time (h)	% Deuteration	
				Run 1	Run 2
1	Et_2O	3	1	40	36
2	^tBuOMe	5	2	46	52
3	2-MeTHF	3	1	52	45

Table 68

As stated above, compound **73** is labelled *via* a 6-mmi, which is known to occur at a rate slower than that of the analogous 5-mmi.[34,35] It was therefore proposed that allowing the reactions to run for a longer period of time and with an increased quantity of catalyst would improve the degree of incorporation achieved (**Scheme 79**, **Table 69**). Unfortunately, no appreciable increase in deuteration was detected. The ligating capabilities of the three solvents under investigation are likely to be substantially more significant than that of DCM, hence coordination of solvent molecules to the iridium metal may be preferred over H-D exchange through a 6-mmi, which is known to occur *via* a higher energy pathway.[34]

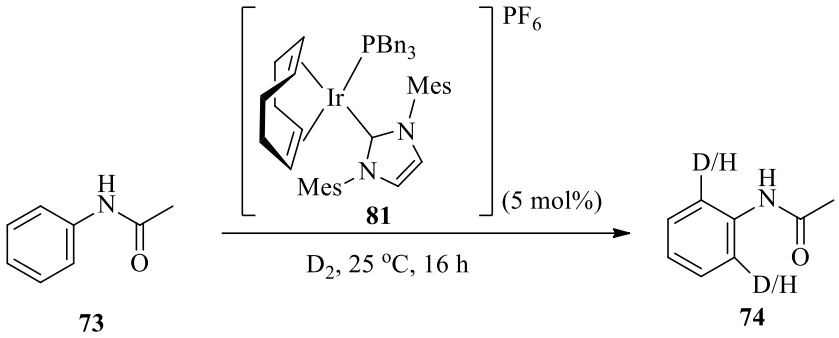

73 **74**

Scheme 79

Entry	Solvent	% Deuteration	
		Run 1	Run 2
1	Et_2O	50	51
2	^tBuOMe	57	57
3	2-MeTHF	62	70

Table 69

The reduced levels of isotope incorporation observed in the labelling of acetanilide **73** and, more specifically, *via* a 6-mmi did, however, provide the opportunity to investigate the degree of selectivity which could be achieved in H-D exchange reactions facilitated by complex **81** in alternative solvents. Many potential drug molecules contain a variety of C-H bonds which may undergo isotopic exchange, positioned either four or five bonds away from an appropriate coordinating functionality. The regioselective labelling at one site over another would therefore enable distinct fragments of the molecule to be traced *in vivo*, thus highlighting any undesired side effects which may result from these metabolites. Accordingly, benzanilide **83** was selected for study (**Scheme 80**). Substrate **83** includes two possible sites of isotope incorporation, *a* and *b*, which are labelled *via* a 5-mmi and 6-mmi, respectively. Previous work within our laboratory had, indeed, shown that the selective labelling of benzanilide was possible at catalyst loadings of 0.5 mol %, giving high levels of deuteration in position *a*, with minimal incorporation occurring at position *b*.[35] As the purity of substrate **83** is crucial to the success of H-D exchange, a test reaction in DCM was

performed utilising freshly recrystallised benzanilide. Pleasingly, the excellent levels of deuterium incorporation expected in each position were achieved (**Table 70**, Entry 1). Attention therefore turned to the deuteration of benzanilide in alternative solvents. As illustrated by the results below, similar outcomes were observed in reactions run in Et_2O and ^tBuOMe; labelling in position *a* proceeded to only moderate levels of isotope incorporation of up to 47%, while that in position *b* was found to reach D loadings in the region of 15% (Entries 2 and 3). The results obtained in reactions performed in 2-MeTHF were extremely encouraging however, displaying high levels of both incorporation and selectivity for exchange in position *a* (Entry 4). Of particular note is the increased quantity of catalyst employed within these reactions. In contrast to the aforementioned reactions which saw high levels of selectivity in the labelling of benzanilide facilitated by just 0.5 mol% of complex **82**,[35] the use of complex **81** in 2-MeTHF delivers a similar degree of selectivity in the presence of a greater catalyst loading of 3 mol%. Such findings may be of great benefit with regards to the labelling of more complex molecules, such as potential drug candidates, which frequently require higher catalyst loadings to achieve acceptable levels of isotope incorporation. The current conditions therefore offer the potential to deliver such loadings of deuterium (or tritium), while maintaining the desired degree of selectivity.

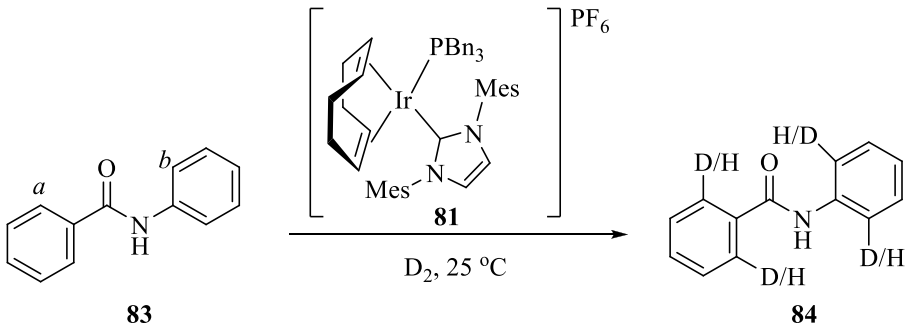

83 **84**

Scheme 80

Entry	Solvent	Catalyst Loading (mol%)	Time (h)	% Deuteration			
				Run 1		Run 2	
				a	*b*	*a*	*b*
1	DCM	5	16	93	90	92	90
2	Et_2O	3	1	36	18	42	15
3	^{t}BuOMe	5	2	43	13	47	15
4	2-MeTHF	3	1	93	12	91	9

Table 70

Efforts to promote the labelling of benzanilide **83** in Et_2O and ^{t}BuOMe centred on the employment of an increased catalyst loading of 5 mol% and a lengthened reaction time of 16 hours (**Scheme 81**). While no considerable improvement in the levels of deuteration were observed in either case (**Table 71**), the initial results from this short study clearly reinforce the advantages associated with performing hydrogen isotope exchange reactions in alternative solvents.

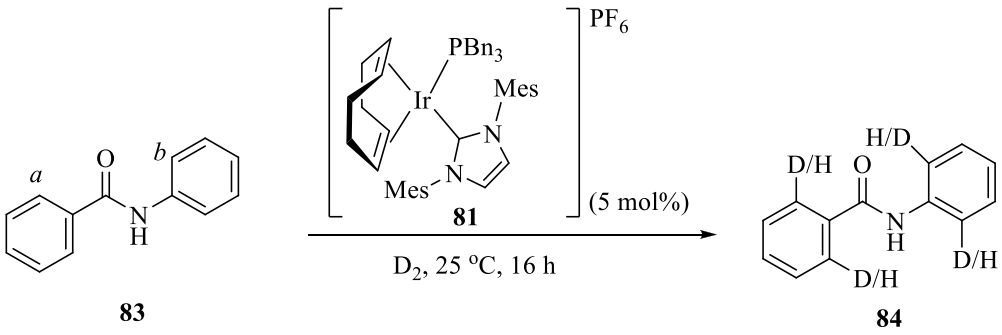

83 **81** **84**

Scheme 81

Entry	Solvent	% Deuteration			
		Run 1		Run 2	
		a	*b*	*a*	*b*
1	Et_2O	41	20	39	27
2	^tBuOMe	43	14	50	14

Table 71

As discussed earlier, a significant benefit offered by solvents identified as possible replacements for DCM in HIE reactions would be their ability to dissolve drug molecules, which invariably contain a number of polar functional groups. To examine such capabilities of Et_2O, ^tBuOMe and 2-MeTHF, the developed conditions were applied to the isotopic labelling of Niclosamide **117**, an anthelmintic manufactured by Bayer which is effective in the treatment of tapeworms.[58] As illustrated in **Scheme 82**, compound **117** has four possible sites at which H-D exchange could occur. Positions *a* and *b* are labelled *via* a 5-mmi directed by the adjacent nitro group, while labelling in position *c*, directed by the amide moiety, is *via* an energetically less favourable 6-mmi. In a manner analogous to *a* and *b*, isotope exchange in position *d* will also proceed *via* a 5-mmi however, in this instance, the carbonyl group located *ortho* to the C-H bond under consideration will coordinate to the metal centre.

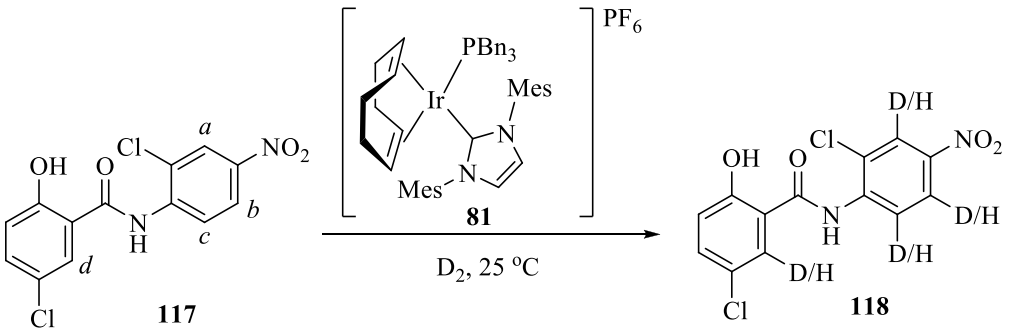

Scheme 82

Entry	Solvent	Catalyst Loading (mol%)	Time (h)	Run	% Deuteration			
					a	*b*	*c*	*d*
1	DCM	5	1	1	51	43	39	54
				2	55	44	40	58
2	Et_2O	3	1	1	75	70	63	76
				2	76	69	57	77
3	^tBuOMe	5	2	1	83	48	37	87
				2	82	42	34	89
4	2-MeTHF	3	1	1	89	55	28	97
				2	86	53	29	97

Table 72

Comparison of the values detailed above in **Table 72** reveals that in each of the three alternative solvents, the levels of deuteration observed are substantially higher than those achieved in reactions employing DCM. It is proposed that such differences could be attributed to the increased solubility of Niclosamide in the more polar reaction media, confirming the benefits associated with identifying solvents as potential replacements of DCM. Furthermore, labelling reactions performed in ^tBuOMe and 2-MeTHF display an enhanced selectivity for H-D exchange which proceeds *via* a 5-mmi, indicating that coordination of the solvent may be more favourable than labelling *via* the energetically more demanding 6-mmi.

From the reasoning outlined above regarding the distance between the activated C-H bond and the relevant directing group, similar levels of deuterium incorporation would be expected in positions *a* and *b*. However, as illustrated in **Table 72**, the degree of labelling in position *b* is substantially different to that observed in position *a*, ranging from approx. 5% in Et_2O to approximately 30% in 2-MeTHF. In view of these observations, it is proposed that there may be a weak ligation to the metal centre by the Cl atoms, enhancing the directing effect for labelling at position *a*.

The final compound to be examined in this study was Celecoxib **119**, a COX-2 inhibitor marketed by Pfizer.[59] As depicted below in **Scheme 83**, substrate **119** contains two suitably positioned C-H bonds which may undergo exchange with deuterium under the reaction conditions: position *a* adjacent to the sulfonamide moiety, and position *b* which is directed by the nitrogen in the 2-position of the pyrazole unit. As demonstrated previously, complex **81** displayed high activity in the labelling of *N*-phenylpyrazole **79** itself in alternative solvents (*vide supra*). In contrast, deuterium incorporation adjacent to a sulfonamide is notoriously difficult; indeed, earlier work carried out within our laboratory has focused on the labelling of various sulfonamide substrates, albeit with only some limited success.[29] Previous results obtained within our laboratory regarding the labelling of Celecoxib **119** with complex **81** had revealed that under the standard conditions employing 5 mol% of the catalyst in DCM over a 1 hour reaction time, H-D exchange proceeded to relatively low levels of incorporation of 3% and 36% in position *a* and *b*, respectively. Pleasingly, increasing the catalyst loading to 10 mol% resulted in a significant improvement in the isotope uptake observed in each position, delivering the desired compound **120** with deuterium incorporations of 19% in position *a*, and an excellent 94% in position *b*.[34] Attention therefore turned to the labelling of substrate **119** in the three solvents identified as suitable replacements for DCM (**Table 73**). Owing to the renowned difficulty of labelling adjacent to a sulfonamide unit, the optimum conditions previously developed for reactions performed in Et_2O and 2-MeTHF were discarded, and initial reactions instead carried out employing a slightly higher catalyst loading of 5 mol%. As the optimum conditions for labelling reactions in ^{t}BuOMe utilised a reaction time of 2 hours, this extended period was maintained for reactions performed in this solvent. Unfortunately, the results obtained were somewhat disappointing. In each case, incorporation in position *a* was relatively low, ranging from 3% in reactions performed in 2-MeTHF to 8% in systems employing Et_2O as the reaction solvent. Furthermore, the degree of H-D exchange adjacent to the pyrazole unit did not compare to the levels of deuteration observed previously in the labelling of substrate **79**. Indeed, the highest extent of deuterium incorporation attained in this instance was a moderate 41% in Et_2O (Entry 1), while reactions performed in 2-MeTHF delivered only a poor 5% deuteration in the equivalent position (Entry 3).

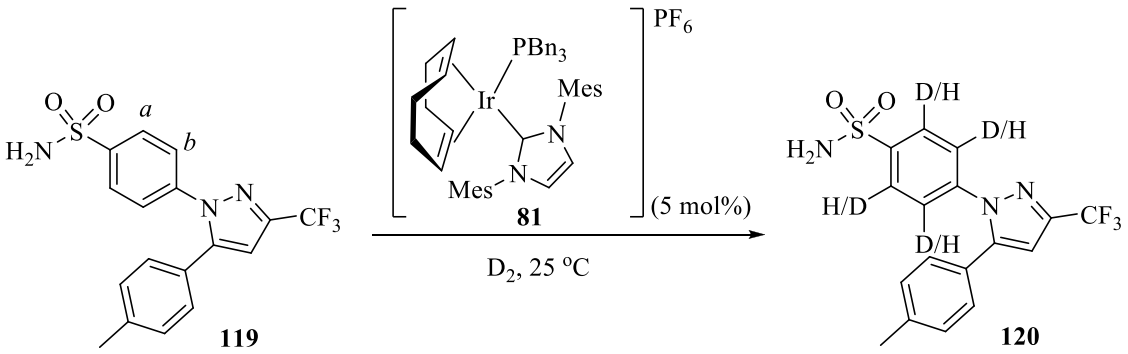

Scheme 83

Entry	Solvent	Time (h)	% Deuteration			
			Run 1		*Run 2*	
			a	*b*	*a*	*b*
1	Et_2O	1	8	41	7	41
2	^tBuOMe	2	5	24	7	23
3	2-MeTHF	1	3	5	4	5

Table 73

As increasing the catalyst loading to 10 mol% had proved beneficial previously, reactions were repeated with this greater quantity of complex **81** (**Scheme 84**). Pleasingly, the results obtained in Et_2O under these modified conditions gave rise to an increase in the levels of H-D exchange observed in both positions *a* and *b*, albeit to a significantly greater extent in the latter position (**Table 74**, Entry 1). Conversely, the levels of isotopic labelling attained in reactions performed in ^tBuOMe and 2-MeTHF did not improve to the degree expected. Only marginal increases were detected in position *b*, with no enhancement obtained in exchange adjacent to the sulfonamide (Entries 2 and 3).

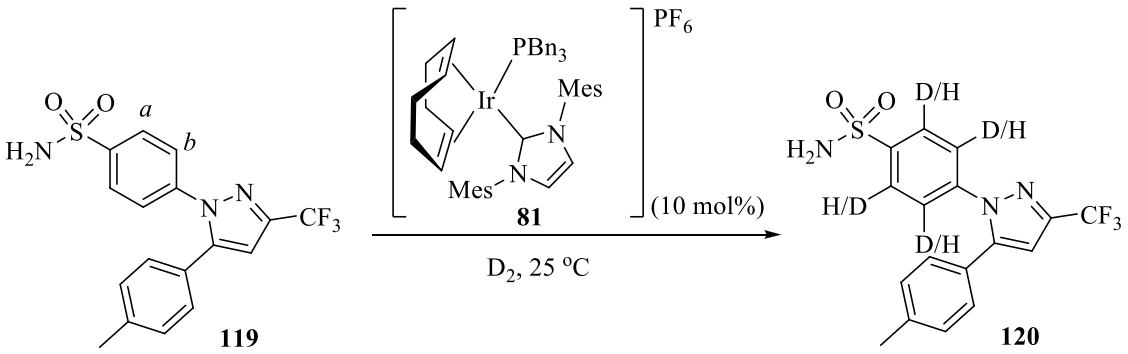

Scheme 84

Entry	Solvent	Time (h)	% Deuteration			
			Run 1		*Run 2*	
			a	*b*	*a*	*b*
1	Et_2O	1	13	72	11	66
2	^tBuOMe	2	7	36	8	30
3	2-MeTHF	1	5	15	5	12

Table 74

The results obtained in this solvent study have revealed complexes of the type $[Ir(COD)(PR_3)(IMes)]PF_6$ to be efficient in hydrogen isotope reactions which are performed under conditions considered to be more industrially acceptable than those described previously.[35] In particular, complex **81** has displayed high catalytic activity in the isotopic labelling of a variety of substrates, operating at catalyst loadings as low as 3 mol%, and in reaction times of 1 hour. The use of 2-MeTHF as an alternative reaction medium to DCM has also displayed a number of advantages, such as the high degree of selectivity attained in the deuteration of benzanilide **83** (**Scheme 80**), together with the increased isotope incorporations and improved levels of selectivity observed in the labelling of the drug molecule, Niclosamide **117** (**Scheme 82**). Such findings highlight significant benefits regarding the identification of alternative reaction media for use in hydrogen isotope exchange reactions,

demonstrating that the replacement of DCM with a solvent which is more environmentally benign may also promote the deuterium loadings achieved.

3.4 Preparation of Novel Iridium(I) Complexes

As described earlier, a further avenue of work to be undertaken within this overall research programme was the synthesis of novel complexes of the type $[Ir(COD)(PR_3)(NHC)]PF_6$. While previous investigations performed within our laboratory have focused on the steric and electronic properties of the tertiary phosphine ligands,[34] no analogous studies regarding the NHC ligands have been carried out. It was therefore proposed that the preparation of Ir(I) complexes bearing alternative NHC ligands, and their subsequent application in the field of hydrogen isotope exchange, may reveal any relationships between the attributes of the NHC ligand and catalyst activity.

Initial investigations into the synthesis of novel Ir(I) complexes focused on the routinely employed synthetic procedure, as described previously (**Scheme 85**). Following addition of NaOEt to Ir dimer **106**, introduction of the required imidazolium salt **121** results in the formation of the stable Cl intermediate **122**. Addition of $AgPF_6$ creates a coordinatively unsaturated Ir species, to which the incoming phosphine can complex, a process indicated by a characteristic orange to red colour change. Recrystallisation techniques are then employed to isolate the desired complex **123**.

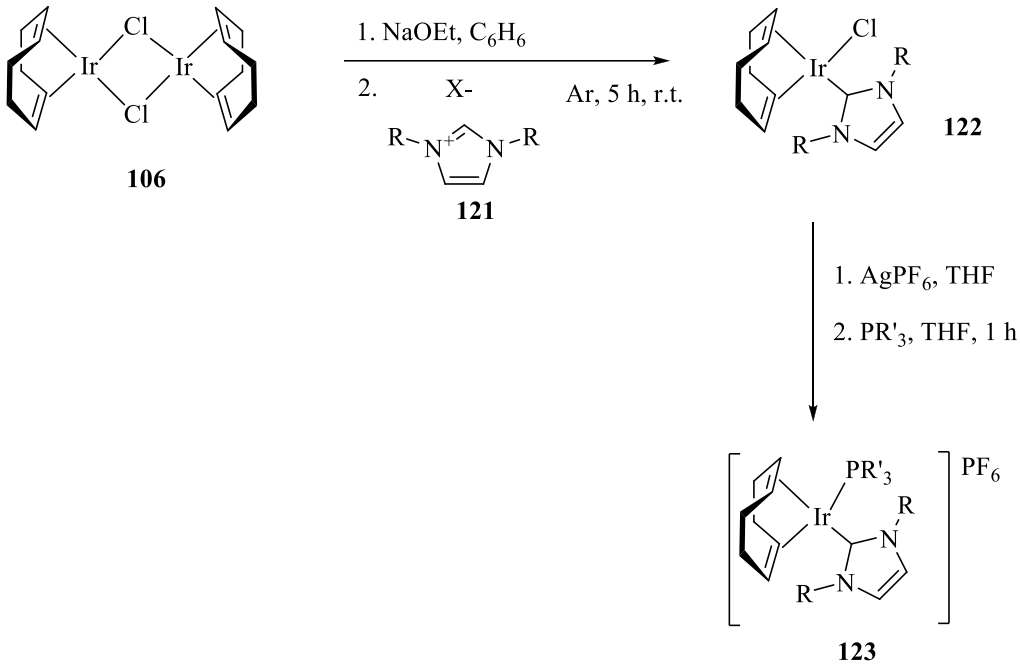

Scheme 85

As opposed to pairing each NHC ligand with each of the three phosphines routinely used within this research area, it was decided to concentrate on one series of complexes initially, in an attempt to establish any patterns in their reactivity. With a cone angle of 145°, the steric influence imparted by triphenylphosphine is between that of tribenzylphosphine and dimethylphenylphosphine, which have cone angles of 165° and 122°, respectively.[36] The former ligand therefore offered an attractive starting point for our synthetic studies.

*Attempted preparation of η^4-Cycloocta-1,5-diene(1,3-dicyclohexylimidazoline-2-ylidene)(triphenylphosphine)iridium(I) Hexafluorophosphate **124***

The first complex to be investigated via this synthetic route was **124**, containing aliphatic substitutents on the NHC, pairing triphenylphosphine with 1,3-dicyclohexylimidazoline-2-ylidene (**Figure 25**).

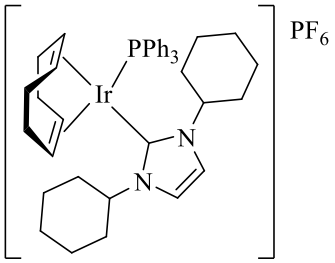

124

Figure 25

Following the standard preparation method described above, a deep red solution was obtained on addition of the phosphine. Removal of the solvent produced a red solid, which was subsequently recrystallised from DCM/Et_2O to give dark red crystals. While analysis by ^1H NMR revealed the desired product to be present, an excess number of signals corresponding to aromatic protons were also visible, indicating the presence of unreacted triphenylphosphine. In addition, the ^{31}P NMR spectrum showed the presence of triphenylphosphine oxide. Further attempts to purify the material through recrystallisation from DCM/Et_2O were unsuccessful, with no change in either NMR spectrum observed.

The reaction was therefore repeated as above, employing freshly recrystallised triphenylphosphine. On this occasion, the red solid obtained in the final step of the synthetic procedure was recrystallised from THF/hexane, a solvent combination which had been previously been used in the isolation of complex **75**.[32] Pleasingly, an orange powder was obtained, ^1H NMR analysis of which indicated the correct product. However, the presence of THF was also apparent which, despite numerous attempts at drying the material, could not be removed. In addition, the use of freshly recrystallised triphenylphosphine had no beneficial effect, as the ^{31}P NMR spectrum again contained a small peak corresponding to $O{=}PPh_3$.

The final attempt at the synthesis of complex **124** *via* the standard preparative procedure involved stirring the solution for an extended period of 5 hours following the addition of the phosphine, to promote complexation of the ligand. Upon removal of the solvent, a red solid

was obtained. Analysis of the crude material by ^{31}P NMR showed the two expected signals, corresponding to the phosphine bound to the iridium, and the PF_6 counter ion. Inspection of the ^{1}H NMR, however, was somewhat confusing. While the correct number of aromatic proton signals was present, the aliphatic peaks integrated to only six protons, a vast reduction from the thirty protons expected.

*Attempted Preparation of η^4-Cycloocta-1,5-diene(1,3-dibenzylimidazoline-2-ylidene) (triphenylphosphine)iridium(I) Hexafluorophosphate **125***

Subsequent investigations into the synthesis of novel Ir(I) complexes bearing alternative NHC ligands focused on the preparation of complex **125**, combining triphenylphosphine with 1,3-dibenzylimidazoline-2-ylidene (**Figure 26**).

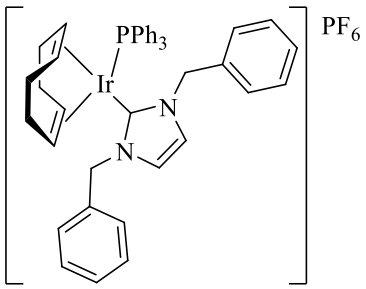

125

Figure 26

Following the standard preparation procedure outlined previously in **Scheme 85**, addition of triphenylphosphine resulted in the characteristic orange to red colour change. However, removal of the solvent yielded an oily gum rather than the expected solid, implying the presence of impurities. Efforts to recrystallise this gum from DCM/Et_2O proved unsuccessful, as the material remained gum-like. The suspicion of impurities present within this gum was confirmed by ^{1}H NMR analysis.

The attempted synthesis of complex **125** was thus repeated. In this instance, a red solid was obtained following removal of the solvent under high vacuum. The material was split into separate portions and different purification techniques were applied in each case. Unfortunately, attempts to isolate the desired product by recrystallisation were unsuccessful; DCM/Et_2O produced an orange/red solid which analysis by ^{31}P NMR revealed the presence of triphenylphosphine oxide, while DCM/hexane resulted in the previously obtained oily gum. As mentioned, known complex **75** had previously been recrystallised from THF/hexane,[32] however the crude material obtained in the synthesis of complex **125** was found to be insoluble in small volumes of THF.

In each case, ^1H NMR analysis of the gum-like material revealed an excess number of peaks in the aromatic region of the spectrum, indicating that residual triphenylphosphine was present within the material obtained. Purification of PPh_3 is achieved by recrystallisation from ethanol, hence it was proposed that if the crude product was dissolved in EtOH, it could be separated from the unreacted phosphine. The attempted synthesis of complex **125** was thus repeated, and the gum obtained following the removal of solvent in the final stages was triturated with EtOH. Encouragingly, a red solid was produced, the ^1H NMR spectrum of which contained the desired number of aromatic signals. Much to our disappointment however, further inspection of the spectrum revealed that although only a small volume had been used, the ethanol had coordinated to the iridium centre. Despite several attempts at drying the solid, the solvent could not be removed.

In a subsequent attempt at the preparation of complex **125**, the presence of residual triphenylphosphine in the crude reaction material was confirmed by analysis by TLC. Thus, purification by column chromatography was carried out, yielding red crystals. Although the number of protons in the aromatic region of the ^1H NMR spectrum decreased significantly, there remained a slight excess, implying that not all the unreacted PPh_3 had been removed.

As all previous attempts at the synthesis of complex **125** had resulted in the presence of unreacted triphenylphosphine, it was proposed that the solution should be left stirring for a longer period of time following the introduction of PPh_3, to ensure complete coordination to the iridium metal. The preparation of complex **125** was therefore repeated once more, and the

red solution left stirring overnight. Pleasingly, the solution remained red, implying no decomposition had occurred. Removal of the solvent produced a red solid however, once again, recrystallisation attempts from DCM/Et_2O yielded a gummy oil, analysis of which revealed the presence of impurities.

Attempted Preparation of η^4-Cycloocta-1,5-diene(1,3-bis(2,6-diisopropylphenyl)imidazoline-2-ylidene)(triphenylphosphine)iridium(I) Hexafluorophosphate ***126***

Undeterred by the frustrating results obtained to this point, attention turned to the synthesis of complex **126**, containing a sterically demanding NHC ligand previously utilised in complexes developed by Nolan[46] (**Figure 27**).

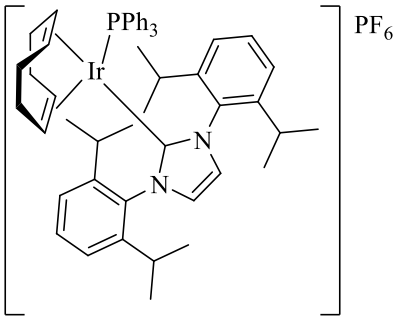

126

Figure 27

Sadly, the initial synthetic attempt at this complex was unsuccessful as, upon addition of triphenylphosphine, the solution remained orange in colour, indicating failure of the phosphine to coordinate to the metal centre. Efforts to aid such a complexation involved the addition of a further two equivalents of triphenylphosphine, however the solution turned yellow, and the formation of a white precipitate was observed. Analysis of the crude reaction mixture by ^1H NMR revealed the desired product had not formed. As allowing the solution to stir for a longer period of time had proved advantageous in the preparation of the previously

discussed complexes, the synthesis of complex **126** was repeated under these conditions. Following filtration under argon to remove the precipitated Ag salts, a clear orange solution was obtained. Unfortunately, but not unexpectedly, addition of PPh_3 did not result in the desired red colour change. The solution was therefore stirred overnight, however, after this time, the reaction mixture had turned brown. Once again, analysis by ^1H NMR indicated that the desired product was not present.

*Attempted Preparation of η^4-Cycloocta-1,5-diene(1,3-bis(diphenylmethyl)imidazoline-2-ylidene)(triphenylphosphine)iridium(I) Hexafluorophosphate **127***

The penultimate complex to be investigated was **127**, bearing the highly sterically encumbered 1,3-bis(diphenylmethyl)imidazoline-2-ylidene NHC ligand (**Figure 28**).

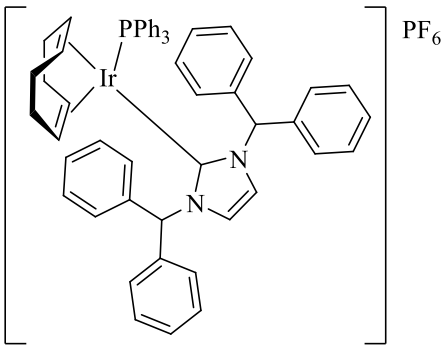

127

Figure 28

In view of the issues encountered in the attempted formation of complex **126**, it was envisaged that similar problems may be presented in efforts to synthesise the current complex, due to the high steric influence imparted by the NHC ligand. Having said this, initial observations in the attempted preparation of the latter complex were encouraging as, upon addition of triphenylphosphine, a distinct orange to red colour change was detected.

Recrystallisation of the crude material obtained delivered red crystals, however analysis by ^{1}H NMR revealed an excess number of aromatic protons in the spectrum.

The attempted synthesis of complex **127** was thus repeated yielding a red solid, TLC analysis of which indicated the presence of unreacted triphenylphosphine. As efforts to separate the free PPh_3 from complex **125** by dissolving in EtOH had resulted in the irreversible coordination of solvent to the iridium centre, purification of complex **127** was attempted using column chromatography. Unfortunately, analysis by ^{1}H NMR revealed that a significant proportion of triphenylphosphine had failed to have been removed.

A final effort to prepare complex **127** involved stirring the solution overnight following addition of the phosphine. Pleasingly, recrystallisation techniques produced a red solid which was subsequently analysed by spectroscopic methods. Examination of the ^{1}H NMR spectrum revealed the expected number of signals in the aromatic region, indicating complete complexation of PPh_3 to the metal centre. Unfortunately, the ^{31}P NMR spectrum did not appear as expected, with 3 additional peaks present along with the signals corresponding to the phosphine bound to the iridium and PF_6 counter ion. It was therefore proposed that the $AgPF_6$ salt used in this instance had started to decompose. Due to insufficient quantities of imidazolium salt **103**, no further investigations regarding the synthesis of complex **127** have been undertaken.

*Attempted Preparation of η^4-Cycloocta-1,5-diene(1,3-bis(1-adamantyl)imidazoline-2-ylidene)(triphenylphosphine)iridium(I) Hexafluorophosphate **128***

The final complex of this series investigated contained the well documented Arduengo's carbene,[51] 1,3-bis(1-adamantyl)imidazol-2-ylidene **100** (**Figure 29**). In contrast to the imidazolium salts examined thus far, compound **100** is available as the free carbene, due to

its renowned stability. Following the general synthetic procedure developed within our laboratory, the synthesis of complex **128** was attempted.

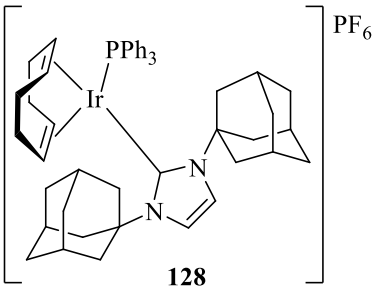

128

Figure 29

Unfortunately, although the synthesis proceeded as expected with the initial colour changes occurring at the appropriate point, addition of the phosphine did not result in the anticipated formation of a final deep red colour. It was suspected that as a result of the steric bulk associated with the adamantyl groups, coordination of the phosphine to the metal centre was more challenging in comparison to complexes containing less sterically encumbered NHCs. Thus, in an attempt to promote such a coordination, a further two equivalents of triphenylphosphine were added. Sadly, however, the solution remained a clear brown. Suspicions that the desired complex had not been obtained were confirmed by ^{1}H NMR analysis.

Attempted Preparation of Chloro(η^4-Cycloocta-1,5-diene(1,3-bis(1-adamantyl)imidazoline-2-ylidene)iridium(I) ***129***

Undeterred by this disappointing outcome, focus turned to the formation of the intermediate chloro species, Ir(COD)(IAd)(Cl) **129** (**Figure 30**), as it was unknown if such a complex had been successfully obtained in the initial preparation. The synthesis was therefore repeated, and the green/brown gum obtained following filtration and removal of Et_2O analysed by ^{1}H

NMR. Unfortunately interpretation of the spectrum revealed that the desired product had not formed.

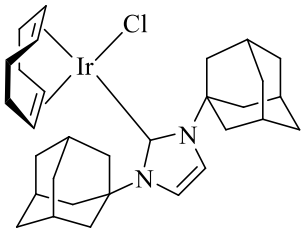

129

Figure 30

As a result of the unsuccessful preparation of Ir(COD)(IAd)Cl **129** via our synthetic route, it was proposed that the difficulties encountered in the isolation of the previous novel Ir(I) complexes may not only be due to the presence of impurities within the final reaction mixture, and that underlying issues regarding the *in-situ* formation of the Cl intermediates may also be present. Attention therefore turned to the isolation of chloro intermediates of the type Ir(COD)(NHC)Cl **122**, to establish the yield and purity of such species.

Preparation of Chloro(η^4–cycloocta–1,5–diene)(1,3-bis(2,6-diisopropylphenyl)imidazoline-2-ylidene)iridium(I) ***130***

As depicted in **Scheme 86**, the synthesis of complex **130** was achieved according to the initial steps of the route routinely employed to prepare our Ir(I) catalysts. Thus, $[Ir(COD)Cl]_2$ **106** was treated with NaOEt, followed by addition of imidazolium salt **105**. Purification of the crude material was achieved by filtration through silica, in a manner analogous to that reported by Nolan.[46] Unfortunately, under the standard reaction conditions, the desired complex was obtained in a low 29% yield (**Table 75**, Entry 1). A considerable increase in yield was obtained in reactions run for extended periods of time (Entries 2 and 3), however the quantities of **130** achieved remained moderate. In an attempt to promote the formation of

130, attention turned to the original synthetic route employed by Herrmann in the synthesis of similar iridium and rhodium complexes.[33] It was noted that, following addition of the appropriate imidazolium salt, the reaction mixture was heated at 60 °C for 2 days, delivering the desired compound in yields of up to 95%. In view of these findings, the preparation of complex **130** was repeated at the slightly elevated temperature of 45 °C. To our delight, a dramatic improvement in yield was obtained (Entry 4). Furthermore, performing the reaction at this higher temperature for an extended period of 48 hours proved even more successful, furnishing the desired complex **130** in an excellent 89% yield (Entry 5).

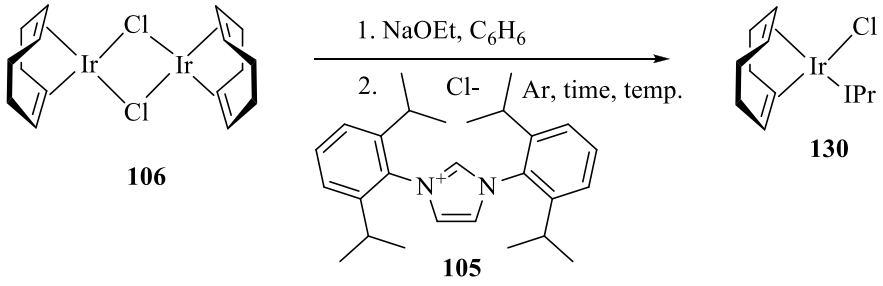

Scheme 86

Entry	Temperature (°C)	Time (h)	Yield of **130**
1	25	24	29
2	25	48	44
3	25	72	51
4	45	24	82
5	45	48	89

Table 75

Preparation *of Chloro(η^4–cycloocta–1,5–diene)(1,3-dicyclohexylimidazoline-2-ylidene)iridium(I)* ***131***

An analogous investigation was undertaken regarding the formation of Ir(COD)(ICy)Cl **131** (**Scheme 87**). As the results in **Table 76** illustrate, under the originally employed conditions, a low yield of 20% was obtained (Entry 1). Consequently, heating the reaction mixture to 45 °C provided the desired product **131** in a significantly improved 82% yield (Entry 2). In an attempt to further promote the formation of **131**, the reaction was run for a longer period of 48 hours, and subsequently 96 hours (Entries 3 and 4). Pleasingly, both reactions delivered slightly increased quantities of **131**, the latter reaction time furnishing the desired product in an admirable 91% yield.

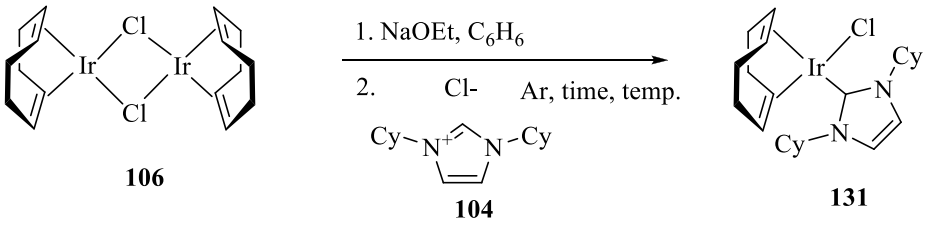

Scheme 87

Entry	Temperature (°C)	Time (h)	Yield of **131**
1	25	24	20
2	45	24	82
3	45	48	87
4	45	96	91

Table 76

Preparation of Chloro(η^4–cycloocta–1,5–diene)(1,3-dibenzylimidazoline-2-ylidene)iridium(I) ***132***

The final species of this series to be prepared was complex **132**, bearing benzyl substituents on the nitrogen atoms of the NHC ligand (**Scheme 88**). As heating the reactions had proved fruitful in the synthesis of complexes **130** and **131**, initial investigations regarding the preparation of **132** employed the slightly higher temperature of 45 °C and a reaction time of 24 hours (**Table 77**, Entry 1). Disappointingly, the desired product **132** was obtained in only a moderate 33% yield, which was considerably lower than the yields of complexes **130** and **131** achieved under the same conditions (**Table 75**, Entry 4 and **Table 76**, Entry 2). It was therefore proposed that the formation of **132** required more forcing conditions; hence, the reaction temperature was increased to 60 °C. After 24 hours, a much improved 60% yield of complex **132** was attained (Entry 2). Extending the reaction period to 48 hours did not result in a significant increase in the amount of **132** formed, however, leaving the reaction for 72 hours proved beneficial, delivering the desired product in an enhanced yield of 80% (Entry 4). Efforts to further promote the formation of complex **132** by allowing the reaction to run for 96 hours did not lead to the production of any additional material, indicating the reaction had reached completion after 3 days (Entry 5).

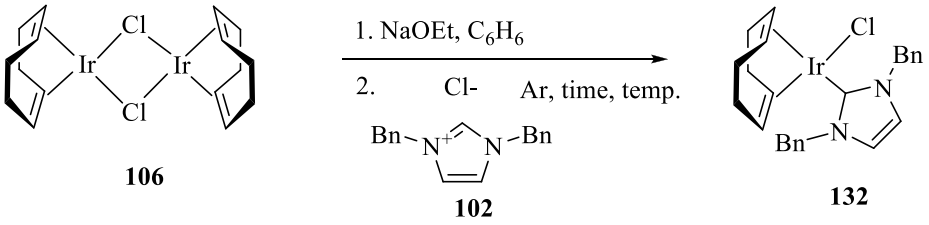

Scheme 88

Entry	Temperature (°C)	Time (h)	Yield of **132**
1	45	24	33
2	60	24	60
3	60	48	67
4	60	72	80
5	60	96	81

Table 77

With sufficient quantities of the required Cl intermediates now available, attention turned to the preparation of the final phosphine-containing Ir(I) complexes.

*Attempted preparation of η^4-Cycloocta-1,5-diene(1,3-bis(2,6-diisopropylphenyl)imidazoline-2-ylidene)(triphenylphosphine)iridium(I) Hexafluorophosphate **126***

Explorations regarding the synthesis of complexes of the type [Ir(COD)(PPh_3)(NHC)]PF_6 via our modified synthetic route began with the attempted formation of complex **126** (**Scheme 89**). Previous efforts to prepare this complex had failed to produce the characteristic orange to red colour change, attributed to the high steric bulk of the NHC ligand which prevented complexation of the phosphine. It was therefore somewhat unsurprising that following filtration to remove precipitated Ag salts, the solution remained clear orange upon addition of PPh_3. After stirring for 1 h, a further equivalent of PPh_3 was added, however this caused the solution to turn yellow and cloudy. Analysis of the crude reaction mixture by ^{1}H NMR revealed the desired product had not formed.

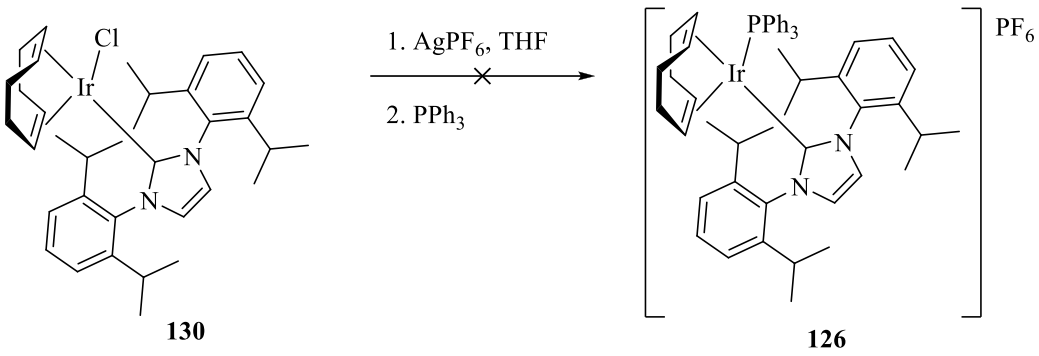

Scheme 89

As the key issue regarding the preparation of complex **126** was believed to be a result of restricted access of triphenylphosphine to the Ir centre, a competition reaction was performed employing dimethylphenylphosphine, which has a significantly smaller cone angle of 122°, compared to the larger 145° associated with PPh_3.[36] As had been observed previously, the reaction mixture remained orange following addition of PPh_3. Upon addition of PMe_2Ph however, a distinct red colour change was detected. Unfortunately, attempts to isolate the desired product were unsuccessful; analysis of the crude mixture by ^{31}P NMR indicating the presence of PMe_2Ph both bound to the Ir and free in solution.

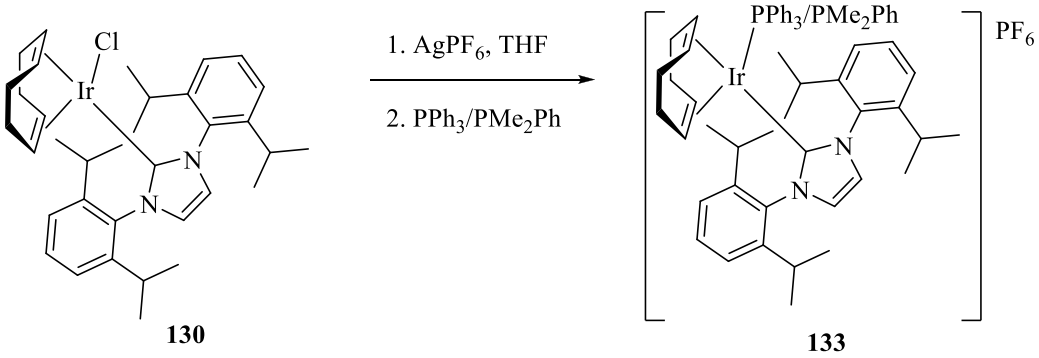

Scheme 90

It was proposed that the complete complexation of PMe_2Ph to the Ir centre in the previous experiment was likely to have been hindered by the presence of PPh_3. In an attempt to aid the

reaction between the smaller phosphine and the metal, the preparation of complex **134** was undertaken as depicted below in **Scheme 91**, without any complications owing to the larger phosphine ligand.

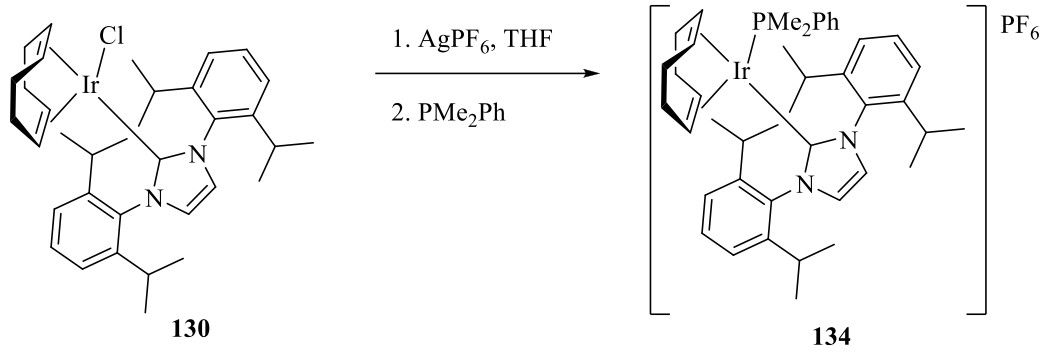

Scheme 91

Pleasingly, the characteristic orange to red colour change expected upon addition of the phosphine was observed. Having stated this, removal of the solvent yielded a yellow gummy residue which, in previous experiments, has indicated the presence of a number of impurities. Indeed, analysis by ^{31}P NMR revealed that, once again, incomplete complexation of PMe_2Ph to the Ir centre had occurred. Recrystallisation techniques were employed in an attempt to separate the desired complex from the unbound phosphine, however, such efforts were deemed unsuccessful.

*Preparation of η^4-Cycloocta-1,5-diene(1,3-dicyclohexylimidazoline-2-ylidene) (triphenylphosphine)iridium(I) Hexafluorophosphate **124***

Undeterred by the disappointing results obtained in the attempted preparation of Ir(I) complexes bearing the sterically encumbered IPr ligand, attention turned to the synthesis of complexes bearing significantly smaller cyclohexyl substituents on the NHC. To our delight, the formation of complex **124** was successfully achieved following the second stage of the

originally employed synthetic route (**Scheme 92**). Thus, upon addition of $AgPF_6$ to Ir(COD)(ICy)Cl **131**, the clear yellow solution turned orange with simultaneous formation of a precipitate. Following filtration under argon, addition of PPh_3 caused the clear orange solution to turn red. The desired product was isolated by recrystallisation techniques, producing novel complex **124** as a bright red solid. As the results shown below in **Table 78** illustrate, the initial preparation of complex **124** delivered the desired product in a relatively low 19% yield (Entry 1). Subsequent attempts at the synthesis of this complex saw a significant enhancement in the quantities of material obtained, with the highest yield attained being a good 75% (Entry 4).

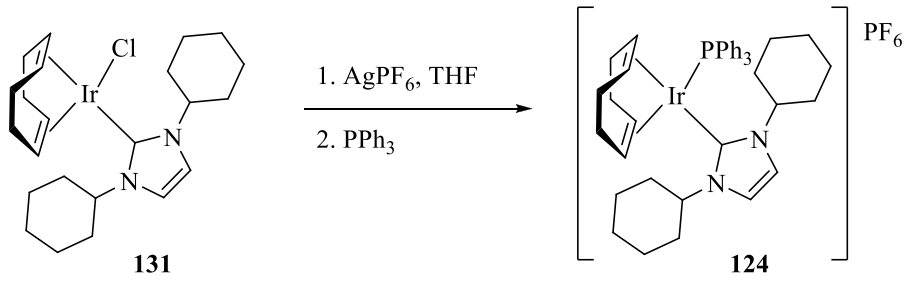

Scheme 92

Entry	Yield of **124**
1	19
2	58
3	69
4	75

Table 78

In an analogous manner to complexes **75**, **81** and **82**, the structure of **124** was confirmed by X-ray crystallography (**Figure 31**; see Appendix 8.1). To our delight, the bond lengths and angles observed were in agreement with the corresponding values noted in the former complexes.[35] Furthermore, comparison of the crystal data with that of the parent imidazolium

salt revealed a number of trends which had previously been reported by Arduengo during the identification of free carbene **100**.[51] Firstly, the N(1)-C(9) bond length of 1.370 Å is found to be slightly longer than the equivalent bond length in the parent imidazolium salt (1.324 Å).[60] In addition, the N(1)-C(9)-N(2) angle of 103.9° is consistent with that expected in singlet carbenes possessing π-donating substituents (100-110°).[61]

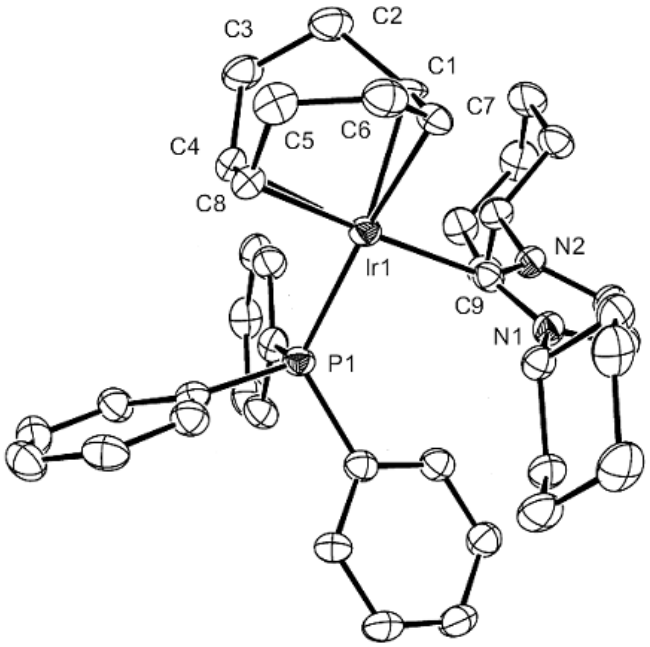

Figure 31

*Preparation of η^4-Cycloocta-1,5-diene(1,3-dicyclohexylimidazoline-2-ylidene) (tribenzylphosphine)iridium(I) Hexafluorophosphate **135***

Extremely pleased that the preparation of complex **124** had proceeded without incident, focus turned to the analogous tribenzylphosphine complex **135** (**Scheme 93**). Again, addition of the phosphine to the coordinatively unsaturated Ir species resulted in the characteristic orange to red colour change. Isolation of the desired product was achieved through recrystallisation techniques, initially furnishing complex **135** in a respectable 57% yield (**Table 79**, Entry 1).

Pleasingly, further attempts at the synthesis of complex **135** resulted in elevated yields of up to 77% being obtained (Entries 2, 3 and 4).

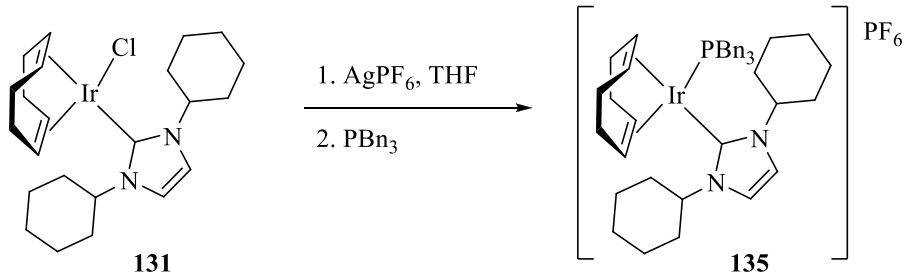

Scheme 93

Entry	Yield of **135**
1	57
2	62
3	68
4	77

Table 79

The formation of [Ir(COD)(PBn_3)(ICy)]PF_6 **135** was also confirmed by X-ray crystallography (**Figure 32**; see Appendix 8.2). Pleasingly, values of a similar magnitude as those recorded in the crystal structure of complex **124** were obtained; the N(1)-C(9) bond length of 1.360 Å is suitably longer than the equivalent length of 1.324 Å in the isolated imidazolium salt,[60] with the N(1)-C(9)-N(2) bond angle of 104.8° also falling within the expected range of 100-110°.[61] It should be noted that due to the solvents used in the recrystallisation of this complex, small amounts of Et_2O and H_2O were found to be present within the crystals analysed by this technique. A slight amount of disorder is therefore observed in the PF_6 unit, as well as in one of the benzyl substituents, however, such disorder is not proposed to affect the overall structure of the complex.

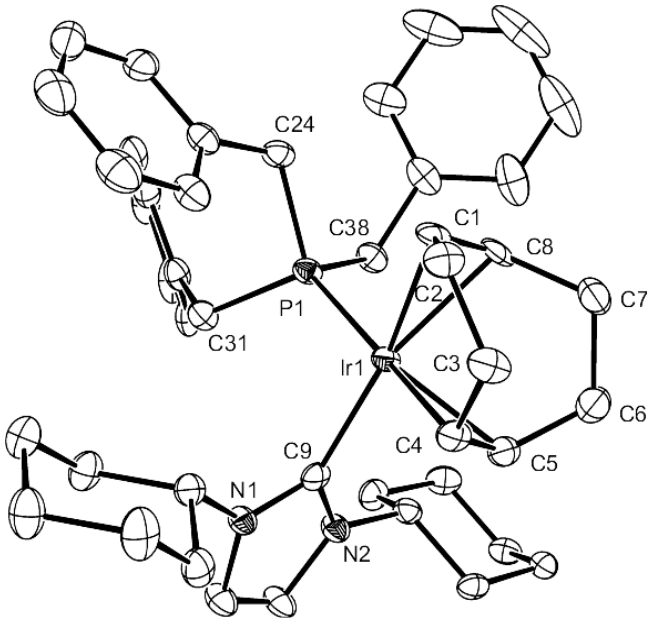

Figure 32

*Preparation of η^4-Cycloocta-1,5-diene(1,3-dicyclohexylimidazoline-2-ylidene) (dimethylphenylphosphine)iridium(I) Hexafluorophosphate **136***

Investigations into the synthesis of complexes bearing the ICy ligand were completed with the formation of complex **136**, pairing the smallest NHC with the smallest phosphine, dimethylphenylphosphine. Following the procedure depicted below in **Scheme 94**, a bright red solution was obtained upon addition of PMe_2Ph. Removal of the solvent gave a red solid, however, inspection of the ^{31}P NMR spectrum corresponding to this material revealed the presence of free phosphine, indicating incomplete complexation of the incoming ligand.

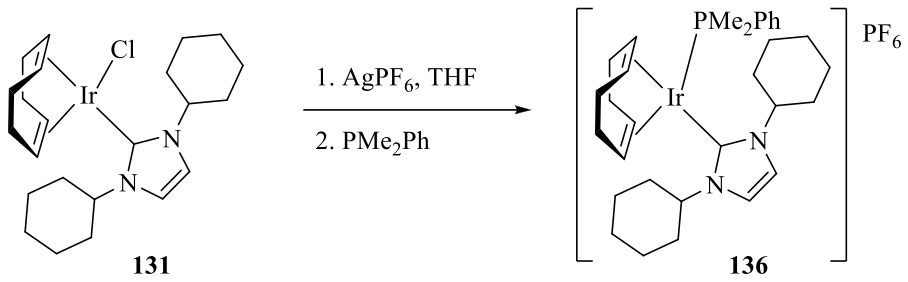

Scheme 94

As the synthesis of complexes **124** and **135** had involved stirring the solution overnight following the addition of the phosphine, it was anticipated that similar conditions may be required for the successful preparation of complex **136**. Having stated this, previous work within our laboratory had revealed complexes bearing dimethylphenylphosphine to be unstable in solution; the conditions for the synthesis of [Ir(COD)(PMe_2Ph)(IMes)]PF_6 **82** requiring a maximum reaction time of 2 hours.[34] Consequently, it was deemed unfavourable to extend the reaction time in the present experimental investigation. Efforts to promote the formation of complex **136** therefore centred on a slight modification to the original synthetic procedure. As opposed to introducing the phosphine to the coordinatively unsaturated Ir species, it was proposed that the incoming ligand should be present in the reaction solution prior to abstraction of the halide by $AgPF_6$. Thus, the reaction was carried out under such conditions as outlined in **Scheme 95**.

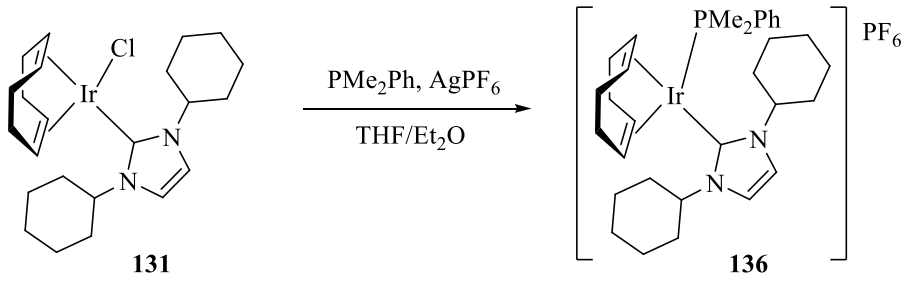

Scheme 95

Pleasingly, upon addition of $AgPF_6$ to a solution of Ir(COD)(ICy)Cl **131** and PMe_2Ph, the distinct orange to red colour change was observed. After stirring for a short period of time, Et_2O was added to the reaction mixture to precipitate the complex from solution, removing any soluble impurities. The resulting red precipitate was then collected *via* filtration through celite under argon and, following recrystallisation techniques, the desired product was isolated as a bright red solid in a moderate 51% yield (**Table 80**, Entry 1). Increased quantities of complex **136** were again obtained upon repetition of the reaction, delivering the novel Ir(I) complex in up to a respectable 62% yield (Entry 4).

Entry	Yield of **136**
1	51
2	57
3	59
4	62

Table 80

The X-ray crystal structure of complex **136** is shown below in **Figure 33** (see Appendix 8.3). Once again, the N(1)-C(1) bond length of 1.358 Å and N(1)-C(1)-N(2) angle of 104.7° are deemed to be of appropriate magnitude for a complex of this type.[51,60,61] It should also be noted that, in each of the three crystal structures obtained, similar bond lengths of approximately 2.203 Å and 2.204 Å were found between the iridium centre and the carbon atoms of the COD ligands opposite the phosphine and NHC ligands, respectively. Such similar values indicate that these ligands exhibit comparable *trans*-directing abilities, and could therefore be considered equivalent in terms of their electron-donation potential.

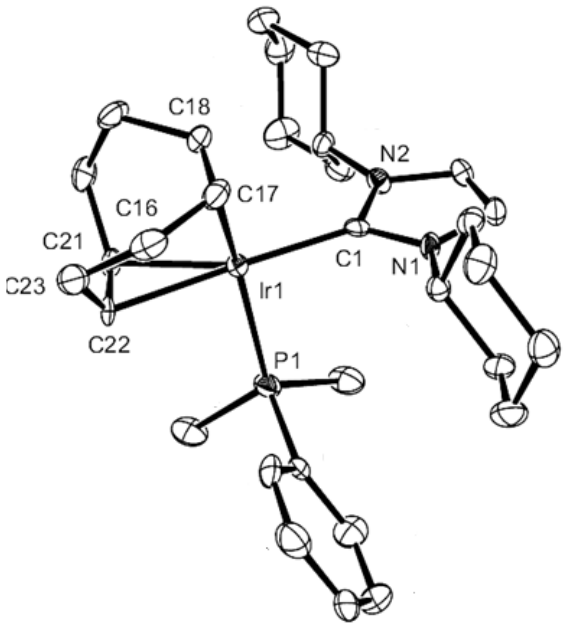

Figure 33

With the complete series of complexes bearing the ICy NHC in hand, focus turned to the preparation of complexes pairing tertiary phosphines with the *N*-benzyl substituted NHC ligand.

Preparation of η^4-Cycloocta-1,5-diene(1,3-dibenzylimidazoline-2-ylidene) (triphenylphosphine)iridium(I) Hexafluorophosphate ***125***

In an analogous manner to previous investigations performed as part of this field of research, explorations began with the attempted synthesis of the triphenylphosphine-containing complex **125**. To our disappointment, returning to the original preparative route proved unsuccessful in this instance as, despite observing the desired orange to red colour change, removal of the solvent at the final stage of the synthesis yielded a sticky red solid. ^{1}H NMR analysis revealed excess protons in the aromatic region; the presence of unreacted triphenylphosphine was confirmed by ^{31}P NMR analysis.

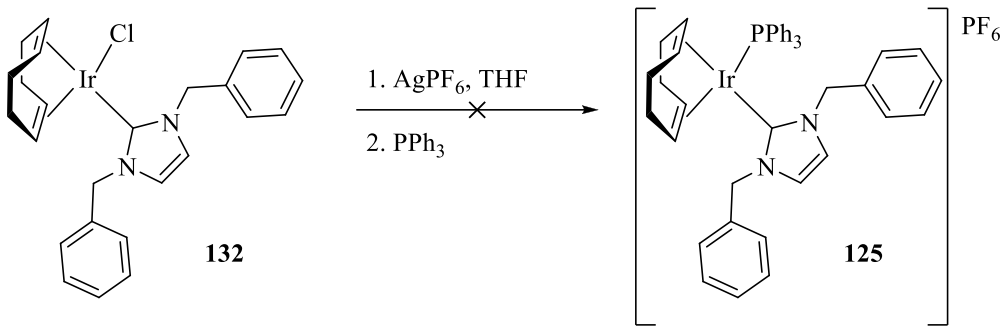

Scheme 96

As limited complexation of triphenylphosphine to the metal centre had occurred, the synthesis of complex **125** was repeated and the solution stirred for an extended period of time following addition of PPh_3. Although the solution remained red, indicating no decomposition had taken place, analysis by ^{1}H and ^{31}P NMR once again revealed the presence of unbound phosphine.

As adding the phosphine to the solution containing the Ir(COD)(NHC)Cl intermediate had proved favourable in the synthesis of complex **136**, it was proposed that an analogous method may provide some success in the formation of complex **125**. Thus, the preparation of complex **125** was repeated as detailed in **Scheme 97**. Following addition of PPh_3 to a solution of **132**, $AgPF_6$ was added causing a distinct yellow to red colour change. After stirring overnight, the solution was filtered through celite under argon, ultimately leading to the formation of a red solid. While ^{1}H NMR analysis of the crude material indicated compound **125** to be present, a number of peaks corresponding to starting material **132** were also visible. The red solid was therefore triturated with Et_2O, and recrystallisation techniques were employed to isolate the desired compound in a respectable 45% yield.

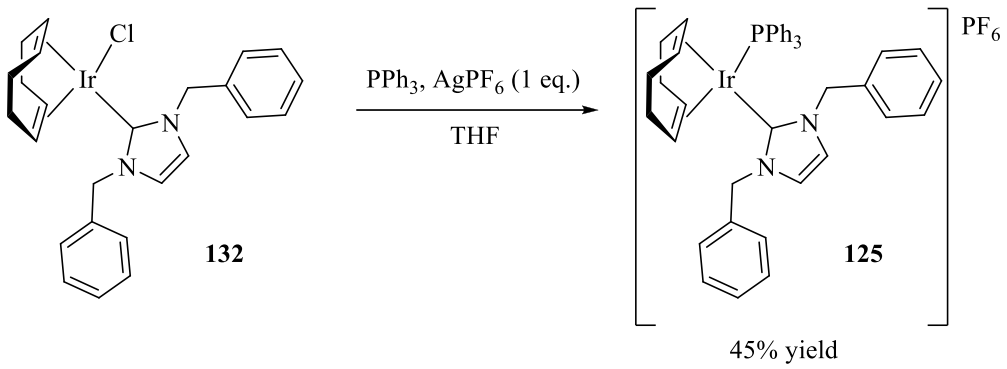

Scheme 97

In an attempt to promote the formation of complex **125** further, a subsequent reaction employed an increased quantity of $AgPF_6$, to ensure complete abstraction of the halide (**Scheme 98**). Pleasingly, recrystallisation of the crude material from DCM/Et_2O delivered only the desired product in an acceptable 53% yield (**Table 81**, Entry 1), with no evidence implying the presence of compound **132**. Upon repetition of this slightly modified synthesis, increased quantities of material were obtained, furnishing the desired complex **125** in enhanced yields of up to 83%.

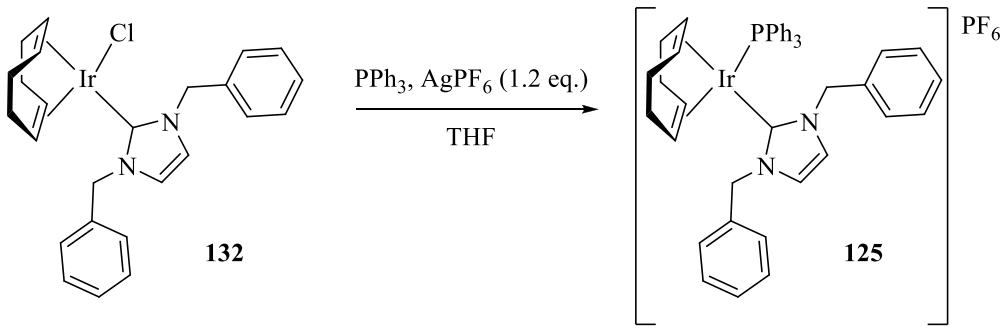

Scheme 98

Entry	Yield of **125**
1	53
2	74
3	83

Table 81

*Preparation of η^4-Cycloocta-1,5-diene(1,3-dibenzylimidazoline-2-ylidene) (tribenzylphosphine)iridium(I) Hexafluorophosphate **137***

With the first of the benzyl-substituted NHC complexes in hand, attention turned to the preparation of the tribenzylphosphine analogue of this series **137** (**Scheme 99**). Pleasingly, upon addition of $AgPF_6$ to a solution of Ir(COD)(IBn)Cl **132** and PBn_3, a distinct yellow to red colour change was observed. Following filtration and removal of the solvent, a red gum was obtained, the ^1H NMR of which revealed the presence of a number of impurities. Attempts to purify the product focused on the routinely employed recrystallisation techniques, however the material remained gum-like, with no changes in the ^1H NMR spectrum being detected.

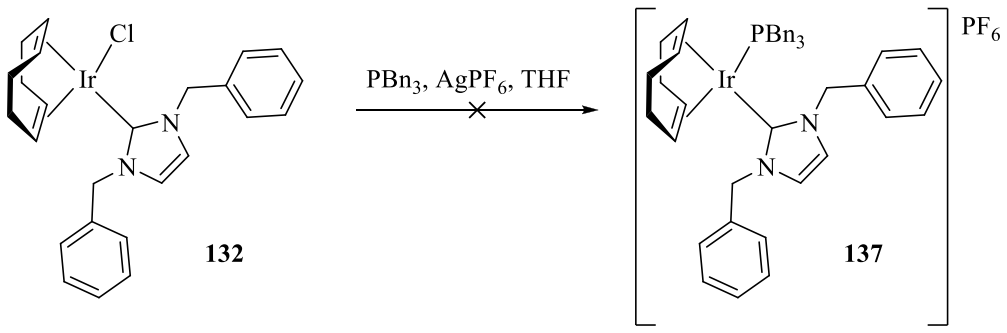

Scheme 99

A second attempt at the synthesis of complex **137** involved adding Et_2O to the solution prior to filtration to aid precipitation of the desired product (**Scheme 100**). Pleasingly, a red solid precipitated from the solution and was subsequently collected and purified, delivering the desired product **137** in a respectable 34% yield.

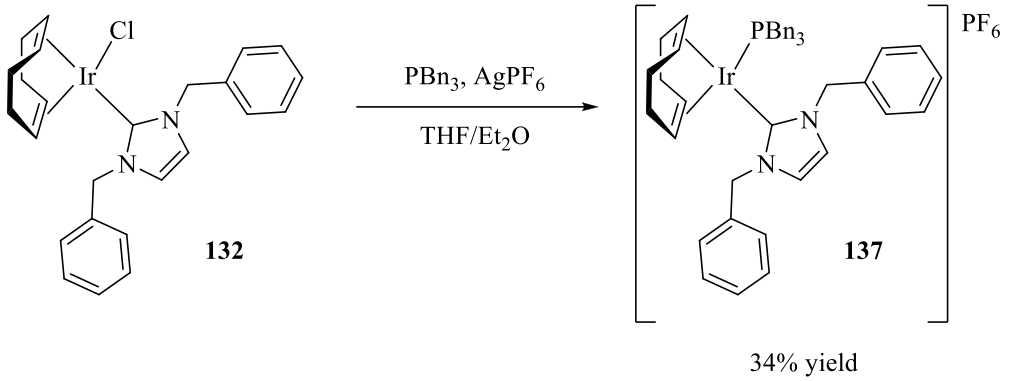

Scheme 100

*Preparation of η^4-Cycloocta-1,5-diene(1,3-dibenzylimidazoline-2-ylidene) (dimethylphenylphosphine)iridium(I) Hexafluorophosphate **138***

Pleased that the synthesis of complex **137** had been achieved, attention turned to the preparation of the final catalyst of this series, bearing the smaller dimethylphenylphosphine. Following the now routinely employed synthetic route as depicted in **Scheme 101**, addition of PMe_2Ph to a solution of compound **132** caused a slight yellow to orange colour change, indicating a small degree of substitution of the halide by the phosphine may have occurred in the absence of $AgPF_6$. Nonetheless, the transition metal salt was added, resulting in the formation of a bright red solution. After some time, a red precipitate became visible which was collected during the subsequent filtration process. Analysis of this material revealed it to be the desired product, with only minor impurities present. Recrystallisation techniques were therefore employed, yielding complex **138** in a respectable 45% yield (**Table 82**, Entry 1). While analysis of the red filtrate obtained also revealed the presence of the desired product, recrystallisation techniques to isolate such material were unsuccessful. Pleasingly, repeated

attempts at the preparation of complex **138** saw a steady increase in the yields of material obtained, the final synthesis delivering the desired product in a good 67% yield (Entry 6).

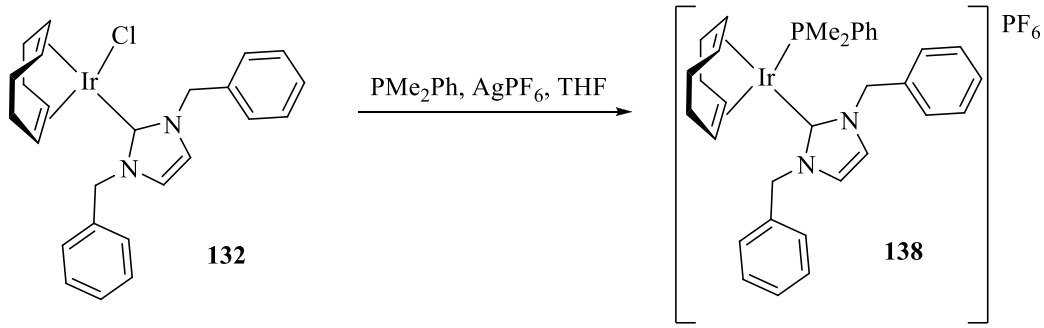

Scheme 101

Entry	Yield of **138**
1	45
2	48
3	54
4	54
5	57
6	67

Table 82

3.5 Application of Novel Ir(I) Complexes in Hydrogen Isotope Exchange

Having successfully prepared the desired Ir(I) complexes bearing different NHC ligands, attention turned to the application of such novel catalysts in hydrogen isotope exchange reactions. The first complex selected was **135**, pairing the bulkiest phosphine, tribenzylphosphine, with the least sterically encumbered NHC, ICy. In an analogous manner

to catalyst activity studies carried out previously, investigations began with the labelling of acetophenone **54** in DCM (**Scheme 102**). As the results shown in **Table 83** illustrate, the excellent levels of isotope incorporation observed after 16 hours (Entry 1) were maintained when the reaction time was reduced considerably to just 1 hour (Entry 3).

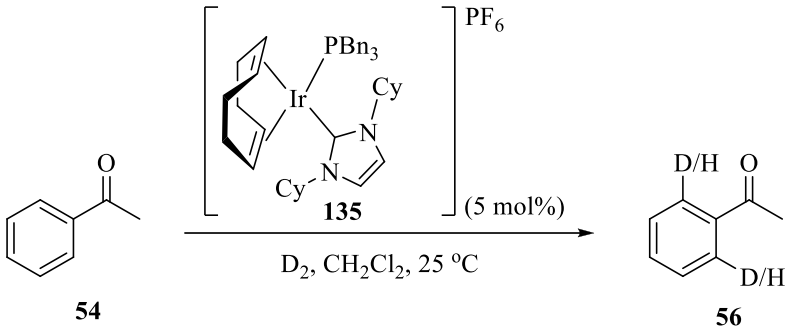

Scheme 102

Entry	Time (h)	% Deuteration	
		Run 1	Run 2
1	16	98	97
2	2	95	94
3	1	97	93

Table 83

The next step in this optimisation process was to determine the lowest catalyst loading which could be employed to facilitate high levels of H-D exchange. Pleasingly, halving the amount of catalyst had no detrimental effect on the deuteration observed after the allotted reaction time (**Table 84**, Entry 1). While the levels of D incorporation achieved with a further reduced catalyst loading to 0.5 mol% were still high (Entry 2), it was proposed that running the reaction for another hour would elevate the incorporation attained further. Indeed, leaving the reaction for 2 hours delivered levels of exchange comparable to those obtained at higher catalyst loadings (Entry 3).

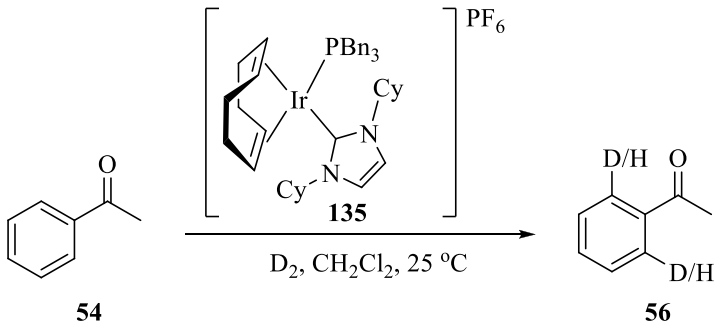

Scheme 103

Entry	Catalyst Loading (mol%)	Time (h)	% Deuteration	
			Run 1	Run 2
1	2.5	1	97	97
2	0.5	1	82	89
3	0.5	2	97	94

Table 84

With the optimised conditions for the use of complex **135** in HIE reactions in hand, focus turned to the second catalyst of this series, **124**. Again, a short time study revealed that in reactions employing 5 mol% of complex **124**, excellent levels of deuteration were observed even after a short reaction time of 1 hour (**Scheme 104**, **Table 85**).

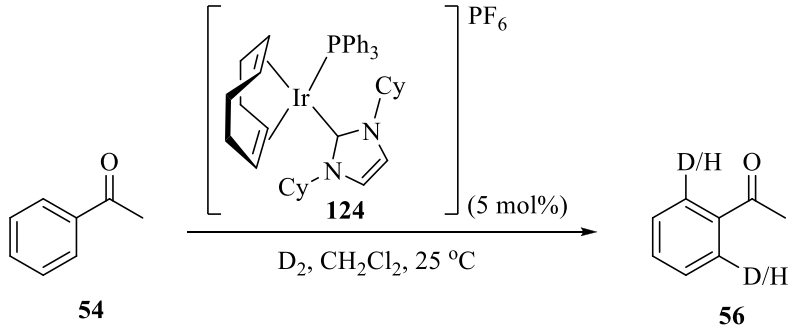

Scheme 104

Entry	Time (h)	% Deuteration	
		Run 1	Run 2
1	16	98	96
2	2	97	97
3	1	96	92

Table 85

Further investigations of H-D exchange reactions employing complex **124** indicated that, akin to the IMes series of catalysts,[35] the activity of **124** was slightly lower than that of its tribenzylphosphine analogue **135**. Upon decreasing the catalyst loading from 2.5 mol% to 0.5 mol%, a substantial reduction in isotope incorporation from 96% to 77% was observed (**Table 86**, Entries 1 and 2). Increasing the reaction time to 2 hours did improve the levels of H-D exchange obtained (Entry 3), however to achieve optimum results, a catalyst loading of 1 mol% was required, with the originally selected 1 hour reaction time (Entry 4).

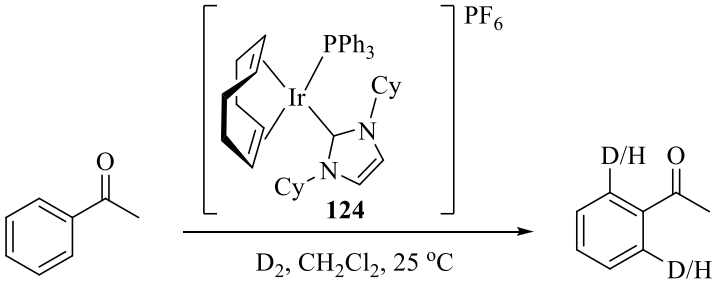

54 **56**

Scheme 105

Entry	Catalyst Loading (mol%)	Time (h)	% Deuteration	
			Run 1	Run 2
1	2.5	1	94	96
2	0.5	1	77	74
3	0.5	2	87	86
4	1	1	96	96

Table 86

The activity of the final complex of this series **136**, pairing dimethylphenylphosphine with ICy, was also examined through a series of optimisation experiments. Once more, the high level of D incorporation achieved was found to be maintained when the reaction time was reduced from 16 hours to 1 hour (**Scheme 106**, **Table 87**).

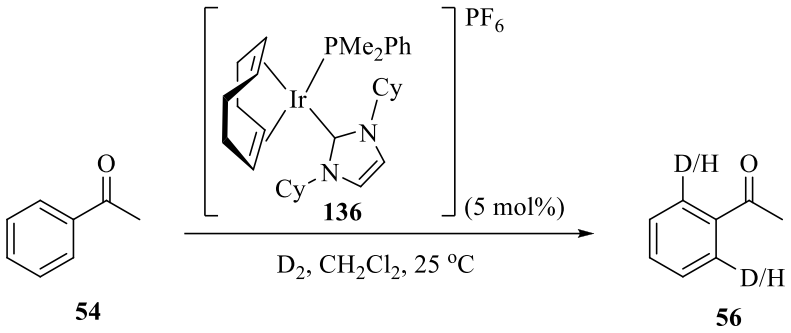

Scheme 106

Entry	Time (h)	% Deuteration	
		Run 1	Run 2
1	16	96	97
2	2	97	98
3	1	97	97

Table 87

In contrast to the results obtained previously with complexes **135** and **124**, reactions employing 3 mol% of complex **136** delivered a slightly diminished level of H-D exchange of up to 88% (**Scheme 107**, **Table 88**, Entry 1). Further probing of the reaction conditions illustrated the need for an extended reaction time, with excellent levels of D incorporation being again achieved after 2 hours at this lower catalyst loading (Entry 2). Unfortunately, reducing the quantity of catalyst further to 1 mol% led to a dramatic decrease in D loading, delivering the isotopically-enriched product in up to a moderate 61% (Entry 3). Despite increased levels of deuteration being achieved when 2 mol% of complex **136** was employed in the reaction (Entry 4), it was decided that for the forthcoming labelling of somewhat more

demanding substrates, the optimum conditions for the use of complex **136** should be selected as a catalyst loading of 3 mol%, and reaction time of 2 hours.

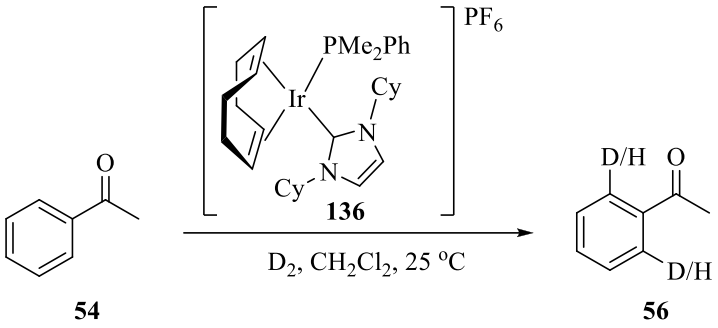

Scheme 107

Entry	Catalyst Loading (mol%)	Time (h)	% Deuteration	
			Run 1	Run 2
1	3	1	85	88
2	3	2	97	96
3	1	2	61	52
4	2	2	91	94

Table 88

Satisfied that a robust and reliable set of conditions had now been developed for the use of complexes of the type [Ir(COD)(ICy)(PR_3)]PF_6 in HIE reactions, attention turned to the second series of complexes which had successfully been prepared, bearing benzyl substituents on the NHC ligand. To date, no details have been reported regarding the steric influence imparted by the IBn NHC ligand within Ir complexes. Having stated this, Nolan has investigated $\%V_{bur}$ values for NHCs in complexes of the type [(NHC)AgCl].[54] The measurement of such coefficients has revealed the benzyl-substituted NHC ligand to display steric properties between those presented by the two alternative NHC ligands investigated as part of this research programme. More specifically, IBn gave rise to an average $\%V_{bur}$ of 30, while the smaller cyclohexyl-substituted NHC ligand displayed a value of 25.8. Unsurprisingly, the $\%V_{bur}$ calculated for the largest NHC employed in this study, IMes, was notably higher at 33.5. It should be stated at this point that, as a result of the time at which

complex **137**, pairing tribenzylphosphine with the IBn ligand, was prepared, and the relatively small quantity which was synthesised, no investigations regarding the application of this catalyst in HIE reactions have been performed. Having stated this, complexes **125** and **138**, bearing the benzyl-substituted NHC in conjunction with triphenylphosphine and dimethylphenylphosphine, respectively, were employed in H-D exchange studies. The initial results obtained within such reactions were extremely encouraging, as the labelling of acetophenone **54** with 5 mol% of complex **125** was found to be essentially complete after only 30 minutes (**Scheme 108**, **Table 89**).

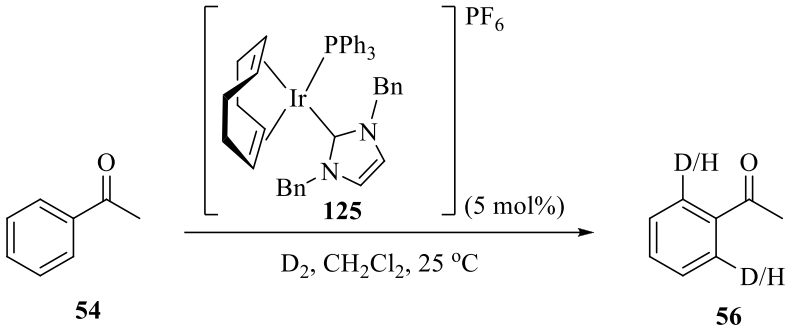

Scheme 108

Entry	Time (h)	% Deuteration	
		Run 1	Run 2
1	16	98	97
2	2	98	98
3	1	98	97
4	0.5	94	93

Table 89

Additional success was achieved in reactions employing decreased quantities of complex **125** (**Table 90**). At a catalyst loading of 3 mol%, deuteration levels equivalent to those previously obtained at the higher catalyst loading of 5 mol% were maintained (Entry 1), while reducing the amount of catalyst further to 1 mol% resulted in only a slight lowering of H-D exchange (Entry 2). As no increase in isotope incorporation was observed in reactions run for 1 hour

(Entry 3), the reaction time was extended to 2 hours, furnishing the desired labelled product with a high 97% incorporation (Entry 4).

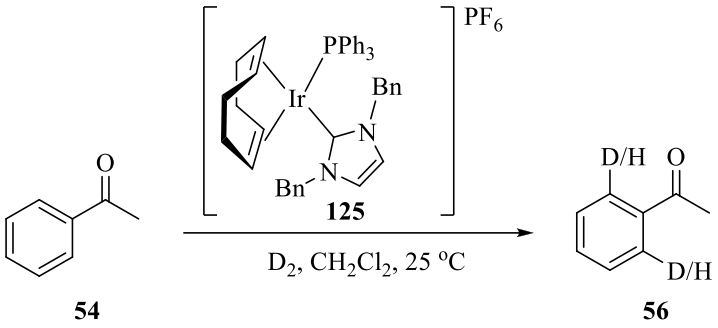

Scheme 109

Entry	Catalyst Loading (mol%)	Time (h)	% Deuteration	
			Run 1	Run 2
1	3	0.5	88	96
2	1	0.5	86	92
3	1	1	87	90
4	1	2	95	97

Table 90

The last complex to be investigated was **138**, pairing dimethylphenylphosphine with the NHC ligand IBn. Once again, as illustrated in **Table 91**, the reaction time could be reduced from 16 hours to just 30 minutes with no loss of D incorporation detected.

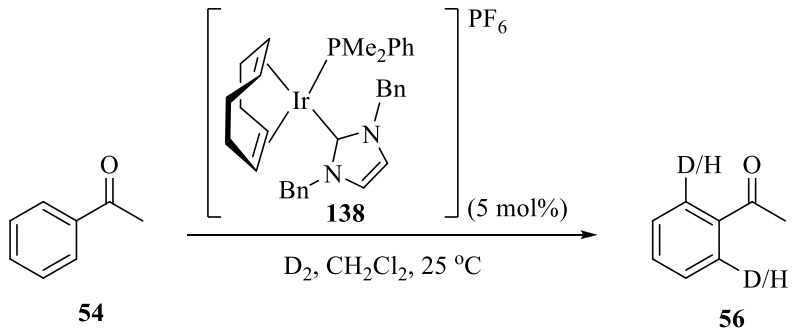

Scheme 110

Entry	Time (h)	% Deuteration	
		Run 1	Run 2
1	16	96	94
2	2	97	96
3	1	98	95
4	0.5	94	96

Table 91

Pleasingly, such high levels of deuteration were maintained after this extremely short reaction time when the catalyst loading was reduced to 3 mol% (**Scheme 111**, **Table 92**, Entry 1). Although lowering the quantity of complex **138** employed in the reaction to 1 mol% did result in a slight decrease in the levels of D incorporation observed, the degree of H-D exchange was still considered very high at up to 87% deuteration (Entry 2). Efforts to promote the labelling of compound **54** in the presence of this lower catalyst loading by running the reaction for extended periods of time were unsuccessful (Entries 3 and 4), as was increasing the amount of catalyst to 2 mol% over a 1 hour reaction time (Entry 5). In each case, the levels of D incorporation attained remained at approximately 83%. In view of these outcomes, the optimum conditions for employing complex **138** in HIE were selected as a catalyst loading of 3 mol%, and a reaction time of 30 minutes.

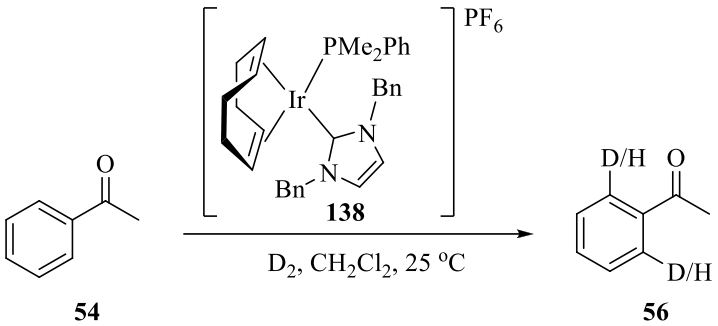

Scheme 111

Entry	Catalyst Loading (mol%)	Time (h)	% Deuteration	
			Run 1	Run 2
1	3	0.5	96	96
2	1	0.5	81	87
3	1	1	81	83
4	1	2	84	83
5	2	1	83	88

Table 92

By systematically altering both the catalyst loading and reaction time, optimised conditions for the use of novel Ir(I) complexes in hydrogen isotope exchange reactions have been developed. In the majority of instances, excellent levels of isotope incorporation were achieved using notably low levels of catalyst loading and short reaction times. A summary of the results as shown in **Table 93** reveal that, of the novel Ir(I) complexes prepared as part of this programme, complex **135** displays the highest activity, operating at the lowest catalyst loading of 0.5 mol%. In contrast, complexes bearing the small dimethylphenylphosphine appear to require slightly higher catalyst loadings of 3 mol% to facilitate H-D exchange to an equivalent level. Another point of interest is the extended time required in reactions employing complex **136**, exposing this catalyst as the least active of the series prepared thus far. Such a result may be somewhat unsurprising, as this complex pairs the smallest phosphine with the smallest NHC ligand, a situation which is likely to be unfavourable in the reductive elimination step of the mechanistic cycle. In addition, the strong electron-donating properties of the same ligands will render the Lewis acidic metal centre of this complex as the most electron-rich, which may impede complexation of the incoming substrate.

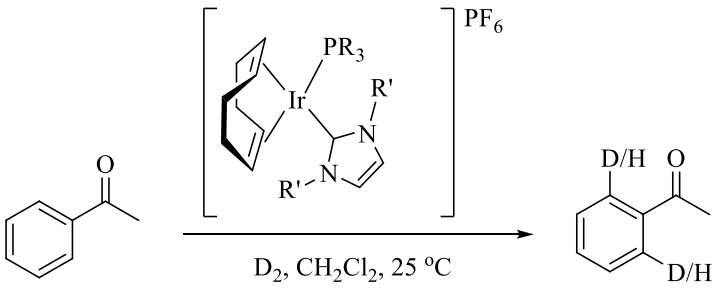

54 **56**

Scheme 112

Complex	PR_3	NHC	Conditions	% Deuteration
135	PBn_3	ICy	0.5 mol%, 2 h	97
124	PPh_3	ICy	1 mol%, 1 h	96
136	PMe_2Ph	ICy	3 mol%, 2 h	97
125	PPh_3	IBn	1 mol%, 2 h	97
138	PMe_2Ph	IBn	3 mol%, 0.5 h	96

Table 93

3.6 Application of Novel Ir(I) Complexes in HIE Reactions for Labelling Alternative Substrates

Following the identification of the optimised conditions, attention turned to the application of such systems in the isotopic labelling of other substrates, the first of which examined was benzophenone **57** (**Scheme 113**). As detailed in earlier, compound **57** is labelled in an analogous fashion to acetophenone, *via* a 5-mmi through coordination of the carbonyl functional group to the iridium centre. The main difference between these two substrates is, therefore, the increased number of positions at which H-D exchange can occur in benzophenone.

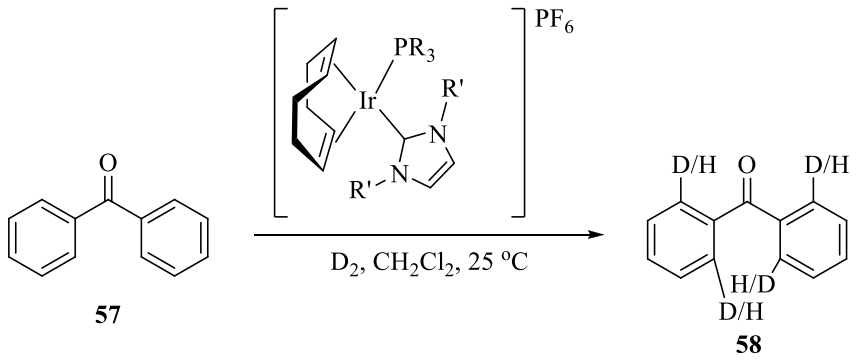

57 **58**

Scheme 113

Entry	Complex	PR_3	NHC	Conditions	% Deuteration	
					Run 1	Run 2
1	**135**	PBn_3	ICy	0.5 mol%, 2 h	71	71
2				5 mol%, 16 h	93	94
3	**124**	PPh_3	ICy	1 mol%, 1 h	79	83
4	**136**	PMe_2Ph	ICy	3 mol%, 2 h	51	51
5				5 mol%, 16 h	85	86
6	**125**	PPh_3	IBn	1 mol%, 2 h	86	87
7	**138**	PMe_2Ph	IBn	3 mol%, 0.5 h	61	58
8				5 mol%, 16 h	85	88

Table 94

As illustrated by the results shown in **Table 94**, moderate to high levels of deuterium incorporation were achieved with each complex under the newly identified optimum conditions. In three of the five cases, it was proposed that the degree of deuteration observed could be improved by performing the reactions with slightly increased quantities of catalyst and extended reaction times. Indeed, repeating reactions employing complexes **135**, **136**, and **138** with a catalyst loading of 5 mol% and a reaction time of 16 hours proved extremely

favourable, delivering the isotopically enriched product **58** with enhanced levels of between 85 and 94% D incorporation (Entries 2, 5 and 8).

The second substrate to be examined as part of this study was the heterocyclic compound 2-phenylpyridine **41** (**Scheme 114**). Unfortunately, the initial results obtained with complex **135** were disappointing, delivering the isotopically labelled product **42** in a poor 2% deuteration (**Table 95**, Entry 1). Increasing the catalyst loading to 5 mol% and extending the reaction time to 16 hours proved to be extremely favourable however, enhancing the levels of D incorporation observed to an excellent 98% (Entry 2). Similar results were obtained with complexes **124** and **125**, each requiring slightly greater quantities of catalyst and longer reaction times to deliver the desired compound **42** with high degrees of deuteration. (Entries 4 and 7).

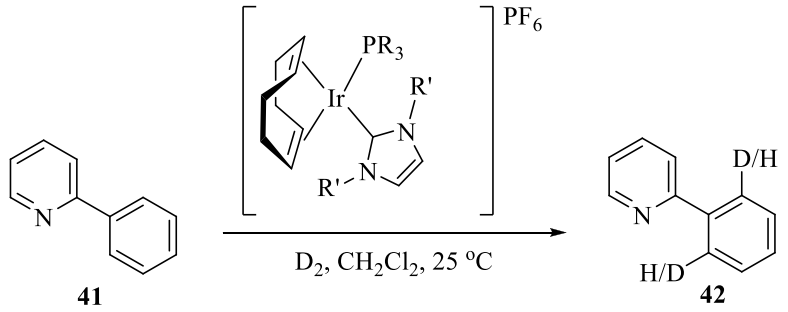

Scheme 114

Entry	Complex	PR_3	NHC	Conditions	% Deuteration	
					Run 1	Run 2
1	**135**	PBn_3	ICy	0.5 mol%, 2 h	2	2
2				5 mol%, 16 h	98	98
3	**124**	PPh_3	ICy	1 mol%, 1 h	3	6
4				5 mol%, 16 h	99	99
5	**136**	PMe_2Ph	ICy	3 mol%, 2 h	91	96
6	**125**	PPh_3	IBn	1 mol%, 2 h	14	16
7				5 mol%, 16 h	97	94
8	**138**	PMe_2Ph	IBn	3 mol%, 0.5 h	90	95

Table 95

Comparison of the results shown in **Table 95** reveals that, in the majority of cases, the isotopic labelling of 2-phenylpyridine **41** under the previously identified optimum conditions proceeds to only poor levels of deuterium incorporation (Entries 1, 3 and 6). Having stated this, reactions employing complexes **136** and **138** deliver the desired isotopically-enriched compound **42** with excellent degrees of deuteration (Entries 5 and 8). Conditions for such reactions utilise a slightly higher catalyst loading of 3 mol%, which may explain the increased levels of deuterium incorporation observed. In an effort to probe the activity of complexes **136** and **138** further, the labelling of substrate **41** was repeated with reduced quantities of each catalyst (**Scheme 115**). In both instances, decreasing the catalyst loading to 2 mol% caused no significant deterioration in the incorporation attained (**Table 96**, Entries 1 and 3). In contrast, reactions employing just 1 mol% of catalyst delivered compound **42** with extremely poor levels of labelling of between 0 and 6% (Entries 2 and 4). In view of these findings, it can be concluded that complexes **136** and **138** do not display a higher reactivity in the labelling of substrate **41**, and the previously low results obtained with complexes **135**, **124** and **125** are attributable to the reduced amount of catalyst present within the system.

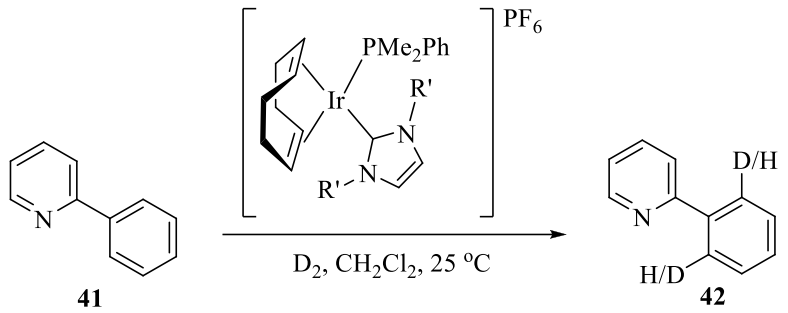

Scheme 115

Entry	Complex	NHC	Conditions	% Deuteration	
				Run 1	Run 2
1	**136**	ICy	2 mol%, 2 h	95	97
2			1 mol%, 2 h	6	2
3	**138**	IBn	2 mol%, 0.5 h	89	93
4			1 mol%, 0.5 h	0	5

Table 96

Investigations into H-D exchange reactions of heterocyclic compounds continued with the labelling of *N*-phenylpyrazole **79** (**Scheme 116**, **Table 97**). Pleasingly, the results obtained with the ICy series of complexes were highly encouraging, delivering the isotopically-enriched product **80** with excellent deuterium incorporations of between 91 and 99% (Entries 1, 2 and 3). In contrast, the labelling of substrate **79** with complex **125** proceeded to only moderate levels of exchange of up to 73%, while reactions employing complex **138** delivered poor incorporations of up to 11% (Entries 4 and 6). Pleasingly, repeating the latter reactions with increased catalyst loadings of 5 mol% and extended reaction times of 16 hours delivered excellent levels of deuteration comparable to those obtained under the optimum conditions with complexes bearing cyclohexyl substituents on the NHC (Entries 5 and 7).

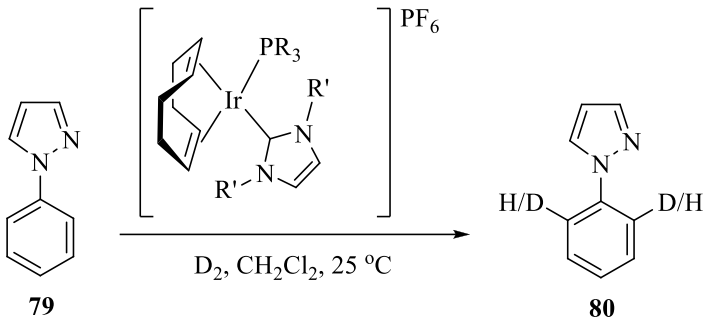

Scheme 116

Entry	Complex	PR_3	NHC	Conditions	% Deuteration	
					Run 1	Run 2
1	**135**	PBn_3	ICy	0.5 mol%, 2 h	98	98
2	**124**	PPh_3	ICy	1 mol%, 1 h	91	95
3	**136**	PMe_2Ph	ICy	3 mol%, 2 h	98	99
4	**125**	PPh_3	IBn	1 mol%, 2 h	68	73
5				5 mol%, 16 h	94	93
6	**138**	PMe_2Ph	IBn	3 mol%, 0.5 h	11	8
7				5 mol%, 16 h	92	98

Table 97

To demonstrate the wider applicability of these novel Ir(I) complexes, the substrate scope was extended from heterocycles to amides, the first of which examined was benzamide **59** (**Scheme 117**). Previous results obtained in the labelling of substrate **59** with complexes featuring the IMes NHC ligand had revealed a maximum deuterium incorporation of 79% to be achieved in reactions employing 5 mol% of complex **81** over a 16 hour reaction time.[35] In comparison to the deuteration of other substrates examined, this lower degree of H-D exchange is thought to be due to the strong ligating capabilities of substrate **59**. The results displayed in **Table 98** are therefore somewhat unsurprising. With each of the novel

complexes, systems employing low catalyst loadings and short reaction times deliver the isotopically-enriched product **60** with poor D loadings of between 4 and 9%. In an attempt to further promote the labelling of benzamide **59**, reactions were repeated in the presence of a greater quantity of Ir(I) catalyst and over extended periods of time. Unfortunately, the use of these slightly more forcing conditions did not lead to a significant increase in the levels of deuteration detected; the highest degree of exchange observed in systems facilitated by complex **136**, furnishing compound **60** with a relatively low 30% deuteration (Entry 6).

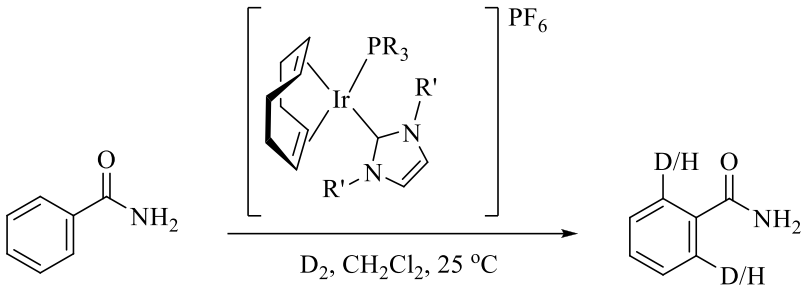

59 **60**

Scheme 117

Entry	Complex	PR_3	NHC	Conditions	% Deuteration	
					Run 1	Run 2
1	**135**	PBn_3	ICy	0.5 mol%, 2 h	6	6
2				5 mol%, 16 h	28	34
3	**124**	PPh_3	ICy	1 mol%, 1 h	7	7
4				5 mol%, 16 h	25	24
5	**136**	PMe_2Ph	ICy	3 mol%, 2 h	7	9
6				5 mol%, 16 h	23	30
7	**125**	PPh_3	IBn	1 mol%, 2 h	4	4
8				5 mol%, 16 h	25	21
9	**138**	PMe_2Ph	IBn	3 mol%, 0.5 h	5	6
10				5 mol%, 16 h	24	20

Table 98

Undeterred by the disappointing results attained in the labelling of benzamide, attention turned to a series of amides bearing alkyl substituents on the amide nitrogen. The first compound of this category to be examined was *N*,*N*,4-trimethylbenzamide **111** (**Scheme 118**). As detailed earlier, isotope incorporation into both the *ortho*-positions of the aromatic ring and the methyl groups on the nitrogen in substrate **111** has previously been observed.[34] As illustrated in **Table 99**, the initial results obtained in reactions facilitated by complexes **135** and **124** were somewhat disappointing, delivering the desired product **114** with a maximum of 11% deuteration in the aromatic ring, with no D incorporation detected in the *N*Me groups (Entries 1 and 3). Such low levels of labelling were presumed to be due to the low quantities of catalyst present in the systems, hence the reactions were repeated under the slightly more forcing conditions employing a 5 mol% catalyst loading and 16 hour reaction time. Pleasingly, the degree of H-D exchange achieved was significantly improved; in each instance, incorporation in the aromatic ring increased to approximately 91%, while labelling in the methyl substituents reached levels of 62% and 20% in reactions catalysed by

complexes **135** and **124**, respectively. In contrast, the previously optimised conditions identified for the use of complex **136** furnished the isotopically-enriched product **114** with moderate levels of deuteration of up to 50% in the aromatic ring only (Entry 5). Subsequent attempts to enhance such levels by increasing both the catalyst loading and reaction time proved to be only slightly beneficial, as D incorporation in the *ortho*-positions improved only marginally to a maximum of 62%, while deuteration in the CH_3 substituent remained minimal (Entry 6).

Results of a similar nature were observed in the labelling of substrate **111** by complexes **125** and **138**, bearing the benzyl-substituted NHC ligand. Under the previously optimised conditions, reactions employing the larger triphenylphosphine-containing complex **125** produced only poor deuterium incorporations of 4% in the aromatic ring, a value which was improved only to respectable levels of up to 73% in the presence of a greater quantity of catalyst and over an extended reaction period (Entries 7 and 8). Conversely, the degree of H-D exchange observed in reactions utilising 3 mol% of complex **138** was detected at moderate levels of 32% in the *ortho*-positions, while analogous reactions performed under slightly more forcing conditions considerably enhanced the deuteration achieved to approximately 90%. Again, it was only at elevated quantities of complex **138** and longer reaction times that any D incorporation into the *N*Me substituents was observed (Entry 10).

The values presented in **Table 99** show that the majority of our novel Ir(I) complexes demonstrate a significant degree of preference for isotope exchange in aryl positions, with low to no incorporation observed in the *N*-methyl substituent. Previous investigations carried out within our laboratory had revealed selectivity of a similar manner, however, in this instance, the level of deuteration detected in the *N*-methyl unit decreased considerably as the cone angle of the phosphine ligand was reduced.[34] In the current study, such a theory may explain the deuterium loadings recorded in reactions facilitated by complexes **135**, **124** and **136**, however, conflicting results were observed in reactions catalysed by complexes **125** and **138**. It is therefore proposed that the degree of selectivity attained in the deuteration of substrate **111** is dependent on a subtle balance of the steric and electronic properties of the

ligands present on the metal centre. Having said this, it should be noted that the high levels of preference displayed by our novel Ir(I) complexes, in comparison with our more sterically encumbered IMes-containing catalysts, may be of significant benefit, offering the potential to selectively label the required positions of analogous substrates by employing the appropriate complex.

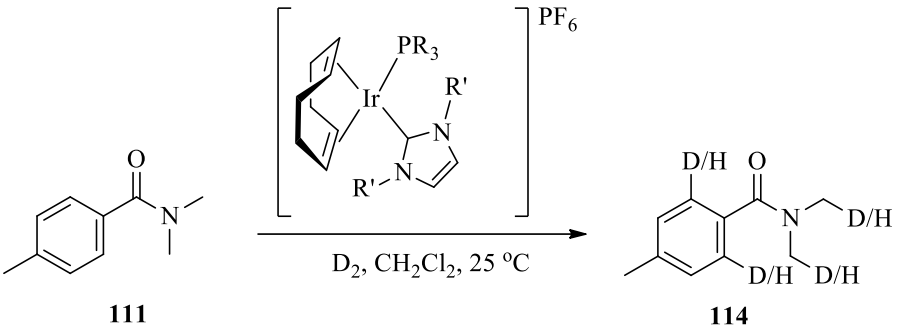

111 **114**

Scheme 118

Entry	Complex	PR_3	NHC	Conditions	% Deuteration			
					Run 1		Run 2	
					ortho	*N*Me	*ortho*	*N*Me
1	**135**	PBn_3	ICy	0.5 mol%, 2 h	7	0	4	0
2				5 mol%, 16 h	91	62	91	61
3	**124**	PPh_3	ICy	1 mol%, 1 h	11	0	7	0
4				5 mol%, 16 h	93	20	90	18
5	**136**	PMe_2Ph	ICy	3 mol%, 2 h	46	0	50	0
6				5 mol%, 16 h	62	2	60	1
7	**125**	PPh_3	IBn	1 mol%, 2 h	4	0	4	0
8				5 mol%, 16 h	68	0	73	0
9	**138**	PMe_2Ph	IBn	3 mol%, 0.5 h	32	0	30	0
10				5 mol%, 16 h	85	4	92	5

Table 99

To determine the effect of increasing the length of the *N*-alkyl substituents on the deuteration levels obtained, the labelling of *N*-ethyl,*N*,4-dimethylbenzamide **112** was investigated (**Scheme 119**). As the results below in **Table 100** reveal, in general, reactions performed under the optimum conditions for each complex provided the isotopically-enriched product **115** with moderate to good levels of D incorporation in the aromatic ring, with deuteration in the methyl substituent observed at between 0 and 6%. In each case, repeating the reactions with a catalyst loading of 5 mol% and reaction time of 16 hours increased the labelling observed to extremely high levels, reaching a maximum of 99% deuteration. Under such conditions, isotope incorporation into the alkyl substituent was noted at moderate levels of approximately 32% in reactions employing complexes **135** and **124**, but remained less than 10% in systems catalysed by complexes **136**, **125** and **138**. No deuteration in the C_2H_5 group was detected in any case. In line with the previously described results regarding the deuteration of substrate **111** (**Table 99**), such values re-emphasise the selective nature of our

new catalyst species, indicating a clear preference for labelling in aryl C-H bonds as opposed to facilitating HIE within the *N*Me unit.

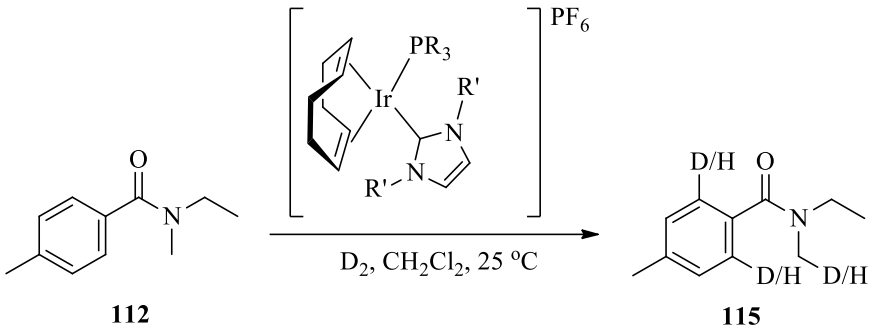

Scheme 119

Entry	Complex	PR_3	NHC	Conditions	% Deuteration			
					Run 1		Run 2	
					ortho	*N*Me	*ortho*	*N*Me
1	**135**	PBn_3	ICy	0.5 mol%, 2 h	34	5	28	6
2				5 mol%, 16 h	94	32	93	35
3	**124**	PPh_3	ICy	1 mol%, 1 h	48	5	52	6
4				5 mol%, 16 h	95	31	96	28
5	**136**	PMe_2Ph	ICy	3 mol%, 2 h	25	6	25	5
6				5 mol%, 16 h	81	8	74	7
7	**125**	PPh_3	IBn	1 mol%, 2 h	41	0	39	0
8				5 mol%, 16 h	99	7	95	9
9	**138**	PMe_2Ph	IBn	3 mol%, 0.5 h	38	3	31	4
10				5 mol%, 16 h	78	4	87	7

Table 100

In line with earlier investigations, the isotopic labelling of *N*,*N*-dialkylsubstituted amides was completed with the deuteration of *N*,*N*-diethyl-4-methylbenzamide **113** (**Scheme 120**). Under the optimum conditions developed for complexes **135** and **136**, only moderate levels of deuteration of between 16 and 37% were attained (**Table** 101, Entries 1 and 4). However, repeating the reactions with a higher catalyst loading of 5 mol% and an extended reaction time of 16 hours delivered the isotopically-enriched product **116** with much improved degrees of exchange of up to an excellent 99% (Entries 2 and 5). In all of the cases reported here no deuteration into the *N*-ethyl units was observed. In contrast, reactions employing the triphenylphosphine analogue of this series of complexes required only a low catalyst loading of 1 mol% and a reaction time of 1 hour to label compound **113** with a high 85% deuterium incorporation. Such a variation in reactivity may be a result of the slight difference in electron density present on the metal of each of the complexes under consideration. Despite being electronically similar, triphenylphosphine is the most electron-deficient of the three phosphine ligands, hence it will donate least electron density to the iridium centre. As substrate **113** is imagined to be fairly electron-rich, it may coordinate to complex **124** more readily than complexes **135** and **136**, hence a higher catalyst activity is observed.

Similar results were detected in the labelling of **113** by complexes **125** and **138** bearing the benzyl-substituted NHC ligand. Again, H-D exchange facilitated by triphenylphosphine-containing complex **125** proceeded to excellent levels in the presence of low quantities of catalyst and over shorter reaction times (Entry 6), while exchange catalysed by the PMe_2Ph complex **138** required increased catalyst loadings and extended periods of time to deliver high isotope incorporations of 79% (Entry 8).

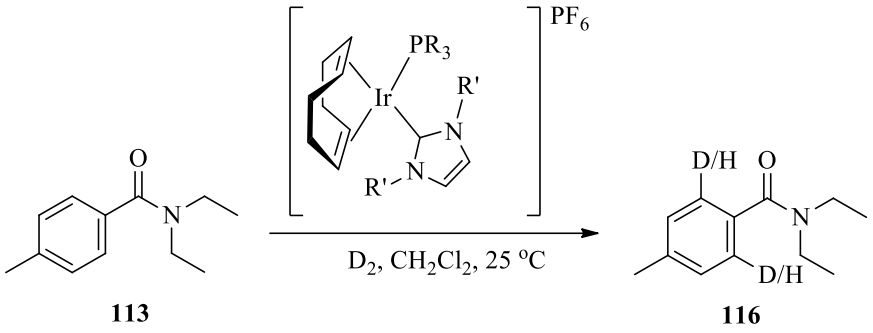

113 **116**

Scheme 120

Entry	Complex	PR_3	NHC	Conditions	% Deuteration	
					Run 1	Run 2
1	**135**	PBn_3	ICy	0.5 mol%, 2 h	29	37
2				5 mol%, 16 h	99	99
3	**124**	PPh_3	ICy	1 mol%, 1 h	85	85
4	**136**	PMe_2Ph	ICy	3 mol%, 2 h	16	18
5				5 mol%, 16 h	93	91
6	**125**	PPh_3	IBn	1 mol%, 2 h	99	97
7	**138**	PMe_2Ph	IBn	3 mol%, 0.5 h	58	58
8				5 mol%, 16 h	78	79

Table 101

Having demonstrated the ability of these novel Ir(I) complexes to label substrates *via* a 5-mmi, attention turned to the deuteration of acetanilide **73**, which is labelled *via* a less energetically favourable 6-mmi (**Scheme 121**). In view of the more demanding nature of substrate **73** in HIE reactions, it was somewhat expected that under the previously optimised conditions for complexes **135**, **124**, **136**, **125**, and **138**, H-D exchange in acetanilide proceeded to only low levels of deuterium incorporation. As shown in **Table 102**, levels of between 6 and 21% were observed. Increasing the catalyst loading to 5 mol% and

lengthening the reaction time to 16 hours proved extremely beneficial in systems employing complexes **135** and **124**, enhancing the deuteration of substrate **73** up to an excellent 95% (**Table 102**, Entries 2 and 4). While improvements in incorporation were also observed under these slightly more forcing conditions in reactions facilitated by complexes **136**, **125**, and **138**, the desired compound **74** was delivered with only moderate to good levels of D loading of up to 70%.

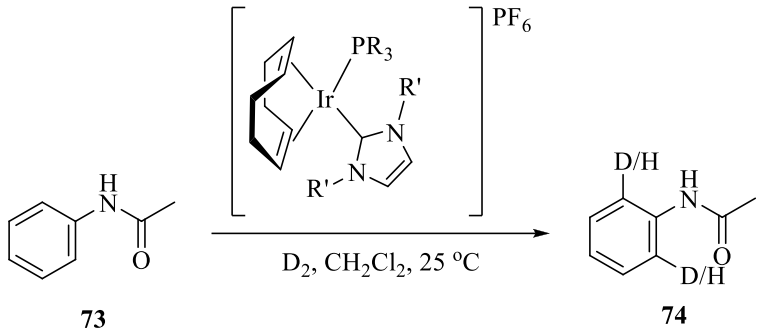

73 **74**

Scheme 121

Entry	Complex	PR_3	NHC	Conditions	% Deuteration	
					Run 1	Run 2
1	**135**	PBn_3	ICy	0.5 mol%, 2 h	18	10
2				5 mol%, 16 h	94	95
3	**124**	PPh_3	ICy	1 mol%, 1 h	15	16
4				5 mol%, 16 h	90	94
5	**136**	PMe_2Ph	ICy	3 mol%, 2 h	21	17
6				5 mol%, 16 h	60	62
7	**125**	PPh_3	IBn	1 mol%, 2 h	6	7
8				5 mol%, 16 h	42	38
9	**138**	PMe_2Ph	IBn	3 mol%, 0.5 h	12	13
10				5 mol%, 16 h	66	70

Table 102

The next substrate to be employed in HIE reactions catalysed by the novel Ir(I) complexes under examination was benzanilide **83**. As described earlier, compound **83** contains two sites at which C-H activation can occur (**Scheme 122**). While exchange in both positions is directed by the carbonyl group of the amide moiety, labelling in position *a* occurs through a 5-mmi, while labelling in position *b* is *via* an energetically less favourable 6-mmi. Previous results reported from within our laboratory focused on the selective labelling of benzanilide, demonstrating the ability of complex **82** to facilitate deuterium incorporation into position *a* to a significantly greater degree than was observed in position *b*.[35] Such discrimination was achieved utilising a catalyst loading of 0.5 mol%, and a reaction time of 16 hours. The initial results obtained in the current study were, therefore, extremely pleasing; after just 2 hours at the equivalent catalyst loading, complex **135** was found to deliver the desired product with similar levels of selectivity. More specifically, incorporation in position *a* was extremely high at up to 95%, while labelling in position *b* proceeded to a maximum of 16% D (**Table 103**, Entry 1). Furthermore, reducing the reaction time to 1 hour caused no significant drop in the

exchange observed at position *a*, while that at position *b* decreased to only negligible levels (Entry 2). Results obtained with complexes **124** and **125** followed a similar trend, although in these instances, comparable reductions were observed in both positions *a* and *b* in the presence of lower catalyst loadings and shorter reaction times (Entries 3 and 4, and 7 and 8). Finally, H-D exchange in substrate **83** catalysed by complex **138** proceeded to good levels of D incorporation of up to 74% in position *a* while, somewhat unsurprisingly, labelling in position *b* was detected at a significantly lower degree of 15% deuteration (Entry 9).

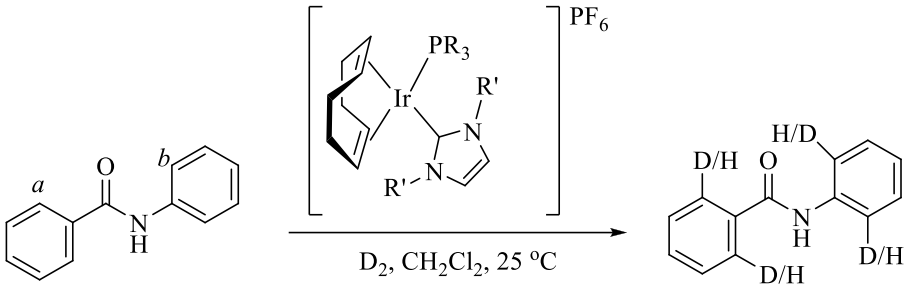

83 **84**

Scheme 122

Entry	Complex	PR_3	NHC	Conditions	% Deuteration			
					Run 1		Run 2	
					a	*b*	*a*	*b*
1	**135**	PBn_3	ICy	0.5 mol%, 2 h	95	16	91	12
2				0.5 mol%, 1 h	91	2	87	3
3	**124**	PPh_3	ICy	1 mol%, 1 h	87	34	93	38
4				0.5 mol%, 1 h	65	11	68	10
5	**136**	PMe_2Ph	ICy	3 mol%, 2 h	88	30	94	32
6				1 mol%, 1 h	73	9	80	9
7	**125**	PPh_3	IBn	1 mol%, 2 h	96	17	96	14
8				1 mol%, 1 h	82	9	88	8
9	**138**	PMe_2Ph	IBn	3 mol%, 0.5 h	67	16	74	15

Table 103

The results to this point clearly demonstrate the high activity of these novel Ir(I) complexes, with the majority of substrates being labelled to excellent levels of deuterium incorporation. Having stated this, the compounds examined thus far have been more simple substrates, each containing only one functional group required to direct the observed C-H activation. Attention therefore turned to the application of these complexes in the isotopic labelling of more complex substrates and, more specifically, in the labelling of real drug molecules, the first of which was Niclosamide **117** (**Scheme 123**). As described previously, Niclosamide has four sites at which labelling may occur: in positions *a* and *b* through coordination to the $–NO_2$ group, and in positions *c* and *d* directed by the carbonyl of the amide moiety, through a 6- and 5-mmi, respectively. As detailed earlier, good levels of deuterium incorporation were achieved in the labelling of substrate **117** catalysed by complex **81**, which pairs the bulky tribenzylphosphine with the sterically encumbered IMes NHC ligand. In DCM solvent, positions *a* and *d* were found to undergo H-D exchange to give incorporations of 55 and 58%, respectively, while the degree of deuteration observed in positions *b* and *c* were slightly

lower at approximately 42% (**Table 72**). Under analogous reaction conditions of a catalyst loading of 5 mol% and reaction time of 1 hour, the labelling of Niclosamide **117** facilitated by complex **135** delivered similar incorporations in positions *a*, *b* and *d*, but displayed a significant discrimination against position c, indicating the preference of complex **135** to label *via* a 5-mmi over a 6-mmi (**Table 104**, Entry 1). The deuteration of substrate **117** by the remaining novel Ir(I) complexes did not compete with the levels of H-D exchange observed in systems employing complex **135**, however each complex did exhibit similar degrees of selectivity. The results from this study, therefore, illustrate the ability of complexes such as **135** to show enhanced levels of selectivity for a 5-mmi over a 6-mmi. Additionally, these observations also reinforce the increased ability of the IMes series of complexes to label positions via the more energetically demanding 6-mmi.

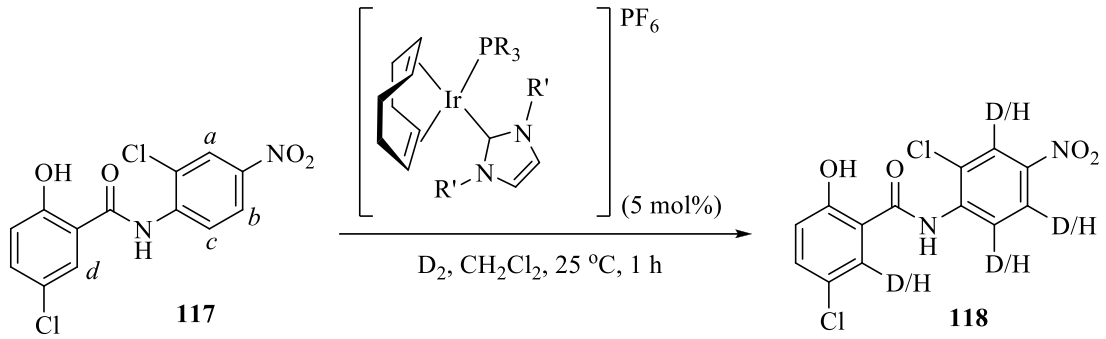

Scheme 123

Entry	Complex	PR_3	NHC	Run	% Deuteration			
					a	*b*	*c*	*d*
1	**135**	PBn_3	ICy	1	55	34	3	68
				2	54	34	4	60
2	**124**	PPh_3	ICy	1	32	16	14	30
				2	29	12	12	31
3	**136**	PMe_2Ph	ICy	1	20	4	4	17
				2	18	1	2	15
4	**125**	PPh_3	IBn	1	22	5	5	20
				2	26	12	11	28
5	**138**	PMe_2Ph	IBn	1	10	1	1	11
				2	12	1	1	10

Table 104

The final substrate to be investigated as part of this study was the COX-2 inhibitor, Celecoxib **119**. As detailed in earlier studies carried out within this research programme, compound **119** contains two C-H positions which can be activated towards substitution with deuterium; positions *a* and *b* as depicted below in **Scheme 124**. In each case, H-D exchange occurs through the formation of a 5-mmi, however position *a* is activated through coordination of the sulfonamide functional group to the iridium, while labelling in position *b* is directed by the pyrazole moiety. Previous results obtained within our laboratory which examined the activity of Ir(I) complexes bearing the NHC ligand IMes had revealed the highest levels of deuteration achieved within Celecoxib to be attained in reactions employing a catalyst loading of 10 mol% and a reaction time of 1 hour.[34] Under such conditions, H-D exchange in position *b* was found to proceed to excellent levels of approximately 94% D loading, with the greatest deuterium incorporation observed in position *a* being 19%. Although this latter result may appear to be relatively low, isotopic labelling adjacent to a sulfonamide is notoriously

difficult and so the ability to catalyse H-D exchange in this position and to this degree was, in fact, extremely pleasing.

In view of the previous conditions utilised, the labelling of substrate **119** with novel Ir(I) complexes bearing alternative NHC ligands was carried out initially using a catalyst loading of 5 mol%, and subsequently with an increased loading of 10 mol%. In each case, reactions employing the lower quantity of catalyst delivered the isotopically-enriched product **120** with higher levels of deuteration than had been achieved previously under analogous reaction conditions with IMes-based complexes **75**, **81** and **82**.[34] More specifically, labelling in position *a* proceeded to D incorporations of between 9 and 13%, while H-D exchange in position *b* was found to be consistently high at up to 99%. While increasing the catalyst loading to 10 mol% had previously proved favourable,[34] in the majority of instances further elevation above the already very good levels of labelling with the new catalyst species was not observed. Having stated this, reactions utilising 10 mol% of complex **135** did furnish the desired product in up to an enhanced 25% deuteration in position *a*, the highest level of labelling adjacent to a sulfonamide which has been achieved to date with catalysts of this type and, indeed, within this area of research, especially with such relatively low levels of catalyst.

The increased activity of complex **135** towards H-D exchange in this position is proposed to arise from a subtle balance between the steric and electronic properties of this Ir(I) complex. Of the novel catalysts examined as part of this programme, complex **135** partners the most electron-donating cyclohexyl-substituted NHC ligand with the second most electron-donating phosphine ligand, PBn_3. Such an elevated level of electron density on the metal centre may, therefore, reduce the coordination of the sulfonamide moiety, aiding the dissociation of the labelled product and, hence, subsequent catalysis. In addition, the large steric influence imparted by the tribenzylphosphine ligand in conjunction with the smaller ICy ligand, may create an optimal space within the coordination sphere of the iridium core, enabling access to the relatively large and encumbering sulfonamide unit.

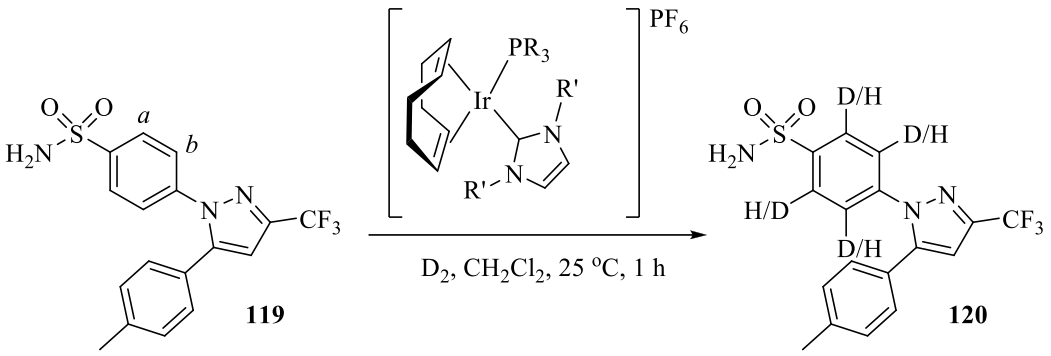

Scheme 124

Entry	Complex	PR_3	NHC	Catalyst Loading (mol%)	% Deuteration			
					Run 1		Run 2	
					a	*b*	*a*	*b*
1	**135**	PBn_3	ICy	5	11	98	9	99
2				10	25	97	18	95
3	**124**	PPh_3	ICy	5	10	98	11	98
4				10	13	96	12	97
5	**136**	PMe_2Ph	ICy	5	12	98	13	97
6				10	12	93	13	95
7	**125**	PPh_3	IBn	5	12	89	12	94
8				10	12	86	10	95
9	**138**	PMe_2Ph	IBn	5	10	99	9	98
10				10	13	99	10	98

Table 105

The application of novel Ir(I) complexes bearing alternative NHC ligands in hydrogen isotope exchange reactions has revealed complexes pairing cyclohexyl- or benzyl-substituted NHCs with tertiary phosphine ligands to display appreciable catalytic activity across a range

of substrates. In the majority of instances, reactions performed under our standard experimental conditions of a 5 mol% catalyst loading and 16 hour reaction time delivered levels of deuterium incorporation comparable to those previously attained in analogous systems facilitated by our original IMes-containing complexes.[34] Novel complexes **135**, **124**, **136**, **125** and **138** have also demonstrated good to high catalytic efficiencies in reactions employing lower quantities of catalyst and shorter reaction times, operating at low catalyst loadings between 0.5 and 3 mol%, over periods as short as 30 minutes. Furthermore, our newly developed complexes appear to display increased levels of selective labelling, when compared to H-D exchange catalysed by complexes bearing mesityl-substituted NHC ligands. More specifically, our more recently prepared Ir(I) complexes show greater preference for isotopic labelling in positions which proceed *via* a 5-mmi, as demonstrated in the deuteration of Niclosamide **117** (**Scheme 123**, p.160). In addition, complex **135** has been identified as a species which can facilitate improved levels of isotope incorporation adjacent to a sulfonamide moiety. The results achieved in this programme of study have, therefore, demonstrated that different complexes affect H-D exchange within different substrates to varying degrees, indicating that the probability of developing a universal HIE catalyst for use with all compounds is very slim. It is significantly more likely that a library of complexes is required, allowing the selection of an appropriate catalyst dependent on the substrate under investigation.

3.7 Application of Novel Ir(I) Complexes in HIE Reactions Conducted in Alternative Solvents

Having demonstrated the ability of novel Ir(I) complexes to facilitate H-D exchange in reactions performed in DCM, attention turned to the application of these catalysts in labelling reactions carried out in alternative reaction media. As described previously, three solvents have been identified as suitable replacements for DCM in this field of research, namely diethyl ether, *tert*-butylmethyl ether, and 2-methyltetrahydrofuran. To determine the compatibility of the new complexes with each of these solvents, the labelling of acetophenone **54** was investigated, employing standard conditions of a 5 mol% catalyst

loading and a 16 hour reaction time. As depicted in **Scheme 125**, explorations in this area began with the use of Et_2O.

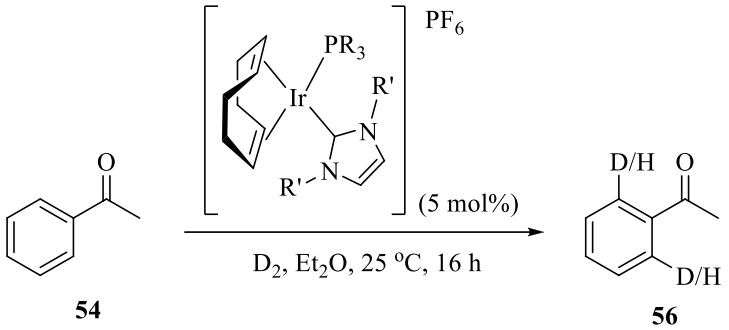

Scheme 125

Entry	Complex	PR_3	NHC	% Deuteration	
				Run 1	Run 2
1	**135**	PBn_3	ICy	5	5
2	**124**	PPh_3	ICy	38	41
3	**136**	PMe_2Ph	ICy	75	84
4	**125**	PPh_3	IBn	48	56
5	**138**	PMe_2Ph	IBn	8	9

Table 106

Unfortunately, the initial results obtained were somewhat disappointing; the labelling of substrate **54** with complex **135** proceeding to only a poor level of 5% D incorporation (**Table 106**, Entry 1). The results obtained with complexes **124** and **136** were more encouraging however, delivering the desired product **56** in up to 41% and 84% deuteration, respectively (Entries 2 and 3). Comparison of these values indicates a clear trend between decreasing size of the phosphine ligand and the level of isotope incorporation observed. With the smallest NHC ligand, complexes within this ICy series undoubtedly present the least steric bulk in the coordination sphere around the metal centre. Greater access to the iridium would therefore be available to solvent molecules, which may restrict coordination of the incoming substrate molecule. As the size of the phosphine ligand decreases in size however, the available space around the metal centre would increase further, improving the probability of a substrate

molecule occupying a vacant coordination site. An enhancement in the levels of incorporation would therefore be observed.

In contrast, the IBn series of complexes displayed the opposite trend. Complex **125** which pairs triphenylphosphine with this NHC catalysed H-D exchange up to a reasonable 56% deuteration (Entry 4), while complex **138** bearing the smaller dimethylphenylphosphine failed to deliver the isotopically-enriched product **56** with more than 9% incorporation (Entry 5).

Satisfied with the results obtained in HIE reactions performed in Et_2O, focus turned to the use of ^{t}BuOMe, the second solvent which had previously been identified as a suitable replacement for DCM in this area of research (**Scheme 126**). As illustrated by the results below in **Table 107**, complexes **135**, **124**, and **136** facilitated the substitution of hydrogen for deuterium to moderate levels, ranging from 24 to 38% D incorporation (Entries 1, 2, and 3). Again, an analogous trend was observed for the IBn series of complexes as had been noted previously in reactions performed in Et_2O. Levels of isotopic labelling achieved with complex **125** reached 46%, while those attained in reactions employing the less sterically encumbered complex **138** were significantly lower at approximately 10% (Entry 5).

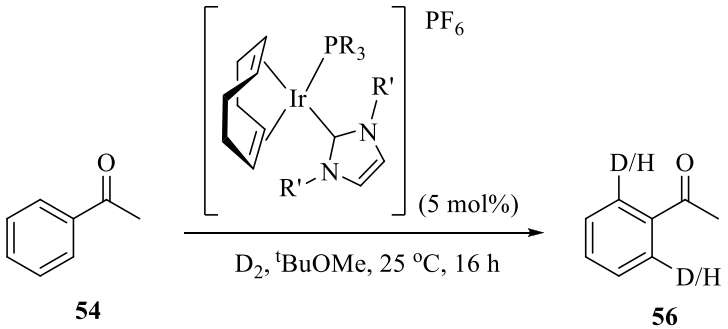

54 **56**

Scheme 126

Entry	Complex	PR_3	NHC	% Deuteration	
				Run 1	Run 2
1	**135**	PBn_3	ICy	35	38
2	**124**	PPh_3	ICy	29	28
3	**136**	PMe_2Ph	ICy	24	32
4	**125**	PPh_3	IBn	46	42
5	**138**	PMe_2Ph	IBn	7	12

Table 107

The final solvent to be examined in hydrogen isotope exchange reactions catalysed by novel Ir(I) complexes was 2-MeTHF (**Scheme 127**). Previous results obtained as part of this programme of study had revealed this solvent to work particularly well in HIE reactions; indeed the majority of substrates examined were labelled to the highest degrees in this solvent in comparison to the incorporations obtained in Et_2O and ^tBuOMe. The results attained in the present study were therefore somewhat disappointing as, in general, the labelling of acetophenone **54** by the novel Ir(I) complexes in 2-MeTHF proceeded to deliver only moderate levels of deuteration (**Table 108**). More encouraging results of approximately 65% D loading were obtained in systems employing complex **136**, however this degree of H-D exchange remains significantly lower than has been detected previously in reactions performed in DCM.

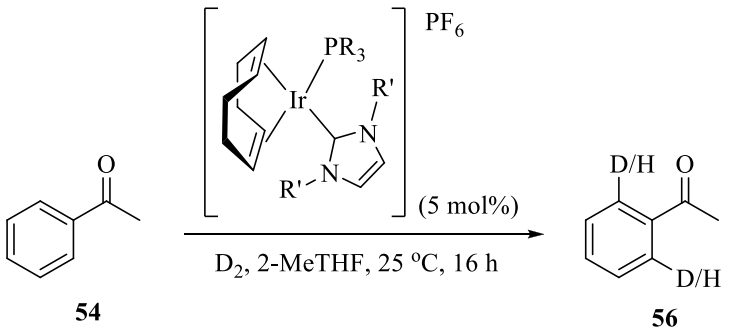

Scheme 127

Entry	Complex	PR_3	NHC	% Deuteration	
				Run 1	Run 2
1	**135**	PBn_3	ICy	33	39
2	**124**	PPh_3	ICy	20	18
3	**136**	PMe_2Ph	ICy	67	60
4	**125**	PPh_3	IBn	17	15
5	**138**	PMe_2Ph	IBn	32	27

Table 108

Unfortunately, comparison of the results obtained in this short solvent study does not reveal any apparent relationship between the combination of phosphine and NHC ligands present in the Ir(I) complex, and the solvent in which the exchange reaction is performed, with the overall level of isotope incorporation attained. From the values displayed in **Table 108**, it could be deduced that an increased electron density on the metal centre may reduce solvent coordination, enabling improved catalytic activity; however, such reasoning is not supported by the degrees of deuteration observed in labelling reactions performed in Et_2O and ^tBuOMe (**Tables 106** and **107**). It is therefore proposed that the performance of our novel Ir(I) complexes in H-D exchange reactions conducted in alternative solvents may be affected by slight changes in the electronic and steric properties of the ligands present within the catalyst, or may, in fact, depend on additional factors, such as the solubility of each species in the selected reaction media.

3.7.1 DFT Studies

To aid our understanding of the relatively poor levels of deuterium incorporation observed in reactions employing our novel Ir(I) complexes in alternative solvents, attention returned to the use of theoretical calculations. Our initial investigations focused on the geometries of the solvent-free iridium complexes, to determine if any significant differences existed between the orientations of each of the NHC ligands. Previous DFT studies performed within this area confirmed the phosphine and NHC ligand to align themselves in a *trans*-configuration around

the metal,[34] providing the structures as depicted in **Figure 34**. Once again, it should be noted that to reduce computational costs the smaller trimethylphosphine ligand was employed in the complexes under investigation.

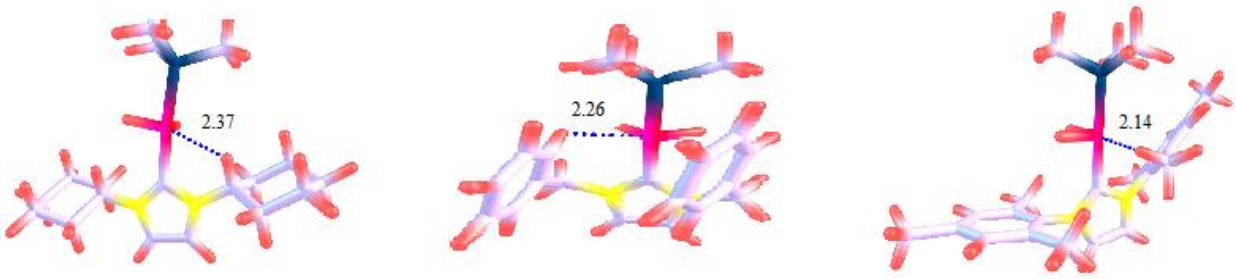

$Ir(D_2)(PMe_3)(ICy)$ $Ir(D_2)(PMe_3)(IBn)$ $Ir(D_2)(PMe_3)(IMes)$

Figure 34 – Optimised geometries of $Ir(D_2)(PMe_3)(NHC)$ complexes computed using the M06 level of theory. Distances shown (in Å) refer to agostic interactions between Ir and a hydrogen atom on the NHC ligand.

Further analysis of these species revealed the presence of agostic interactions between a hydrogen on the NHC ligand and the iridium centre. In the case of the IBn ligand, such an interaction was found between the metal and an aryl hydrogen, as opposed to a C-H bond situated at the benzylic position. The distances between the metal and the associated hydrogen were determined as 2.37 Å for the complex bearing the ICy ligand, 2.26 Å for that containing the benzyl-substituted NHC, and 2.14 Å for the originally employed IMes ligand. While each value lies broadly within the 1.8-2.3 Å range designated for agostic bonds,[62] the shorter distance calculated in the latter complex indicates a greater stabilisation in comparison to that found in the former two complexes, which may provide some explanation for the generally higher reactivity displayed by catalysts bearing this sterically encumbered ligand.

While the identification of the differing magnitudes of forces between the metal centre and neighbouring hydrogens offers some explanation regarding the stability of the three $Ir(PMe_3)(NHC)$ complexes, it was proposed that additional, and perhaps more insightful,

information could be obtained through the implementation of computational studies analogous to those performed previously for the solvated IMes containing complexes. The solvent binding energies of the bi-solvated iridium complexes were therefore determined by means of the following equation:

$$Ir(D_2)(PMe_3)(NHC) + 2S \rightleftharpoons Ir(D_2)(PMe_3)(NHC)(S)_2$$

$$\Delta E = E[Ir(D_2)(PMe_3)(NHC)(S)_2] – E[Ir(D_2)(PMe_3)(NHC)] - 2E[S]$$

As illustrated by the results shown in **Table 109**, the relative solvent binding energies for the four reaction media examined as part of this study follow the same trend as identified in our earlier theoretical investigations (the previous values calculated for our IMes complexes are included for comparison). In each case, the least coordinating solvent is DCM, followed by ^{t}BuOMe, Et_2O and finally 2-MeTHF. While the results from our practical experiments offered no apparent direct correlation with the calculated outcomes between the NHC present in the iridium catalyst and its performance in HIE reactions conducted in different solvents, our theoretical findings imply that, as a result of lower solvent binding energies, catalysts bearing the dibenzyl-substituted NHC should display the highest catalytic activity. Furthermore, the significantly stronger coordination of solvent molecules to complexes containing the ICy ligand suggest this series of catalysts to be the least efficient facilitators of H-D exchange, with our original IMes-containing complexes demonstrating an apparent intermediate activity.

Entry	Solvent	Complex	Binding Energy (kcal/mol)	
			Gas Phase	Solvent
1	DCM	$Ir(D)_2(ICy)(PMe_3)(DCM)_2$	-25.67	-15.13
2	Et_2O	$Ir(D)_2(ICy)(PMe_3)(Et_2O)_2$	-40.37	-31.41
3	^{t}BuOMe	$Ir(D)_2(ICy)(PMe_3)(^t BuOMe)_2$	-39.00	-
4	2-MeTHF	$Ir(D)_2(ICy)(PMe_3)(2\text{-}MeTHF)_2$	-44.27	-
5	DCM	$Ir(D)_2(IBn)(PMe_3)(DCM)_2$	-8.51	-2.33
6	Et_2O	$Ir(D)_2(IBn)(PMe_3)(Et_2O)_2$	-19.95	-14.64
7	^{t}BuOMe	$Ir(D)_2(IBn)(PMe_3)(^t BuOMe)_2$	-18.80	-
8	2-MeTHF	$Ir(D)_2(IBn)(PMe_3)(2\text{-}MeTHF)_2$	-29.94	-
9	DCM	$Ir(D)_2(IMes)(PMe_3)(DCM)_2$	-16.19	-11.46
10	Et_2O	$Ir(D)_2(IMes)(PMe_3)(Et_2O)_2$	-31.56	-26.97
11	^{t}BuOMe	$Ir(D)_2(IMes)(PMe_3)(^t BuOMe)_2$	-23.87	-
12	2-MeTHF	$Ir(D)_2(IMes)(PMe_3)(2\text{-}MeTHF)_2$	-37.29	-

Table 109 – Binding energies of bi-solvated complexes containing alternative NHC ligands

As before, the energies of complexes containing one substrate molecule in place of a solvent ligand were also calculated to identify the extent of stabilisation resulting from such a substitution. From the results illustrated in **Table 110** (which again include the previously calculated values for the IMes complex in various solvents), it is evident that in each of the three complexes, the replacement of a solvent molecule with one of acetophenone stabilises the system to the highest degree when the solvent of interest is DCM (Entries 1, 5 and 9). With regards to species containing the dibenzyl-substituted NHC ligand, the ordering of the ethereal solvents is identical to that observed previously; complexes to which ^{t}BuOMe is bound are stabilised by the coordination of a substrate molecule more than those containing Et_2O ligands, with systems involving 2-MeTHF solvent molecules displaying the lowest binding energies (Entries 6, 7 and 8). A slight anomaly was detected in the analogous calculations performed for complexes bearing the cyclohexyl-substituted NHC ligand as, in this instance, the presence of 2-MeTHF was found to stabilise the system to a greater degree

than that computed for complexes containing Et_2O (Entries 2 and 4). In view of the initial findings which reveal 2-MeTHF to bind more strongly to the iridium centre (**Table 109**, Entries 2 and 4), it is proposed that this discrepancy is, in fact, a methodological error and, if the values were to be recalculated, a lower binding energy would be determined for the cyclic ether.

Entry	Solvent	Complex	Binding Energy (kcal/mol)	
			Gas Phase	Solvent
1	DCM	$Ir(D)_2(ICy)(PMe_3)(DCM)(PhCOOMe)$	-11.63	-7.92
2	Et_2O	$Ir(D)_2(ICy)(PMe_3)(Et_2O)(PhCOOMe)$	-4.42	-1.97
3	^{t}BuOMe	$Ir(D)_2(ICy)(PMe_3)(^t BuOMe)(PhCOOMe)$	-8.31	-
4	2-MeTHF	$Ir(D)_2(ICy)(PMe_3)(2\text{-}MeTHF)(PhCOOMe)$	-6.15	-
5	DCM	$Ir(D)_2(IBn)(PMe_3)(DCM)(PhCOOMe)$	-15.12	-12.21
6	Et_2O	$Ir(D)_2(IBn)(PMe_3)(Et_2O)(PhCOOMe)$	-10.57	-8.49
7	^{t}BuOMe	$Ir(D)_2(IBn)(PMe_3)(^t BuOMe)(PhCOOMe)$	-11.46	-
8	2-MeTHF	$Ir(D)_2(IBn)(PMe_3)(2\text{-}MeTHF)(PhCOOMe)$	-3.20	-
9	DCM	$Ir(D)_2(IMes)(PMe_3)(DCM)(PhCOOMe)$	-14.03	-10.31
10	Et_2O	$Ir(D)_2(IMes)(PMe_3)(Et_2O)(PhCOOMe)$	-6.35	-4.58
11	^{t}BuOMe	$Ir(D)_2(IMes)(PMe_3)(^t BuOMe)(PhCOOMe)$	-11.85	-
12	2-MeTHF	$Ir(D)_2(IMes)(PMe_3)(2\text{-}MeTHF)(PhCOOMe)$	-4.30	-

Table 110 - Calculated binding energies for mono-solvated species containing alternative NHC ligands, and one substrate ligand

As mentioned, our laboratory experimental results provided no obvious relationship regarding the degree of H-D exchange which occurs in reactions facilitated by complexes bearing different NHC ligands and the solvent in which the labelling process takes place. It is therefore extremely difficult to draw any definitive conclusions from our more recent theoretical investigations, as they are not consistent with previous findings which indicate

complexes containing the mesityl-substituted NHC ligand to display the highest catalytic activity. Having stated this, it should be noted that the efficiency displayed by HIE catalysts will be dependent on a significant number of factors, as opposed to the strength of solvent binding alone. With regards to the proposed mechanism by which H-D exchange occurs (**Scheme 11**, p.12) Heys postulated that the coordinatively unsaturated Ir(I) species formed following the loss of the COD ligand would be stabilised by two coordinating molecules.[20] While our theoretical calculations have assumed such ligands to be solvent molecules, it should be acknowledged that alternative species may be involved in the stabilisation of the metal core, such as additional substrate molecules, or dihydrogen. In addition, it is not known exactly how many ligands may be bound to the Ir complex, a factor which is almost certainly dependent on the steric properties associated with each ligand.

Further investigations into the different efficiencies of our novel Ir(I) complexes therefore focused more closely on the catalytic cycle itself. In Heys' initial report, it was suggested that the rate determining step of the HIE process is the oxidative insertion of iridium into the aromatic C-H bond positioned *ortho* to the coordinating functionality.[20] If this were the case, the presence of strongly electron-donating ligands on the metal core would lower the energy associated with this transition, and accelerate the rate of the overall reaction. In addition, the steric influence of the ligands is likely to play an important role in the catalytic activity of an efficient HIE complex, as additional energy will be required in the reductive elimination step of the mechanistic cycle. In view of the different electronic and steric properties of our novel Ir(I) complexes, it was proposed that examining the reaction energetics associated with each complex may provide further information regarding the performance of complexes bearing alternative NHC ligands, in comparison to that displayed by our original IMes-containing catalysts. Computational experiments were therefore carried out to determine the energies associated with the key steps of the reaction pathway as depicted in **Scheme 128**.

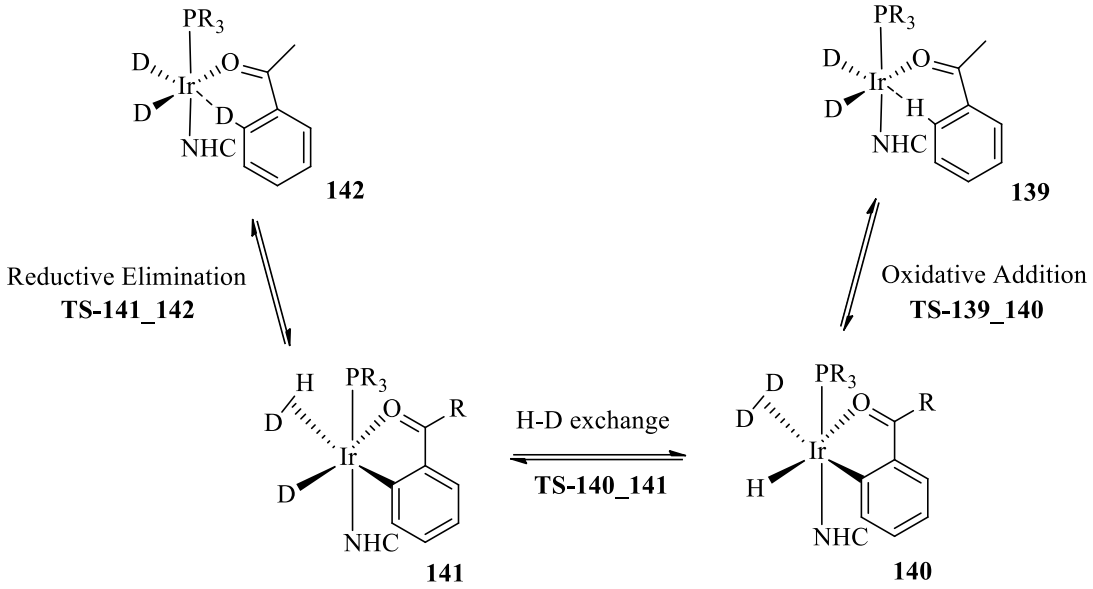

Scheme 128

Calculations were performed to determine the relative energies (ΔE), enthalpies (ΔH), and Gibbs' free energies (ΔG) for the oxidative addition, H-D exchange and reductive elimination processes involved in the isotopic labeling of acetophenone **54** by our Ir(I) complexes bearing different NHCs. As revealed by the results shown in **Table 111** and, perhaps more clearly illustrated, in **Figure 35**, the rate-limiting process for H-D exchange facilitated by complexes bearing either the cyclohexyl- or benzyl-substituted NHC ligand appears to be reductive elimination while, in contrast, the oxidative addition step requires more energy when catalysts containing the IMes ligand are employed. Such findings are likely a result of the increased electron-donating ability of the ICy and IBn ligands, which would assist the oxidative insertion process, together with the greater steric bulk of the mesityl-substituted NHC ligand, a feature which would undoubtedly aid reductive elimination.

The values presented in **Table 111** (and in **Figure 35**) demonstrate a clear relationship between the NHC ligand present in the Ir(I) complex under investigation, and the relative energies associated with the oxidative addition and reductive elimination processes which occur within the H-D exchange reaction pathway. In conjunction with the results described previously, regarding the analogous reaction energetics calculated for the reaction of our

IMes-containing complexes with different substrates,[34] this study constitutes the most detailed examination, to date, of the relative energies of the central mechanistic processes involved with the HIE catalytic cycle.

Species	ΔE (kcal/mol)	ΔH (kcal/mol)	ΔG (kcal/mol)
$Ir(D)_2(ICy)(PMe_3)(PhCOCH_3)$ (**139**)	0.00	0.00	0.00
TS-$(ICy)(PMe_3)(PhCOCH_3\_C_6H_4COCH_3)(H)$ (**TS-139_140**)	15.80	15.17	17.40
$Ir(D)_2(ICy)(PMe_3)(H)(C_6H_4COCH_3)$ (**140**)	-4.99	-5.13	-4.26
TS-$(ICy)(PMe_3)$(H-D exchange) (**TS-140_141**)	-2.54	-2.59	-2.70
$Ir(ICy)(PMe_3)(DH)(D)(C_6H_4COCH_3)$ (**141**)	-5.03	-5.20	-4.25
TS-$(ICy)(PMe_3)(C_6H_4COCH_3\_C_6H_4DCOCH_3)$ (**TS-141_142**)	16.14	15.48	17.73
$Ir(DH)(D)(ICy)(PMe_3)(PhCOCH_3)$ (**142**)	-0.42	-0.45	-0.40
$Ir(D)_2(IBn)(PMe_3)(PhCOCH_3)$ (**139**)	0.00	0.00	0.00
TS-$(IBn)(PMe_3)(PhCOCH_3\_C_6H_4COCH_3)(H)$ (**TS-139_140**)	16.96	16.44	17.48
$Ir(D)_2(IBn)(PMe_3)(H)(C_6H_4COCH_3)$ (**140**)	0.21	-0.10	1.28
*TS-$(IBn)(PMe_3)$(H-D exchange) (**TS-140_141**)	-	-	-
$Ir(IBn)(PMe_3)(DH)(D)(C_6H_4COCH_3)$ (**141**)	0.13	-0.21	1.25
TS-$(IBn)(PMe_3)(C_6H_4COCH_3\_C_6H_4DCOCH_3)$ (**TS-141_142**)	17.26	16.71	17.79
$Ir(DH)(D)(IBn)(PMe_3)(PhCOCH_3)$ (**142**)	-0.38	-0.41	-0.37

* The calculation of the energies for this TS are currently ongoing.

Table 111 - Relative energies (ΔE), enthalpies (ΔH) and Gibb's free energies (ΔG) for the oxidative addition, H/D exchange and reductive elimination steps calculated at M06 level of theory (continued on next page)

$Ir(D)_2(IMes)(PMe_3)(PhCOCH_3)$ (**139**)	0.00	0.00	0.00
TS-$(IMes)(PMe_3)(PhCOCH_3\_C_6H_4COCH_3)(H)$ (**TS-139_140**)	18.14	18.13	18.35
$Ir(D)_2(IMes)(PMe_3)(H)(C_6H_4COCH_3)$ (**140**)	0.93	1.20	0.26
TS-($IMes)(PMe_3)$(H-D exchange) (**TS-140_141**)	3.17	3.66	2.10
$Ir(IMes)(PMe_3)(DH)(D)(C_6H_4COCH_3)$ (**141**)	0.93	1.19	0.30
TS-($IMes)(PMe_3)(C_6H_4COCH_3\_C_6H_4DCOCH_3)$ (**TS-141_142**)	18.39	18.35	18.62
$Ir(DH)(D)($ $IMes)(PMe_3)(PhCOCH_3)$ (**142**)	-0.44	-0.48	-0.42

Table 111 continued - Relative energies (ΔE), enthalpies (ΔH) and Gibb's free energies (ΔG) for the oxidative addition, H/D exchange and reductive elimination steps calculated at M06 level of theory

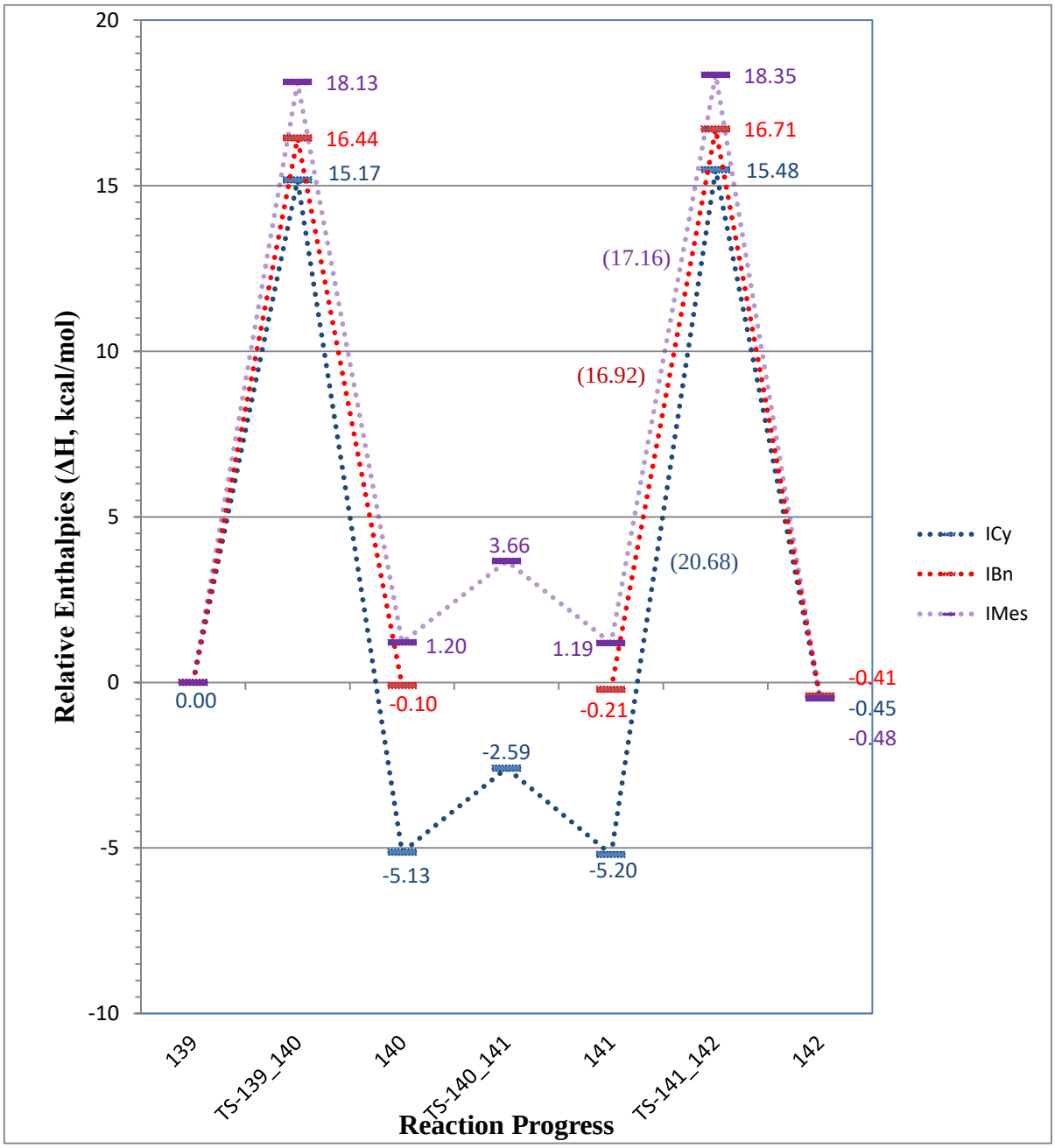

Figure 35 – Graph illustrating the relative energies associated with the key steps of the proposed HIE mechanistic cycle

In an attempt to confirm our results regarding the rate-limiting processes of the hydrogen isotope exchange mechanism, we concluded our computational studies by examining the existence of kinetic isotope effects (KIEs) within the proposed rate-determining steps for each of the three NHC-containing complexes. Such a value had previously been investigated

through practical experiments utilising complex **81**; the rate of Ir-catalysed H-D exchange in acetophenone **54** was compared to the rate of the reverse exchange process (**Scheme 129**).[34] As depicted below, a slight kinetic isotope effect of 1.18 was found to exist. Having stated this, the values recorded were considered to be outwith the range expected for a primary kinetic isotope effect (PKIE), implying that only a secondary kinetic isotope effect (SKIE) occurs.

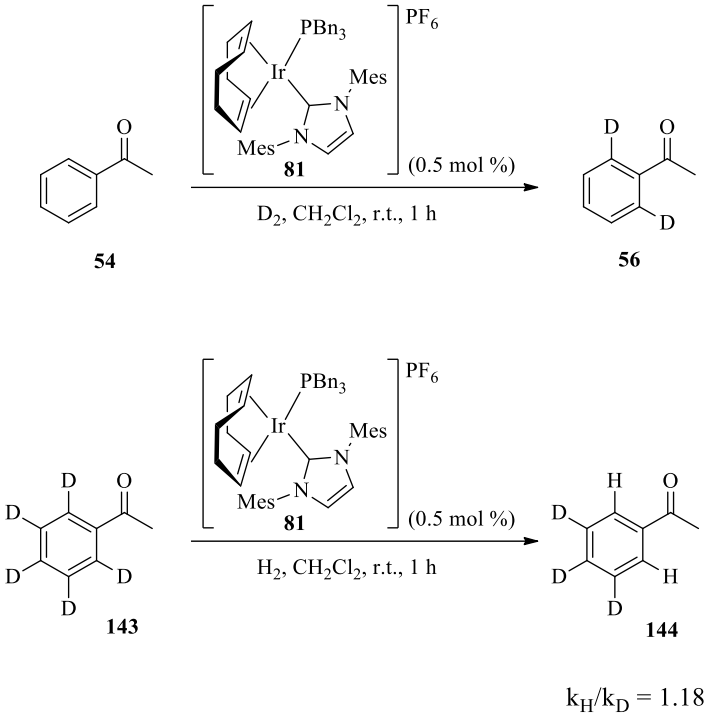

Scheme 129

The corresponding theoretical rate constants were determined by considering the enthalpy of activation ($\Delta H^{\ddagger}$) associated with the oxidative addition and reductive elimination processes. The enthalpy of activation involving deuterium ($\Delta H_D^{\ddagger}$) was calculated using a geometrically optimised species in which two of the participating hydrogen atoms were replaced with deuterium. The existence of a kinetic isotope effect was therefore examined by means of the following equation:

$$\frac{k_H}{k_D} = \frac{e^{-(\Delta H_H^{\ddagger}/RT)}}{e^{-(\Delta H_D^{\ddagger}/RT)}}$$

While a value of 1.20 was obtained for the oxidative addition process in our theoretical calculations, an increased KIE of 1.54 was observed for the associated reductive elimination step (**Table 112**, Entry 1). Such findings conflict with our previous computational results, which indicate the rate-determining step of HIE catalysed by the IMes complexes to be the insertion of the iridium into the aromatic C-H bond. In contrast, the values determined for the reductive elimination processes in H-D exchange facilitated by complexes bearing the cyclohexyl- or benzyl-substituted NHC are higher than those found for the corresponding oxidative addition steps, as predicted by our earlier studies (Entries 2 and 3). However, it should once again be noted that k_H/k_D values of 1.66 and 1.63 are not regarded as being high enough as to denote a PKIE, and are likely to correspond to a lesser SKIE.

NHC	k_H/k_D	
	Oxidative Addition	Reductive Elimination
IMes	1.20	1.54
ICy	1.17	1.66
IBn	1.10	1.63

Table 112 - KIE values calculated for oxidative addition and reductive elimination steps as depicted in **Scheme 128**

The results obtained in the theoretical studies described above represent a significant development in investigations regarding the process of H-D exchange, catalyzed by Ir(I) complexes. As mentioned, such detailed analysis of the reaction energetics had not previously been performed, with only speculation highlighting oxidative insertion as the rate limiting step within the proposed catalytic cycle. In view of the current findings, it has become apparent that the steric and electronic properties of the ligands present on the metal centre may impart a considerable degree of influence on the energies associated with the key mechanistic steps. It is therefore suggested that the rate limiting step of isotope exchange may

differ between reactions, and is perhaps dependent on the individual complex employed in each instance.

3.8 Application of Ir(COD)(NHC)Cl in Hydrogen Isotope Exchange

As little success had been achieved in the synthesis of complex **126** bearing the sterically encumbered IPr ligand, it was proposed that the Cl derivative **130** which had been prepared in high yields may serve as an efficient hydrogen isotope exchange catalyst. Previous work carried out within our laboratory had examined the application of the analogous IMes complex **108** in such reactions, delivering a number of isotopically-enriched ketones and heterocycles with high levels of incorporation.[34] The range of substrates which could be labelled efficiently with complex **108** was relatively limited however, with only low to moderate degrees of deuteration observed in reactions employing amides and anilides (**Scheme 130**).

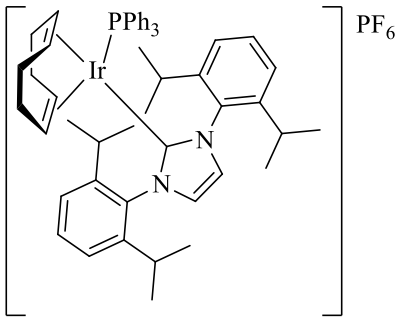

126

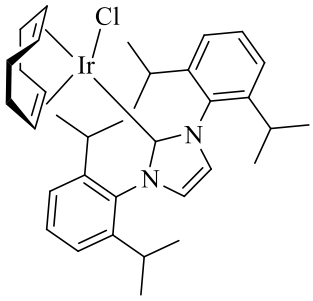

130

Figure 36

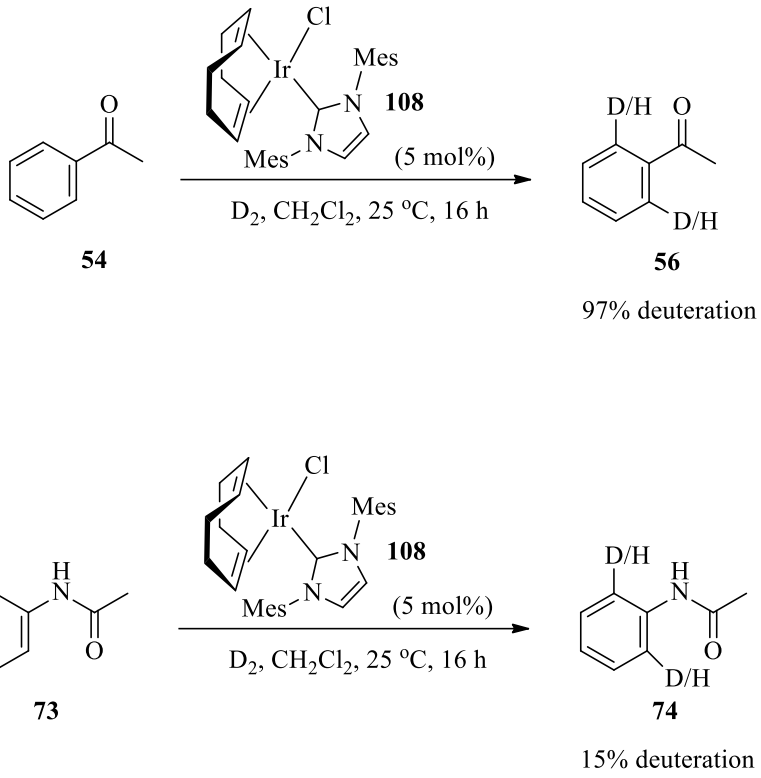

Scheme 130

To ascertain whether comparable activity would be displayed by complexes **130**, **131** and **132**, the isotopic labelling of acetophenone **54** was investigated (**Scheme 131**). As the results below in **Table 113** reveal, poor incorporations of up to only 7% were obtained with complexes **131** and **132** (Entries 1 and 2). Such low levels of incorporation are likely to be a result of the significantly smaller size of the complexes in comparison to their phosphine derivatives **124** and **125**, a feature which would be unfavourable in the reductive elimination step of the catalytic cycle, and which may also enable the formation of inactive Ir clusters as have been identified with Crabtree's catalyst (*vide supra*).[18] In contrast, H-D exchange facilitated by complex **130** proceeded to excellent levels, furnishing the desired compound **56** in up to 91% D incorporation (Entry 3). The ability of complex **130** to catalyse H-D exchange to such elevated levels clearly indicates the high stability of this species, undoubtedly due to the steric influence imparted by the IPr ligand.

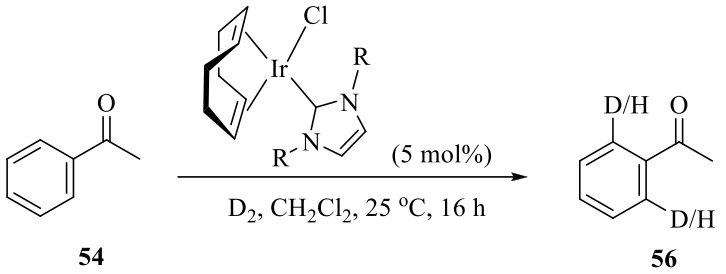

54 **56**

Scheme 131

Entry	Complex	NHC	% Deuteration	
			Run 1	Run 2
1	**131**	ICy	7	6
2	**132**	IBn	6	3
3	**130**	IPr	91	83

Table 113

Whilst only a limited number of chloro intermediates have been examined, the results obtained in the current study, as well as in previous investigations,[34] clearly demonstrate the appreciable efficiency of complexes of this type, bearing sterically encumbered NHC ligands, to facilitate the process of hydrogen isotope exchange. Due to the relative ease with which these complexes can be prepared, there exists the potential to readily access a range of chloro catalysts, and to subsequently examine their activity within this area of interest.

4 Conclusions

Investigations into the replacement of DCM as a solvent for hydrogen isotope exchange reactions have resulted in the identification of three suitable alternative reaction media considered more industrially acceptable than the current solvent of choice. A series of optimisation studies have been conducted, revealing that complexes of the type $[Ir(COD)(PR_3)(IMes)]PF_6$ can facilitate isotopic labelling in systems performed in Et_2O, ^tBuOMe and 2-MeTHF, operating at low catalyst loadings and over short reaction times. These newly identified reaction conditions have been employed in the deuteration of numerous substrates, containing various functional groups such as ketones, amides, heterocycles, and anilides. In the majority of cases high levels of H-D exchange were achieved, comparable to those attained previously in the original reaction solvent, DCM.

Of particular success was the isotopic labelling of the drug molecule Niclosamide **117** (**Scheme 132**). Comparison of the results displayed in **Table 114** illustrate the higher incorporations achieved in each of the alternative solvents, thought to be a result of the increased solubility of compound **117** in the ethereal solvents.

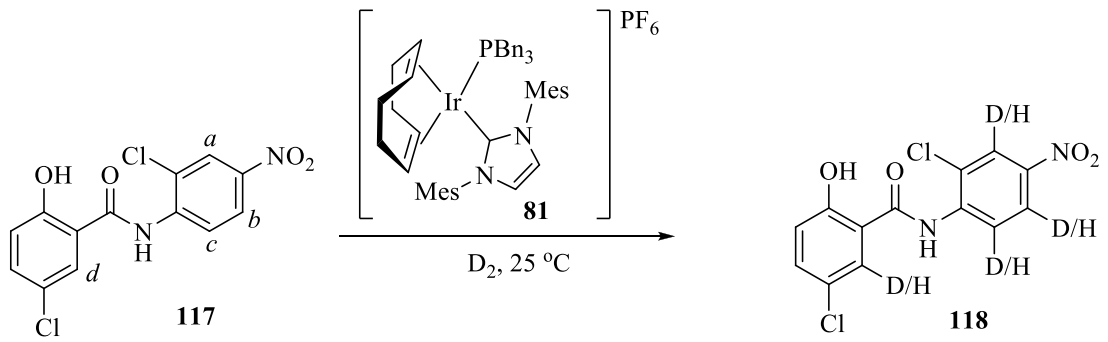

Scheme 132

Solvent	Catalyst Loading (mol%)	Time (h)	% Deuteration			
			a	*b*	*c*	*d*
DCM	5	1	55	44	40	58
Et_2O	3	1	75	70	63	76
^tBuOMe	5	2	83	48	37	87
2-MeTHF	3	1	89	55	28	97

Table 114

Further development of the Ir(I) complexes themselves has also been achieved. Investigations into the use of alternative NHC ligands have led to the successful preparation of six novel complexes (**Figure 37**). More specifically, complexes pairing each of our routinely employed phosphine ligands with cyclohexyl- and benzyl-substituted NHCs have been synthesised in moderate to high yields.

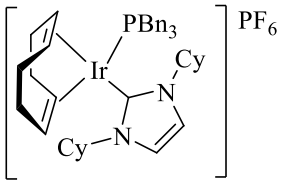

135

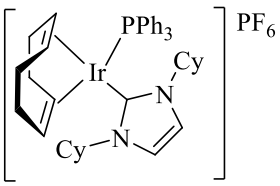

124

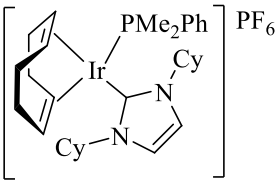

136

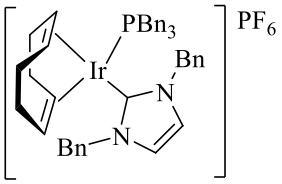

137

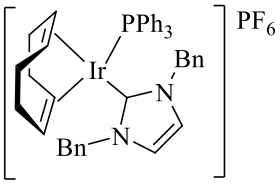

125

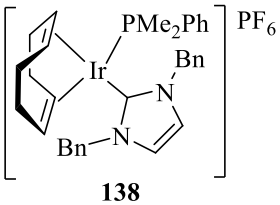

138

Figure 37

Following their synthesis, the novel complexes depicted above were applied to the field of hydrogen isotope exchange, demonstrating high catalytic activity in the isotopic labelling of a range of substrates. Once again, great success was achieved in the deuteration of marketed

drug molecules. In particular, under the conditions outlined in **Scheme 133**, complex **135** was found to deliver the highest levels of deuterium incorporation adjacent to a sulfonamide moiety observed to date with complexes of this type.

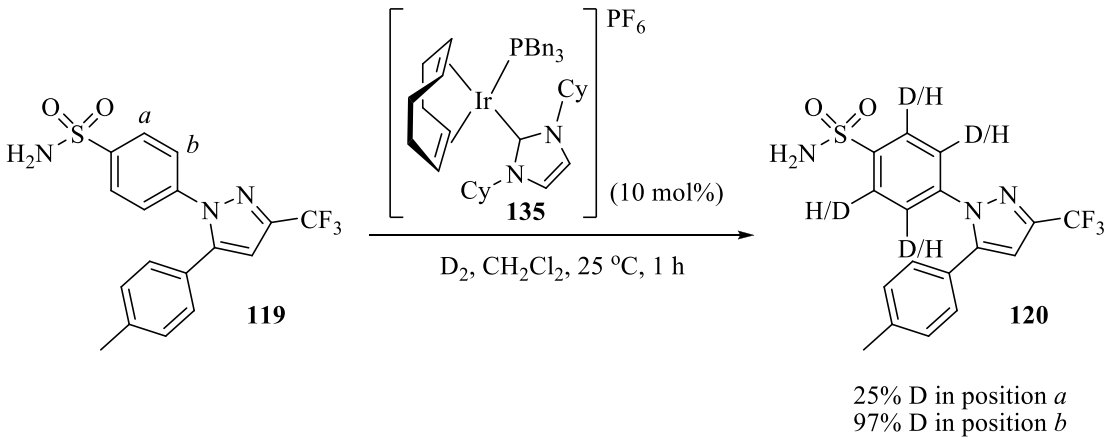

Scheme 133

To complement the practical work carried out as part of this overall programme, a variety of DFT studies have been performed, initially focusing on the solvent binding energies of the different reaction media examined as part of this investigation. Unfortunately, our theoretical findings did not directly correlate with those from our laboratory experiments, indicating that additional factors, not included in our computational calculations, may indeed play an important role in HIE reactions catalysed by our Ir(I) complexes in alternative solvents.

To more thoroughly investigate the processes under active investigation, further explorations included analysis of the relative energies of the key processes in the catalytic cycle itself. Here appreciable advances were made in the identification of different rate limiting steps dependent on the NHC ligand present in the complex.

5 Future Work

The scope for future work in this area is vast, expanding from within the field of hydrogen isotope exchange to demonstrating the potential applicability of our Ir(I) complexes in new roles. A number of results obtained within this programme of study have highlighted possible routes by which further explorations could be directed, such as the investigation into the labelling of a range of sulfonamides by novel Ir(I) complexes. More specifically, the activity of complex **135**, which displayed the highest efficiency in H-D exchange adjacent to such a functionality, should be employed in the deuteration of substrates containing the sulfonamide moiety to determine if results of a similar level are obtained (**Scheme 134**).

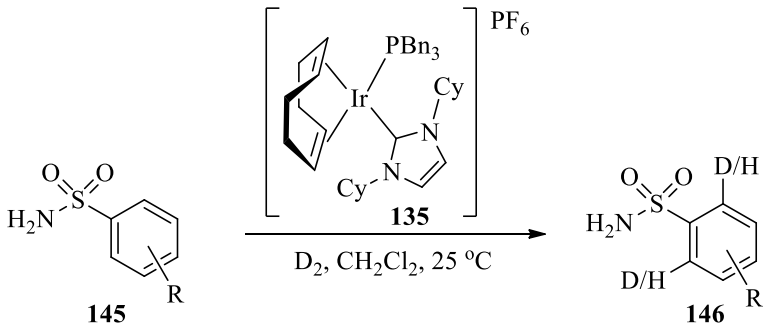

Scheme 134

In addition, the efficiency of novel complexes in alternative reaction media should be explored further. Previous work carried out within our laboratory focused on the use of EtOH and 1,4-dioxane as additional replacements for DCM.[63] During such studies it was determined that reactions performed in the former solvent proceeded to significantly higher levels of deuterium incorporation when heated to 40 °C. It is therefore proposed that a similar improvement may be attained in labelling reactions employing ^{t}BuOMe and 2-MeTHF if run at slightly elevated temperatures.

While attempts at the synthesis of complex **126** did not led to formation of the desired product, the successfully prepared Cl derivative **130** was revealed to display high efficiency in the isotopic labelling of acetophenone **54**. To investigate the activity of this complex further, alternative substrates bearing different functional groups should be examined (**Scheme 135**), and the outcomes compared to those obtained previously with the analogous IMes complex **108**.

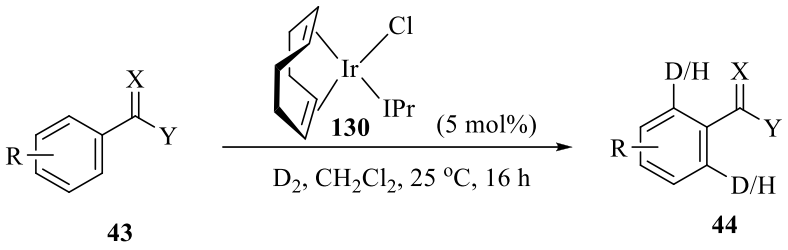

43 44

Scheme 135

Concerning the novel Ir(I) complexes themselves, attention should return to the synthesis of complex **127**. Due to insufficient quantities of material, the preparation of the analogous Cl intermediate **147** was not attempted; however, it is proposed that application of the newly devised synthetic procedure, which would involve the isolation and purification of the latter species, may lead to the successful preparation of the desired complex **127** (**Figure 38**).

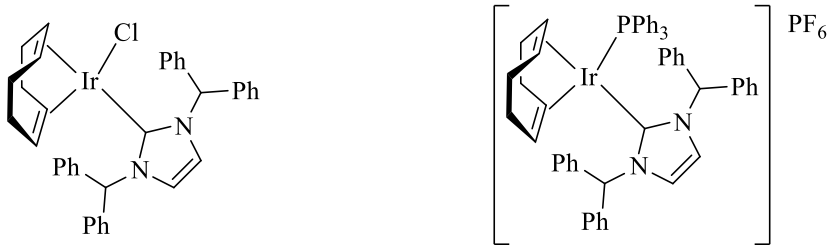

147 127

Figure 38

The extensive coverage of iridium-catalysed processes in current literature offers numerous opportunities to demonstrate the wider applicability of our expanding series of complexes. One area which is of continual interest to our group is the formation of cyclopentenones via the Pauson-Khand reaction.[64] Research by Shibata and co-workers has detailed the use of $[Ir(COD)Cl]_2$ **106** in conjunction with a phosphine ligand to facilitate this carbonylative coupling of an alkyne and alkene, a system which undoubtedly involves the *in-situ* formation of an iridium-phosphine complex.[65] It would therefore be of great interest to investigate the potential to utilise our Ir(I) complexes in an analogous process to determine if any catalytic activity is observed (**Scheme 136**).

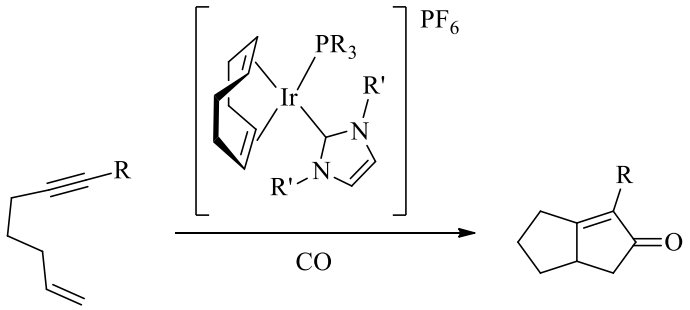

148 **149**

Scheme 136

6 Experimental

6.1 General

All reagents were obtained from commercial suppliers (Aldrich, Alfa Aesar or Strem) and used without further purification, unless otherwise stated. Purification was carried out according to standard laboratory methods.[66]

- Tetrahydrofuran was dried by heating to reflux over sodium wire using benzophenone ketyl as an indicator, and then distilled under nitrogen.
- Diethyl ether and benzene were dried by heating to reflux over sodium wire, and then distilled under nitrogen.
- Dichloromethane and 2-methyltetrahydrofuran were dried by heating to reflux over calcium hydride, and then distilled under nitrogen.
- *tert*-Butylmethyl ether was dried by heating to reflux over calcium sulfate, and then distilled under nitrogen.
- Toluene was obtained from a PureSolv SPS-400-5 Solvent Purification System.
- Hexane was obtained from a PureSolv SPS-400-5 Solvent Purification System and deoxygenated by bubbling argon through for a minimum of thirty minutes.
- Petrol refers to petroleum ether distilling in the range of 40-60 °C.
- Acetanilide, benzanilide, benzamide and triphenylphosphine were purified by recrystallisation from ethanol.

Thin layer chromatography was carried out using Camlab silica plates coated with fluorescent indicator UV_{254}. This was analysed using a Mineralight UVGL-25 lamp or developed using vanillin solution.

Flash column chromatography was carried out using Prolabo silica gel (230-400 mesh).

IR spectra were obtained on an A_2 Technologies ML FTTR machine.

^{1}H, ^{13}C and ^{31}P spectra were recorded on a Bruker DPX 400 spectrometer at 400 MHz, 100 MHz, and 162 MHz, respectively. Chemical shifts are reported in ppm. Coupling constants are reported in Hz and refer to $^{3}J_{H\text{-}H}$ interactions unless otherwise specified.

Melting points were obtained (uncorrected) on a Gallenkamp Griffin melting point apparatus.

High resolution mass spectra were recorded on a Finnigan MAT 90XLT instrument at the EPSRC Mass Spectrometry facility at the University of Wales, Swansea.

Elemental analyses were obtained using a Carlo Erba 1106 CHN analyser.

Density functional theory[67,68] (DFT) was employed to calculate the relative energies for the iridium complexes. Initial pre-optimisation of the structures was carried out with the gradient corrected BP86 functional,[69] in order to take advantage of the resolution-of-the-identity (RI)-DFT approach,[70] as implemented in TurboMole.[71] Calculations involving the iridium atom employed a large-core, quasi-relativistic, effective core potential[72] with the associated basis set; all other atoms were described with the def2-TZVP or def2-SVP basis set.[73] The final optimisation of structures and their characterisation was performed with the Gaussian 09 program suite.[74] These calculations have been performed at the M06 level of theory[75] in conjunction with the 6-31G(*d*,*p*) basis set[76] for all main group elements, and the Stuttgart RSC effective core potential and the associated basis set for Ir.[77] Frequency calculations were performed at the same level of theory to characterise the minima and the first order saddle points. More information regarding the calculations performed as well as all optimised structures may be found on the enclosed CD.[78]

6.2 General Procedures

General Procedure A – Preparation of Iridium(I) Complexes, [Ir(COD)(PR_3)(IMes)]PF_6

A 1 M sodium ethoxide solution was prepared by dissolving 0.25 g of sodium metal in ethanol (10 ml).

To a previously flame-dried Schlenk tube containing η^4-cycloocta-1,5-dieneiridium(I) chloride dimer **106** dissolved in dry benzene (10 ml), was added 1 M sodium ethoxide solution, resulting in a red to yellow colour change. The solution was stirred at r.t. for 10 minutes, followed by the addition of 1,3-dimesitylimidazolium chloride **107**. The solution was stirred under an atmosphere of argon for 5 hours, after which time the solvent was removed under high vacuum. The residue was triturated with dry diethyl ether (15 ml) and filtered through celite under argon. The solvent was again removed under high vacuum yielding a yellow solid which was subsequently dissolved in dry THF (10 ml). Addition of silver hexafluorophosphate resulted in a yellow to orange colour change, and the formation of a precipitate was observed. The solution was stirred for 30 minutes prior to filtration through celite under argon, to give a clear orange solution. On addition of the phosphine, the solution turned from orange to deep red. After stirring for 1 hour, the solvent was once again removed under high vacuum, yielding a red solid. The product was isolated by recrystallisation from DCM/Et_2O, and analysed by ^1H, ^{31}P and ^{13}C NMR, and IR spectroscopy.

General Procedure B – Preparation of Iridium(I) Complexes of the Type Ir(COD)(NHC)Cl

To a previously flame-dried Schlenk tube containing η^4-cycloocta-1,5-dieneiridium(I) chloride dimer **106** dissolved in dry benzene (10 ml), was added 1 M sodium ethoxide solution, resulting in a red to yellow colour change. The solution was stirred at r.t. for 10 minutes, followed by the addition of the imidazolium salt. The Schlenk tube was then placed in an oil bath set at the required temperature, and the solution stirred under an atmosphere of argon. After the allotted time, the solvent was removed under high vacuum and the residue purified directly through a short plug of silica, yielding the desired product as a yellow solid.

General Procedure C – Deuteration of Substrates Using Iridium(I) Complexes

To a previously flame-dried three necked round bottomed flask, fitted with stopcock valves and a suba seal, was added the iridium(I) complex and substrate. The solvent was added and the suba seal replaced with a glass stopper fitted with a Teflon sleeve. The stirring solution was immediately placed in a dry ice/acetone slurry bath and cooled to -78 °C. The flask was evacuated three times, re-filled with nitrogen in the first two instances, and with deuterium in

the third. The flask was then removed from the slurry bath and placed in a water bath set at 25 °C. The solution was left stirring vigorously for the allotted reaction time.

The flask was evacuated to remove excess deuterium from the system. The contents of the flask and washings were then transferred to a single necked flask, and concentrated *in vacuo*. The catalyst was precipitated from the residue by addition of diethyl ether (~10 ml) and the solution filtered through a short plug of silica. The solvent was then removed under reduced pressure.

The level of incorporation achieved was determined by ^{1}H NMR. The relevant integral for the signal corresponding to the site of incorporation was compared to that of a site where exchange would not be expected to occur. The following formula was then used to calculate the extent of labelling:

% Deuteration = 100 – ((relative integral/number of possible labelled sites)*100)

6.3 Preparation of Iridium(I) Complexes

Following *General Procedure A*, results are reported as a) amount of **106**, b) amount of NaOEt, c) amount of imidazolium salt, d) amount of $AgPF_6$, e) amount of phosphine, and f) product yield.

*Preparation of η^4–Cycloocta-1,5-diene(1,3-dimesitylimidazoline-2-ylidene) (triphenylphosphine)iridium(I) hexafluorophosphate **75***[35]

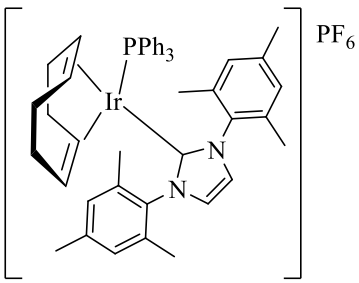

Table 27, Run 1

a) 0.2 g, 0.298 mmol, b) 0.6 ml, 0.6 mmol, c) 1,3-dimesitylimidazolium chloride **107**, 0.203 g, 0.595 mmol, d) 0.150 g, 0.595 mmol, e) triphenylphosphine, 0.156 g, 0.595 mmol, and f) 0.198 g, 33%.

Table 27, Run 2

a) 0.4 g, 0.595 mmol, b) 1.2 ml, 1.2 mmol, c) 1,3-dimesitylimidazolium chloride **107**, 0.406 g, 1.191 mmol, d) 0.301 g, 1.191 mmol, e) triphenylphosphine, 0.312 g, 1.191 mmol, and f) 0.570 g, 47%.

Table 27, Run 3

a) 0.4 g, 0.595 mmol, b) 1.2 ml, 1.2 mmol, c) 1,3-dimesitylimidazolium chloride **107**, 0.406 g, 1.191 mmol, d) 0.301 g, 1.191 mmol, e) triphenylphosphine, 0.312 g, 1.191 mmol, and f) 0.615 g, 51%.

Table 27, Run 4

a) 0.2 g, 0.298 mmol, b) 0.6 ml, 0.6 mmol, c) 1,3-dimesitylimidazolium chloride **107**, 0.203 g, 0.595 mmol, d) 0.150 g, 0.595 mmol, e) triphenylphosphine, 0.156 g, 0.595 mmol, and f) 0.336 g, 56%.

Table 27, Run 5

a) 0.4 g, 0.595 mmol, b) 1.2 ml, 1.2 mmol, c) 1,3-dimesitylimidazolium chloride **107**, 0.406 g, 1.191 mmol, d) 0.301 g, 1.191 mmol, e) triphenylphosphine, 0.312 g, 1.191 mmol, and f) 0.689 g, 57%.

FTIR (CH_2Cl_2): 3061, 2884, 1610, 1588 cm^{-1}.

^1H NMR (400 MHz, $CDCl_3$): δ 7.47-7.43 (m, 5H, ArH), 7.33-7.27 (m, 6H, ArH), 7.15-7.10 (m, 6H, ArH), 7.03 (s, 2H, ArH), 6.65 (s, 2H, olefinic CH), 4.41-4.40 (m, 2H, COD CH), 3.31 (m, 2H, COD CH), 2.36 (s, 6H, $ArCH_3$), 2.12 (s, 6H, $ArCH_3$), 1.66 (s, 6H, $ArCH_3$), 1.63-1.51 (m, 6H, COD CH_2), 1.49 (m, 2H, COD CH_2).

^{13}C NMR (100 MHz, $CDCl_3$): δ 176.7, 139.7, 135.7, 135.6, 135.2, 134.8, 131.2, 130.8, 130.3, 129.7, 128.5, 126.9, 80.5, 80.4, 77.9, 31.9, 30.1, 21.2, 20.9, 19.0.

^{31}P NMR (162 MHz, $CDCl_3$): δ 16.3 (PPh_3), -144.3 (PF_6).

Preparation of η^4–Cycloocta-1,5-diene(1,3-dimesitylimidazoline-2-ylidene) (tribenzylphosphine)iridium(I) hexafluorophosphate ***81***[35]

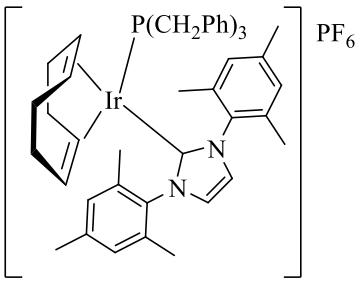

Table 28, Run 1

a) 0.2 g, 0.298 mmol, b) 0.6 ml, 0.6 mmol, c) 1,3-dimesitylimidazolium chloride **107**, 0.203 g, 0.595 mmol, d) 0.150 g, 0.595 mmol, e) tribenzylphosphine, 0.181 g, 0.595 mmol, and f) 0.199 g, 32%.

Table 28, Run 2

a) 0.4 g, 0.595 mmol, b) 1.2 ml, 1.2 mmol, c) 1,3-dimesitylimidazolium chloride **107**, 0.406 g, 1.191 mmol, d) 0.301 g, 1.191 mmol, e) tribenzylphosphine, 0.363 g, 1.191 mmol, and f) 0.547 g, 44%.

Table 28, Run 3

a) 0.4 g, 0.595 mmol, b) 1.2 ml, 1.2 mmol, c) 1,3-dimesitylimidazolium chloride **107**, 0.406 g, 1.191 mmol, d) 0.301 g, 1.191 mmol, e) tribenzylphosphine, 0.363 g, 1.191 mmol, and f) 0.713 g, 57%.

Table 28, Run 4

a) 0.2 g, 0.298 mmol, b) 0.6 ml, 0.6 mmol, c) 1,3-dimesitylimidazolium chloride **107**, 0.203 g, 0.595 mmol, d) 0.150 g, 0.595 mmol, e) tribenzylphosphine, 0.181 g, 0.595 mmol, and f) 0.397 g, 63%.

Table 28, Run 5

a) 0.4 g, 0.595 mmol, b) 1.2 ml, 1.2 mmol, c) 1,3-dimesitylimidazolium chloride **107**, 0.406 g, 1.191 mmol, d) 0.301 g, 1.191 mmol, e) tribenzylphosphine, 0.363 g, 1.191 mmol, and f) 0.751 g, 60%.

FTIR (CH_2Cl_2): 3064, 2917, 1603, 1581 cm^{-1}.

^1H NMR (400 MHz, d_6-acetone): δ 7.79 (s, 2H, olefinic CH), 7.40 (s, 2H, ArH), 7.34 (s, 2H, ArH), 7.30-7.27 (m, 9H, ArH), 6.99-6.97 (m, 6H, ArH), 4.72-4.69 (m, 2H, COD CH), 3.64-3.61 (m, 2H, COD CH), 3.02 (d, $^2J_{P\text{-}H}$ = 8.8 Hz, 6H, PCH_2Ar), 2.57 (s, 6H, $ArCH_3$), 2.47 (s, 6H, $ArCH_3$), 2.39 (s, 6H, $ArCH_3$), 1.80-1.77 (m, 2H, COD CH_2), 1.58-1.49 (m, 4H, COD CH_2), 1.34-1.32 (m, 2H, COD CH_2).

^{13}C NMR (100 MHz, d_6-acetone): δ 175.6, 140.4, 136.3, 136.0, 134.9, 132.9, 132.8, 130.3, 129.9, 129.8, 128.8, 127.4, 126.9, 86.7, 75.3, 31.7, 31.4, 30.5, 30.3, 21.1, 20.2, 19.7.

^{31}P NMR (162 MHz, d_6-acetone): δ -6.8 ($P(CH_2Ph)_3$), -144.2 (PF_6).

*Preparation of η^4–Cycloocta-1,5-diene(1,3-dimesitylimidazoline-2-ylidene) (dimethylphenylphosphine)iridium(I) hexafluorophosphate **82***[35]

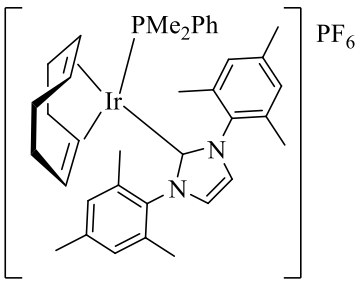

Table 29, Run 1

a) 0.2 g, 0.298 mmol, b) 0.6 ml, 0.6 mmol, c) 1,3-dimesitylimidazolium chloride **107**, 0.203 g, 0.595 mmol, d) 0.150 g, 0.595 mmol, e) dimethylphenylphosphine, 0.082 g, 0.595 mmol, and f) 0.116 g, 22%.

Table 29, Run 2

a) 0.2 g, 0.298 mmol, b) 0.6 ml, 0.6 mmol, c) 1,3-dimesitylimidazolium chloride **107**, 0.203 g, 0.595 mmol, d) 0.150 g, 0.595 mmol, e) dimethylphenylphosphine, 0.082 g, 0.595 mmol, and f) 0.169 g, 32%.

Table 29, Run 3

a) 0.4 g, 0.595 mmol, b) 1.2 ml, 1.2 mmol, c) 1,3-dimesitylimidazolium chloride **107**, 0.406 g, 1.191 mmol, d) 0.301 g, 1.191 mmol, e) dimethylphenylphosphine, 0.164 g, 1.191 mmol, and f) 0.454 g, 43%.

Table 29, Run 4

a) 0.2 g, 0.298 mmol, b) 0.6 ml, 0.6 mmol, c) 1,3-dimesitylimidazolium chloride **107**, 0.203 g, 0.595 mmol, d) 0.150 g, 0.595 mmol, e) dimethylphenylphosphine, 0.082 g, 0.595 mmol, and f) 0.253 g, 48%.

Table 29, Run 5

a) 0.2 g, 0.298 mmol, b) 0.6 ml, 0.6 mmol, c) 1,3-dimesitylimidazolium chloride **107**, 0.203 g, 0.595 mmol, d) 0.150 g, 0.595 mmol, e) dimethylphenylphosphine, 0.082 g, 0.595 mmol, and f) 0.296 g, 56%.

FTIR (CH_2Cl_2): 3006, 2920, 1607, 1577 cm^{-1}.

^{1}H NMR (400 MHz, $CDCl_3$): δ 7.43-7.37 (m, 4H, ArH), 7.31-7.27 (m, 3H, ArH and olefinic CH), 7.06 (s, 2H, ArH), 6.92 (s, 2H, ArH), 4.30-4.28 (m, 2H, COD CH), 3.47-3.44 (m, 2H, COD CH), 2.39 (s, 6H, $ArCH_3$), 2.21 (s, 6H, $ArCH_3$), 2.14 (s, 6H, CH_3), 1.77-1.56 (m, 8H, COD CH_2), 1.51 (d, $^{2}J_{P\text{-}H}$ = 8.4 Hz, 6H, CH_3).

^{13}C NMR (100 MHz, $CDCl_3$): δ 177.1, 139.4, 135.0, 134.9, 134.0, 131.3, 130.1, 129.5, 129.2, 128.2, 125.3, 82.8, 82.7, 75.3, 30.8, 29.9, 20.4, 19.6, 18.6, 15.9, 15.6.

^{31}P NMR (162 MHz, $CDCl_3$): δ -14.1 (PMe_2Ph), -144.3 (PF_6).

6.4 Preparation of Substrates

Preparation of N,N,*4-Trimethylbenzamide* ***111***[79]

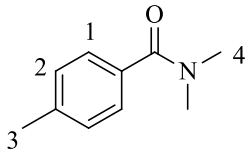

Prior to use, dimethylamine was extracted from a 40% solution in water (8.18 ml, 0.0646 mmol) with DCM (4 x 10 ml).

A solution of *p*-toluoyl chloride **110** (1.99 g, 0.0129 mol) in DCM was cooled to 0 °C in an ice bath, and a solution of dimethylamine in DCM (3.26 ml, 0.0646 mol) was added dropwise. The reaction mixture was allowed to warm to r.t. and stirred for 4 hours. After this time, analysis by TLC (30% Et_2O/petrol) showed complete consumption of the starting material. The reaction mixture was washed with 3 M HCl (3 x 100 ml), saturated $NaHCO_3$ (100 ml), and dried over $NaSO_4$. Filtration followed by removal of solvent under reduced pressure yielded the desired product **111** as a yellow oil (2.078 g, 99%).

FTIR (CH_2Cl_2): 3044, 2934, 1624, 1487 cm^{-1}.
^{1}H NMR (400 MHz, $CDCl_3$): δ 7.32 (d, *J* = 8.0 Hz, 2H, ^{1}CH), 7.19 (d, *J* = 8.0 Hz, 2H, ^{2}CH), 3.00 (br s, 6H, ^{4}CH), 2.38 (s, 3H, ^{3}CH).
^{13}C NMR (100 MHz, $CDCl_3$): δ 171.1, 138.9, 132.8, 128.3, 126.6, 39.0, 34.7, 20.7.

Preparation of N-*Ethyl*,N,*4-dimethylbenzamide* ***112***[34]

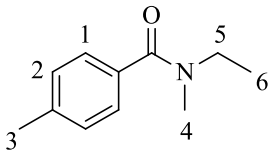

A solution of *p*-toluoyl chloride **110** (1.99 g, 0.0129 mol) in DCM was cooled to 0 °C in an ice bath, and *N*-ethylmethylamine (2.78 ml, 0.0323 mol) was added dropwise. The solution was stirred for 30 minutes at 0 °C and then for 2 hours at r.t. After this time, analysis by TLC (30% Et_2O/petrol) showed complete consumption of the starting material. The reaction mixture was washed with 3 M HCl (3 x 100 ml), saturated $NaHCO_3$ (100 ml), and dried over $NaSO_4$. Filtration followed by removal of solvent under reduced pressure yielded the desired product **112** as a colourless oil (2.229 g, 98%).

FTIR (CH_2Cl_2): 3044, 2918, 2873, 1616, 1457 cm^{-1}.
^{1}H NMR (400 MHz, d_6-acetone): δ 7.30 (d, *J* = 8.0 Hz, 2H, ^{1}CH), 7.24 (d, *J* = 8.0 Hz, 2H, ^{2}CH), 3.39 (br s, 2H, ^{5}CH), 2.98 (s, 3H, ^{4}CH), 2.37 (s, 3H, ^{3}CH), 1.15 (br s, 3H, ^{6}CH).
^{13}C NMR (100 MHz, $CDCl_3$): δ 171.4, 139.1, 133.8, 128.7, 126.6, 45.7, 36.6, 21.1, 12.2.

Preparation of N,N-*Diethyl-4-methylbenzamide* ***113***[80]

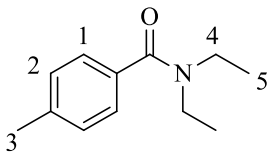

A solution of *p*-toluoyl chloride **110** (1.99 g, 0.0129 mol) in DCM was cooled to 0 °C in an ice bath, and diethylamine (3.34 ml, 0.0323 mol) was added dropwise. The solution was stirred for 30 minutes at 0 °C, allowed to warm to r.t., and stirred overnight. After this time, analysis by TLC (30% Et_2O/petrol) showed complete consumption of the starting material. The reaction mixture was washed with 3 M HCl (3 x 100 ml), saturated $NaHCO_3$ (100 ml), and dried over $NaSO_4$. Filtration followed by removal of solvent under reduced pressure yielded the desired product **113** as a white crystalline solid (2.0591 g, 83%).

m.p. = 55-56 °C (lit. ref. 53.5-55.5 °C)[79]
FTIR (CH_2Cl_2): 2972, 2874, 1618, 1429 cm^{-1}.
^{1}H NMR (400 MHz, d_6-acetone): δ 7.27-7.22 (m, 4H, ^{1}CH and ^{2}CH), 3.38 (br s, 4H, ^{4}CH), 2.36 (s, 3H, ^{3}CH), 1.14 (s, 6H, ^{5}CH).

^{13}C NMR (100 MHz, $CDCl_3$): δ 171.4, 139.0, 134.4, 128.9, 126.3, 43.3, 39.2, 21.3, 14.2, 12.9.

6.5 Application of Iridium(I) Complexes in Hydrogen Isotope Exchange

*Deuteration of Acetophenone **54***

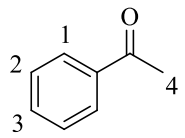

^{1}H NMR (400 MHz, $CDCl_3$): δ 7.93 (d, *J* = 7.5 Hz, 2H, ^{1}CH), 7.54 (t, *J* = 7.4 Hz, 1H, ^{3}CH), 7.40 (t, *J* = 7.4 Hz, 2H, ^{2}CH), 2.58 (s, 3H, ^{4}CH).

Incorporation expected at δ 7.93. Determined against integral at δ 2.58.

Following *General Procedure C*, results are reported as a) amount of substrate, b) amount of catalyst, c) solvent, volume of solvent, d) reaction time, and e) level of incorporation.

Table 30, Entry 1, Run 1

a) acetophenone **54**, 0.026 g, 0.215 mmol, b) complex **75**, 0.001 g, 0.001 mmol, 0.5 mol%, c) DCM, 2.5 ml, d) 2 h, and e) 97%.

Table 30, Entry 1, Run 2

a) acetophenone **54**, 0.026 g, 0.215 mmol, b) complex **75**, 0.001 g, 0.001 mmol, 0.5 mol%, c) DCM, 2.5 ml, d) 2 h, and e) 96%.

Table 30, Entry 2, Run 1

a) acetophenone **54**, 0.026 g, 0.215 mmol, b) complex **81**, 0.0011 g, 0.001 mmol, 0.5 mol%, c) DCM, 2.5 ml, d) 1 h, and e) 97%.

Table 30, Entry 2, Run 2

a) acetophenone **54**, 0.026 g, 0.215 mmol, b) complex **81**, 0.0011 g, 0.001 mmol, 0.5 mol%, c) DCM, 2.5 ml, d) 1 h, and e) 97%.

Table 30, Entry 3, Run 1

a) acetophenone **54**, 0.026 g, 0.215 mmol, b) complex **82**, 0.0009 g, 0.001 mmol, 0.5 mol%, c) DCM, 2.5 ml, d) 1.5 h, and e) 97%.

Table 30, Entry 3, Run 2

a) acetophenone **54**, 0.026 g, 0.215 mmol, b) complex **82**, 0.0009 g, 0.001 mmol, 0.5 mol%, c) DCM, 2.5 ml, d) 1.5 h, and e) 97%.

6.5.1 Solvent Investigations

*Deuteration of Acetophenone **54** in Various Solvents*

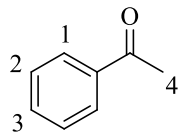

^{1}H NMR (400 MHz, $CDCl_3$): δ 7.93 (d, *J* = 7.5 Hz, 2H, ^{1}CH), 7.54 (t, *J* = 7.4 Hz, 1H, ^{3}CH), 7.40 (t, *J* = 7.4 Hz, 2H, ^{2}CH), 2.58 (s, 3H, ^{4}CH).

Incorporation expected at δ 7.93. Determined against integral at δ 2.58.

Following *General Procedure C*, results are reported as a) amount of substrate, b) amount of catalyst, c) solvent, volume of solvent, d) reaction time, and e) level of incorporation.

Table 31, Entry 1, Run 1

a) acetophenone **54**, 0.026 g, 0.215 mmol, b) complex **75**, 0.01 g, 0.01 mmol, 5 mol%, c) toluene, 4 ml, d) 16 h, and e) 57%.

Table 31, Entry 1, Run 2

a) acetophenone **54**, 0.026 g, 0.215 mmol, b) complex **75**, 0.01 g, 0.01 mmol, 5 mol%, c) toluene, 4 ml, d) 16 h, and e) 44%.

Table 31, Entry 2, Run 1

a) acetophenone **54**, 0.026 g, 0.215 mmol, b) complex **75**, 0.01 g, 0.01 mmol, 5 mol%, c) Et_2O, 4 ml, d) 16 h, and e) 93%.

Table 31, Entry 2, Run 2

a) acetophenone **54**, 0.026 g, 0.215 mmol, b) complex **75**, 0.01 g, 0.01 mmol, 5 mol%, c) Et_2O, 4 ml, d) 16 h, and e) 94%.

Table 31, Entry 3, Run 1

a) acetophenone **54**, 0.026 g, 0.215 mmol, b) complex **75**, 0.01 g, 0.01 mmol, 5 mol%, c) ^{t}BuOMe, 4 ml, d) 16 h, and e) 90%.

Table 31, Entry 3, Run 2

a) acetophenone **54**, 0.026 g, 0.215 mmol, b) complex **75**, 0.01 g, 0.01 mmol, 5 mol%, c) ^{t}BuOMe, 4 ml, d) 16 h, and e) 92%.

Table 31, Entry 4, Run 1

a) acetophenone **54**, 0.026 g, 0.215 mmol, b) complex **75**, 0.01 g, 0.01 mmol, 5 mol%, c) acetone, 2.5 ml, d) 16 h, and e) 41%.

Table 31, Entry 4, Run 2

a) acetophenone **54**, 0.026 g, 0.215 mmol, b) complex **75**, 0.01 g, 0.01 mmol, 5 mol%, c) acetone, 2.5 ml, d) 16 h, and e) 45%.

Table 31, Entry 5, Run 1

a) acetophenone **54**, 0.026 g, 0.215 mmol, b) complex **75**, 0.01 g, 0.01 mmol, 5 mol%, c) THF, 2.5 ml, d) 16 h, and e) 38%.

Table 31, Entry 5, Run 2

a) acetophenone **54**, 0.026 g, 0.215 mmol, b) complex **75**, 0.01 g, 0.01 mmol, 5 mol%, c) THF, 2.5 ml, d) 16 h, and e) 48%.

Table 31, Entry 6, Run 1

a) acetophenone **54**, 0.026 g, 0.215 mmol, b) complex **75**, 0.01 g, 0.01 mmol, 5 mol%, c) 2-MeTHF, 2.5 ml, d) 16 h, and e) 95%.

Table 31, Entry 6, Run 2

a) acetophenone **54**, 0.026 g, 0.215 mmol, b) complex **75**, 0.01 g, 0.01 mmol, 5 mol%, c) 2-MeTHF, 2.5 ml, d) 16 h, and e) 94%.

6.5.2 Rate and Activity Studies

*Deuteration of Acetophenone **54** in Et_2O*

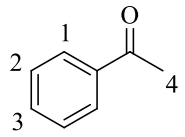

^{1}H NMR (400 MHz, $CDCl_3$): δ 7.93 (d, *J* = 7.5 Hz, 2H, ^{1}CH), 7.54 (t, *J* = 7.4 Hz, 1H, ^{3}CH), 7.40 (t, *J* = 7.4 Hz, 2H, ^{2}CH), 2.58 (s, 3H, ^{4}CH).

Incorporation expected at δ 7.93. Determined against integral at δ 2.58.

Following *General Procedure C*, results are reported as a) amount of substrate, b) amount of catalyst, c) solvent, volume of solvent, d) reaction time, and e) level of incorporation.

Table 34, Entry 1, Run 1

a) acetophenone **54**, 0.026 g, 0.215 mmol, b) complex **81**, 0.011 g, 0.01 mmol, 5 mol%, c) Et_2O, 4 ml, d) 16 h, and e) 93%.

Table 34, Entry 1, Run 2

a) acetophenone **54**, 0.026 g, 0.215 mmol, b) complex **81**, 0.011 g, 0.01 mmol, 5 mol%, c) Et_2O, 4 ml, d) 16 h, and e) 94%.

Table 34, Entry 2, Run 1

a) acetophenone **54**, 0.026 g, 0.215 mmol, b) complex **81**, 0.011 g, 0.01 mmol, 5 mol%, c) Et_2O, 4 ml, d) 2 h, and e) 96%.

Table 34, Entry 2, Run 2

a) acetophenone **54**, 0.026 g, 0.215 mmol, b) complex **81**, 0.011 g, 0.01 mmol, 5 mol%, c) Et_2O, 4 ml, d) 2 h, and e) 95%.

Table 34, Entry 3, Run 1

a) acetophenone **54**, 0.026 g, 0.215 mmol, b) complex **81**, 0.011 g, 0.01 mmol, 5 mol%, c) Et_2O, 4 ml, d) 1 h, and e) 94%.

Table 34, Entry 3, Run 2

a) acetophenone **54**, 0.026 g, 0.215 mmol, b) complex **81**, 0.011 g, 0.01 mmol, 5 mol%, c) Et_2O, 4 ml, d) 1 h, and e) 92%.

Table 34, Entry 4, Run 1

a) acetophenone **54**, 0.026 g, 0.215 mmol, b) complex **81**, 0.011 g, 0.01 mmol, 5 mol%, c) Et_2O, 4 ml, d) 0.5 h, and e) 63%.

Table 34, Entry 4, Run 2

a) acetophenone **54**, 0.026 g, 0.215 mmol, b) complex **81**, 0.011 g, 0.01 mmol, 5 mol%, c) Et_2O, 4 ml, d) 0.5 h, and e) 65%.

Table 35, Entry 1, Run 1

a) acetophenone **54**, 0.026 g, 0.215 mmol, b) complex **81**, 0.0068 g, 0.0065 mmol, 3 mol%, c) Et_2O, 4 ml, d) 1 h, and e) 96%.

Table 35, Entry 1, Run 2

a) acetophenone **54**, 0.026 g, 0.215 mmol, b) complex **81**, 0.0068 g, 0.0065 mmol, 3 mol%, c) Et_2O, 4 ml, d) 1 h, and e) 97%.

Table 35, Entry 2, Run 1

a) acetophenone **54**, 0.026 g, 0.215 mmol, b) complex **81**, 0.0023 g, 0.0022 mmol, 1 mol%, c) Et_2O, 4 ml, d) 1 h, and e) 72%.

Table 35, Entry 2, Run 2

a) acetophenone **54**, 0.026 g, 0.215 mmol, b) complex **81**, 0.0023 g, 0.0022 mmol, 1 mol%, c) Et_2O, 4 ml, d) 1 h, and e) 67%.

Table 36, Entry 1, Run 1

a) acetophenone **54**, 0.026 g, 0.215 mmol, b) complex **75**, 0.01 g, 0.01 mmol, 5 mol%, c) Et_2O, 4 ml, d) 16 h, and e) 93%.

Table 36, Entry 1, Run 2

a) acetophenone **54**, 0.026 g, 0.215 mmol, b) complex **75**, 0.01 g, 0.01 mmol, 5 mol%, c) Et_2O, 4 ml, d) 16 h, and e) 94%.

Table 36, Entry 2, Run 1

a) acetophenone **54**, 0.026 g, 0.215 mmol, b) complex **75**, 0.01 g, 0.01 mmol, 5 mol%, c) Et_2O, 4 ml, d) 2 h, and e) 94%.

Table 36, Entry 2, Run 2

a) acetophenone **54**, 0.026 g, 0.215 mmol, b) complex **75**, 0.01 g, 0.01 mmol, 5 mol%, c) Et_2O, 4 ml, d) 2 h, and e) 94%.

Table 36, Entry 3, Run 1

a) acetophenone **54**, 0.026 g, 0.215 mmol, b) complex **75**, 0.01 g, 0.01 mmol, 5 mol%, c) Et_2O, 4 ml, d) 1 h, and e) 94%.

Table 36, Entry 3, Run 2

a) acetophenone **54**, 0.026 g, 0.215 mmol, b) complex **75**, 0.01 g, 0.01 mmol, 5 mol%, c) Et_2O, 4 ml, d) 1 h, and e) 93%.

Table 36, Entry 4, Run 1

a) acetophenone **54**, 0.026 g, 0.215 mmol, b) complex **75**, 0.01 g, 0.01 mmol, 5 mol%, c) Et_2O, 4 ml, d) 0.5 h, and e) 84%.

Table 36, Entry 4, Run 2

a) acetophenone **54**, 0.026 g, 0.215 mmol, b) complex **75**, 0.01 g, 0.01 mmol, 5 mol%, c) Et_2O, 4 ml, d) 0.5 h, and e) 84%.

Table 37, Entry 1, Run 1

a) acetophenone **54**, 0.026 g, 0.215 mmol, b) complex **75**, 0.0065 g, 0.0065 mmol, 3 mol%, c) Et_2O, 4 ml, d) 1 h, and e) 77%.

Table 37, Entry 1, Run 2

a) acetophenone **54**, 0.026 g, 0.215 mmol, b) complex **75**, 0.0065 g, 0.0065 mmol, 3 mol%, c) Et_2O, 4 ml, d) 1 h, and e) 72%.

Table 37, Entry 2, Run 1

a) acetophenone **54**, 0.026 g, 0.215 mmol, b) complex **75**, 0.0065 g, 0.0065 mmol, 3 mol%, c) Et_2O, 4 ml, d) 2 h, and e) 92%.

Table 37, Entry 2, Run 2

a) acetophenone **54**, 0.026 g, 0.215 mmol, b) complex **75**, 0.0065 g, 0.0065 mmol, 3 mol%, c) Et_2O, 4 ml, d) 2 h, and e) 90%.

Table 38, Entry 1, Run 1

a) acetophenone **54**, 0.026 g, 0.215 mmol, b) complex **82**, 0.009 g, 0.01 mmol, 5 mol%, c) Et_2O, 4 ml, d) 16 h, and e) 94%.

Table 38, Entry 1, Run 2

a) acetophenone **54**, 0.026 g, 0.215 mmol, b) complex **82**, 0.009 g, 0.01 mmol, 5 mol%, c) Et_2O, 4 ml, d) 16 h, and e) 95%.

Table 38, Entry 2, Run 1

a) acetophenone **54**, 0.026 g, 0.215 mmol, b) complex **82**, 0.009 g, 0.01 mmol, 5 mol%, c) Et_2O, 4 ml, d) 2 h, and e) 97%.

Table 38, Entry 2, Run 2

a) acetophenone **54**, 0.026 g, 0.215 mmol, b) complex **82**, 0.009 g, 0.01 mmol, 5 mol%, c) Et_2O, 4 ml, d) 2 h, and e) 96%.

Table 38, Entry 3, Run 1

a) acetophenone **54**, 0.026 g, 0.215 mmol, b) complex **82**, 0.009 g, 0.01 mmol, 5 mol%, c) Et_2O, 4 ml, d) 1 h, and e) 96%.

Table 38, Entry 3, Run 2

a) acetophenone **54**, 0.026 g, 0.215 mmol, b) complex **82**, 0.009 g, 0.01 mmol, 5 mol%, c) Et_2O, 4 ml, d) 1 h, and e) 96%.

Table 38, Entry 4, Run 1

a) acetophenone **54**, 0.026 g, 0.215 mmol, b) complex **82**, 0.009 g, 0.01 mmol, 5 mol%, c) Et_2O, 4 ml, d) 0.5 h, and e) 98%.

Table 38, Entry 4, Run 2

a) acetophenone **54**, 0.026 g, 0.215 mmol, b) complex **82**, 0.009 g, 0.01 mmol, 5 mol%, c) Et_2O, 4 ml, d) 0.5 h, and e) 97%.

Table 39, Entry 1, Run 1

a) acetophenone **54**, 0.026 g, 0.215 mmol, b) complex **82**, 0.006 g, 0.0065 mmol, 3 mol%, c) Et_2O, 4 ml, d) 0.5 h, and e) 98%.

Table 39, Entry 1, Run 2

a) acetophenone **54**, 0.026 g, 0.215 mmol, b) complex **82**, 0.006 g, 0.0065 mmol, 3 mol%, c) Et_2O, 4 ml, d) 0.5 h, and e) 92%.

Table 39, Entry 2, Run 1

a) acetophenone **54**, 0.026 g, 0.215 mmol, b) complex **82**, 0.002 g, 0.0022 mmol, 1 mol%, c) Et_2O, 4 ml, d) 0.5 h, and e) 34%.

Table 39, Entry 2, Run 2

a) acetophenone **54**, 0.026 g, 0.215 mmol, b) complex **82**, 0.002 g, 0.0022 mmol, 1 mol%, c) Et_2O, 4 ml, d) 0.5 h, and e) 34%.

Table 39, Entry 3, Run 1

a) acetophenone **54**, 0.026 g, 0.215 mmol, b) complex **82**, 0.002 g, 0.0022 mmol, 1 mol%, c) Et_2O, 4 ml, d) 1 h, and e) 80%.

Table 39, Entry 3, Run 2

a) acetophenone **54**, 0.026 g, 0.215 mmol, b) complex **82**, 0.002 g, 0.0022 mmol, 1 mol%, c) Et_2O, 4 ml, d) 1 h, and e) 88%.

Table 39, Entry 4, Run 1

a) acetophenone **54**, 0.026 g, 0.215 mmol, b) complex **82**, 0.002 g, 0.0022 mmol, 1 mol%, c) Et_2O, 4 ml, d) 2 h, and e) 96%.

Table 39, Entry 4, Run 2

a) acetophenone **54**, 0.026 g, 0.215 mmol, b) complex **82**, 0.002 g, 0.0022 mmol, 1 mol%, c) Et_2O, 4 ml, d) 2 h, and e) 90%.

*Deuteration of Acetophenone **54** in ^{t}BuOMe*

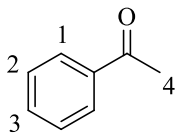

^{1}H NMR (400 MHz, $CDCl_3$): δ 7.93 (d, *J* = 7.5 Hz, 2H, ^{1}CH), 7.54 (t, *J* = 7.4 Hz, 1H, ^{3}CH), 7.40 (t, *J* = 7.4 Hz, 2H, ^{2}CH), 2.58 (s, 3H, ^{4}CH).

Incorporation expected at δ 7.93. Determined against integral at δ 2.58.

Following *General Procedure C,* results are reported as a) amount of substrate, b) amount of catalyst, c) solvent, volume of solvent, d) reaction time, and e) level of incorporation.

Table 40, Entry 1, Run 1

a) acetophenone **54**, 0.026 g, 0.215 mmol, b) complex **81**, 0.011 g, 0.01 mmol, 5 mol%, c) ^{t}BuOMe, 4 ml, d) 16 h, and e) 92%.

Table 40, Entry 1, Run 2

a) acetophenone **54**, 0.026 g, 0.215 mmol, b) complex **81**, 0.011 g, 0.01 mmol, 5 mol%, c) ^{t}BuOMe, 4 ml, d) 16 h, and e) 97%.

Table 40, Entry 2, Run 1

a) acetophenone **54**, 0.026 g, 0.215 mmol, b) complex **81**, 0.011 g, 0.01 mmol, 5 mol%, c) ^{t}BuOMe, 4 ml, d) 2 h, and e) 94%.

Table 40, Entry 2, Run 2

a) acetophenone **54**, 0.026 g, 0.215 mmol, b) complex **81**, 0.011 g, 0.01 mmol, 5 mol%, c) ^{t}BuOMe, 4 ml, d) 2 h, and e) 90%.

Table 40, Entry 3, Run 1

a) acetophenone **54**, 0.026 g, 0.215 mmol, b) complex **81**, 0.011 g, 0.01 mmol, 5 mol%, c) ^{t}BuOMe, 4 ml, d) 1 h, and e) 63%.

Table 40, Entry 3, Run 2

a) acetophenone **54**, 0.026 g, 0.215 mmol, b) complex **81**, 0.011 g, 0.01 mmol, 5 mol%, c) ^{t}BuOMe, 4 ml, d) 1 h, and e) 52%.

Table 41, Entry 1, Run 1

a) acetophenone **54**, 0.026 g, 0.215 mmol, b) complex **81**, 0.0068 g, 0.0065 mmol, 3 mol%, c) ^{t}BuOMe, 4 ml, d) 2 h, and e) 79%.

Table 41, Entry 1, Run 2

a) acetophenone **54**, 0.026 g, 0.215 mmol, b) complex **81**, 0.0068 g, 0.0065 mmol, 3 mol%, c) ^{t}BuOMe, 4 ml, d) 2 h, and e) 87%.

Table 41, Entry 2, Run 1

a) acetophenone **54**, 0.026 g, 0.215 mmol, b) complex **81**, 0.0068 g, 0.0065 mmol, 3 mol%, c) ^{t}BuOMe, 4 ml, d) 3 h, and e) 90%.

Table 41, Entry 2, Run 2

a) acetophenone **54**, 0.026 g, 0.215 mmol, b) complex **81**, 0.0068 g, 0.0065 mmol, 3 mol%, c) ^{t}BuOMe, 4 ml, d) 3 h, and e) 85%.

Table 42, Entry 1, Run 1

a) acetophenone **54**, 0.026 g, 0.215 mmol, b) complex **75**, 0.01 g, 0.01 mmol, 5 mol%, c) ^{t}BuOMe, 4 ml, d) 16 h, and e) 90%.

Table 42, Entry 1, Run 2

a) acetophenone **54**, 0.026 g, 0.215 mmol, b) complex **75**, 0.01 g, 0.01 mmol, 5 mol%, c) ^{t}BuOMe, 4 ml, d) 16 h, and e) 92%.

Table 42, Entry 2, Run 1

a) acetophenone **54**, 0.026 g, 0.215 mmol, b) complex **75**, 0.01 g, 0.01 mmol, 5 mol%, c) ^{t}BuOMe, 4 ml, d) 2 h, and e) 89%.

Table 42, Entry 2, Run 2

a) acetophenone **54**, 0.026 g, 0.215 mmol, b) complex **75**, 0.01 g, 0.01 mmol, 5 mol%, c) ^{t}BuOMe, 4 ml, d) 2 h, and e) 91%.

Table 42, Entry 3, Run 1

a) acetophenone **54**, 0.026 g, 0.215 mmol, b) complex **75**, 0.01 g, 0.01 mmol, 5 mol%, c) ^{t}BuOMe, 4 ml, d) 1 h, and e) 78%.

Table 42, Entry 3, Run 2

a) acetophenone **54**, 0.026 g, 0.215 mmol, b) complex **75**, 0.01 g, 0.01 mmol, 5 mol%, c) ^{t}BuOMe, 4 ml, d) 1 h, and e) 76%.

Table 42, Entry 4, Run 1

a) acetophenone **54**, 0.026 g, 0.215 mmol, b) complex **75**, 0.01 g, 0.01 mmol, 5 mol%, c) ^{t}BuOMe, 4 ml, d) 0.5 h, and e) 63%.

Table 42, Entry 4, Run 2

a) acetophenone **54**, 0.026 g, 0.215 mmol, b) complex **75**, 0.01 g, 0.01 mmol, 5 mol%, c) ^{t}BuOMe, 4 ml, d) 0.5 h, and e) 55%.

Table 43, Entry 1, Run 1

a) acetophenone **54**, 0.026 g, 0.215 mmol, b) complex **75**, 0.0065 g, 0.0065 mmol, 3 mol%, c) ^{t}BuOMe, 4 ml, d) 2 h, and e) 66%.

Table 43, Entry 1, Run 2

a) acetophenone **54**, 0.026 g, 0.215 mmol, b) complex **75**, 0.0065 g, 0.0065 mmol, 3 mol%, c) ^{t}BuOMe, 4 ml, d) 2 h, and e) 75%.

Table 44, Entry 1, Run 1

a) acetophenone **54**, 0.026 g, 0.215 mmol, b) complex **82**, 0.009 g, 0.01 mmol, 5 mol%, c) ^{t}BuOMe, 4 ml, d) 16 h, and e) 90%.

Table 44, Entry 1, Run 2

a) acetophenone **54**, 0.026 g, 0.215 mmol, b) complex **82**, 0.009 g, 0.01 mmol, 5 mol%, c) ^{t}BuOMe, 4 ml, d) 16 h, and e) 88%.

Table 44, Entry 2, Run 1

a) acetophenone **54**, 0.026 g, 0.215 mmol, b) complex **82**, 0.009 g, 0.01 mmol, 5 mol%, c) ^{t}BuOMe, 4 ml, d) 2 h, and e) 93%.

Table 44, Entry 2, Run 2

a) acetophenone **54**, 0.026 g, 0.215 mmol, b) complex **82**, 0.009 g, 0.01 mmol, 5 mol%, c) ^{t}BuOMe, 4 ml, d) 2 h, and e) 86%.

Table 44, Entry 3, Run 1

a) acetophenone **54**, 0.026 g, 0.215 mmol, b) complex **82**, 0.009 g, 0.01 mmol, 5 mol%, c) ^{t}BuOMe, 4 ml, d) 1 h, and e) 96%.

Table 44, Entry 3, Run 2

a) acetophenone **54**, 0.026 g, 0.215 mmol, b) complex **82**, 0.009 g, 0.01 mmol, 5 mol%, c) ^{t}BuOMe, 4 ml, d) 1 h, and e) 94%.

Table 44, Entry 4, Run 1

a) acetophenone **54**, 0.026 g, 0.215 mmol, b) complex **82**, 0.009 g, 0.01 mmol, 5 mol%, c) ^{t}BuOMe, 4 ml, d) 0.5 h, and e) 80%.

Table 44, Entry 4, Run 2

a) acetophenone **54**, 0.026 g, 0.215 mmol, b) complex **82**, 0.009 g, 0.01 mmol, 5 mol%, c) ^{t}BuOMe, 4 ml, d) 0.5 h, and e) 76%.

Table 45, Entry 1, Run 1

a) acetophenone **54**, 0.026 g, 0.215 mmol, b) complex **82**, 0.006 g, 0.0065 mmol, 3 mol%, c) ^{t}BuOMe, 4 ml, d) 1 h, and e) 94%.

Table 45, Entry 1, Run 2

a) acetophenone **54**, 0.026 g, 0.215 mmol, b) complex **82**, 0.006 g, 0.0065 mmol, 3 mol%, c) ^{t}BuOMe, 4 ml, d) 1 h, and e) 86%.

Table 45, Entry 2, Run 1

a) acetophenone **54**, 0.026 g, 0.215 mmol, b) complex **82**, 0.002 g, 0.0022 mmol, 1 mol%, c) ^{t}BuOMe, 4 ml, d) 1 h, and e) 68%.

Table 45, Entry 2, Run 2

a) acetophenone **54**, 0.026 g, 0.215 mmol, b) complex **82**, 0.002 g, 0.0022 mmol, 1 mol%, c) ^{t}BuOMe, 4 ml, d) 1 h, and e) 72%.

*Deuteration of Acetophenone **54** in 2-MeTHF*

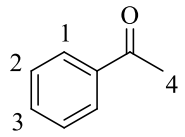

^{1}H NMR (400 MHz, $CDCl_3$): δ 7.93 (d, *J* = 7.5 Hz, 2H, ^{1}CH), 7.54 (t, *J* = 7.4 Hz, 1H, ^{3}CH), 7.40 (t, *J* = 7.4 Hz, 2H, ^{2}CH), 2.58 (s, 3H, ^{4}CH).

Incorporation expected at δ 7.93. Determined against integral at δ 2.58.

Following *General Procedure C*, results are reported as a) amount of substrate, b) amount of catalyst, c) solvent, volume of solvent, d) reaction time, and e) level of incorporation.

Table 46, Entry 1, Run 1

a) acetophenone **54**, 0.026 g, 0.215 mmol, b) complex **81**, 0.011 g, 0.01 mmol, 5 mol%, c) 2-MeTHF, 2.5 ml, d) 16 h, and e) 97%.

Table 46, Entry 1, Run 2

a) acetophenone **54**, 0.026 g, 0.215 mmol, b) complex **81**, 0.011 g, 0.01 mmol, 5 mol%, c) 2-MeTHF, 2.5 ml, d) 16 h, and e) 92%.

Table 46, Entry 2, Run 1

a) acetophenone **54**, 0.026 g, 0.215 mmol, b) complex **81**, 0.011 g, 0.01 mmol, 5 mol%, c) 2-MeTHF, 2.5 ml, d) 2 h, and e) 97%.

Table 46, Entry 2, Run 2

a) acetophenone **54**, 0.026 g, 0.215 mmol, b) complex **81**, 0.011 g, 0.01 mmol, 5 mol%, c) 2-MeTHF, 2.5 ml, d) 2 h, and e) 95%.

Table 46, Entry 3, Run 1

a) acetophenone **54**, 0.026 g, 0.215 mmol, b) complex **81**, 0.011 g, 0.01 mmol, 5 mol%, c) 2-MeTHF, 2.5 ml, d) 1 h, and e) 95%.

Table 46, Entry 3, Run 2

a) acetophenone **54**, 0.026 g, 0.215 mmol, b) complex **81**, 0.011 g, 0.01 mmol, 5 mol%, c) 2-MeTHF, 2.5 ml, d) 1 h, and e) 92%.

Table 46, Entry 4, Run 1

a) acetophenone **54**, 0.026 g, 0.215 mmol, b) complex **81**, 0.011 g, 0.01 mmol, 5 mol%, c) 2-MeTHF, 2.5 ml, d) 0.5 h, and e) 94%.

Table 46, Entry 4, Run 2

a) acetophenone **54**, 0.026 g, 0.215 mmol, b) complex **81**, 0.011 g, 0.01 mmol, 5 mol%, c) 2-MeTHF, 2.5 ml, d) 0.5 h, and e) 91%.

Table 47, Entry 1, Run 1

a) acetophenone **54**, 0.026 g, 0.215 mmol, b) complex **81**, 0.0068 g, 0.0065 mmol, 3 mol%, c) 2-MeTHF, 2.5 ml, d) 0.5 h, and e) 55%.

Table 47, Entry 1, Run 2

a) acetophenone **54**, 0.026 g, 0.215 mmol, b) complex **81**, 0.0068 g, 0.0065 mmol, 3 mol%, c) 2-MeTHF, 2.5 ml, d) 0.5 h, and e) 59%.

Table 47, Entry 2, Run 1

a) acetophenone **54**, 0.026 g, 0.215 mmol, b) complex **81**, 0.0068 g, 0.0065 mmol, 3 mol%, c) 2-MeTHF, 2.5 ml, d) 1 h, and e) 96%.

Table 47, Entry 2, Run 2

a) acetophenone **54**, 0.026 g, 0.215 mmol, b) complex **81**, 0.0068 g, 0.0065 mmol, 3 mol%, c) 2-MeTHF, 2.5 ml, d) 1 h, and e) 90%.

Table 48, Entry 1, Run 1

a) acetophenone **54**, 0.026 g, 0.215 mmol, b) complex **75**, 0.01 g, 0.01 mmol, 5 mol%, c) 2-MeTHF, 2.5 ml, d) 16 h, and e) 95%.

Table 48, Entry 1, Run 2

a) acetophenone **54**, 0.026 g, 0.215 mmol, b) complex **75**, 0.01 g, 0.01 mmol, 5 mol%, c) 2-MeTHF, 2.5 ml, d) 16 h, and e) 94%.

Table 48, Entry 2, Run 1

a) acetophenone **54**, 0.026 g, 0.215 mmol, b) complex **75**, 0.01 g, 0.01 mmol, 5 mol%, c) 2-MeTHF, 2.5 ml, d) 2 h, and e) 97%.

Table 48, Entry 2, Run 2

a) acetophenone **54**, 0.026 g, 0.215 mmol, b) complex **75**, 0.01 g, 0.01 mmol, 5 mol%, c) 2-MeTHF, 2.5 ml, d) 2 h, and e) 96%.

Table 48, Entry 3, Run 1

a) acetophenone **54**, 0.026 g, 0.215 mmol, b) complex **75**, 0.01 g, 0.01 mmol, 5 mol%, c) 2-MeTHF, 2.5 ml, d) 1 h, and e) 91%.

Table 48, Entry 3, Run 2

a) acetophenone **54**, 0.026 g, 0.215 mmol, b) complex **75**, 0.01 g, 0.01 mmol, 5 mol%, c) 2-MeTHF, 2.5 ml, d) 1 h, and e) 94%.

Table 48, Entry 4, Run 1

a) acetophenone **54**, 0.026 g, 0.215 mmol, b) complex **75**, 0.01 g, 0.01 mmol, 5 mol%, c) 2-MeTHF, 2.5 ml, d) 0.5 h, and e) 76%.

Table 48, Entry 4, Run 2

a) acetophenone **54**, 0.026 g, 0.215 mmol, b) complex **75**, 0.01 g, 0.01 mmol, 5 mol%, c) 2-MeTHF, 2.5 ml, d) 0.5 h, and e) 63%.

Table 49, Entry 1, Run 1

a) acetophenone **54**, 0.026 g, 0.215 mmol, b) complex **75**, 0.0065 g, 0.0065 mmol, 3 mol%, c) 2-MeTHF, 2.5 ml, d) 2 h, and e) 95%.

Table 49, Entry 1, Run 2

a) acetophenone **54**, 0.026 g, 0.215 mmol, b) complex **75**, 0.0065 g, 0.0065 mmol, 3 mol%, c) 2-MeTHF, 2.5 ml, d) 2 h, and e) 88%.

Table 49, Entry 2, Run 1

a) acetophenone **54**, 0.026 g, 0.215 mmol, b) complex **75**, 0.0022 g, 0.0022 mmol, 1 mol%, c) 2-MeTHF, 2.5 ml, d) 2 h, and e) 26%.

Table 49, Entry 2, Run 2

a) acetophenone **54**, 0.026 g, 0.215 mmol, b) complex **75**, 0.0022 g, 0.0022 mmol, 1 mol%, c) 2-MeTHF, 2.5 ml, d) 2 h, and e) 20%.

Table 50, Entry 1, Run 1

a) acetophenone **54**, 0.026 g, 0.215 mmol, b) complex **82**, 0.009 g, 0.01 mmol, 5 mol%, c) 2-MeTHF, 2.5 ml, d) 16 h, and e) 98%.

Table 50, Entry 1, Run 2

a) acetophenone **54**, 0.026 g, 0.215 mmol, b) complex **82**, 0.009 g, 0.01 mmol, 5 mol%, c) 2-MeTHF, 2.5 ml, d) 16 h, and e) 98%.

Table 50, Entry 2, Run 1

a) acetophenone **54**, 0.026 g, 0.215 mmol, b) complex **82**, 0.009 g, 0.01 mmol, 5 mol%, c) 2-MeTHF, 2.5 ml, d) 1 h, and e) 96%.

Table 50, Entry 2, Run 2

a) acetophenone **54**, 0.026 g, 0.215 mmol, b) complex **82**, 0.009 g, 0.01 mmol, 5 mol%, c) 2-MeTHF, 2.5 ml, d) 1 h, and e) 98%.

Table 50, Entry 3, Run 1

a) acetophenone **54**, 0.026 g, 0.215 mmol, b) complex **82**, 0.009 g, 0.01 mmol, 5 mol%, c) 2-MeTHF, 2.5 ml, d) 0.5 h, and e) 96%.

Table 50, Entry 3, Run 2

a) acetophenone **54**, 0.026 g, 0.215 mmol, b) complex **82**, 0.009 g, 0.01 mmol, 5 mol%, c) 2-MeTHF, 2.5 ml, d) 0.5 h, and e) 90%.

Table 51, Entry 1, Run 1

a) acetophenone **54**, 0.026 g, 0.215 mmol, b) complex **82**, 0.006 g, 0.0065 mmol, 3 mol%, c) 2-MeTHF, 2.5 ml, d) 0.5 h, and e) 98%.

Table 51, Entry 1, Run 2

a) acetophenone **54**, 0.026 g, 0.215 mmol, b) complex **82**, 0.006 g, 0.0065 mmol, 3 mol%, c) 2-MeTHF, 2.5 ml, d) 0.5 h, and e) 95%.

Table 51, Entry 2, Run 1

a) acetophenone **54**, 0.026 g, 0.215 mmol, b) complex **82**, 0.002 g, 0.0022 mmol, 1 mol%, c) 2-MeTHF, 2.5 ml, d) 0.5 h, and e) 33%.

Table 51, Entry 2, Run 2

a) acetophenone **54**, 0.026 g, 0.215 mmol, b) complex **82**, 0.002 g, 0.0022 mmol, 1 mol%, c) 2-MeTHF, 2.5 ml, d) 0.5 h, and e) 37%.

*Deuteration of Benzophenone **57***

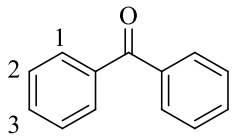

^{1}H NMR (400 MHz, $CDCl_3$): δ 7.81 (d, *J* = 8.0 Hz, 4H, ^{1}CH), 7.60 (t, *J* = 8.0 Hz, 2H, ^{3}CH), 7.49 (t, *J* = 7.7 Hz, 4H, ^{2}CH).

Incorporation expected at δ7.81. Determined against integral at δ7.60.

Following *General Procedure C*, results are reported as a) amount of substrate, b) amount of catalyst, c) solvent, volume of solvent, d) reaction time, and e) level of incorporation.

Table 53, Entry 1, Run 1

a) benzophenone **57**, 0.039 g, 0.215 mmol, b) complex **81**, 0.0068 g, 0.0065 mmol, 3 mol%, c) Et_2O, 4 ml, d) 1 h, and e) 83%.

Table 53, Entry 1, Run 2

a) benzophenone **57**, 0.039 g, 0.215 mmol, b) complex **81**, 0.0068 g, 0.0065 mmol, 3 mol%, c) Et_2O, 4 ml, d) 1 h, and e) 76%.

Table 53, Entry 2, Run 1

a) benzophenone **57**, 0.039 g, 0.215 mmol, b) complex **75**, 0.0065 g, 0.0065 mmol, 3 mol%, c) Et_2O, 4 ml, d) 2 h, and e) 87%.

Table 53, Entry 2, Run 2

a) benzophenone **57**, 0.039 g, 0.215 mmol, b) complex **75**, 0.0065 g, 0.0065 mmol, 3 mol%, c) Et_2O, 4 ml, d) 2 h, and e) 85%.

Table 53, Entry 3, Run 1

a) benzophenone **57**, 0.039 g, 0.215 mmol, b) complex **82**, 0.002 g, 0.0022 mmol, 1 mol%, c) Et_2O, 4 ml, d) 2 h, and e) 94%.

Table 53, Entry 3, Run 2

a) benzophenone **57**, 0.039 g, 0.215 mmol, b) complex **82**, 0.002 g, 0.0022 mmol, 1 mol%, c) Et_2O, 4 ml, d) 2 h, and e) 94%.

Table 54, Entry 1, Run 1

a) benzophenone **57**, 0.039 g, 0.215 mmol, b) complex **81**, 0.011 g, 0.01 mmol, 5 mol%, c) ^{t}BuOMe, 4 ml, d) 2 h, and e) 68%.

Table 54, Entry 1, Run 2

a) benzophenone **57**, 0.039 g, 0.215 mmol, b) complex **81**, 0.011 g, 0.01 mmol, 5 mol%, c) ^{t}BuOMe, 4 ml, d) 2 h, and e) 66%.

Table 54, Entry 2, Run 1

a) benzophenone **57**, 0.039 g, 0.215 mmol, b) complex **75**, 0.01 g, 0.01 mmol, 5 mol%, c) ^{t}BuOMe, 4 ml, d) 2 h, and e) 72%.

Table 54, Entry 2, Run 2

a) benzophenone **57**, 0.039 g, 0.215 mmol, b) complex **75**, 0.01 g, 0.01 mmol, 5 mol%, c) ^{t}BuOMe, 4 ml, d) 2 h, and e) 81%.

Table 54, Entry 3, Run 1

a) benzophenone **57**, 0.039 g, 0.215 mmol, b) complex **82**, 0.006 g, 0.0065 mmol, 3 mol%, c) ^{t}BuOMe, 4 ml, d) 1 h, and e) 72%.

Table 54, Entry 3, Run 2

a) benzophenone **57**, 0.039 g, 0.215 mmol, b) complex **82**, 0.006 g, 0.0065 mmol, 3 mol%, c) ^{t}BuOMe, 4 ml, d) 1 h, and e) 68%.

Table 54, Entry 4, Run 1

a) benzophenone **57**, 0.039 g, 0.215 mmol, b) complex **82**, 0.009 g, 0.01 mmol, 5 mol%, c) ^{t}BuOMe, 4 ml, d) 16 h, and e) 92%.

Table 54, Entry 4, Run 2

a) benzophenone **57**, 0.039 g, 0.215 mmol, b) complex **82**, 0.009 g, 0.01 mmol, 5 mol%, c) ^{t}BuOMe, 4 ml, d) 16 h, and e) 88%.

Table 55, Entry 1, Run 1

a) benzophenone **57**, 0.039 g, 0.215 mmol, b) complex **81**, 0.0068 g, 0.0065 mmol, 3 mol%, c) 2-MeTHF, 2.5 ml, d) 1 h, and e) 76%.

Table 55, Entry 1, Run 2

a) benzophenone **57**, 0.039 g, 0.215 mmol, b) complex **81**, 0.0068 g, 0.0065 mmol, 3 mol%, c) 2-MeTHF, 2.5 ml, d) 1 h, and e) 73%.

Table 55, Entry 2, Run 1

a) benzophenone **57**, 0.039 g, 0.215 mmol, b) complex **75**, 0.0065 g, 0.0065 mmol, 3 mol%, c) 2-MeTHF, 2.5 ml, d) 2 h, and e) 70%.

Table 55, Entry 2, Run 2

a) benzophenone **57**, 0.039 g, 0.215 mmol, b) complex **75**, 0.0065 g, 0.0065 mmol, 3 mol%, c) 2-MeTHF, 2.5 ml, d) 2 h, and e) 72%.

Table 55, Entry 3, Run 1

a) benzophenone **57**, 0.039 g, 0.215 mmol, b) complex **82**, 0.006 g, 0.0065 mmol, 3 mol%, c) 2-MeTHF, 2.5 ml, d) 0.5 h, and e) 87%.

Table 55, Entry 3, Run 2

a) benzophenone **57**, 0.039 g, 0.215 mmol, b) complex **82**, 0.006 g, 0.0065 mmol, 3 mol%, c) 2-MeTHF, 2.5 ml, d) 0.5 h, and e) 89%.

*Deuteration of 2-Phenylpyridine **41***

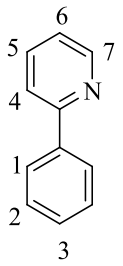

^{1}H NMR (400 MHz, $CDCl_3$): δ 8.71 (d, *J* = 4.7 Hz, 1H, ^{7}CH), 8.01 (d, *J* = 6.9 Hz, 2H, ^{1}CH), 7.75-7.71 (m, 2H, ^{5}CH and ^{6}CH), 7.51-7.41 (m, 3H, ^{2}CH and ^{3}CH), 7.27-7.22 (m, 1H, ^{4}CH).

Incorporation expected at δ 8.01. Determined against integral at δ 7.75-7.71.

Following *General Procedure C*, results are reported as a) amount of substrate, b) amount of catalyst, c) solvent, volume of solvent, d) reaction time, and e) level of incorporation.

Scheme 65

a) 2-phenylpyridine **41**, 0.033 g, 0.215 mmol, b) complex **81**, 0.011 g, 0.01 mmol, 5 mol%, c) DCM, 2.5 ml, d) 16 h, and e) 95%.

Table 56, Entry 1, Run 1

a) 2-phenylpyridine **41**, 0.033 g, 0.215 mmol, b) complex **81**, 0.0068 g, 0.0065 mmol, 3 mol%, c) Et_2O, 4 ml, d) 1 h, and e) 96%.

Table 56, Entry 1, Run 2

a) 2-phenylpyridine **41**, 0.033 g, 0.215 mmol, b) complex **81**, 0.0068 g, 0.0065 mmol, 3 mol%, c) Et_2O, 4 ml, d) 1 h, and e) 95%.

Table 56, Entry 2, Run 1

a) 2-phenylpyridine **41**, 0.033 g, 0.215 mmol, b) complex **75**, 0.0065 g, 0.0065 mmol, 3 mol%, c) Et_2O, 4 ml, d) 2 h, and e) 96%.

Table 56, Entry 2, Run 2

a) 2-phenylpyridine **41**, 0.033 g, 0.215 mmol, b) complex **75**, 0.0065 g, 0.0065 mmol, 3 mol%, c) Et_2O, 4 ml, d) 2 h, and e) 94%.

Table 56, Entry 3, Run 1

a) 2-phenylpyridine **41**, 0.033 g, 0.215 mmol, b) complex **82**, 0.002 g, 0.0022 mmol, 1 mol%, c) Et_2O, 4 ml, d) 2 h, and e) 52%.

Table 56, Entry 3, Run 2

a) 2-phenylpyridine **41**, 0.033 g, 0.215 mmol, b) complex **82**, 0.002 g, 0.0022 mmol, 1 mol%, c) Et_2O, 4 ml, d) 2 h, and e) 53%.

Table 56, Entry 4, Run 1

a) 2-phenylpyridine **41**, 0.033 g, 0.215 mmol, b) complex **82**, 0.009 g, 0.01 mmol, 5 mol%, c) Et_2O, 4 ml, d) 16 h, and e) 55%.

Table 56, Entry 4, Run 2

a) 2-phenylpyridine **41**, 0.033 g, 0.215 mmol, b) complex **82**, 0.009 g, 0.01 mmol, 5 mol%, c) Et_2O, 4 ml, d) 16 h, and e) 57%.

Table 57, Entry 1, Run 1

a) 2-phenylpyridine **41**, 0.033 g, 0.215 mmol, b) complex **81**, 0.011 g, 0.01 mmol, 5 mol%, c) ^tBuOMe, 4 ml, d) 2 h, and e) 97%.

Table 57, Entry 1, Run 2

a) 2-phenylpyridine **41**, 0.033 g, 0.215 mmol, b) complex **81**, 0.011 g, 0.01 mmol, 5 mol%, c) ^{t}BuOMe, 4 ml, d) 2 h, and e) 92%.

Table 57, Entry 2, Run 1

a) 2-phenylpyridine **41**, 0.033 g, 0.215 mmol, b) complex **75**, 0.01 g, 0.01 mmol, 5 mol%, c) ^{t}BuOMe, 4 ml, d) 2 h, and e) 91%.

Table 57, Entry 2, Run 2

a) 2-phenylpyridine **41**, 0.033 g, 0.215 mmol, b) complex **75**, 0.01 g, 0.01 mmol, 5 mol%, c) ^{t}BuOMe, 4 ml, d) 2 h, and e) 90%.

Table 57, Entry 3, Run 1

a) 2-phenylpyridine **41**, 0.033 g, 0.215 mmol, b) complex **82**, 0.006 g, 0.0065 mmol, 3 mol%, c) ^{t}BuOMe, 4 ml, d) 1 h, and e) 10%.

Table 57, Entry 3, Run 2

a) 2-phenylpyridine **41**, 0.033 g, 0.215 mmol, b) complex **82**, 0.006 g, 0.0065 mmol, 3 mol%, c) ^{t}BuOMe, 4 ml, d) 1 h, and e) 7%.

Table 57, Entry 4, Run 1

a) 2-phenylpyridine **41**, 0.033 g, 0.215 mmol, b) complex **82**, 0.009 g, 0.01 mmol, 5 mol%, c) ^{t}BuOMe, 4 ml, d) 16 h, and e) 95%.

Table 57, Entry 4, Run 2

a) 2-phenylpyridine **41**, 0.033 g, 0.215 mmol, b) complex **82**, 0.009 g, 0.01 mmol, 5 mol%, c) ^{t}BuOMe, 4 ml, d) 16 h, and e) 93%.

Table 58, Entry 1, Run 1

a) 2-phenylpyridine **41**, 0.033 g, 0.215 mmol, b) complex **81**, 0.0068 g, 0.0065 mmol, 3 mol%, c) 2-MeTHF, 2.5 ml, d) 1 h, and e) 88%.

Table 58, Entry 1, Run 2

a) 2-phenylpyridine **41**, 0.033 g, 0.215 mmol, b) complex **81**, 0.0068 g, 0.0065 mmol, 3 mol%, c) 2-MeTHF, 2.5 ml, d) 1 h, and e) 96%.

Table 58, Entry 2, Run 1

a) 2-phenylpyridine **41**, 0.033 g, 0.215 mmol, b) complex **75**, 0.0065 g, 0.0065 mmol, 3 mol%, c) 2-MeTHF, 2.5 ml, d) 2 h, and e) 91%.

Table 58, Entry 2, Run 2

a) 2-phenylpyridine **41**, 0.033 g, 0.215 mmol, b) complex **75**, 0.0065 g, 0.0065 mmol, 3 mol%, c) 2-MeTHF, 2.5 ml, d) 2 h, and e) 97%.

Table 58, Entry 3, Run 1

a) 2-phenylpyridine **41**, 0.033 g, 0.215 mmol, b) complex **82**, 0.006 g, 0.0065 mmol, 3 mol%, c) 2-MeTHF, 2.5 ml, d) 0.5 h, and e) 5%.

Table 58, Entry 3, Run 2

a) 2-phenylpyridine **41**, 0.033 g, 0.215 mmol, b) complex **82**, 0.006 g, 0.0065 mmol, 3 mol%, c) 2-MeTHF, 2.5 ml, d) 0.5 h, and e) 5%.

Table 58, Entry 4, Run 1

a) 2-phenylpyridine **41**, 0.033 g, 0.215 mmol, b) complex **82**, 0.009 g, 0.01 mmol, 5 mol%, c) 2-MeTHF, 2.5 ml, d) 16 h, and e) 32%.

Table 58, Entry 4, Run 2

a) 2-phenylpyridine **41**, 0.033 g, 0.215 mmol, b) complex **82**, 0.009 g, 0.01 mmol, 5 mol%, c) 2-MeTHF, 2.5 ml, d) 16 h, and e) 24%.

Deuteration of N-*Phenylpyrazole* ***79***

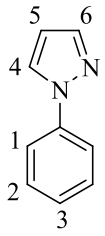

^{1}H NMR (400 MHz, $CDCl_3$): δ 7.92 (d, *J* = 4.0 Hz, 1H, ^{4}CH), 7.75-7.70 (m, 3H, ^{1}CH and ^{6}CH), 7.45 (t, *J* = 8.0 Hz, 2H, ^{2}CH), 7.29 (t, *J* = 8.0 Hz, 1H, ^{3}CH), 6.47 (t, *J* = 2.0 Hz, 1H, ^{5}CH).

Incorporation expected at δ 7.75-7.70. Determined against integral at δ 6.47.

Following *General Procedure C*, results are reported as a) amount of substrate, b) amount of catalyst, c) solvent, volume of solvent, d) reaction time, and e) level of incorporation.

Table 59, Entry 1, Run 1

a) *N*-phenylpyrazole **79**, 0.031 g, 0.215 mmol, b) complex **81**, 0.0068 g, 0.0065 mmol, 3 mol%, c) Et_2O, 4 ml, d) 1 h, and e) 94%.

Table 59, Entry 1, Run 2

a) *N*-phenylpyrazole **79**, 0.031 g, 0.215 mmol, b) complex **81**, 0.0068 g, 0.0065 mmol, 3 mol%, c) Et_2O, 4 ml, d) 1 h, and e) 92%.

Table 59, Entry 2, Run 1

a) *N*-phenylpyrazole **79**, 0.031 g, 0.215 mmol, b) complex **75**, 0.0065 g, 0.0065 mmol, 3 mol%, c) Et_2O, 4 ml, d) 2 h, and e) 95%.

Table 59, Entry 2, Run 2

a) *N*-phenylpyrazole **79**, 0.031 g, 0.215 mmol, b) complex **75**, 0.0065 g, 0.0065 mmol, 3 mol%, c) Et_2O, 4 ml, d) 2 h, and e) 94%.

Table 59, Entry 3, Run 1

a) *N*-phenylpyrazole **79**, 0.031 g, 0.215 mmol, b) complex **82**, 0.002 g, 0.0022 mmol, 1 mol%, c) Et_2O, 4 ml, d) 2 h, and e) 72%.

Table 59, Entry 3, Run 2

a) *N*-phenylpyrazole **79**, 0.031 g, 0.215 mmol, b) complex **82**, 0.002 g, 0.0022 mmol, 1 mol%, c) Et_2O, 4 ml, d) 2 h, and e) 68%.

Table 60, Entry 1, Run 1

a) *N*-phenylpyrazole **79**, 0.031 g, 0.215 mmol, b) complex **81**, 0.011 g, 0.01 mmol, 5 mol%, c) ^{t}BuOMe, 4 ml, d) 2 h, and e) 82%.

Table 60, Entry 1, Run 2

a) *N*-phenylpyrazole **79**, 0.031 g, 0.215 mmol, b) complex **81**, 0.011 g, 0.01 mmol, 5 mol%, c) ^{t}BuOMe, 4 ml, d) 2 h, and e) 82%.

Table 60, Entry 2, Run 1

a) *N*-phenylpyrazole **79**, 0.031 g, 0.215 mmol, b) complex **75**, 0.01 g, 0.01 mmol, 5 mol%, c) ^{t}BuOMe, 4 ml, d) 2 h, and e) 83%.

Table 60, Entry 2, Run 2

a) *N*-phenylpyrazole **79**, 0.031 g, 0.215 mmol, b) complex **75**, 0.01 g, 0.01 mmol, 5 mol%, c) ^{t}BuOMe, 4 ml, d) 2 h, and e) 84%.

Table 60, Entry 3, Run 1

a) *N*-phenylpyrazole **79**, 0.031 g, 0.215 mmol, b) complex **82**, 0.006 g, 0.0065 mmol, 3 mol%, c) ^{t}BuOMe, 4 ml, d) 1 h, and e) 92%.

Table 60, Entry 3, Run 2

a) *N*-phenylpyrazole **79**, 0.031 g, 0.215 mmol, b) complex **82**, 0.006 g, 0.0065 mmol, 3 mol%, c) ^{t}BuOMe, 4 ml, d) 1 h, and e) 91%.

Table 61, Entry 1, Run 1

a) *N*-phenylpyrazole **79**, 0.031 g, 0.215 mmol, b) complex **81**, 0.0068 g, 0.0065 mmol, 3 mol%, c) 2-MeTHF, 2.5 ml, d) 1 h, and e) 94%.

Table 61, Entry 1, Run 2

a) *N*-phenylpyrazole **79**, 0.031 g, 0.215 mmol, b) complex **81**, 0.0068 g, 0.0065 mmol, 3 mol%, c) 2-MeTHF, 2.5 ml, d) 1 h, and e) 92%.

Table 61, Entry 2, Run 1

a) *N*-phenylpyrazole **79**, 0.031 g, 0.215 mmol, b) complex **75**, 0.0065 g, 0.0065 mmol, 3 mol%, c) 2-MeTHF, 2.5 ml, d) 2 h, and e) 89%.

Table 61, Entry 2, Run 2

a) *N*-phenylpyrazole **79**, 0.031 g, 0.215 mmol, b) complex **75**, 0.0065 g, 0.0065 mmol, 3 mol%, c) 2-MeTHF, 2.5 ml, d) 2 h, and e) 96%.

Table 61, Entry 3, Run 1

a) *N*-phenylpyrazole **79**, 0.031 g, 0.215 mmol, b) complex **82**, 0.006 g, 0.0065 mmol, 3 mol%, c) 2-MeTHF, 2.5 ml, d) 0.5 h, and e) 97%.

Table 61, Entry 3, Run 2

a) *N*-phenylpyrazole **79**, 0.031 g, 0.215 mmol, b) complex **82**, 0.006 g, 0.0065 mmol, 3 mol%, c) 2-MeTHF, 2.5 ml, d) 0.5 h, and e) 97%.

6.5.3 Labelling of Further Substrates Using [Ir(COD)(PBn$_3$)(IMes)]PF$_6$

*Deuteration of Benzamide **59***

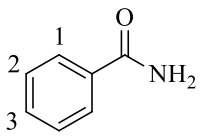

^{1}H NMR (400 MHz, d$_6$-acetone): δ 7.95 (d, *J* = 7.2 Hz, 2H, ^{1}CH), 7.53 (t, *J* = 7.3 Hz, 1H, ^{3}CH), 7.44 (t, *J* = 7.3 Hz, 2H, ^{2}CH).

Incorporation expected at δ 7.95. Determined against integral at δ 7.53.

Following *General Procedure C*, results are reported as a) amount of substrate, b) amount of catalyst, c) solvent, volume of solvent, d) reaction time, and e) level of incorporation.

Table 62, Entry 1, Run 1

a) benzamide **59**, 0.026 g, 0.215 mmol, b) complex **81**, 0.011 g, 0.01 mmol, 5 mol%, c) DCM, 2.5 ml, d) 16 h, and e) 86%.

Table 62, Entry 1, Run 2

a) benzamide **59**, 0.026 g, 0.215 mmol, b) complex **81**, 0.011 g, 0.01 mmol, 5 mol%, c) DCM, 2.5 ml, d) 16 h, and e) 92%.

Table 62, Entry 2, Run 1

a) benzamide **59**, 0.026 g, 0.215 mmol, b) complex **81**, 0.0068 g, 0.0065 mmol, 3 mol%, c) Et$_2$O, 4 ml, d) 1 h, and e) 28%.

Table 62, Entry 2, Run 2

a) benzamide **59**, 0.026 g, 0.215 mmol, b) complex **81**, 0.0068 g, 0.0065 mmol, 3 mol%, c) Et$_2$O, 4 ml, d) 1 h, and e) 24%.

Table 62, Entry 3, Run 1

a) benzamide **59**, 0.026 g, 0.215 mmol, b) complex **81**, 0.011 g, 0.01 mmol, 5 mol%, c) ^{t}BuOMe, 4 ml, d) 2 h, and e) 38%.

Table 62, Entry 3, Run 2

a) benzamide **59**, 0.026 g, 0.215 mmol, b) complex **81**, 0.011 g, 0.01 mmol, 5 mol%, c) ^{t}BuOMe, 4 ml, d) 2 h, and e) 43%.

Table 62, Entry 4, Run 1

a) benzamide **59**, 0.026 g, 0.215 mmol, b) complex **81**, 0.0068 g, 0.0065 mmol, 3 mol%, c) 2-MeTHF, 2.5 ml, d) 1 h, and e) 64%.

Table 62, Entry 4, Run 2

a) benzamide **59**, 0.026 g, 0.215 mmol, b) complex **81**, 0.0068 g, 0.0065 mmol, 3 mol%, c) 2-MeTHF, 2.5 ml, d) 1 h, and e) 64%.

Table 63, Entry 1, Run 1

a) benzamide **59**, 0.026 g, 0.215 mmol, b) complex **81**, 0.011 g, 0.01 mmol, 5 mol%, c) Et_2O, 4 ml, d) 16 h, and e) 27%.

Table 63, Entry 1, Run 2

a) benzamide **59**, 0.026 g, 0.215 mmol, b) complex **81**, 0.011 g, 0.01 mmol, 5 mol%, c) Et_2O, 4 ml, d) 16 h, and e) 29%.

Table 63, Entry 2, Run 1

a) benzamide **59**, 0.026 g, 0.215 mmol, b) complex **81**, 0.011 g, 0.01 mmol, 5 mol%, c) ^{t}BuOMe, 4 ml, d) 16 h, and e) 57%.

Table 63, Entry 2, Run 2

a) benzamide **59**, 0.026 g, 0.215 mmol, b) complex **81**, 0.011 g, 0.01 mmol, 5 mol%, c) ^{t}BuOMe, 4 ml, d) 16 h, and e) 49%.

Table 63, Entry 3, Run 1

a) benzamide **59**, 0.026 g, 0.215 mmol, b) complex **81**, 0.011 g, 0.01 mmol, 5 mol%, c) 2-MeTHF, 2.5 ml, d) 16 h, and e) 89%.

Table 63, Entry 3, Run 2

a) benzamide **59**, 0.026 g, 0.215 mmol, b) complex **81**, 0.011 g, 0.01 mmol, 5 mol%, c) 2-MeTHF, 2.5 ml, d) 16 h, and e) 79%.

*Deuteration of N,N,4-Trimethylbenzamide **111***

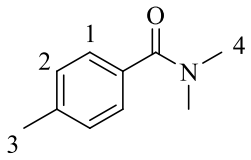

^{1}H NMR (400 MHz, $CDCl_3$): δ 7.32 (d, *J* = 8.0 Hz, 2H, ^{1}CH), 7.19 (d, *J* = 8.0 Hz, 2H, ^{2}CH), 3.00 (br s, 6H, ^{4}CH), 2.38 (s, 3H, ^{3}CH).

Incorporation expected at δ 7.32 and 3.00. Determined against integral at δ 2.38.

Following *General Procedure C*, results are reported as a) amount of substrate, b) amount of catalyst, c) solvent, volume of solvent, d) reaction time, and e) level of incorporation.

Table 64, Entry 1, Run 1

a) *N*,*N*,4-trimethylbenzamide **111**, 0.035 g, 0.215 mmol, b) complex **81**, 0.0068 g, 0.0065 mmol, 3 mol%, c) Et_2O, 4 ml, d) 1 h, and e) 81% at δ 7.32 and 13% at δ 3.00.

Table 64, Entry 1, Run 2

a) *N*,*N*,4-trimethylbenzamide **111**, 0.035 g, 0.215 mmol, b) complex **81**, 0.0068 g, 0.0065 mmol, 3 mol%, c) Et_2O, 4 ml, d) 1 h, and e) 83% at δ 7.32 and 13% at δ 3.00.

Table 64, Entry 2, Run 1

a) *N*,*N*,4-trimethylbenzamide **111**, 0.035 g, 0.215 mmol, b) complex **81**, 0.011 g, 0.01 mmol, 5 mol%, c) ^{t}BuOMe, 4 ml, d) 2 h, and e) 96% at δ 7.32 and 18% at δ 3.00.

Table 64, Entry 2, Run 2

a) *N*,*N*,4-trimethylbenzamide **111**, 0.035 g, 0.215 mmol, b) complex **81**, 0.011 g, 0.01 mmol, 5 mol%, c) ^{t}BuOMe, 4 ml, d) 2 h, and e) 93% at δ 7.32 and 24% at δ 3.00.

Table 64, Entry 3, Run 1

a) *N*,*N*,4-trimethylbenzamide **111**, 0.035 g, 0.215 mmol, b) complex **81**, 0.0068 g, 0.0065 mmol, 3 mol%, c) 2-MeTHF, 2.5 ml, d) 1 h, and e) 95% at δ 7.32 and 22% at δ 3.00.

Table 64, Entry 3, Run 2

a) *N*,*N*,4-trimethylbenzamide **111**, 0.035 g, 0.215 mmol, b) complex **81**, 0.0068 g, 0.0065 mmol, 3 mol%, c) 2-MeTHF, 2.5 ml, d) 1 h, and e) 94% at δ 7.32 and 24% at δ 3.00.

Deuteration of N-*Ethyl*-N,*4-dimethylbenzamide **112***

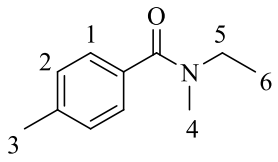

^{1}H NMR (400 MHz, d_6-acetone): δ 7.30 (d, *J* = 8.0 Hz, 2H, ^{1}CH), 7.24 (d, *J* = 8.0 Hz, 2H, ^{2}CH), 3.39 (br s, 2H, ^{5}CH), 2.98 (s, 3H, ^{4}CH), 2.37 (s, 3H, ^{3}CH), 1.15 (br s, 3H, ^{6}CH).

Incorporation expected at δ 7.30 and 2.98. Determined against integral at δ 2.37.

Following *General Procedure C*, results are reported as a) amount of substrate, b) amount of catalyst, c) solvent, volume of solvent, d) reaction time, and e) level of incorporation.

Table 65, Entry 1, Run 1

a) *N*-ethyl-*N*,4-dimethylbenzamide **112**, 0.038 g, 0.215 mmol, b) complex **81**, 0.0068 g, 0.0065 mmol, 3 mol%, c) Et_2O, 4 ml, d) 1 h, and e) 91% at δ 7.30 and 22% at δ 2.98.

Table 65, Entry 1, Run 2

a) *N*-ethyl-*N*,4-dimethylbenzamide **112**, 0.038 g, 0.215 mmol, b) complex **81**, 0.0068 g, 0.0065 mmol, 3 mol%, c) Et_2O, 4 ml, d) 1 h, and e) 88% at δ 7.30 and 21% at δ 2.98.

Table 65, Entry 2, Run 1

a) *N*-ethyl-*N*,4-dimethylbenzamide **112**, 0.038 g, 0.215 mmol, b) complex **81**, 0.011 g, 0.01 mmol, 5 mol%, c) ^{t}BuOMe, 4 ml, d) 2 h, and e) 95% at δ 7.30 and 31% at δ 2.98.

Table 65, Entry 2, Run 2

a) *N*-ethyl-*N*,4-dimethylbenzamide **112**, 0.038 g, 0.215 mmol, b) complex **81**, 0.011 g, 0.01 mmol, 5 mol%, c) ^{t}BuOMe, 4 ml, d) 2 h, and e) 95% at δ 7.30 and 30% at δ 2.98.

Table 65, Entry 3, Run 1

a) *N*-ethyl-*N*,4-dimethylbenzamide **112**, 0.038 g, 0.215 mmol, b) complex **81**, 0.0068 g, 0.0065 mmol, 3 mol%, c) 2-MeTHF, 2.5 ml, d) 1 h, and e) 91% at δ 7.30 and 17% at δ 2.98.

Table 65, Entry 3, Run 2

a) *N*-ethyl-*N*,4-dimethylbenzamide **112**, 0.038 g, 0.215 mmol, b) complex **81**, 0.0068 g, 0.0065 mmol, 3 mol%, c) 2-MeTHF, 2.5 ml, d) 1 h, and e) 85% at δ 7.30 and 13% at δ 2.98.

Deuteration of N,N-*Diethyl-4-methylbenzamide **113***

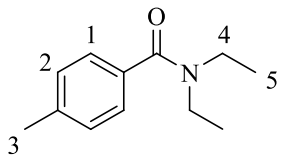

^{1}H NMR (400 MHz, d_6-acetone): δ 7.27-7.22 (m, 4H, ^{1}CH and ^{2}CH), 3.38 (br s, 4H, ^{4}CH), 2.36 (s, 3H, ^{3}CH), 1.14 (s, 6H, ^{5}CH).

Incorporation expected at δ 7.27-7.22. Determined against integral at δ 2.36.

Following *General Procedure C*, results are reported as a) amount of substrate, b) amount of catalyst, c) solvent, volume of solvent, d) reaction time, and e) level of incorporation.

Table 66, Entry 1, Run 1

a) *N*,*N*-diethyl-4-methylbenzamide **113**, 0.041 g, 0.215 mmol, b) complex **81**, 0.0068 g, 0.0065 mmol, 3 mol%, c) Et_2O, 4 ml, d) 1 h, and e) 51%.

Table 66, Entry 1, Run 2

a) *N*,*N*-diethyl-4-methylbenzamide **113**, 0.041 g, 0.215 mmol, b) complex **81**, 0.0068 g, 0.0065 mmol, 3 mol%, c) Et_2O, 4 ml, d) 1 h, and e) 56%.

Table 66, Entry 2, Run 1

a) *N*,*N*-diethyl-4-methylbenzamide **113**, 0.041 g, 0.215 mmol, b) complex **81**, 0.011 g, 0.01 mmol, 5 mol%, c) ^{t}BuOMe, 4 ml, d) 2 h, and e) 47%.

Table 66, Entry 2, Run 2

a) *N*,*N*-diethyl-4-methylbenzamide **113**, 0.041 g, 0.215 mmol, b) complex **81**, 0.011 g, 0.01 mmol, 5 mol%, c) ^{t}BuOMe, 4 ml, d) 2 h, and e) 46%.

Table 66, Entry 3, Run 1

a) *N*,*N*-diethyl-4-methylbenzamide **113**, 0.041 g, 0.215 mmol, b) complex **81**, 0.0068 g, 0.0065 mmol, 3 mol%, c) 2-MeTHF, 2.5 ml, d) 1 h, and e) 62%.

Table 66, Entry 3, Run 2

a) *N*,*N*-diethyl-4-methylbenzamide **113**, 0.041 g, 0.215 mmol, b) complex **81**, 0.0068 g, 0.0065 mmol, 3 mol%, c) 2-MeTHF, 2.5 ml, d) 1 h, and e) 61%.

Table 67, Entry 1, Run 1

a) *N*,*N*-diethyl-4-methylbenzamide **113**, 0.041 g, 0.215 mmol, b) complex **81**, 0.011 g, 0.01 mmol, 5 mol%, c) Et_2O, 4 ml, d) 16 h, and e) 71%.

Table 67, Entry 1, Run 2

a) *N*,*N*-diethyl-4-methylbenzamide **113**, 0.041 g, 0.215 mmol, b) complex **81**, 0.011 g, 0.01 mmol, 5 mol%, c) Et_2O, 4 ml, d) 16 h, and e) 74%.

Table 67, Entry 2, Run 1

a) *N*,*N*-diethyl-4-methylbenzamide **113**, 0.041 g, 0.215 mmol, b) complex **81**, 0.011 g, 0.01 mmol, 5 mol%, c) ^{t}BuOMe, 4 ml, d) 16 h, and e) 53%.

Table 67, Entry 2, Run 2

a) *N*,*N*-diethyl-4-methylbenzamide **113**, 0.041 g, 0.215 mmol, b) complex **81**, 0.011 g, 0.01 mmol, 5 mol%, c) ^{t}BuOMe, 4 ml, d) 16 h, and e) 54%.

Table 67, Entry 3, Run 1

a) *N*,*N*-diethyl-4-methylbenzamide **113**, 0.041 g, 0.215 mmol, b) complex **81**, 0.011 g, 0.01 mmol, 5 mol%, c) 2-MeTHF, 2.5 ml, d) 16 h, and e) 85%.

Table 67, Entry 3, Run 2

a) *N*,*N*-diethyl-4-methylbenzamide **113**, 0.041 g, 0.215 mmol, b) complex **81**, 0.011 g, 0.01 mmol, 5 mol%, c) 2-MeTHF, 2.5 ml, d) 16 h, and e) 78%.

*Deuteration of Acetanilide **73***

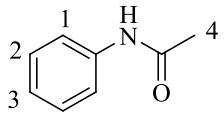

^{1}H NMR (400 MHz, MeOD): δ 7.50 (d, *J* = 7.9 Hz, 2H, ^{1}CH), 7.32 (t, *J* = 7.9 Hz, 2H, ^{2}CH), 7.11 (t, *J* = 7.4 Hz, 1H, ^{3}CH), 2.12 (s, 3H, ^{4}CH).

Incorporation expected at δ 7.50. Determined against integral at δ 2.12.

Following *General Procedure C*, results are reported as a) amount of substrate, b) amount of catalyst, c) solvent, volume of solvent, d) reaction time, and e) level of incorporation.

Table 68, Entry 1, Run 1

a) acetanilide **73**, 0.029 g, 0.215 mmol, b) complex **81**, 0.0068 g, 0.0065 mmol, 3 mol%, c) Et_2O, 4 ml, d) 1 h, and e) 40%.

Table 68, Entry 1, Run 2

a) acetanilide **73**, 0.029 g, 0.215 mmol, b) complex **81**, 0.0068 g, 0.0065 mmol, 3 mol%, c) Et_2O, 4 ml, d) 1 h, and e) 36%.

Table 68, Entry 2, Run 1

a) acetanilide **73**, 0.029 g, 0.215 mmol, b) complex **81**, 0.011 g, 0.01 mmol, 5 mol%, c) ^{t}BuOMe, 4 ml, d) 2 h, and e) 46%.

Table 68, Entry 2, Run 2

a) acetanilide **73**, 0.029 g, 0.215 mmol, b) complex **81**, 0.011 g, 0.01 mmol, 5 mol%, c) ^{t}BuOMe, 4 ml, d) 2 h, and e) 52%.

Table 68, Entry 3, Run 1

a) acetanilide **73**, 0.029 g, 0.215 mmol, b) complex **81**, 0.0068 g, 0.0065 mmol, 3 mol%, c) 2-MeTHF, 2.5 ml, d) 1 h, and e) 52%.

Table 68, Entry 3, Run 2

a) acetanilide **73**, 0.029 g, 0.215 mmol, b) complex **81**, 0.0068 g, 0.0065 mmol, 3 mol%, c) 2-MeTHF, 2.5 ml, d) 1 h, and e) 45%.

Table 69, Entry 1, Run 1

a) acetanilide **73**, 0.029 g, 0.215 mmol, b) complex **81**, 0.011 g, 0.01 mmol, 5 mol%, c) Et_2O, 4 ml, d) 16 h, and e) 50%.

Table 69, Entry 1, Run 2

a) acetanilide **73**, 0.029 g, 0.215 mmol, b) complex **81**, 0.011 g, 0.01 mmol, 5 mol%, c) Et_2O, 4 ml, d) 16 h, and e) 51%.

Table 69, Entry 2, Run 1

a) acetanilide **73**, 0.029 g, 0.215 mmol, b) complex **81**, 0.011 g, 0.01 mmol, 5 mol%, c) ^{t}BuOMe, 4 ml, d) 16 h, and e) 57%.

Table 69, Entry 2, Run 2

a) acetanilide **73**, 0.029 g, 0.215 mmol, b) complex **81**, 0.011 g, 0.01 mmol, 5 mol%, c) ^{t}BuOMe, 4 ml, d) 16 h, and e) 57%.

Table 69, Entry 3, Run 1

a) acetanilide **73**, 0.029 g, 0.0215 mmol, b) complex **81**, 0.011 g, 0.01 mmol, 5 mol%, c) 2-MeTHF, 2.5 ml, d) 16 h, and e) 62%.

Table 69, Entry 3, Run 2

a) acetanilide **73**, 0.029 g, 0.215 mmol, b) complex **81**, 0.011 g, 0.01 mmol, 5 mol%, c) 2-MeTHF, 2.5 ml, d) 16 h, and e) 70%.

*Deuteration of Benzanilide **83***

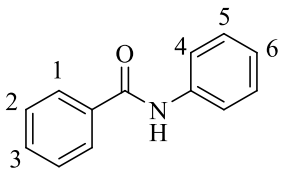

^{1}H NMR (400 MHz, d_6-acetone): δ 9.50 (s, 1H, NH), 7.99 (dd, *J* = 7.0 Hz, ^{4}J = 1.5 Hz, 2H, ^{1}CH), 7.86 (d, *J* = 8.0 Hz, 2H, ^{4}CH), 7.60-7.50 (m, 3H, ^{2}CH and ^{3}CH), 7.36 (t, *J* = 7.0 Hz, 2H, ^{5}CH), 7.11 (t, *J* = 7.3 Hz, 1H, ^{6}CH).

Incorporation expected at δ 7.99 and 7.86. Determined against integral at δ 7.11.

Following *General Procedure C*, results are reported as a) amount of substrate, b) amount of catalyst, c) solvent, volume of solvent, d) reaction time, and e) level of incorporation.

Table 70, Entry 1, Run 1

a) benzanilide **83**, 0.042 g, 0.215 mmol, b) complex **81**, 0.011 g, 0.01 mmol, 5 mol%, c) DCM, 2.5 ml, d) 16 h, and e) 93% at δ 7.99 and 90% at δ 7.86.

Table 70, Entry 1, Run 2

a) benzanilide **83**, 0.042 g, 0.215 mmol, b) complex **81**, 0.011 g, 0.01 mmol, 5 mol%, c) DCM, 2.5 ml, d) 16 h, and e) 92% at δ 7.99 and 90% at δ 7.86.

Table 70, Entry 2, Run 1

a) benzanilide **83**, 0.042 g, 0.215 mmol, b) complex **81**, 0.0068 g, 0.0065 mmol, 3 mol%, c) Et_2O, 4 ml, d) 1 h, and e) 36% at δ 7.99 and 18% at δ 7.86.

Table 70, Entry 2, Run 2

a) benzanilide **83**, 0.042 g, 0.215 mmol, b) complex **81**, 0.0068 g, 0.0065 mmol, 3 mol%, c) Et_2O, 4 ml, d) 1 h, and e) 42% at δ 7.99 and 15% at δ 7.86.

Table 70, Entry 3, Run 1

a) benzanilide **83**, 0.042 g, 0.215 mmol, b) complex **81**, 0.011 g, 0.01 mmol, 5 mol%, c) ^tBuOMe, 4 ml, d) 2 h, and e) 43% at δ 7.99 and 13% at δ 7.86.

Table 70, Entry 3, Run 2

a) benzanilide **83**, 0.042 g, 0.215 mmol, b) complex **81**, 0.011 g, 0.01 mmol, 5 mol%, c) ^tBuOMe, 4 ml, d) 2 h, and e) 47% at δ 7.99 and 15% at δ 7.86.

Table 70, Entry 4, Run 1

a) benzanilide **83**, 0.042 g, 0.215 mmol, b) complex **81**, 0.0068 g, 0.0065 mmol, 3 mol%, c) 2-MeTHF, 2.5 ml, d) 1 h, and e) 93% at δ 7.99 and 12% at δ 7.86.

Table 70, Entry 4, Run 2

a) benzanilide **83**, 0.042 g, 0.215 mmol, b) complex **81**, 0.0068 g, 0.0065 mmol, 3 mol%, c) 2-MeTHF, 2.5 ml, d) 1 h, and e) 91% at δ 7.99 and 9% at δ 7.86.

Table 71, Entry 1, Run 1

a) benzanilide **83**, 0.042 g, 0.215 mmol, b) complex **81**, 0.011 g, 0.01 mmol, 5 mol%, c) Et_2O, 4 ml, d) 16 h, and e) 41% at δ 7.99 and 20% at δ 7.86.

Table 71, Entry 1, Run 2

a) benzanilide **83**, 0.042 g, 0.215 mmol, b) complex **81**, 0.011 g, 0.01 mmol, 5 mol%, c) Et_2O, 4 ml, d) 16 h, and e) 39% at δ 7.99 and 27% at δ 7.86.

Table 71, Entry 2, Run 1

a) benzanilide **83**, 0.042 g, 0.215 mmol, b) complex **81**, 0.011 g, 0.01 mmol, 5 mol%, c) ^tBuOMe, 4 ml, d) 16 h, and e) 43% at δ 7.99 and 14% at δ 7.86.

Table 71, Entry 2, Run 2

a) benzanilide **83**, 0.042 g, 0.215 mmol, b) complex **81**, 0.011 g, 0.01 mmol, 5 mol%, c) ^{t}BuOMe, 4 ml, d) 16 h, and e) 50% at δ 7.99 and 14% at δ 7.86.

*Deuteration of Niclosamide **117***

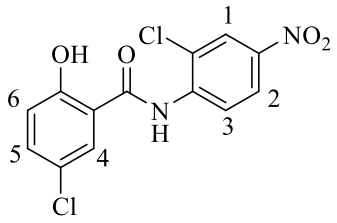

^{1}H NMR (400 MHz, d_6-DMSO): δ 11.37 (br s, 1H, OH), 8.81 (d, *J* = 9.2 Hz, 1H, ^{3}CH), 8.41 (d, ^{4}J = 2.8 Hz, 1H, ^{1}CH), 8.29 (dd, *J* = 9.2 Hz, ^{4}J = 2.8 Hz, 1H, ^{2}CH), 7.95 (d, ^{4}J = 2.8 Hz, 1H, ^{4}CH), 7.53 (dd, *J* = 8.8 Hz, ^{4}J = 2.8 Hz, 1H, ^{5}CH), 7.08 (d, *J* = 8.4 Hz, 1H, ^{6}CH).

Incorporation expected at δ 8.81, 8.41, 8.29, and 7.95. Determined against integral at δ 7.08.

Following *General Procedure C*, results are reported as a) amount of substrate, b) amount of catalyst, c) solvent, volume of solvent, d) reaction time, and e) level of incorporation.

Table 72, Entry 1, Run 1

a) Niclosamide **117**, 0.016 g, 0.05 mmol, b) complex **81**, 0.0026 g, 0.0025 mmol, 5 mol%, c) DCM, 2.5 ml, d) 1 h, and e) 39% at δ 8.81, 51% at δ 8.41, 43% at δ 8.29, and 54% at δ 7.95.

Table 72, Entry 1, Run 2

a) Niclosamide **117**, 0.016 g, 0.05 mmol, b) complex **81**, 0.0026 g, 0.0025 mmol, 5 mol%, c) DCM, 2.5 ml, d) 1 h, and e) 40% at δ 8.81, 55% at δ 8.41, 44% at δ 8.29, and 58% at δ 7.95.

Table 72, Entry 2, Run 1

a) Niclosamide **117**, 0.016 g, 0.05 mmol, b) complex **81**, 0.0016 g, 0.0015 mmol, 3 mol%, c) Et_2O, 4 ml, d) 1 h, and e) 63% at δ 8.81, 75% at δ 8.41, 70% at δ 8.29, and 76% at δ 7.95.

Table 72, Entry 2, Run 2

a) Niclosamide **117**, 0.016 g, 0.05 mmol, b) complex **81**, 0.0016 g, 0.0015 mmol, 3 mol%, c) Et_2O, 4 ml, d) 1 h, and e) 57% at δ 8.81, 76% at δ 8.41, 69% at δ 8.29, and 77% at δ 7.95.

Table 72, Entry 3, Run 1

a) Niclosamide **117**, 0.016 g, 0.05 mmol, b) complex **81**, 0.0026 g, 0.0025 mmol, 5 mol%, c) ^tBuOMe, 4 ml, d) 2 h, and e) 37% at δ 8.81, 83% at δ 8.41, 48% at δ 8.29, and 87% at δ 7.95.

Table 72, Entry 3, Run 2

a) Niclosamide **117**, 0.016 g, 0.05 mmol, b) complex **81**, 0.0026 g, 0.0025 mmol, 5 mol%, c) ^tBuOMe, 4 ml, d) 2 h, and e) 34% at δ 8.81, 82% at δ 8.41, 42% at δ 8.29, and 89% at δ 7.95.

Table 72, Entry 4, Run 1

a) Niclosamide **117**, 0.016 g, 0.05 mmol, b) complex **81**, 0.0016 g, 0.0015 mmol, 3 mol%, c) 2-MeTHF, 2.5 ml, d) 1 h, and e) 28% at δ 8.81, 89% at δ 8.41, 55% at δ 8.29, and 97% at δ 7.95.

Table 72, Entry 4, Run 2

a) Niclosamide **117**, 0.016 g, 0.05 mmol, b) complex **81**, 0.0016 g, 0.0015 mmol, 3 mol%, c) 2-MeTHF, 2.5 ml, d) 1 h, and e) 29% at δ 8.81, 86% at δ 8.41, 53% at δ 8.29, and 97% at δ 7.95.

*Deuteration of Celecoxib **119***

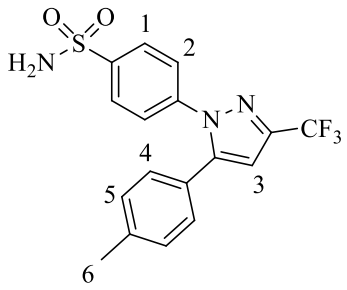

^{1}H NMR (400 MHz, MeOD) δ: 7.93 (d, *J* = 8.8 Hz, 2H, ^{1}CH), 7.49 (d, *J* = 8.8 Hz, 2H, ^{2}CH), 7.21-7.16 (m, 4H, ^{4}CH and ^{5}CH), 6.90 (s, 1H, ^{3}CH), 2.35 (s, 3H, ^{6}CH).

Incorporation expected at δ 7.93 and 7.49. Determined against integral at δ 2.35.

Following *General Procedure C*, results are reported as a) amount of substrate, b) amount of catalyst, c) solvent, volume of solvent, d) reaction time, and e) level of incorporation.

Table 73, Entry 1, Run 1

a) Celecoxib **119**, 0.019 g, 0.05 mmol, b) complex **81**, 0.0026 g, 0.0025 mmol, 5 mol%, c) Et_2O, 4 ml, d) 1 h, and e) 8% at δ 7.93 and 41% at δ 7.49.

Table 73, Entry 1, Run 2

a) Celecoxib **119**, 0.019 g, 0.05 mmol, b) complex **81**, 0.0026 g, 0.0025 mmol, 5 mol%, c) Et_2O, 4 ml, d) 1 h, and e) 7% at δ 7.93 and 41% at δ 7.49.

Table 73, Entry 2, Run 1

a) Celecoxib **119**, 0.019 g, 0.05 mmol, b) complex **81**, 0.0026 g, 0.0025 mmol, 5 mol%, c) ^{t}BuOMe, 4 ml, d) 2 h, and e) 5% at δ 7.93 and 24% at δ 7.49.

Table 73, Entry 2, Run 2

a) Celecoxib **119**, 0.019 g, 0.05 mmol, b) complex **81**, 0.0026 g, 0.0025 mmol, 5 mol%, c) ^{t}BuOMe, 4 ml, d) 2 h, and e) 7% at δ 7.93 and 23% at δ 7.49.

Table 73, Entry 3, Run 1

a) Celecoxib **119**, 0.019 g, 0.05 mmol, b) complex **81**, 0.0026 g, 0.0025 mmol, 5 mol%, c) 2-MeTHF, 2.5 ml, d) 1 h, and e) 3% at δ 7.93 and 5% at δ 7.49.

Table 73, Entry 3, Run 2

a) Celecoxib **119**, 0.019 g, 0.05 mmol, b) complex **81**, 0.0026 g, 0.0025 mmol, 5 mol%, c) 2-MeTHF, 2.5 ml, d) 1 h, and e) 4% at δ 7.93 and 5% at δ 7.49.

Table 74, Entry 1, Run 1

a) Celecoxib **119**, 0.019 g, 0.05 mmol, b) complex **81**, 0.0052 g, 0.005 mmol, 10 mol%, c) Et_2O, 4 ml, d) 1 h, and e) 13% at δ 7.93 and 72% at δ 7.49.

Table 74, Entry 1, Run 2

a) Celecoxib **119**, 0.019 g, 0.05 mmol, b) complex **81**, 0.0052 g, 0.005 mmol, 10 mol%, c) Et_2O, 4 ml, d) 1 h, and e) 11% at δ 7.93 and 66% at δ 7.49.

Table 74, Entry 2, Run 1

a) Celecoxib **119**, 0.019 g, 0.05 mmol, b) complex **81**, 0.0052 g, 0.005 mmol, 10 mol%, c) ^{t}BuOMe, 4 ml, d) 2 h, and e) 7% at δ 7.93 and 36% at δ 7.49.

Table 74, Entry 2, Run 2

a) Celecoxib **119**, 0.019 g, 0.05 mmol, b) complex **81**, 0.0052 g, 0.005 mmol, 10 mol%, c) ^{t}BuOMe, 4 ml, d) 2 h, and e) 8% at δ 7.93 and 30% at δ 7.49.

Table 74, Entry 3, Run 1

a) Celecoxib **119**, 0.019 g, 0.05 mmol, b) complex **81**, 0.0052 g, 0.005 mmol, 10 mol%, c) 2-MeTHF, 2.5 ml, d) 1 h, and e) 5% at δ 7.93 and 15% at δ 7.49.

Table 74, Entry 3, Run 2

a) Celecoxib **119**, 0.019 g, 0.05 mmol, b) complex **81**, 0.0052 g, 0.005 mmol, 10 mol%, c) 2-MeTHF, 2.5 ml, d) 1 h, and e) 5% at δ 7.93 and 12% at δ 7.49.

6.6 Preparation of Novel Iridium(I) Complexes

*Attempted Preparation of η^4-Cycloocta-1,5-diene(1,3-dicyclohexylimidazoline-2-ylidene)(triphenylphosphine)iridium(I) Hexafluorophosphate **124***

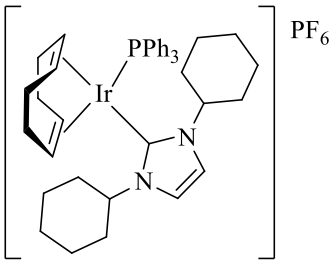

A 1 M sodium ethoxide solution was prepared by dissolving 0.25 g of sodium metal in ethanol (10 ml).

To a previously flame-dried Schlenk tube containing η^4-cycloocta-1,5-dieneiridium(I) chloride dimer **106**, dissolved in dry benzene (10 ml), was added 1 M sodium ethoxide solution, resulting in a red to yellow colour change. The solution was stirred at r.t. for 10 minutes, followed by the addition of the 1,3-dicyclohexylimidazolium chloride **104**. The solution was stirred under an atmosphere of argon for 5 hours, after which time the solvent was removed under high vacuum. The residue was triturated with dry diethyl ether (15 ml) and filtered through celite under argon. The solvent was again removed under high vacuum yielding a yellow solid which was subsequently dissolved in dry THF (10 ml). Addition of silver hexafluorophosphate resulted in a yellow to orange colour change, and the formation of a precipitate was observed. The solution was stirred for 30 minutes prior to filtration through celite under argon, to give a clear orange solution. On addition of the phosphine, the solution turned from orange to deep red. After stirring for the allotted time, the solvent was once again removed under high vacuum and purification techniques were employed in an attempt to isolate the desired product.

Following the above procedure, results are reported as a) amount of **106**, b) amount of NaOEt, c) amount of **104**, d) amount of $AgPF_6$, e) amount of triphenylphosphine, f) solution stirring time, g) appearance of material obtained, purification conditions and analysis, and h) product yield.

a) 0.2 g, 0.298 mmol, b) 0.6 ml, 0.6 mmol, c) 0.16 g, 0.595 mmol, d) 0.15 g, 0.595 mmol, e) 0.156 g, 0.595 mmol, f) 1 h, g) recrystallisation of residue from DCM/Et_2O produced dark red crystals; ^1H NMR showed excess aromatic protons, ^{31}P NMR showed presence of $O=PPh_3$. Subsequent attempts at recrystallisation from DCM/Et_2O failed to remove impurities, and h) 0 g.

a) 0.2 g, 0.298 mmol, b) 0.6 ml, 0.6 mmol, c) 0.16 g, 0.595 mmol, d) 0.15 g, 0.595 mmol, e) 0.156 g, 0.595 mmol, f) 1 h, g) red solid obtained; recrystallisation from THF/hexane produced orange powder. THF persisted in ^1H NMR despite prolonged periods drying in vacuum oven and under high vacuum. ^{31}P NMR showed presence of $O=PPh_3$, and h) 0 g.

a) 0.4 g, 0.595 mmol, b) 1.2 ml, 1.2 mmol, c) 0.32 g, 1.191 mmol, d) 0.301 g, 1.191 mmol, e) 0.312 g, 1.191 mmol, f) 5 h, g) red solid obtained; ^{31}P NMR showed expected peaks at 17.1 ppm (Ir-PPh_3) and -144.2 ppm (PF_6), ^1H NMR correct in aromatic region, but aliphatic region integrated to only 6 protons, and h) 0 g.

Attempted Preparation of η^4-Cycloocta-1,5-diene(1,3-dibenzylimidazoline-2-ylidene)(triphenylphosphine)iridium(I) Hexafluorophosphate ***125***

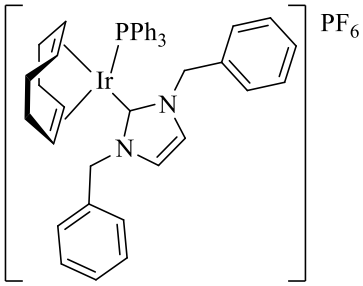

A 1 M sodium ethoxide solution was prepared by dissolving 0.25 g of sodium metal in ethanol (10 ml).

To a previously flame-dried Schlenk tube containing η^4-cycloocta-1,5-dieneiridium(I) chloride dimer **106** dissolved in dry benzene (10 ml), was added 1 M sodium ethoxide solution, resulting in a red to yellow colour change. The solution was stirred at r.t. for 10 minutes, followed by the addition of the 1,3-dibenzylimidazolium chloride **102**. The solution was stirred under an atmosphere of argon for 5 hours, after which time the solvent was removed under high vacuum. The residue was triturated with dry diethyl ether (15 ml) and filtered through celite under argon. The solvent was again removed under high vacuum yielding a yellow solid which was subsequently dissolved in dry THF (10 ml). Addition of silver hexafluorophosphate resulted in a yellow to orange colour change, and the formation of a precipitate was observed. The solution was stirred for 30 minutes prior to filtration through celite under argon, to give a clear orange solution. On addition of the phosphine, the solution turned from orange to deep red. After stirring for the allotted time, the solvent was once again removed under high vacuum and purification techniques were employed in an attempt to isolate the desired product.

Following the above procedure, results are reported as a) amount of **106**, b) amount of NaOEt, c) amount of **102**, d) amount of $AgPF_6$, e) amount of triphenylphosphine, f) solution stirring time, g) appearance of material obtained, purification conditions and analysis, and h) product yield.

a) 0.4 g, 0.595 mmol, b) 1.2 ml, 1.2 mmol, c) 1,3-dibenzylimidazolium chloride **102**, 0.339 g, 1.191 mmol, d) 0.301 g, 1.191 mmol, e) 0.312 g, 1.191 mmol, f) 1 h, g) oily gum obtained; recrystallisation attempt from DCM/Et_2O unsuccessful, and h) 0 g.

a) 0.4 g, 0.595 mmol, b) 1.2 ml, 1.2 mmol, c) 1,3-dibenzylimidazolium chloride **102**, 0.339 g, 1.191 mmol, d) 0.301 g, 1.191 mmol, e) 0.312 g, 1.191 mmol, f) 1 h, g) red solid obtained; on splitting into separate portions individual purification methods were attempted: recrystallisation from DCM/Et_2O gave orange-red solid, with the ^{31}P NMR spectrum showing the presence of $O=PPh_3$; recrystallisation from DCM/hexane resulted in an oily gum; crude material insoluble in small volumes of THF (as part of THF/hexane recrystallisation), and h) 0 g.

a) 0.4 g, 0.595 mmol, b) 1.2 ml, 1.2 mmol, c) 1,3-dibenzylimidazolium chloride **102**, 0.339 g, 1.191 mmol, d) 0.301 g, 1.191 mmol, e) 0.312 g, 1.191 mmol, f) 1 h, g) crude material triturated with EtOH then filtered to give a red solid; ^{1}H NMR spectrum showed presence of EtOH, and h) 0 g.

a) 0.4 g, 0.595 mmol, b) 1.2 ml, 1.2 mmol, c) 1,3-dibenzylimidazolium chloride **102**, 0.339 g, 1.191 mmol, d) 0.301 g, 1.191 mmol, e) 0.312 g, 1.191 mmol, f) 1 h, g) red crystals obtained following column chromatography (DCM then 10% MeOH/DCM); ^{1}H NMR showed excess aromatic protons (PPh_3), and h) 0 g.

a) 0.4 g, 0.595 mmol, b) 1.2 ml, 1.2 mmol, c) 1,3-dibenzylimidazolium chloride **102**, 0.339 g, 1.191 mmol, d) 0.301 g, 1.191 mmol, e) 0.312 g, 1.191 mmol, f) 16 h, g) red solid obtained; recrystallisation attempt from DCM/Et_2O yielded oily gum, ^{1}H NMR of which showed presence of impurities, and h) 0 g.

*Attempted Preparation of η^4-Cycloocta-1,5-diene(1,3-bis(2,6-diisopropylphenyl) imidazoline-2-ylidene)(triphenylphosphine)iridium(I) Hexafluorophosphate **126***

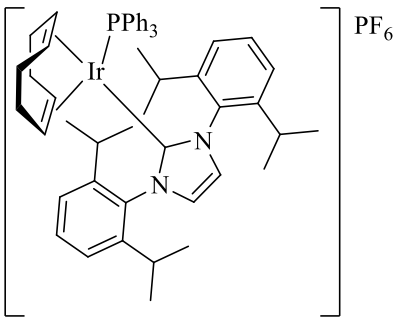

A 1 M sodium ethoxide solution was prepared by dissolving 0.25 g of sodium metal in ethanol (10 ml).

To a previously flame-dried Schlenk tube containing η^4-cycloocta-1,5-dieneiridium(I) chloride dimer **106** dissolved in dry benzene (10 ml), was added 1 M sodium ethoxide solution, resulting in a red to yellow colour change. The solution was stirred at r.t. for 10 minutes, followed by the addition of 1,3-bis(2,6-diisopropylphenyl)imidazolium chloride

105. The solution was stirred under an atmosphere of argon for 5 hours, after which time the solvent was removed under high vacuum. The residue was triturated with dry diethyl ether (15 ml) and filtered through celite under argon. The solvent was again removed under high vacuum yielding a yellow solid which was subsequently dissolved in dry THF. Addition of silver hexafluorophosphate resulted in a yellow to orange colour change, and the formation of a precipitate was observed. The solution was stirred for 30 minutes prior to filtration through celite under argon, to give a clear orange solution. Following addition of triphenylphosphine, the solution was stirred for the allotted period of time and then analysed by ^{1}H NMR.

Following the above procedure, results are reported as a) amount of **106**, b) amount of NaOEt, c) amount of **105**, d) amount of $AgPF_6$, e) amount of triphenylphosphine, f) solution stirring time, g) appearance of material obtained, purification conditions and analysis, and h) product yield.

a) 0.4 g, 0.595 mmol, b) 1.2 ml, 1.2 mmol, c) 0.406 g, 1.191 mmol, d) 0.301 g, 1.191 mmol, e) 0.312 g, 1.191 mmol, f) 1 h, g) solution remained orange following addition of PPh_3. Further 2 eq. PPh_3 added (0.312 g, 1.191 mmol); solution turned yellow with formation of white precipitate. ^{1}H NMR showed no desired product, and h) 0 g.

a) 0.2 g, 0.298 mmol, b) 0.6 ml, 0.6 mmol, c) 0.253 g, 0.595 mmol, d) 0.15 g, 0.595 mmol, e) 0.156 g, 0.595 mmol, f) 16 h, g) solution remained orange following addition of PPh_3. Stirred overnight, solution turned brown. ^{1}H NMR showed no desired product, and h) 0 g.

*Attempted Preparation of η^4-Cycloocta-1,5-diene(1,3-bis(diphenylmethyl)imidazoline-2-ylidene)(triphenylphosphine)iridium(I) Hexafluorophosphate **127***

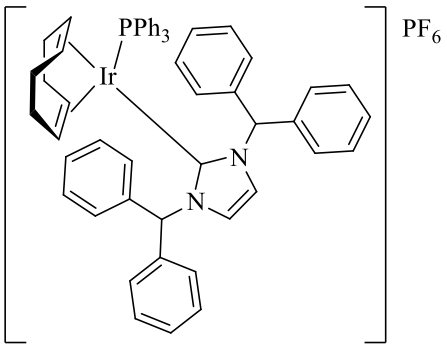

A 1 M sodium ethoxide solution was prepared by dissolving 0.25 g of sodium metal in ethanol (10 ml).

To a previously flame-dried Schlenk tube containing η^4-cycloocta-1,5-dieneiridium(I) chloride dimer **106** dissolved in dry benzene (10 ml), was added 1 M sodium ethoxide solution, resulting in a red to yellow colour change. The solution was stirred at r.t. for 10 minutes, followed by the addition of 1,3-bis(diphenylmethyl)imidazolium chloride **103**. The solution was stirred under an atmosphere of argon for 5 hours, after which time the solvent was removed under high vacuum. The residue was triturated with dry diethyl ether (15 ml) and filtered through celite under argon. The solvent was again removed under high vacuum yielding a yellow solid which was subsequently dissolved in dry THF. Addition of silver hexafluorophosphate resulted in a yellow to orange colour change, and the formation of a precipitate was observed. The solution was stirred for 30 minutes prior to filtration through celite under argon, to give a clear orange solution. Following addition of triphenylphosphine, the solution was stirred for the allotted period of time and then analysed by ^{1}H NMR.

Following the above procedure, results are reported as a) amount of **106**, b) amount of NaOEt, c) amount of **103**, d) amount of $AgPF_6$, e) amount of triphenylphosphine, f) solution stirring time, g) appearance of material obtained, purification conditions and analysis, and h) product yield.

a) 0.2 g, 0.298 mmol, b) 0.6 ml, 0.6 mmol, c) 0.26 g, 0.595 mmol, d) 0.15 g, 0.595 mmol, e) 0.156 g, 0.595 mmol, f) 1 h, g) recrystallisation from DCM/Et_2O produced red crystals; ^{1}H NMR spectrum contained an excess number of aromatic protons, and h) 0 g.

a) 0.4 g, 0.595 mmol, b) 1.2 ml, 1.2 mmol, c) 0.52 g, 1.191 mmol, d) 0.301 g, 1.191 mmol, e) 0.312 g, 1.191 mmol, f) 1 h, g) red crystals obtained following column chromatography (DCM then 10% MeOH/DCM); ^{1}H NMR showed excess aromatic protons, and h) 0 g.

a) 0.4 g, 0.595 mmol, b) 1.2 ml, 1.2 mmol, c) 0.52 g, 1.191 mmol, d) 0.301 g, 1.191 mmol, e) 0.312 g, 1.191 mmol, f) 16 h, g) red crystals obtained following recrystallisation from DCM/Et_2O; correct number of protons visible in ^{1}H NMR spectrum but ^{31}P NMR spectrum contained excess peaks, and h) 0 g.

Attempted Preparation of η^4-Cycloocta-1,5-diene(1,3-bis(1-adamantyl)imidazoline-2-ylidene)(triphenylphosphine)iridium(I) Hexafluorophosphate ***128***

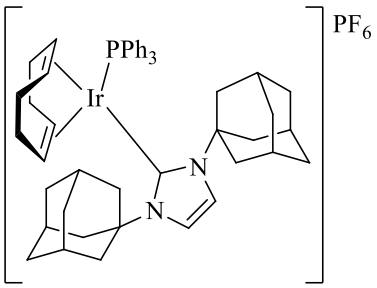

A 1 M sodium ethoxide solution was prepared by dissolving 0.25 g of sodium metal in ethanol (10 ml).

To a previously flame-dried Schlenk tube containing η^4-cycloocta-1,5-dieneiridium(I) chloride dimer **106** (0.25 g, 0.372 mmol) dissolved in dry benzene (10 ml), was added 1 M sodium ethoxide solution (0.74 ml, 0.743 mmol), resulting in a red to yellow colour change. The solution was stirred at r.t. for 10 minutes, followed by the addition of 1,3-bis(1-adamantyl)imidazol-2-ylidene **100** (0.25 g, 0.743 mmol). The solution was stirred under an atmosphere of argon for 5 hours, after which time the solvent was removed under high

vacuum. The residue was triturated with dry diethyl ether (15 ml) and filtered through celite under argon. The solvent was again removed under high vacuum, yielding a green/brown gum which was subsequently dissolved in dry THF (10 ml). Addition of $AgPF_6$ (0.188 g, 0.743 mmol) resulted in a green to brown colour change, and the formation of a precipitate was observed. The solution was stirred for 30 minutes prior to filtration through celite under argon to give a clear brown solution. Upon addition of triphenylphosphine (0.195 g, 0.743 mmol) the solution remained brown. A further portion of triphenylphosphine (0.195 g, 0.743 mmol) was added, however, the solution remained brown. After stirring for 1 hour, the solvent was once again removed under high vacuum, yielding a brown gum. Analysis by ^1H NMR revealed no desired product to be present.

Attempted Preparation of η^4-Cycloocta-1,5-diene(1,3-bis(1-adamantyl)imidazoline-2-ylidene)(chloride)iridium(I) ***129***[46]

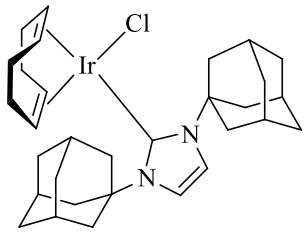

A 1 M sodium ethoxide solution was prepared by dissolving 0.25 g of sodium metal in ethanol (10 ml).

To a previously flame-dried Schlenk tube containing η^4-cycloocta-1,5-dieneiridium(I) chloride dimer **106** (0.25 g, 0.372 mmol) dissolved in dry benzene (10 ml), was added 1 M sodium ethoxide solution (0.74 ml, 0.743 mmol), resulting in a red to yellow colour change. The solution was stirred at r.t. for 10 minutes, followed by the addition of carbene **100** (0.25 g, 0.743 mmol). The solution was stirred under an atmosphere of argon for 5 hours, after which time the solvent was removed under high vacuum. The residue was triturated with dry diethyl ether (15 ml) and filtered through celite under argon. The solvent was again removed under high vacuum, yielding a green/brown gum. Analysis by ^1H NMR revealed no desired product to be present.

Preparation of Ir(COD)(NHC)Cl

Following *General Procedure B*, results are reported as a) amount of **106**, b) amount of NaOEt, c) amount of imidazolium salt, d) reaction temperature, e) reaction time, f) solvent used to elute material from silica, and g) product yield.

Preparation of Chloro(η^4–cycloocta–1,5–diene)(1,3-bis(2,6-diisopropyl-phenyl)imidazoline-2-ylidene) iridium(I) ***130***[46]

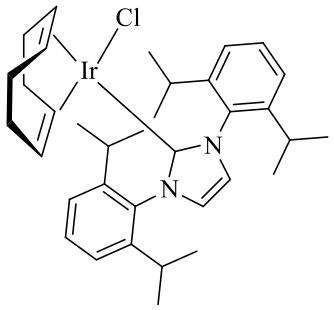

Table 75, Entry 1

a) 0.4 g, 0.595 mmol, b) 1.2 ml, 1.2 mmol, c) 1,3-bis(2,6-diisopropylphenyl)imidazolium chloride **105**, 0.506 g, 1.191 mmol, d) 25 °C, e) 24 h, f) EtOAc, and g) 0.247 g, 29%.

Table 75, Entry 2

a) 0.4 g, 0.595 mmol, b) 1.2 ml, 1.2 mmol, c) 1,3-bis(2,6-diisopropylphenyl)imidazolium chloride **105**, 0.506 g, 1.191 mmol, d) 25 °C, e) 48 h, f) EtOAc, and g) 0.380 g, 44%.

Table 75, Entry 3

a) 0.4 g, 0.595 mmol, b) 1.2 ml, 1.2 mmol, c) 1,3-bis(2,6-diisopropylphenyl)imidazolium chloride **105**, 0.506 g, 1.191 mmol, d) 25 °C, e) 72 h, f) EtOAc, and g) 0.442 g, 51%.

Table 75, Entry 4

a) 0.2 g, 0.298 mmol, b) 0.6 ml, 0.6 mmol, c) 1,3-bis(2,6-diisopropylphenyl)imidazolium chloride **105**, 0.253 g, 0.595 mmol, d) 45 °C, e) 24 h, f) EtOAc, and g) 0.354 g, 82%.

Table 75, Entry 5

a) 0.2 g, 0.298 mmol, b) 0.6 ml, 0.6 mmol, c) 1,3-bis(2,6-diisopropylphenyl)imidazolium chloride **105**, 0.253 g, 0.595 mmol, d) 45 °C, e) 48 h, f) EtOAc, and g) 0.386 g, 89%.

m.p. = decomposes at > 195 °C

FTIR: 2927, 2871, 1596, 1567 cm^{-1}

^{1}H NMR (400 MHz, $CDCl_3$): δ 7.48 (t, *J* = 7.8 Hz, 2H, ArH), 7.26-7.34 (m, 4H, ArH), 7.03 (s, 2H, olefinic CH), 4.19-4.21 (m, 2H, COD CH), 3.50-3.44 (m, 2H, $CH(CH_3)_2$), 2.89-2.91 (m, 2H, COD CH), 2.71-2.70 (m, 2H, $CH(CH_3)_2$), 1.75-1.64 (m, 2H, COD CH_2), 1.54-1.29 (m, 16H, COD CH_2 and $CH(CH_3)_2$), 1.28-1.25 (m, 2H, COD CH_2), 1.11 (d, *J* = 6.8 Hz, 12H, $CH(CH_3)_2$).

^{13}C NMR (100 MHz, $CDCl_3$): δ 181.9, 135.7, 129.3, 123.8, 122.4, 82.3, 50.9, 33.0, 28.4, 28.2, 25.9, 22.7, 22.0.

Preparation of Chloro(η^4–cycloocta–1,5–diene)(1,3-dicyclohexylimidazoline-2-ylidene) iridium(I) ***131***[46]

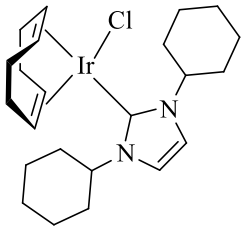

Table 76, Entry 1

a) 0.605 g, 0.9 mmol, b) 1.8 ml, 1.8 mmol, c) 1,3-dicyclohexylimidazolium chloride **104**, 0.484 g, 1.8 mmol, d) 25 °C, e) 24 h, f) EtOAc, and g) 0.196 g, 20%.

Table 76, Entry 2

a) 0.6 g, 0.893 mmol, b) 1.8 ml, 1.8 mmol, c) 1,3-dicyclohexylimidazolium chloride **104**, 0.480 g, 1.8 mmol, d) 45 °C, e) 24 h, f) EtOAc, and g) 0.814 g, 82%.

Table 76, Entry 3

a) 0.2 g, 0.298 mmol, b) 0.6 ml, 0.6 mmol, c) 1,3-dicyclohexylimidazolium chloride **104**, 0.160 g, 0.595 mmol, d) 45 °C, e) 48 h, f) EtOAc, and g) 0.288 g, 87%.

Table 76, Entry 4

a) 0.4 g, 0.595 mmol, b) 1.2 ml, 1.2 mmol, c) 1,3-dicyclohexylimidazolium chloride **104**, 0.320 g, 1.191 mmol, d) 45 °C, e) 96 h, f) EtOAc, and g) 0.602 g, 91%.

m.p. = decomposes at > 180 °C

FTIR: 2932, 2846, 1567, 1426 cm^{-1}

^{1}H NMR (400 MHz, $CDCl_3$): δ 6.84 (s, 2H, olefinic CH), 5.14-5.16 (m, 2H, CH), 4.57-4.59 (m, 2H, COD CH), 2.94-2.95 (m, 2H, COD CH), 2.17-2.29 (m, 6H, CH_2), 2.02 (d, J = 12.0 Hz, 2H, CH_2), 1.95 (dd, J = 13.1 Hz, ^{4}J = 2.1 Hz, 2H, CH_2), 1.85 (dd, J = 13.4 Hz, ^{4}J = 2.2 Hz, 2H, CH_2), 1.72-1.78 (m, 4H, CH_2), 1.57-1.66 (m, 4H, COD CH_2), 1.46-1.55 (m, 4H, COD CH_2), 1.18-1.39 (m, 4H, CH_2).

^{13}C NMR (100 MHz, $CDCl_3$): δ 177.4, 116.4, 82.8, 59.4, 50.3, 33.8, 33.7, 33.3, 29.2, 25.6, 25.3, 24.9.

Preparation of Chloro(η^4–cycloocta–1,5–diene)(1,3-dibenzylimidazoline-2-ylidene) iridium(I) ***132***[81]

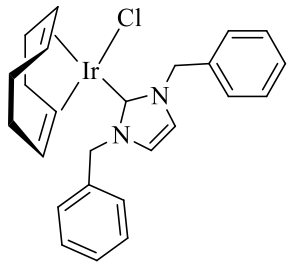

Table 77, Entry 1

a) 0.2 g, 0.298 mmol, b) 0.6 ml, 0.6 mmol, c) 1,3-dibenzylimidazolium chloride **102**, 0.169 g, 0.595 mmol, d) 45 °C, e) 24 h, f) DCM, and g) 0.116 g, 33%.

Table 77, Entry 2

a) 0.4 g, 0.595 mmol, b) 1.2 ml, 1.2 mmol, c) 1,3-dibenzylimidazolium chloride **102**, 0.339 g, 1.191 mmol, d) 60 °C, e) 24 h, f) DCM, and g) 0.418 g, 60%.

Table 77, Entry 3

a) 0.2 g, 0.298 mmol, b) 0.6 ml, 0.6 mmol, c) 1,3-dibenzylimidazolium chloride **102**, 0.169 g, 0.595 mmol, d) 60 °C, e) 48 h, f) DCM, and g) 0.234 g, 67%.

Table 77, Entry 4

a) 0.4 g, 0.595 mmol, b) 1.2 ml, 1.2 mmol, c) 1,3-dibenzylimidazolium chloride **102**, 0.339 g, 1.191 mmol, d) 60 °C, e) 72 h, f) DCM, and g) 0.553 g, 80%.

Table 77, Entry 5

a) 0.4 g, 0.595 mmol, b) 1.2 ml, 1.2 mmol, c) 1,3-dibenzylimidazolium chloride **102**, 0.339 g, 1.191 mmol, d) 60 °C, e) 96 h, f) DCM, and g) 0.562 g, 81%.

m.p. = decomposes at > 195 °C

FTIR: 3171, 3111, 2951, 1569, 1500 cm^{-1}

^{1}H NMR (400 MHz, $CDCl_3$): δ 7.39-7.32 (m, 10H, ArH), 6.77 (s, 2H, olefinic CH), 5.78 (d, *J* = 14.8 Hz, 2H, $ArCH_2$), 5.62 (d, *J* = 14.8 Hz, 2H, $ArCH_2$), 4.67 (m, 2H, COD CH), 2.98 (m, 2H, COD CH), 2.11-2.22 (m, 4H, COD CH_2), 1.76-1.71 (m, 2H, COD CH_2), 1.61-1.56 (m, 2H, COD CH_2).

^{13}C NMR (100 MHz, $CDCl_3$): δ 180.5, 135.8, 128.4, 127.7, 127.6, 120.0, 84.6, 53.9, 51.4, 33.1, 29.0.

Attempted Preparation of η^4-Cycloocta-1,5-diene(1,3-bis(2,6-diisopropylphenyl) imidazoline-2-ylidene)(triphenylphosphine)iridium(I) Hexafluorophosphate ***126***

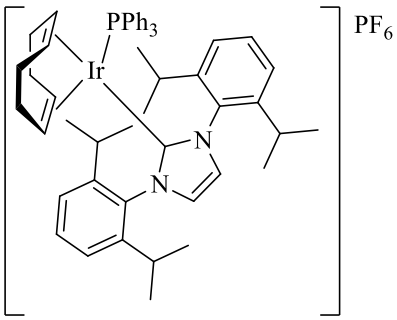

Scheme 89

To a stirring solution of Ir(COD)(IPr)Cl **130** (0.3 g, 0.414 mmol) in dry THF (6 ml) under an argon atmosphere was added $AgPF_6$ (0.150 g, 0.414 mmol), causing the clear yellow solution to turn orange and the formation of a precipitate was observed. The solution was stirred for 30 minutes prior to filtration through celite under argon, to give a clear orange solution. On addition of triphenylphosphine (0.109 g, 0.414 mmol) the solution remained orange. The reaction mixture was stirred for 1 h, then a second equivalent of PPh_3 (0.109 g, 0.414 mmol) was added, causing the solution to turn yellow, with the appearance of a white precipitate. After stirring for a further 1 h, the solution was filtered and the yellow filtrate concentrated *in vacuo*, yielding a yellow/brown gum, the ^1H NMR ($CDCl_3$) spectrum of which did not reveal the desired product.

Scheme 90

To a stirring solution of Ir(COD)(IPr)Cl **130** (0.187 g, 0.26 mmol) in dry THF (3 ml) under an argon atmosphere was added $AgPF_6$ (0.066 g, 0.26 mmol), causing the clear yellow solution to turn orange and the formation of a precipitate was observed. The solution was stirred for 30 minutes prior to filtration through celite under argon, to give a clear orange solution. On addition of triphenylphosphine (0.068 g, 0.26 mmol) the solution remained orange. Addition of dimethylphenylphosphine (0.036 g, 0.26 mmol) caused the solution to turn bright red. After stirring for 1 h, the solvent was removed under reduced pressure,

yielding a yellow gum. While analysis by ^{31}P NMR ($CDCl_3$) confirmed some complexation of PMe_2Ph to the Ir centre had occurred (-14.12 ppm), there also existed a (more intense) signal corresponding to unbound PMe_2Ph (-45.53 ppm).

Attempted Preparation of η^4-Cycloocta-1,5-diene(1,3-bis(2,6-diisopropylphenyl)imidazoline-2-ylidene)(dimethylphenylphosphine)iridium(I) Hexafluorophosphate ***134***

Scheme 91

To a stirring solution of Ir(COD)(IPr)Cl **130** (0.203 g, 0.28 mmol) in dry THF (3 ml) under an argon atmosphere was added $AgPF_6$ (0.071 g, 0.28 mmol), causing the clear yellow solution to turn orange and the formation of a precipitate was observed. The solution was stirred for 30 minutes prior to filtration through celite under argon, to give a clear orange solution. Upon addition of dimethylphenylphosphine (0.039 g, 0.28 mmol) the solution turned from orange to bright red. The solution was stirred for 2 h, before the solvent was removed under high vacuum, yielding a yellow gummy residue. While analysis by ^{31}P NMR ($CDCl_3$) confirmed some complexation of PMe_2Ph to the Ir centre had occurred (-14.13 ppm), there also existed a (more intense) signal corresponding to unbound PMe_2Ph (-45.63 ppm). Attempts to separate the desired product from the unreacted phosphine by recrystallisation from DCM/Et_2O were unsuccessful, with no clean material being isolated.

Preparation of η^4-Cycloocta-1,5-diene(1,3-dicyclohexyllimidazoline-2-ylidene)(triphenylphosphine)iridium(I) Hexafluorophosphate, ***124***

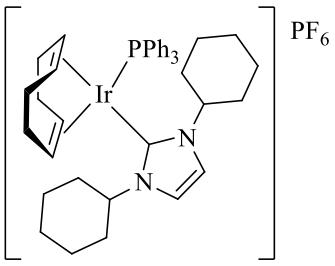

Scheme 92

To a stirring solution of Ir(COD)(ICy)Cl **131** in dry THF under an argon atmosphere was added $AgPF_6$, causing the clear yellow solution to turn orange and the formation of a precipitate was observed. The solution was stirred for 30 minutes prior to filtration through celite under argon, to give a clear orange solution. On addition of triphenylphosphine, the solution turned from orange to deep red. After stirring for 16 hours, the solvent was removed under high vacuum. The desired product **124** was isolated as a red solid following recrystallisation from DCM/Et_2O.

Following the above procedure, results are reported as a) amount of **131**, b) volume of THF, c) amount of $AgPF_6$, d) amount of triphenylphosphine, and e) product yield.

Table 78, Entry 1
a) 0.277 g, 0.5 mmol, b) 4 ml, c) 0.126 g, 0.5 mmol, d) 0.131 g, 0.5 mmol, and e) 0.091 g, 19%.

Table 78, Entry 2
a) 0.2 g, 0.36 mmol, b) 4 ml, c) 0.091 g, 0.36 mmol, d) 0.094 g, 0.36 mmol, and e) 0.195 g, 58%.

Table 78, Entry 3
a) 0.2 g, 0.36 mmol, b) 4 ml, c) 0.091 g, 0.36 mmol, d) 0.094 g, 0.36 mmol, and e) 0.232 g, 69%.

Table 78, Entry 4
a) 0.4 g, 0.72 mmol, b) 6 ml, c) 0.182 g, 0.72 mmol, d) 0.189 g, 0.72 mmol, and e) 0.506 g, 75%.

m.p. = decomposition began at 195 °C
FTIR: 3057, 2941, 2857, 1573, 1484 cm^{-1}

^{1}H NMR (400 MHz, $CDCl_3$): δ7.50-7.46 (m, 3H, ArH), 7.42-7.39 (m, 6H, ArH), 7.17-7.15 (m, 8H, ArH and olefinic CH), 4.57-4.52 (m, 2H, CH), 4.43-4.42 (m, 2H, COD CH), 3.61-3.60 (m, 2H, COD CH), 2.29-2.28 (m, 4H, CH_2), 2.18-2.16 (m, 2H, CH_2), 2.04-1.97 (m, 6H, CH_2), 1.72-1.66 (m, 4H, CH_2), 1.59-1.56 (m, 2H, CH_2), 1.45-1.1.35 (m, 2H, CH_2), 1.27-1.15 (m, 4H, CH_2), 1.09-1.03 (m, 2H, CH_2), 0.56-0.53 (m, 2H, CH_2).
^{13}C NMR (100 MHz, $CDCl_3$): δ 168.8, 133.1, 130.9, 130.1, 129.6, 128.7, 119.5, 84.8, 79.0, 60.8, 34.9, 31.5, 30.8, 30.0, 25.6, 25.4, 24.3.
^{31}P NMR (162 MHz, $CDCl_3$): δ 18.5 (PPh_3), -144.3 (PF_6).
HRMS (ESI): m/z calcd for $C_{41}H_{51}{}^{191}IrN_2P$ $[M\text{-}PF_6]^+$: 793.3390; found: 793.3390.
For crystal structure data, see Appendix (section 8.1).

Preparation of η^4-Cycloocta-1,5-diene(1,3-dicyclohexyllimidazoline-2-ylidene) (tribenzylphosphine)iridium(I) Hexafluorophosphate, ***135***

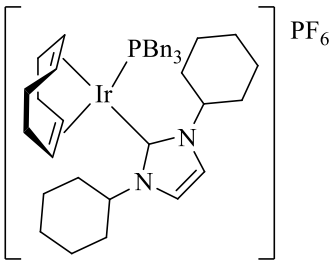

Scheme 93

To a stirring solution of Ir(COD)(ICy)Cl **131** in dry THF under an argon atmosphere was added $AgPF_6$, causing the clear yellow solution to turn orange and the formation of a precipitate was observed. The solution was stirred for 30 minutes prior to filtration through celite under argon, to give a clear orange solution. On addition of tribenzylphosphine, the solution turned from orange to deep red. After stirring for 16 hours, the solvent was removed under high vacuum. The desired product **135** was isolated as a red solid following recrystallisation from DCM/Et_2O.

Following the above procedure, results are reported as a) amount of **131**, b) volume of THF, c) amount of $AgPF_6$, d) amount of tribenzylphosphine, and e) product yield.

Table 79, Entry 1

a) 0.2 g, 0.36 mmol, b) 4 ml, c) 0.091 g, 0.36 mmol, d) 0.110 g, 0.36 mmol, and e) 0.203 g, 57%.

Table 79, Entry 2

a) 0.2 g, 0.36 mmol, b) 4 ml, c) 0.091 g, 0.36 mmol, d) 0.110 g, 0.36 mmol, and e) 0.219 g, 62%.

Table 79, Entry 3

a) 0.2 g, 0.36 mmol, b) 4 ml, c) 0.091 g, 0.36 mmol, d) 0.110 g, 0.36 mmol, and e) 0.242 g, 68%.

Table 79, Entry 4

a) 0.2 g, 0.36 mmol, b) 4 ml, c) 0.091 g, 0.36 mmol, d) 0.110 g, 0.36 mmol, and e) 0.274 g, 77%.

m.p. = decomposition began at 185 °C

FTIR: 2938, 1595, 1491 cm^{-1}

^{1}H NMR (400 MHz, $CDCl_3$): δ 7.75 (s, 2H, olefinic CH), 7.45-7.41 (m, 6H, ArH), 7.39-7.37 (m, 3H, ArH), 7.35-7.31 (m, 6H, ArH), 5.08-5.07 (m, 2H, CH), 4.64-4.61 (m, 2H, COD CH), 3.46-3.45 (m, 2H, COD CH), 3.17 (d, $^{2}J_{P\text{-}H}$ = 8.8 Hz, 6H, CH_2Ar), 2.37-2.28 (m, 2H, CH_2), 2.24-2.17 (m, 4H, CH_2), 2.12-2.03 (m, 10H, CH_2), 2.00-1.95 (m, 2H, CH_2), 1.88-1.81 (m, 4H, CH_2), 1.76-1.64 (m, 4H, CH_2), 1.47-1.39 (m, 2H, CH_2).

^{13}C NMR (100 MHz, $CDCl_3$): δ 170.0, 132.0, 129.3, 129.2, 128.6, 127.2, 119.8, 86.6, 77.6, 60.0, 35.1, 33.9, 31.9, 31.7, 30.7, 30.4, 25.8, 25.4, 24.3.

^{31}P NMR (162 MHz, $CDCl_3$): δ -4.54 (PPh_3), -144.3 (PF_6).

HRMS (ESI): m/z calcd for $C_{44}H_{57}{}^{191}IrN_2P$ $[M\text{-}PF_6]^+$: 835.3860; found: 835.3861.

For crystal structure data, see Appendix (section 8.2).

*Preparation of η^4-Cycloocta-1,5-diene(1,3-dicyclohexyllimidazoline-2-ylidene)(dimethylphenylphosphine)iridium(I) Hexafluorophosphate **136***

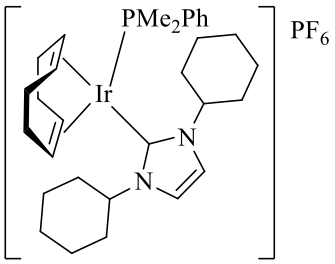

Scheme 94

To a stirring solution of Ir(COD)(ICy)Cl **131** (0.2 g, 0.36 mmol) in dry THF (3 ml) under an argon atmosphere was added $AgPF_6$ (0.091 g, 0.36 mmol), causing the clear yellow solution to turn orange and the formation of a precipitate was observed. The solution was stirred for 30 minutes prior to filtration through celite under argon, to give a clear orange solution. On addition of dimethylphenylphosphine (0.05 g, 0.36 mmol) the solution turned from orange to deep red. After stirring for 4 h, the solvent was removed under high vacuum yielding a red solid. Analysis by ^{31}P NMR revealed the presence of a peak corresponding to free PMe_2Ph.

Scheme 95

To a stirring solution of Ir(COD)(ICy)Cl **131** (0.2 g, 0.36 mmol) in dry THF (6 ml) under an argon atmosphere was added dimethylphenylphosphine (0.05 g, 0.36 mmol). $AgPF_6$ (0.109 g, 0.432 mmol) was then added, causing the clear yellow solution to turn red. The solution was stirred for 1.5 h, after which time dry Et_2O (5 ml) was added, resulting in the formation of a red precipitate. The solution was stirred for a further 20 minutes, then filtered through celite under argon. The red precipitate was washed from the celite with DCM, and the resulting clear red filtrate concentrated under reduced pressure. The desired product **136** was isolated as a red solid following recrystallisation from DCM/Et_2O. Analysis of the red solution obtained during filtration under argon revealed a small quantity of product to be present within the filtrate, however attempts to isolate this material through recrystallisation by DCM/Et_2O were unsuccessful.

Following the above procedure, results are reported as a) product yield.

Table 80, Entry 1

a) 0.150 g, 51%.

Table 80, Entry 2

a) 0.168 g, 57%.

Table 80, Entry 3

a) 0.172 g, 59%.

Table 80, Entry 4

a) 0.181 g, 62%.

m.p. = decomposition began at 190 °C

FTIR: 2932, 2854, 1456 cm^{-1}

^{1}H NMR (400 MHz, $CDCl_3$): δ 7.67-7.61 (m, 2H, ArH), 7.54-7.49 (m, 3H, ArH), 7.15 (s, 2H, olefinic CH), 4.57-4.41 (m, 2H, CH), 4.41-4.40 (m, 2H, COD CH), 3.96-3.95 (m, 2H, COD CH), 2.28-2.25 (m, 4H, CH_2), 2.13-1.99 (m, 8H, CH_2), 1.91-1.90 (m, 2H, CH_2), 1.80-1.78 (m, 2H, CH_2), 1.73-1.66 (m, 6H, CH_2), 1.59 (d, $^{2}J_{P\text{-}H}$ = 8.8 Hz, 6H, CH_3), 1.45-1.42 (m, 2H, CH_2), 1.33-1.27 (m, 4H, CH_2).

^{13}C NMR (100 MHz, $CDCl_3$): δ 171.2, 133.6, 130.7, 130.2, 128.9, 128.6, 118.9, 85.7, 60.5, 35.0, 33.2, 30.7, 30.6, 25.4, 25.1, 24.4, 15.0, 14.6, 13.9, 13.7.

^{31}P NMR (162 MHz, $CDCl_3$): δ -11.8 (PMe_2Ph), -144.3 (PF_6).

HRMS (ESI): m/z calcd for $C_{31}H_{45}{}^{191}IrN_2P$ $[M\text{-}2H\text{-}PF_6]^+$: 667.2921; found: 667.2919.

For crystal structure data, see Appendix (section 8.3).

*Preparation of η^4–Cycloocta-1,5-diene(1,3-dibenzylimidazoline-2-ylidene) (triphenylphosphine)iridium(I) hexafluorophosphate **125***

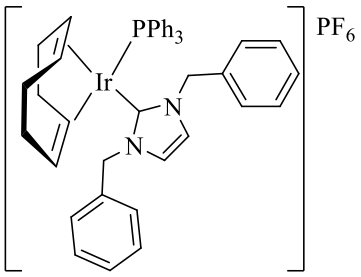

Scheme 96

To a stirring solution of Ir(COD)(IBn)Cl **132** in dry THF under an argon atmosphere was added $AgPF_6$, causing the clear yellow solution to turn orange and the formation of a precipitate was observed. The solution was stirred for 30 minutes prior to filtration through celite under argon, to give a clear orange solution. On addition of triphenylphosphine, the solution turned from orange to deep red. After stirring for the allotted time, the solvent was removed under high vacuum and purification techniques were employed in an attempt to isolate the desired product.

Following the above procedure, results are reported as a) amount of **132**, b) volume of THF, c) amount of $AgPF_6$, d) amount of triphenylphosphine, e) solution stirring time, f) appearance of material obtained, purification conditions and analysis, and g) product yield.

a) 0.351 g, 0.6 mmol, b) 7 ml, c) 0.152 g, 0.6 mmol, d) 0.157 g, 0.6 mmol, e) 4 h, f) sticky red solid obtained; excess protons in ^1H NMR spectrum and peak in ^{31}P NMR spectrum corresponding to free PPh_3, and g) 0 g.

a) 0.129 g, 0.22 mmol, b) 4 ml, c) 0.056 g, 0.22 mmol, d) 0.058 g, 0.22 mmol, e) 16 h, f) red solid obtained; excess protons in ^1H NMR spectrum and peak in ^{31}P NMR spectrum corresponding to free PPh_3, and g) 0 g.

Scheme 97

To a stirring solution of Ir(COD)(IBn)Cl **132** (0.094 g, 0.16 mmol) in dry THF under an argon atmosphere was added triphenylphosphine (0.042 g, 0.16 mmol). $AgPF_6$ (0.040 g, 0.16 mmol) was then added, causing the clear yellow solution to turn red. The solution was stirred overnight, and then filtered through celite under argon and the red filtrate concentrated under reduced pressure yielding a red solid. Analysis by ^1H NMR showed the desired product to be present, however signals corresponding to starting material **102** were also apparent. The material was triturated with dry Et_2O (5 x 2 ml) to remove impurities and the clean product **125** isolated as a red solid following recrystallisation from DCM/Et_2O (0.069 g, 45%).

Scheme 98

To a stirring solution of Ir(COD)(IBn)Cl **132** in dry THF under an argon atmosphere was added triphenylphosphine. $AgPF_6$ was then added, causing the clear yellow solution to turn red. The solution was stirred overnight, and then filtered through celite under argon and the red filtrate was concentrated under reduced pressure. The desired product **125** was isolated as a red solid following recrystallisation from DCM/Et_2O.

Following the above procedure, results are reported as a) amount of **132**, b) volume of THF, c) amount of triphenylphosphine, d) amount of $AgPF_6$, and e) product yield.

Table 81, Entry 1

a) 0.351 g, 0.6 mmol, b) 8 ml, c) 0.157, 0.6 mmol, d) 0.182 g, 0.72 mmol, and e) 0.302 g, 53%.

Table 81, Entry 2

a) 0.2 g, 0.34 mmol, b) 8 ml, c) 0.089 g, 0.34 mmol, d) 0.104 g, 0.41 mmol, and e) 0.239 g, 74%

Table 81, Entry 3

a) 0.263 g, 0.45 mmol, b) 5 ml, c), 0.118 g, 0.45 mmol, d) 0.137 g, 0.54 mmol, and e) 0.357 g, 83%.

m.p. = decomposition began at 190 °C

FTIR: 3169, 3140, 2962, 1571, 1482 cm^{-1}

^{1}H NMR (400 MHz, $CDCl_3$): δ 7.56-7.52 (m, 3H, ArH), 7.49-7.45 (m, 6H, ArH), 7.36-7.31 (m, 12H, ArH), 6.99-6.98 (m, 4H, ArH), 6.79 (s, 2H, olefinic CH), 5.52 (d, ^{2}J = 15.2 Hz, 2H, $ArCH_2$), 4.54 (d, ^{2}J = 14.8 Hz, 2H, $ArCH_2$), 4.41-4.40 (m, 2H, COD CH), 3.87-3.86 (m, 2H, COD CH), 2.29-2.23 (m, 2H, COD CH_2), 2.15-2.11 (m, 2H, COD CH_2), 2.03-1.96 (m, 4H, COD CH_2).

^{13}C NMR (100 MHz, $CDCl_3$): δ 174.8, 134.4, 133.8, 133.7, 131.5, 130.3, 129.8, 129.3, 129.2, 128.7, 127.7, 122.6, 86.7, 80.6, 54.3, 31.1, 30.6.

^{31}P NMR (162 Hz, $CDCl_3$): δ 18.2 (PPh_3), -144.3 (PF_6).

HRMS (ESI): m/z calcd for $C_{43}H_{43}{}^{191}IrN_2P$ $[M\text{-}PF_6]^+$: 809.2764; found: 809.2764.

*Preparation of η^4–Cycloocta-1,5-diene(1,3-dibenzylimidazoline-2-ylidene) (tribenzylphosphine)iridium(I) hexafluorophosphate **137***

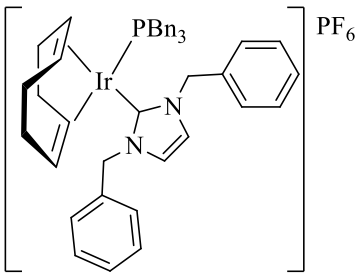

Scheme 99

To a stirring solution of Ir(COD)(IBn)Cl **132** (0.094 g, 0.16 mmol) in dry THF (4 ml) under an argon atmosphere was added tribenzylphosphine (0.049 g, 0.16 mmol). $AgPF_6$ (0.049 g, 0.192 mmol) was then added, causing the clear yellow solution to turn red. The solution was stirred overnight, and then filtered through celite under argon. The solvent was removed under high vacuum yielding a red gum, ^{1}H NMR analysis of which showed impurities.

Attempts to recrystallise the crude material from DCM/Et_2O were unsuccessful; the material remained as a gummy oil with no change in the ^1H NMR spectrum being observed.

Scheme 100

To a stirring solution of Ir(COD)(IBn)Cl **132** (0.1 g, 0.17 mmol) in dry THF (4 ml) under an argon atmosphere was added tribenzylphosphine (0.052 g, 0.17 mmol). $AgPF_6$ (0.052 g, 0.204 mmol) was then added, causing the clear yellow solution to turn red. The solution was stirred for 2 hours, prior to the addition of dry Et_2O (5 ml). After stirring for 20 minutes, the solution was filtered through celite under an argon atmosphere. The red precipitate which collected on the celite was washed with DCM and the solvent removed under reduced pressure. The desired product was isolated by recrystallisation from DCM/Et_2O, yielding complex **137** as a red solid (0.059 g, 34%).

m.p. = decomposition began at 190 °C
FTIR: 3168, 3039, 2884, 1497 cm^{-1}
^1H NMR (400 MHz, $CDCl_3$): δ 7.46-7.43 (m, 4H, ArH), 7.40-7.30 (m, 11H, ArH), 7.26-7.20 (m, 10H, ArH), 7.12 (s, 2H, olefinic CH), 5.81 (d, ^2J = 15.6 Hz, 2H, $ArCH_2$), 5.39 (d, ^2J = 15.6 Hz, 2H, $ArCH_2$), 4.33-4.32 (m, 2H, COD CH), 3.68-3.67 (m, 2H, COD CH), 2.02-1.78 (m, 8H, COD CH_2).
^{13}C NMR (100 MHz, $CDCl_3$): δ 175.5, 135.1, 132.9, 130.2, 130.0, 129.4, 128.9, 128.6, 127.6, 126.9, 126.9, 126.8, 123.1, 87.2, 79.3, 76.6, 54.2, 32.2, 32.0, 31.2, 30.6, 14.9.
^{31}P NMR (162 MHz, $CDCl_3$): δ -1.63 (PBn_3), -144.2 (PF_6).
HRMS (ESI): m/z calcd for $C_{46}H_{49}{}^{191}IrN_2P$ $[M\text{-}PF_6]^+$: 851.3215; found: 851.3224.

*Preparation of η^4–Cycloocta-1,5-diene(1,3-dibenzylimidazoline-2-ylidene) (dimethylphenylphosphine)iridium(I) hexafluorophosphate **138***

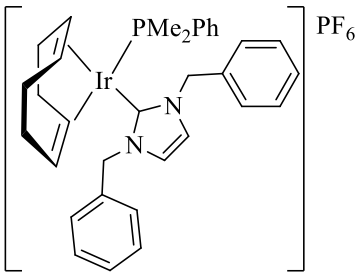

Scheme 101

To a stirring solution of Ir(COD)(IBn)Cl **132** in dry THF under an argon atmosphere was added dimethylphenylphosphine, resulting in a yellow to orange-red colour change. $AgPF_6$ was then added, causing the red colour of the solution to intensify. The solution was stirred for 1.5 h, during which time the formation of a red precipitate was observed. The solution was filtered through celite under argon, and the collected precipitate washed from the celite with DCM. The resulting clear red filtrate was concentrated under reduced pressure, and the desired product **138** was isolated as a red solid following recrystallisation from DCM/Et_2O. Analysis of the red solution originally obtained during filtration under argon revealed a small quantity of product to be present within the filtrate, however attempts to isolate this material through recrystallisation by DCM/Et_2O were unsuccessful.

Following the above procedure, results are reported as a) amount of **132**, b) volume of THF, c) amount of dimethylphenylphosphine, d) amount of $AgPF_6$, and e) product yield.

Table 82, Entry 1

a) 0.2 g, 0.34 mmol, b) 6 ml, c) 0.047 g, 0.34 mmol, d) 0.103 g, 0.408 mmol, and e) 0.128 g, 45%.

Table 82, Entry 2

a) 0.3 g, 0.51 mmol, b) 8 ml, c) 0.07 g, 0.51 mmol, d) 0.155 g, 0.612 mmol, and e) 0.202 g, 48%.

Table 82, Entry 3

a) 0.2 g, 0.34 mmol, b) 6 ml, c) 0.047 g, 0.34 mmol, d) 0.103 g, 0.408 mmol, and e) 0.154 g, 54%.

Table 82, Entry 4

a) 0.2 g, 0.34 mmol, b) 6 ml, c) 0.047 g, 0.34 mmol, d) 0.103 g, 0.408 mmol, and e) 0.153 g, 54%.

Table 82, Entry 5

a) 0.2 g, 0.34 mmol, b) 6 ml, c) 0.047 g, 0.34 mmol, d) 0.103 g, 0.408 mmol, and e) 0.162 g, 57%.

Table 82, Entry 6

a) 0.2 g, 0.34 mmol, b) 6 ml, c) 0.047 g, 0.34 mmol, d) 0.103 g, 0.408 mmol, and e) 0.189 g, 67%.

m.p. = decomposition began at 195 °C

FTIR: 3030, 2947, 2891, 1610, 1500 cm^{-1}

^{1}H NMR (400 MHz, $CDCl_3$): δ 7.51-7.47 (m, 5H, ArH), 7.39-7.32 (m, 6H, ArH), 7.09 (d, *J* = 7.2 Hz, 4H, ArH), 6.99 (s, 2H, olefinic CH), 5.57 (d, *J* = 15.6 Hz, 2H, $ArCH_2$), 4.79 (d, *J* = 15.2 Hz, 2H, $ArCH_2$), 4.20-4.18 (m, 4H, COD CH), 2.26-2.20 (m, 2H, COD CH_2), 2.03-1.84 (m, 6H, COD CH_2), 1.66 (d, $^{2}J_{P\text{-}H}$ = 8.8 Hz, 6H, CH_3).

^{13}C NMR (100 MHz, $CDCl_3$): δ 176.0, 135.0, 130.2, 129.6, 129.5, 128.9, 128.8, 128.7, 127.9, 126.3, 122.3, 86.0, 53.5, 30.7, 30.4, 12.8, 12.5.

^{31}P NMR (162 MHz, $CDCl_3$): δ -10.6 (PMe_2Ph), -144.2 (PF_6).

HRMS (ESI): m/z calcd for $C_{33}H_{37}{}^{191}IrN_2P$ $[M\text{-}2H\text{-}PF_6]^+$: 683.2295; found: 683.2294.

Elemental Analysis: Found: C, 47.56; H, 4.70; N, 3.55. Calc. for $C_{33}H_{39}F_6IrN_2P_2$: C, 47.65; H, 4.73; N, 3.37%.

6.7 Application of Novel Ir(I) Complexes in Hydrogen Isotope Exchange

*Deuteration of Acetophenone **54***

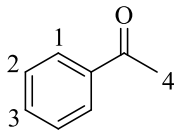

^{1}H NMR (400 MHz, $CDCl_3$): δ 7.93 (d, *J* = 7.5 Hz, 2H ^{1}CH), 7.54 (t, *J* = 7.4 Hz, 1H, ^{3}CH), 7.40 (t, *J* = 7.4 Hz, 2H ^{2}CH), 2.58 (s, 3H, ^{4}CH).

Incorporation expected at δ 7.93. Determined against integral at δ 2.58.

Following *General Procedure C*, results are reported as a) amount of substrate, b) amount of catalyst, c) solvent, volume of solvent, d) reaction time, and e) level of incorporation.

Table 83, Entry 1, Run 1

a) acetophenone **54**, 0.026 g, 0.215 mmol, b) complex **135**, 0.0098 g, 0.01 mmol, 5 mol%, c) DCM, 2.5 ml, d) 16 h, and e) 98%.

Table 83, Entry 1, Run 2

a) acetophenone **54**, 0.026 g, 0.215 mmol, b) complex **135**, 0.0098 g, 0.01 mmol, 5 mol%, c) DCM, 2.5 ml, d) 16 h, and e) 97%.

Table 83, Entry 2, Run 1

a) acetophenone **54**, 0.026 g, 0.215 mmol, b) complex **135**, 0.0098 g, 0.01 mmol, 5 mol%, c) DCM, 2.5 ml, d) 2 h, and e) 95%.

Table 83, Entry 2, Run 2

a) acetophenone **54**, 0.026 g, 0.215 mmol, b) complex **135**, 0.0098 g, 0.01 mmol, 5 mol%, c) DCM, 2.5 ml, d) 2 h, and e) 94%.

Table 83, Entry 3, Run 1

a) acetophenone **54**, 0.026 g, 0.215 mmol, b) complex **135**, 0.0098 g, 0.01 mmol, 5 mol%, c) DCM, 2.5 ml, d) 1 h, and e) 97%.

Table 83, Entry 3, Run 2

a) acetophenone **54**, 0.026 g, 0.215 mmol, b) complex **135**, 0.0098 g, 0.01 mmol, 5 mol%, c) DCM, 2.5 ml, d) 1 h, and e) 93%.

Table 84, Entry 1, Run 1

a) acetophenone **54**, 0.026 g, 0.215 mmol, b) complex **135**, 0.0049 g, 0.005 mmol, 2.5 mol%, c) DCM, 2.5 ml, d) 1 h, and e) 97%.

Table 84, Entry 1, Run 2

a) acetophenone **54**, 0.026 g, 0.215 mmol, b) complex **135**, 0.0049 g, 0.005 mmol, 2.5 mol%, c) DCM, 2.5 ml, d) 1 h, and e) 97%.

Table 84, Entry 2, Run 1

a) acetophenone **54**, 0.026 g, 0.215 mmol, b) complex **135**, 0.001 g, 0.001 mmol, 0.5 mol%, c) DCM, 2.5 ml, d) 1 h, and e) 82%.

Table 84, Entry 2, Run 2

a) acetophenone **54**, 0.026 g, 0.215 mmol, b) complex **135**, 0.001 g, 0.001 mmol, 0.5 mol%, c) DCM, 2.5 ml, d) 1 h, and e) 89%.

Table 84, Entry 3, Run 1

a) acetophenone **54**, 0.026 g, 0.215 mmol, b) complex **135**, 0.001 g, 0.001 mmol, 0.5 mol%, c) DCM, 2.5 ml, d) 2 h, and e) 97%.

Table 84, Entry 3, Run 2

a) acetophenone **54**, 0.026 g, 0.215 mmol, b) complex **135**, 0.001 g, 0.001 mmol, 0.5 mol%, c) DCM, 2.5 ml, d) 2 h, and e) 94%.

Table 85, Entry 1, Run 1

a) acetophenone **54**, 0.026 g, 0.215 mmol, b) complex **124**, 0.0094 g, 0.01 mmol, 5 mol%, c) DCM, 2.5 ml, d) 16 h, and e) 98%.

Table 85, Entry 1, Run 2

a) acetophenone **54**, 0.026 g, 0.215 mmol, b) complex **124**, 0.0094 g, 0.01 mmol, 5 mol%, c) DCM, 2.5 ml, d) 16 h, and e) 96%.

Table 85, Entry 2, Run 1

a) acetophenone **54**, 0.026 g, 0.215 mmol, b) complex **124**, 0.0094 g, 0.01 mmol, 5 mol%, c) DCM, 2.5 ml, d) 2 h, and e) 97%.

Table 85, Entry 2, Run 2

a) acetophenone **54**, 0.026 g, 0.215 mmol, b) complex **124**, 0.0094 g, 0.01 mmol, 5 mol%, c) DCM, 2.5 ml, d) 2 h, and e) 97%.

Table 85, Entry 3, Run 1

a) acetophenone **54**, 0.026 g, 0.215 mmol, b) complex **124**, 0.0096 g, 0.01 mmol, 5 mol%, c) DCM, 2.5 ml, d) 1 h, and e) 96%.

Table 85, Entry 3, Run 2

a) acetophenone **54**, 0.026 g, 0.215 mmol, b) complex **124**, 0.0096 g, 0.01 mmol, 5 mol%, c) DCM, 2.5 ml, d) 1 h, and e) 92%.

Table 86, Entry 1, Run 1

a) acetophenone **54**, 0.026 g, 0.215 mmol, b) complex **124**, 0.0047 g, 0.005 mmol, 2.5 mol%, c) DCM, 2.5 ml, d) 1 h, and e) 94%.

Table 86, Entry 1, Run 2

a) acetophenone **54**, 0.026 g, 0.215 mmol, b) complex **124**, 0.0047 g, 0.005 mmol, 2.5 mol%, c) DCM, 2.5 ml, d) 1 h, and e) 96%.

Table 86, Entry 2, Run 1

a) acetophenone **54**, 0.026 g, 0.215 mmol, b) complex **124**, 0.001 g, 0.001 mmol, 0.5 mol%, c) DCM, 2.5 ml, d) 1 h, and e) 77%.

Table 86, Entry 2, Run 2

a) acetophenone **54**, 0.026 g, 0.215 mmol, b) complex **124**, 0.001 g, 0.001 mmol, 0.5 mol%, c) DCM, 2.5 ml, d) 1 h, and e) 74%.

Table 86, Entry 3, Run 1

a) acetophenone **54**, 0.026 g, 0.215 mmol, b) complex **124**, 0.001 g, 0.001 mmol, 0.5 mol%, c) DCM, 2.5 ml, d) 2 h, and e) 87%.

Table 86, Entry 3, Run 2

a) acetophenone **54**, 0.026 g, 0.215 mmol, b) complex **124**, 0.001 g, 0.001 mmol, 0.5 mol%, c) DCM, 2.5 ml, d) 2 h, and e) 86%.

Table 86, Entry 4, Run 1

a) acetophenone **54**, 0.026 g, 0.215 mmol, b) complex **124**, 0.002 g, 0.002 mmol, 1 mol%, c) DCM, 2.5 ml, d) 1 h, and e) 96%.

Table 86, Entry 4, Run 2

a) acetophenone **54**, 0.026 g, 0.215 mmol, b) complex **124**, 0.002 g, 0.002 mmol, 1 mol%, c) DCM, 2.5 ml, d) 1 h, and e) 96%.

Table 87, Entry 1, Run 1

a) acetophenone **54**, 0.026 g, 0.215 mmol, b) complex **136**, 0.0082 g, 0.01 mmol, 5 mol%, c) DCM, 2.5 ml, d) 16 h, and e) 96%.

Table 87, Entry 1, Run 2

a) acetophenone **54**, 0.026 g, 0.215 mmol, b) complex **136**, 0.0082 g, 0.01 mmol, 5 mol%, c) DCM, 2.5 ml, d) 16 h, and e) 97%.

Table 87, Entry 2, Run 1

a) acetophenone **54**, 0.026 g, 0.215 mmol, b) complex **136**, 0.0082 g, 0.01 mmol, 5 mol%, c) DCM, 2.5 ml, d) 2 h, and e) 97%.

Table 87, Entry 2, Run 2

a) acetophenone **54**, 0.026 g, 0.215 mmol, b) complex **136**, 0.0082 g, 0.01 mmol, 5 mol%, c) DCM, 2.5 ml, d) 2 h, and e) 98%.

Table 87, Entry 3, Run 1

a) acetophenone **54**, 0.026 g, 0.215 mmol, b) complex **136**, 0.0082 g, 0.01 mmol, 5 mol%, c) DCM, 2.5 ml, d) 1 h, and e) 97%.

Table 87, Entry 3, Run 2

a) acetophenone **54**, 0.026 g, 0.215 mmol, b) complex **136**, 0.0082 g, 0.01 mmol, 5 mol%, c) DCM, 2.5 ml, d) 1 h, and e) 97%.

Table 88, Entry 1, Run 1

a) acetophenone **54**, 0.026 g, 0.215 mmol, b) complex **136**, 0.0049 g, 0.006 mmol, 3 mol%, c) DCM, 2.5 ml, d) 1 h, and e) 85%.

Table 88, Entry 1, Run 2

a) acetophenone **54**, 0.026 g, 0.215 mmol, b) complex **136**, 0.0049 g, 0.006 mmol, 3 mol%, c) DCM, 2.5 ml, d) 1 h, and e) 88%.

Table 88, Entry 2, Run 1

a) acetophenone **54**, 0.026 g, 0.215 mmol, b) complex **136**, 0.0049 g, 0.006 mmol, 3 mol%, c) DCM, 2.5 ml, d) 2 h, and e) 97%.

Table 88, Entry 2, Run 2

a) acetophenone **54**, 0.026 g, 0.215 mmol, b) complex **136**, 0.0049 g, 0.006 mmol, 3 mol%, c) DCM, 2.5 ml, d) 2 h, and e) 96%.

Table 88, Entry 3, Run 1

a) acetophenone **54**, 0.026 g, 0.215 mmol, b) complex **136**, 0.0016 g, 0.002 mmol, 1 mol%, c) DCM, 2.5 ml, d) 2 h, and e) 61%.

Table 88, Entry 3, Run 2

a) acetophenone **54**, 0.026 g, 0.215 mmol, b) complex **136**, 0.0016 g, 0.002 mmol, 1 mol%, c) DCM, 2.5 ml, d) 2 h, and e) 52%.

Table 88, Entry 4, Run 1

a) acetophenone **54**, 0.026 g, 0.215 mmol, b) complex **136**, 0.0033 g, 0.004 mmol, 2 mol%, c) DCM, 2.5 ml, d) 2 h, and e) 91%.

Table 88, Entry 4, Run 2

a) acetophenone **54**, 0.026 g, 0.215 mmol, b) complex **136**, 0.0033 g, 0.004 mmol, 2 mol%, c) DCM, 2.5 ml, d) 2 h, and e) 94%.

Table 89, Entry 1, Run 1

a) acetophenone **54**, 0.026 g, 0.215 mmol, b) complex **125**, 0.0096 g, 0.01 mmol, 5 mol%, c) DCM, 2.5 ml, d) 16 h, and e) 98%.

Table 89, Entry 1, Run 2

a) acetophenone **54**, 0.026 g, 0.215 mmol, b) complex **125**, 0.0096 g, 0.01 mmol, 5 mol%, c) DCM, 2.5 ml, d) 16 h, and e) 97%.

Table 89, Entry 2, Run 1

a) acetophenone **54**, 0.026 g, 0.215 mmol, b) complex **125**, 0.0096 g, 0.01 mmol, 5 mol%, c) DCM, 2.5 ml, d) 2 h, and e) 98%.

Table 89, Entry 2, Run 2

a) acetophenone **54**, 0.026 g, 0.215 mmol, b) complex **125**, 0.0096 g, 0.01 mmol, 5 mol%, c) DCM, 2.5 ml, d) 2 h, and e) 98%.

Table 89, Entry 3, Run 1

a) acetophenone **54**, 0.026 g, 0.215 mmol, b) complex **125**, 0.0096 g, 0.01 mmol, 5 mol%, c) DCM, 2.5 ml, d) 1 h, and e) 98%.

Table 89, Entry 3, Run 2

a) acetophenone **54**, 0.026 g, 0.215 mmol, b) complex **125**, 0.0096 g, 0.01 mmol, 5 mol%, c) DCM, 2.5 ml, d) 1 h, and e) 97%.

Table 89, Entry 4, Run 1

a) acetophenone **54**, 0.026 g, 0.215 mmol, b) complex **125**, 0.0096 g, 0.01 mmol, 5 mol%, c) DCM, 2.5 ml, d) 0.5 h, and e) 94%.

Table 89, Entry 4, Run 2

a) acetophenone **54**, 0.026 g, 0.215 mmol, b) complex **125**, 0.0096 g, 0.01 mmol, 5 mol%, c) DCM, 2.5 ml, d) 0.5 h, and e) 93%.

Table 90, Entry 1, Run 1

a) acetophenone **54**, 0.026 g, 0.215 mmol, b) complex **125**, 0.0062 g, 0.006 mmol, 3 mol%, c) DCM, 2.5 ml, d) 0.5 h, and e) 88%.

Table 90, Entry 1, Run 2

a) acetophenone **54**, 0.026 g, 0.215 mmol, b) complex **125**, 0.0062 g, 0.006 mmol, 3 mol%, c) DCM, 2.5 ml, d) 0.5 h, and e) 96%.

Table 90, Entry 2, Run 1

a) acetophenone **54**, 0.026 g, 0.215 mmol, b) complex **125**, 0.0021 g, 0.002 mmol, 1 mol%, c) DCM, 2.5 ml, d) 0.5 h, and e) 86%.

Table 90, Entry 2, Run 2

a) acetophenone **54**, 0.026 g, 0.215 mmol, b) complex **125**, 0.0021 g, 0.002 mmol, 1 mol%, c) DCM, 2.5 ml, d) 0.5 h, and e) 92%.

Table 90, Entry 3, Run 1

a) acetophenone **54**, 0.026 g, 0.215 mmol, b) complex **125**, 0.0021 g, 0.002 mmol, 1 mol%, c) DCM, 2.5 ml, d) 1 h, and e) 87%.

Table 90, Entry 3, Run 2

a) acetophenone **54**, 0.026 g, 0.215 mmol, b) complex **125**, 0.0021 g, 0.002 mmol, 1 mol%, c) DCM, 2.5 ml, d) 1 h, and e) 90%.

Table 90, Entry 4, Run 1

a) acetophenone **54**, 0.026 g, 0.215 mmol, b) complex **125**, 0.0021 g, 0.002 mmol, 1 mol%, c) DCM, 2.5 ml, d) 2 h, and e) 95%.

Table 90, Entry 4, Run 2

a) acetophenone **54**, 0.026 g, 0.215 mmol, b) complex **125**, 0.0021 g, 0.002 mmol, 1 mol%, c) DCM, 2.5 ml, d) 2 h, and e) 97%.

Table 91, Entry 1, Run 1

a) acetophenone **54**, 0.026 g, 0.215 mmol, b) complex **138**, 0.0083 g, 0.01 mmol, 5 mol%, c) DCM, 2.5 ml, d) 16 h, and e) 96%.

Table 91, Entry 1, Run 2

a) acetophenone **54**, 0.026 g, 0.215 mmol, b) complex **138**, 0.0083 g, 0.01 mmol, 5 mol%, c) DCM, 2.5 ml, d) 16 h, and e) 94%.

Table 91, Entry 2, Run 1

a) acetophenone **54**, 0.026 g, 0.215 mmol, b) complex **138**, 0.0083 g, 0.01 mmol, 5 mol%, c) DCM, 2.5 ml, d) 2 h, and e) 97%.

Table 91, Entry 2, Run 2

a) acetophenone **54**, 0.026 g, 0.215 mmol, b) complex **138**, 0.0083 g, 0.01 mmol, 5 mol%, c) DCM, 2.5 ml, d) 2 h, and e) 96%.

Table 91, Entry 3, Run 1

a) acetophenone **54**, 0.026 g, 0.215 mmol, b) complex **138**, 0.0083 g, 0.01 mmol, 5 mol%, c) DCM, 2.5 ml, d) 1 h, and e) 98%.

Table 91, Entry 3, Run 2

a) acetophenone **54**, 0.026 g, 0.215 mmol, b) complex **138**, 0.0083 g, 0.01 mmol, 5 mol%, c) DCM, 2.5 ml, d) 1 h, and e) 95%.

Table 91, Entry 4, Run 1

a) acetophenone **54**, 0.026 g, 0.215 mmol, b) complex **138**, 0.0083 g, 0.01 mmol, 5 mol%, c) DCM, 2.5 ml, d) 0.5 h, and e) 94%.

Table 91, Entry 4, Run 2

a) acetophenone **54**, 0.026 g, 0.215 mmol, b) complex **138**, 0.0083 g, 0.01 mmol, 5 mol%, c) DCM, 2.5 ml, d) 0.5 h, and e) 96%.

Table 92, Entry 1, Run 1

a) acetophenone **54**, 0.026 g, 0.215 mmol, b) complex **138**, 0.005 g, 0.006 mmol, 3 mol%, c) DCM, 2.5 ml, d) 0.5 h, and e) 96%.

Table 92, Entry 1, Run 2

a) acetophenone **54**, 0.026 g, 0.215 mmol, b) complex **138**, 0.005 g, 0.006 mmol, 3 mol%, c) DCM, 2.5 ml, d) 0.5 h, and e) 96%.

Table 92, Entry 2, Run 1

a) acetophenone **54**, 0.026 g, 0.215 mmol, b) complex **138**, 0.0017 g, 0.002 mmol, 1 mol%, c) DCM, 2.5 ml, d) 0.5 h, and e) 81%.

Table 92, Entry 2, Run 2

a) acetophenone **54**, 0.026 g, 0.215 mmol, b) complex **138**, 0.0017 g, 0.002 mmol, 1 mol%, c) DCM, 2.5 ml, d) 0.5 h, and e) 87%.

Table 92, Entry 3, Run 1

a) acetophenone **54**, 0.026 g, 0.215 mmol, b) complex **138**, 0.0017 g, 0.002 mmol, 1 mol%, c) DCM, 2.5 ml, d) 1 h, and e) 81%.

Table 92, Entry 3, Run 2

a) acetophenone **54**, 0.026 g, 0.215 mmol, b) complex **138**, 0.0017 g, 0.002 mmol, 1 mol%, c) DCM, 2.5 ml, d) 1 h, and e) 83%.

Table 92, Entry 4, Run 1

a) acetophenone **54**, 0.026 g, 0.215 mmol, b) complex **138**, 0.0017 g, 0.002 mmol, 1 mol%, c) DCM, 2.5 ml, d) 2 h, and e) 84%.

Table 92, Entry 4, Run 2

a) acetophenone **54**, 0.026 g, 0.215 mmol, b) complex **138**, 0.0017 g, 0.002 mmol, 1 mol%, c) DCM, 2.5 ml, d) 2 h, and e) 83%.

Table 92, Entry 5, Run 1

a) acetophenone **54**, 0.026 g, 0.215 mmol, b) complex **138**, 0.0034 g, 0.004 mmol, 2 mol%, c) DCM, 2.5 ml, d) 1 h, and e) 83%.

Table 92, Entry 5, Run 2

a) acetophenone **54**, 0.026 g, 0.215 mmol, b) complex **138**, 0.0034 g, 0.004 mmol, 2 mol%, c) DCM, 2.5 ml, d) 1 h, and e) 88%.

6.8 Application of Novel Ir(I) Complexes in HIE Reactions for Labelling Alternative Substrates

*Deuteration of Benzophenone **57***

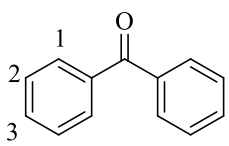

^{1}H NMR (400 MHz, $CDCl_3$): δ 7.81 (d, *J* = 8.0 Hz, 4H, ^{1}CH), 7.60 (t, *J* = 8.0 Hz, 2H, ^{3}CH), 7.49 (t, *J* = 7.7 Hz, 4H, ^{2}CH).

Incorporation expected at δ 7.81. Determined against integral at δ 7.60.

Following *General Procedure C*, results are reported as a) amount of substrate, b) amount of catalyst, c) solvent, volume of solvent, d) reaction time, and e) level of incorporation.

Table 94, Entry 1, Run 1

a) benzophenone **57**, 0.039 g, 0.215 mmol, b) complex **135**, 0.001 g, 0.001 mmol, 0.5 mol%, c) DCM, 2.5 ml, d) 2 h, and e) 71%.

Table 94, Entry 1, Run 2

a) benzophenone **57**, 0.039 g, 0.215 mmol, b) complex **135**, 0.001 g, 0.001 mmol, 0.5 mol%, c) DCM, 2.5 ml, d) 2 h, and e) 71%.

Table 94, Entry 2, Run 1

a) benzophenone **57**, 0.039 g, 0.215 mmol, b) complex **135**, 0.0098 g, 0.01 mmol, 5 mol%, c) DCM, 2.5 ml, d) 16 h, and e) 93%.

Table 94, Entry 2, Run 2

a) benzophenone **57**, 0.039 g, 0.215 mmol, b) complex **135**, 0.0098 g, 0.01 mmol, 5 mol%, c) DCM, 2.5 ml, d) 16 h, and e) 94%.

Table 94, Entry 3, Run 1

a) benzophenone **57**, 0.039 g, 0.215 mmol, b) complex **124**, 0.002 g, 0.002 mmol, 1 mol%, c) DCM, 2.5 ml, d) 1 h, and e) 79%.

Table 94, Entry 3, Run 2

a) benzophenone **57**, 0.039 g, 0.215 mmol, b) complex **124**, 0.002 g, 0.002 mmol, 1 mol%, c) DCM, 2.5 ml, d) 1 h, and e) 83%.

Table 94, Entry 4, Run 1

a) benzophenone **57**, 0.039 g, 0.215 mmol, b) complex **136**, 0.0049 g, 0.006 mmol, 3 mol%, c) DCM, 2.5 ml, d) 2 h, and e) 51%.

Table 94, Entry 4, Run 2

a) benzophenone **57**, 0.039 g, 0.215 mmol, b) complex **136**, 0.0049 g, 0.006 mmol, 3 mol%, c) DCM, 2.5 ml, d) 2 h, and e) 51%.

Table 94, Entry 5, Run 1

a) benzophenone **57**, 0.039 g, 0.215 mmol, b) complex **136**, 0.0082 g, 0.01 mmol, 5 mol%, c) DCM, 2.5 ml, d) 16 h, and e) 85%.

Table 94, Entry 5, Run 2

a) benzophenone **57**, 0.039 g, 0.215 mmol, b) complex **136**, 0.0082 g, 0.01 mmol, 5 mol%, c) DCM, 2.5 ml, d) 16 h, and e) 86%.

Table 94 Entry 6, Run 1

a) benzophenone **57**, 0.039 g, 0.215 mmol, b) complex **125**, 0.0021 g, 0.002 mmol, 1 mol%, c) DCM, 2.5 ml, d) 2 h, and e) 86%.

Table 94, Entry 6, Run 2

a) benzophenone **57**, 0.039 g, 0.215 mmol, b) complex **125**, 0.0021 g, 0.002 mmol, 1 mol%, c) DCM, 2.5 ml, d) 2 h, and e) 87%.

Table 94, Entry 7, Run 1

a) benzophenone **57**, 0.039 g, 0.215 mmol, b) complex **138**, 0.005 g, 0.006 mmol, 3 mol%, c) DCM, 2.5 ml, d) 0.5 h, and e) 61%.

Table 94, Entry 7, Run 2

a) benzophenone **57**, 0.039 g, 0.215 mmol, b) complex **138**, 0.005 g, 0.006 mmol, 3 mol%, c) DCM, 2.5 ml, d) 0.5 h, and e) 58%.

Table 94, Entry 8, Run 1

a) benzophenone **57**, 0.039 g, 0.215 mmol, b) complex **138**, 0.0083 g, 0.01 mmol, 5 mol%, c) DCM, 2.5 ml, d) 16 h, and e) 85%.

Table 94, Entry 8, Run 2

a) benzophenone **57**, 0.039 g, 0.215 mmol, b) complex **138**, 0.0083 g, 0.01 mmol, 5 mol%, c) DCM, 2.5 ml, d) 16 h, and e) 88%.

*Deuteration of 2-Phenylpyridine **41***

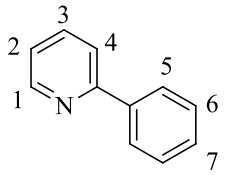

^{1}H NMR (400 MHz, $CDCl_3$): δ 8.71 (d, *J* = 4.7 Hz, 1H, ^{1}CH), 8.01 (d, *J* = 6.9 Hz, 2H, ^{5}CH), 7.75-7.71 (m, 2H, ^{2}CH and ^{3}CH), 7.51-7.41 (m, 3H, ^{6}CH and ^{7}CH), 7.27-7.22 (m, 1H, ^{4}CH).

Incorporation expected at δ 8.01. Determined against integral at δ 7.75-7.71.

Following *General Procedure C*, results are reported as a) amount of substrate, b) amount of catalyst, c) solvent, volume of solvent, d) reaction time, and e) level of incorporation.

Table 95, Entry 1, Run 1

a) 2-phenylpyridine **41**, 0.033 g, 0.215 mmol, b) complex **135**, 0.001 g, 0.001 mmol, 0.5 mol%, c) DCM, 2.5 ml, d) 2 h, and e) 2%.

Table 95, Entry 1, Run 2

a) 2-phenylpyridine **41**, 0.033 g, 0.215 mmol, b) complex **135**, 0.001 g, 0.001 mmol, 0.5 mol%, c) DCM, 2.5 ml, d) 2 h, and e) 2%.

Table 95, Entry 2, Run 1

a) 2-phenylpyridine **41**, 0.033 g, 0.215 mmol, b) complex **135**, 0.0098 g, 0.01 mmol, 5 mol%, c) DCM, 2.5 ml, d) 16 h, and e) 98%.

Table 95, Entry 2, Run 2

a) 2-phenylpyridine **41**, 0.033 g, 0.215 mmol, b) complex **135**, 0.0098 g, 0.01 mmol, 5 mol%, c) DCM, 2.5 ml, d) 16 h, and e) 98%.

Table 95, Entry 3, Run 1

a) 2-phenylpyridine **41**, 0.033 g, 0.215 mmol, b) complex **124**, 0.002 g, 0.002 mmol, 1 mol%, c) DCM, 2.5 ml, d) 1 h, and e) 3%.

Table 95, Entry 3, Run 2

a) 2-phenylpyridine **41**, 0.033 g, 0.215 mmol, b) complex **124**, 0.002 g, 0.002 mmol, 1 mol%, c) DCM, 2.5 ml, d) 1 h, and e) 6%.

Table 95, Entry 4, Run 1

a) 2-phenylpyridine **41**, 0.033 g, 0.215 mmol, b) complex **124**, 0.0094 g, 0.01 mmol, 5 mol%, c) DCM, 2.5 ml, d) 16 h, and e) 99%.

Table 95, Entry 4, Run 2

a) 2-phenylpyridine **41**, 0.033 g, 0.215 mmol, b) complex **124**, 0.0094 g, 0.01 mmol, 5 mol%, c) DCM, 2.5 ml, d) 16 h, and e) 99%.

Table 95, Entry 5, Run 1

a) 2-phenylpyridine **41**, 0.033 g, 0.215 mmol, b) complex **136**, 0.0049 g, 0.006 mmol, 3 mol%, c) DCM, 2.5 ml, d) 2 h, and e) 91%.

Table 95, Entry 5, Run 2

a) 2-phenylpyridine **41**, 0.033 g, 0.215 mmol, b) complex **136**, 0.0049 g, 0.006 mmol, 3 mol%, c) DCM, 2.5 ml, d) 2 h, and e) 96%.

Table 95, Entry 6, Run 1

a) 2-phenylpyridine **41**, 0.033 g, 0.215 mmol, b) complex **125**, 0.0021 g, 0.002 mmol, 1 mol%, c) DCM, 2.5 ml, d) 2 h, and e) 14%.

Table 95, Entry 6, Run 2

a) 2-phenylpyridine **41**, 0.033 g, 0.215 mmol, b) complex **125**, 0.0021 g, 0.002 mmol, 1 mol%, c) DCM, 2.5 ml, d) 2 h, and e) 16%.

Table 95, Entry 7, Run 1

a) 2-phenylpyridine **41**, 0.033 g, 0.215 mmol, b) complex **125**, 0.0096 g, 0.01 mmol, 5 mol%, c) DCM, 2.5 ml, d) 16 h, and e) 97%.

Table 95, Entry 7, Run 2

a) 2-phenylpyridine **41**, 0.033 g, 0.215 mmol, b) complex **125**, 0.0096 g, 0.01 mmol, 5 mol%, c) DCM, 2.5 ml, d) 16 h, and e) 94%.

Table 95, Entry 8, Run 1

a) 2-phenylpyridine **41**, 0.033 g, 0.215 mmol, b) complex **138**, 0.005 g, 0.006 mmol, 3 mol%, c) DCM, 2.5 ml, d) 0.5 h, and e) 90%.

Table 95, Entry 8, Run 2

a) 2-phenylpyridine **41**, 0.033 g, 0.215 mmol, b) complex **138**, 0.005 g, 0.006 mmol, 3 mol%, c) DCM, 2.5 ml, d) 0.5 h, and e) 95%.

Table 96, Entry 1, Run 1

a) 2-phenylpyridine **41**, 0.033 g, 0.215 mmol, b) complex **136**, 0.0033 g, 0.004 mmol, 2 mol%, c) DCM, 2.5 ml, d) 2 h, and e) 95%.

Table 96, Entry 1, Run 2

a) 2-phenylpyridine **41**, 0.033 g, 0.215 mmol, b) complex **136**, 0.0033 g, 0.004 mmol, 2 mol%, c) DCM, 2.5 ml, d) 2 h, and e) 97%.

Table 96, Entry 2, Run 1

a) 2-phenylpyridine **41**, 0.033 g, 0.215 mmol, b) complex **136**, 0.0016 g, 0.002 mmol, 1 mol%, c) DCM, 2.5 ml, d) 2 h, and e) 6%.

Table 96, Entry 2, Run 2

a) 2-phenylpyridine **41**, 0.033 g, 0.215 mmol, b) complex **136**, 0.0016 g, 0.002 mmol, 1 mol%, c) DCM, 2.5 ml, d) 2 h, and e) 2%.

Table 96, Entry 3, Run 1

a) 2-phenylpyridine **41**, 0.033 g, 0.215 mmol, b) complex **138**, 0.0034 g, 0.004 mmol, 2 mol%, c) DCM, 2.5 ml, d) 0.5 h, and e) 89%.

Table 96, Entry 3, Run 2

a) 2-phenylpyridine **41**, 0.033 g, 0.215 mmol, b) complex **138**, 0.0034 g, 0.004 mmol, 2 mol%, c) DCM, 2.5 ml, d) 0.5 h, and e) 93%.

Table 96, Entry 4, Run 1

a) 2-phenylpyridine **41**, 0.033 g, 0.215 mmol, b) complex **138**, 0.0017 g, 0.002 mmol, 1 mol%, c) DCM, 2.5 ml, d) 0.5 h, and e) 0%.

Table 96, Entry 4, Run 2

a) 2-phenylpyridine **41**, 0.033 g, 0.215 mmol, b) complex **138**, 0.0017 g, 0.002 mmol, 1 mol%, c) DCM, 2.5 ml, d) 0.5 h, and e) 5%.

Deuteration of N-*Phenylpyrazole **79***

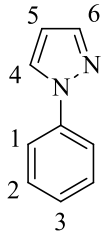

^{1}H NMR (400 MHz, $CDCl_3$): δ 7.92 (d, *J* = 4.0 Hz, 1H, ^{4}CH), 7.75-7.70 (m, 3H, ^{1}CH and ^{6}CH), 7.45 (t, *J* = 8.0 Hz, 2H, ^{2}CH), 7.29 (t, *J* = 8.0 Hz, 1H, ^{3}CH), 6.47 (t, *J* = 2.0 Hz, 1H, ^{5}CH).

Incorporation expected at δ 7.75-7.70. Determined against integral at δ 6.47.

Following *General Procedure C*, results are reported as a) amount of substrate, b) amount of catalyst, c) solvent, volume of solvent, d) reaction time, and e) level of incorporation.

Table 97, Entry 1, Run 1

a) *N*-phenylpyrazole **79**, 0.031 g, 0.215 mmol, b) complex **135**, 0.001 g, 0.001 mmol, 0.5 mol%, c) DCM, 2.5 ml, d) 2 h, and e) 98%.

Table 97, Entry 1, Run 2

a) *N*-phenylpyrazole **79**, 0.031 g, 0.215 mmol, b) complex **135**, 0.001 g, 0.001 mmol, 0.5 mol%, c) DCM, 2.5 ml, d) 2 h, and e) 98%.

Table 97, Entry 2, Run 1

a) *N*-phenylpyrazole **79**, 0.031 g, 0.215 mmol, b) complex **124**, 0.002 g, 0.002 mmol, 1 mol%, c) DCM, 2.5 ml, d) 1 h, and e) 91%.

Table 97, Entry 2, Run 2

a) *N*-phenylpyrazole **79**, 0.031 g, 0.215 mmol, b) complex **124**, 0.002 g, 0.002 mmol, 1 mol%, c) DCM, 2.5 ml, d) 1 h, and e) 95%.

Table 97, Entry 3, Run 1

a) *N*-phenylpyrazole **79**, 0.031 g, 0.215 mmol, b) complex **136**, 0.0049 g, 0.006 mmol, 3 mol%, c) DCM, 2.5 ml, d) 2 h, and e) 98%.

Table 97, Entry 3, Run 2

a) *N*-phenylpyrazole **79**, 0.031 g, 0.215 mmol, b) complex **136**, 0.0049 g, 0.006 mmol, 3 mol%, c) DCM, 2.5 ml, d) 2 h, and e) 99%.

Table 97, Entry 4, Run 1

a) *N*-phenylpyrazole **79**, 0.031 g, 0.215 mmol, b) complex **125**, 0.0021 g, 0.002 mmol, 1 mol%, c) DCM, 2.5 ml, d) 2 h, and e) 68%.

Table 97, Entry 4, Run 2

a) *N*-phenylpyrazole **79**, 0.031 g, 0.215 mmol, b) complex **125**, 0.0021 g, 0.002 mmol, 1 mol%, c) DCM, 2.5 ml, d) 2 h, and e) 73%.

Table 97, Entry 5, Run 1

a) *N*-phenylpyrazole **79**, 0.031 g, 0.215 mmol, b) complex **125**, 0.0096 g, 0.01 mmol, 5 mol%, c) DCM, 2.5 ml, d) 16 h, and e) 94%.

Table 97, Entry 5, Run 2

a) *N*-phenylpyrazole **79**, 0.031 g, 0.215 mmol, b) complex **125**, 0.0096 g, 0.01 mmol, 5 mol%, c) DCM, 2.5 ml, d) 16 h, and e) 93%.

Table 97, Entry 6, Run 1

a) *N*-phenylpyrazole **79**, 0.031 g, 0.215 mmol, b) complex **138**, 0.005 g, 0.006 mmol, 3 mol%, c) DCM, 2.5 ml, d) 0.5 h, and e) 11%.

Table 97, Entry 6, Run 1

a) *N*-phenylpyrazole **79**, 0.031 g, 0.215 mmol, b) complex **138**, 0.005 g, 0.006 mmol, 3 mol%, c) DCM, 2.5 ml, d) 0.5 h, and e) 8%.

Table 97, Entry 7, Run 1

a) *N*-phenylpyrazole **79**, 0.031 g, 0.215 mmol, b) complex **138**, 0.0083 g, 0.01 mmol, 5 mol%, c) DCM, 2.5 ml, d) 16 h, and e) 92%.

Table 97, Entry 7, Run 2

a) *N*-phenylpyrazole **79**, 0.031 g, 0.215 mmol, b) complex **138**, 0.0083 g, 0.01 mmol, 5 mol%, c) DCM, 2.5 ml, d) 16 h, and e) 98%.

*Deuteration of Benzamide **59***

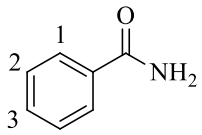

^{1}H NMR (400 MHz, d_6-acetone): δ 7.95 (d, *J* = 7.2 Hz, 2H, ^{1}CH), 7.53 (t, *J* = 7.3 Hz, 1H, ^{3}CH), 7.44 (t, *J* = 7.3 Hz, 2H, ^{2}CH).

Incorporation expected at δ 7.95. Determined against integral at δ 7.53.

Following *General Procedure C*, results are reported as a) amount of substrate, b) amount of catalyst, c) solvent, volume of solvent, d) reaction time, and e) level of incorporation.

Table 98, Entry 1, Run 1

a) benzamide **59**, 0.026 g, 0.215 mmol, b) complex **135**, 0.001 g, 0.001 mmol, 0.5 mol%, c) DCM, 2.5 ml, d) 2 h, and e) 6%.

Table 98, Entry 1, Run 2

a) benzamide **59**, 0.026 g, 0.215 mmol, b) complex **135**, 0.001 g, 0.001 mmol, 0.5 mol%, c) DCM, 2.5 ml, d) 2 h, and e) 6%.

Table 98, Entry 2, Run 1

a) benzamide **59**, 0.026 g, 0.215 mmol, b) complex **135**, 0.0098 g, 0.01 mmol, 5 mol%, c) DCM, 2.5 ml, d) 16 h, and e) 28%.

Table 98, Entry 2, Run 2

a) benzamide **59**, 0.026 g, 0.215 mmol, b) complex **135**, 0.0098 g, 0.01 mmol, 5 mol%, c) DCM, 2.5 ml, d) 16 h, and e) 34%.

Table 98, Entry 3, Run 1

a) benzamide **59**, 0.026 g, 0.215 mmol, b) complex **124**, 0.002 g, 0.002 mmol, 1 mol%, c) DCM, 2.5 ml, d) 1 h, and e) 7%.

Table 98, Entry 3, Run 2

a) benzamide **59**, 0.026 g, 0.215 mmol, b) complex **124**, 0.002 g, 0.002 mmol, 1 mol%, c) DCM, 2.5 ml, d) 1 h, and e) 7%.

Table 98, Entry 4, Run 1

a) benzamide **59**, 0.026 g, 0.215 mmol, b) complex **124**, 0.0094 g, 0.01 mmol, 5 mol%, c) DCM, 2.5 ml, d) 16 h, and e) 25%.

Table 98, Entry 4, Run 2

a) benzamide **59**, 0.026 g, 0.215 mmol, b) complex **124**, 0.0094 g, 0.01 mmol, 5 mol%, c) DCM, 2.5 ml, d) 16 h, and e) 24%.

Table 98, Entry 5, Run 1

a) benzamide **59**, 0.026 g, 0.215 mmol, b) complex **136**, 0.0049 g, 0.006 mmol, 3 mol%, c) DCM, 2.5 ml, d) 2 h, and e) 7%.

Table 98, Entry 5, Run 2

a) benzamide **59**, 0.026 g, 0.215 mmol, b) complex **136**, 0.0049 g, 0.006 mmol, 3 mol%, c) DCM, 2.5 ml, d) 2 h, and e) 9%.

Table 98, Entry 6, Run 1

a) benzamide **59**, 0.026 g, 0.215 mmol, b) complex **136**, 0.0082 g, 0.01 mmol, 5 mol%, c) DCM, 2.5 ml, d) 16 h, and e) 23%.

Table 98, Entry 6, Run 2

a) benzamide **59**, 0.026 g, 0.215 mmol, b) complex **136**, 0.0082 g, 0.01 mmol, 5 mol%, c) DCM, 2.5 ml, d) 16 h, and e) 30%.

Table 98, Entry 7, Run 1

a) benzamide **59**, 0.026 g, 0.215 mmol, b) complex **125**, 0.0021 g, 0.002 mmol, 1 mol%, c) DCM, 2.5 ml, d) 2 h, and e) 4%.

Table 98, Entry 7, Run 2

a) benzamide **59**, 0.026 g, 0.215 mmol, b) complex **125**, 0.0021 g, 0.002 mmol, 1 mol%, c) DCM, 2.5 ml, d) 2 h, and e) 4%.

Table 98, Entry 8, Run 1

a) benzamide **59**, 0.026 g, 0.215 mmol, b) complex **125**, 0.0096 g, 0.01 mmol, 5 mol%, c) DCM, 2.5 ml, d) 16 h, and e) 25%.

Table 98, Entry 8, Run 2

a) benzamide **59**, 0.026 g, 0.215 mmol, b) complex **125**, 0.0096 g, 0.01 mmol, 5 mol%, c) DCM, 2.5 ml, d) 16 h, and e) 21%.

Table 98, Entry 9, Run 1

a) benzamide **59**, 0.026 g, 0.215 mmol, b) complex **138**, 0.005 g, 0.006 mmol, 3 mol%, c) DCM, 2.5 ml, d) 0.5 h, and e) 5%.

Table 98, Entry 9, Run 2

a) benzamide **59**, 0.026 g, 0.215 mmol, b) complex **138**, 0.005 g, 0.006 mmol, 3 mol%, c) DCM, 2.5 ml, d) 0.5 h, and e) 6%.

Table 98, Entry 10, Run 1

a) benzamide **59**, 0.026 g, 0.215 mmol, b) complex **138**, 0.0083 g, 0.01 mmol, 5 mol%, c) DCM, 2.5 ml, d) 16 h, and e) 24%.

Table 98, Entry 10, Run 2

a) benzamide **59**, 0.026 g, 0.215 mmol, b) complex **138**, 0.0083 g, 0.01 mmol, 5 mol%, c) DCM, 2.5 ml, d) 16 h, and e) 20%.

*Deuteration of N,N,4-Trimethylbenzamide **111***

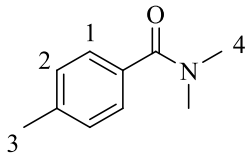

^{1}H NMR (400 MHz, $CDCl_3$): δ 7.32 (d, *J* = 8.0 Hz, 2H, ^{1}CH), 7.19 (d, *J* = 8.0 Hz, 2H, ^{2}CH), 3.00 (br s, 6H, ^{4}CH), 2.38 (s, 3H, ^{3}CH).

Incorporation expected at δ 7.32 and 3.00. Determined against integral at δ 2.38.

Following *General Procedure C*, results are reported as a) amount of substrate, b) amount of catalyst, c) solvent, volume of solvent, d) reaction time, and e) level of incorporation.

Table 99, Entry 1, Run 1

a) *N*,*N*,4-trimethylbenzamide **111**, 0.035 g, 0.215 mmol, b) complex **135**, 0.001 g, 0.001 mmol, 0.5 mol%, c) DCM, 2.5 ml, d) 2 h, and e) 7% at δ 7.32 and 0% at δ 3.00.

Table 99, Entry 1, Run 2

a) *N*,*N*,4-trimethylbenzamide **111**, 0.035 g, 0.215 mmol, b) complex **135**, 0.001 g, 0.001 mmol, 0.5 mol%, c) DCM, 2.5 ml, d) 2 h, and e) 4% at δ 7.32 and 0% at δ 3.00.

Table 99, Entry 2, Run 1

a) *N*,*N*,4-trimethylbenzamide **111**, 0.035 g, 0.215 mmol, b) complex **135**, 0.0098 g, 0.01 mmol, 5 mol%, c) DCM, 2.5 ml, d) 16 h, and e) 91% at δ 7.32 and 62% at δ 3.00.

Table 99, Entry 2, Run 2

a) *N*,*N*,4-trimethylbenzamide **111**, 0.035 g, 0.215 mmol, b) complex **135**, 0.0098 g, 0.01 mmol, 5 mol%, c) DCM, 2.5 ml, d) 16 h, and e) 91% at δ 7.32 and 61% at δ 3.00.

Table 99, Entry 3, Run 1

a) *N*,*N*,4-trimethylbenzamide **111**, 0.035 g, 0.215 mmol, b) complex **124**, 0.002 g, 0.002 mmol, 1 mol%, c) DCM, 2.5 ml, d) 1 h, and e) 11% at δ 7.32 and 0% at δ 3.00.

Table 99, Entry 3, Run 2

a) *N*,*N*,4-trimethylbenzamide **111**, 0.035 g, 0.215 mmol, b) complex **124**, 0.002 g, 0.002 mmol, 1 mol%, c) DCM, 2.5 ml, d) 1 h, and e) 7% at δ 7.32 and 0% at δ 3.00.

Table 99, Entry 4, Run 1

a) *N*,*N*,4-trimethylbenzamide **111**, 0.035 g, 0.215 mmol, b) complex **124**, 0.0094 g, 0.01 mmol, 5 mol%, c) DCM, 2.5 ml, d) 16 h, and e) 93% at δ 7.32 and 20% at δ 3.00.

Table 99, Entry 4, Run 2

a) *N*,*N*,4-trimethylbenzamide **111**, 0.035 g, 0.215 mmol, b) complex **124**, 0.0094 g, 0.01 mmol, 5 mol%, c) DCM, 2.5 ml, d) 16 h, and e) 90% at δ 7.32 and 18% at δ 3.00.

Table 99, Entry 5, Run 1

a) *N*,*N*,4-trimethylbenzamide **111**, 0.035 g, 0.215 mmol, b) complex **136**, 0.0049 g, 0.006 mmol, 3 mol%, c) DCM, 2.5 ml, d) 2 h, and e) 46% at δ 7.32 and 0% at δ 3.00.

Table 99, Entry 5, Run 2

a) *N*,*N*,4-trimethylbenzamide **111**, 0.035 g, 0.215 mmol, b) complex **136**, 0.0049 g, 0.006 mmol, 3 mol%, c) DCM, 2.5 ml, d) 2 h, and e) 50% at δ 7.32 and 0% at δ 3.00.

Table 99, Entry 6, Run 1

a) *N*,*N*,4-trimethylbenzamide **111**, 0.035 g, 0.215 mmol, b) complex **136**, 0.0082 g, 0.01 mmol, 5 mol%, c) DCM, 2.5 ml, d) 16 h, and e) 62% at δ 7.32 and 2% at δ 3.00.

Table 99, Entry 6, Run 2

a) *N*,*N*,4-trimethylbenzamide **111**, 0.035 g, 0.215 mmol, b) complex **136**, 0.0082 g, 0.01 mmol, 5 mol%, c) DCM, 2.5 ml, d) 16 h, and e) 60% at δ 7.32 and 1% at δ 3.00.

Table 99, Entry 7, Run 1

a) *N*,*N*,4-trimethylbenzamide **111**, 0.035 g, 0.215 mmol, b) complex **125**, 0.0021 g, 0.002 mmol, 1 mol%, c) DCM, 2.5 ml, d) 2 h, and e) 4% at δ 7.32 and 0% at δ 3.00.

Table 99, Entry 7, Run 2

a) *N*,*N*,4-trimethylbenzamide **111**, 0.035 g, 0.215 mmol, b) complex **125**, 0.0021 g, 0.002 mmol, 1 mol%, c) DCM, 2.5 ml, d) 2 h, and e) 4% at δ 7.32 and 0% at δ 3.00.

Table 99, Entry 8, Run 1

a) *N*,*N*,4-trimethylbenzamide **111**, 0.035 g, 0.215 mmol, b) complex **125**, 0.0096 g, 0.01 mmol, 5 mol%, c) DCM, 2.5 ml, d) 16 h, and e) 68% at δ 7.32 and 0% at δ 3.00.

Table 99, Entry 8, Run 2

a) *N*,*N*,4-trimethylbenzamide **111**, 0.035 g, 0.215 mmol, b) complex **125**, 0.0096 g, 0.01 mmol, 5 mol%, c) DCM, 2.5 ml, d) 16 h, and e) 73% at δ 7.32 and 0% at δ 3.00.

Table 99, Entry 9, Run 1

a) *N*,*N*,4-trimethylbenzamide **111**, 0.035 g, 0.215 mmol, b) complex **138**, 0.005 g, 0.006 mmol, 3 mol%, c) DCM, 2.5 ml, d) 0.5 h, and e) 32% at δ 7.32 and 0% at δ 3.00.

Table 99, Entry 9, Run 2

a) *N*,*N*,4-trimethylbenzamide **111**, 0.035 g, 0.215 mmol, b) complex **138**, 0.005 g, 0.006 mmol, 3 mol%, c) DCM, 2.5 ml, d) 0.5 h, and e) 30% at δ 7.32 and 0% at δ 3.00.

Table 99, Entry 10, Run 1

a) *N*,*N*,4-trimethylbenzamide **111**, 0.035 g, 0.215 mmol, b) complex **138**, 0.0083 g, 0.01 mmol, 5 mol%, c) DCM, 2.5 ml, d) 16 h, and e) 85% at δ 7.32 and 4% at δ 3.00.

Table 99, Entry 10, Run 2

a) *N*,*N*,4-trimethylbenzamide **111**, 0.035 g, 0.215 mmol, b) complex **138**, 0.0083 g, 0.01 mmol, 5 mol%, c) DCM, 2.5 ml, d) 16 h, and e) 92% at δ 7.32 and 5% at δ 3.00.

Deuteration of N-*Ethyl*-N,*4-dimethylbenzamide **112***

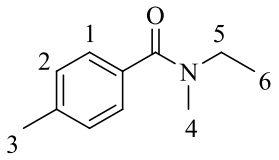

^{1}H NMR (400 MHz, d_6-acetone): δ 7.30 (d, *J* = 8.0 Hz, 2H, ^{1}CH), 7.24 (d, *J* = 8.0 Hz, 2H, ^{2}CH), 3.39 (br s, 2H, ^{5}CH), 2.98 (s, 3H, ^{4}CH), 2.37 (s, 3H, ^{3}CH), 1.15 (br s, 3H, ^{6}CH).

Incorporation expected at δ 7.30 and 2.98. Determined against integral at δ 2.37.

Following *General Procedure C*, results are reported as a) amount of substrate, b) amount of catalyst, c) solvent, volume of solvent, d) reaction time, and e) level of incorporation.

Table 100, Entry 1, Run 1

a) *N*-ethyl-*N*,4-dimethylbenzamide **112**, 0.038 g, 0.215 mmol, b) complex **135**, 0.001 g, 0.001 mmol, 0.5 mol%, c) DCM, 2.5 ml, d) 2 h, and e) 34% at δ 7.30 and 5% at δ 2.98.

Table 100, Entry 1, Run 2

a) *N*-ethyl-*N*,4-dimethylbenzamide **112**, 0.038 g, 0.215 mmol, b) complex **135**, 0.001 g, 0.001 mmol, 0.5 mol%, c) DCM, 2.5 ml, d) 2 h, and e) 28% at δ 7.30 and 6% at δ 2.98.

Table 100, Entry 2, Run 1

a) *N*-ethyl-*N*,4-dimethylbenzamide **112**, 0.038 g, 0.215 mmol, b) complex **135**, 0.0098 g, 0.01 mmol, 5 mol%, c) DCM, 2.5 ml, d) 16 h, and e) 94% at δ 7.30 and 32% at δ 2.98.

Table 100, Entry 2, Run 2

a) *N*-ethyl-*N*,4-dimethylbenzamide **112**, 0.038 g, 0.215 mmol, b) complex **135**, 0.0098 g, 0.01 mmol, 5 mol%, c) DCM, 2.5 ml, d) 16 h, and e) 93% at δ 7.30 and 35% at δ 2.98.

Table 100, Entry 3, Run 1

a) *N*-ethyl-*N*,4-dimethylbenzamide **112**, 0.038 g, 0.215 mmol, b) complex **124**, 0.002 g, 0.002 mmol, 1 mol%, c) DCM, 2.5 ml, d) 1 h, and e) 48% at δ 7.30 and 5% at δ 2.98.

Table 100, Entry 3, Run 2

a) *N*-ethyl-*N*,4-dimethylbenzamide **112**, 0.038 g, 0.215 mmol, b) complex **124**, 0.002 g, 0.002 mmol, 1 mol%, c) DCM, 2.5 ml, d) 1 h, and e) 52% at δ 7.30 and 6% at δ 2.98.

Table 100, Entry 4, Run 1

a) *N*-ethyl-*N*,4-dimethylbenzamide **112**, 0.038 g, 0.215 mmol, b) complex **124**, 0.0094 g, 0.01 mmol, 5 mol%, c) DCM, 2.5 ml, d) 16 h, and e) 95% at δ 7.30 and 31% at δ 2.98.

Table 100, Entry 4, Run 2

a) *N*-ethyl-*N*,4-dimethylbenzamide **112**, 0.038 g, 0.215 mmol, b) complex **124**, 0.0094 g, 0.01 mmol, 5 mol%, c) DCM, 2.5 ml, d) 16 h, and e) 96% at δ 7.30 and 28% at δ 2.98.

Table 100, Entry 5, Run 1

a) *N*-ethyl-*N*,4-dimethylbenzamide **112**, 0.038 g, 0.215 mmol, b) complex **136**, 0.0049 g, 0.006 mmol, 3 mol%, c) DCM, 2.5 ml, d) 2 h, and e) 25% at δ 7.30 and 6% at δ 2.98.

Table 100, Entry 5, Run 2

a) *N*-ethyl-*N*,4-dimethylbenzamide **112**, 0.038 g, 0.215 mmol, b) complex **136**, 0.0049 g, 0.006 mmol, 3 mol%, c) DCM, 2.5 ml, d) 2 h, and e) 25% at δ 7.30 and 5% at δ 2.98.

Table 100, Entry 6, Run 1

a) *N*-ethyl-*N*,4-dimethylbenzamide **112**, 0.038 g, 0.215 mmol, b) complex **136**, 0.0082 g, 0.01 mmol, 5 mol%, c) DCM, 2.5 ml, d) 16 h, and e) 81% at δ 7.30 and 8% at δ 2.98.

Table 100, Entry 6, Run 2

a) *N*-ethyl-*N*,4-dimethylbenzamide **112**, 0.038 g, 0.215 mmol, b) complex **136**, 0.0082 g, 0.01 mmol, 5 mol%, c) DCM, 2.5 ml, d) 16 h, and e) 74% at δ 7.30 and 7% at δ 2.98.

Table 100, Entry 7, Run 1

a) *N*-ethyl-*N*,4-dimethylbenzamide **112**, 0.038 g, 0.215 mmol, b) complex **125**, 0.0021 g, 0.002 mmol, 1 mol%, c) DCM, 2.5 ml, d) 2 h, and e) 41% at δ 7.30 and 0% at δ 2.98.

Table 100, Entry 7, Run 2

a) *N*-ethyl-*N*,4-dimethylbenzamide **112**, 0.038 g, 0.215 mmol, b) complex **125**, 0.0021 g, 0.002 mmol, 1 mol%, c) DCM, 2.5 ml, d) 2 h, and e) 39% at δ 7.30 and 0% at δ 2.98.

Table 100, Entry 8, Run 1

a) *N*-ethyl-*N*,4-dimethylbenzamide **112**, 0.038 g, 0.215 mmol, b) complex **125**, 0.0096 g, 0.01 mmol, 5 mol%, c) DCM, 2.5 ml, d) 16 h, and e) 99% at δ 7.30 and 7% at δ 2.98.

Table 100, Entry 8, Run 2

a) *N*-ethyl-*N*,4-dimethylbenzamide **112**, 0.038 g, 0.215 mmol, b) complex **125**, 0.0096 g, 0.01 mmol, 5 mol%, c) DCM, 2.5 ml, d) 16 h, and e) 95% at δ 7.30 and 9% at δ 2.98

Table 100, Entry 9, Run 1

a) *N*-ethyl-*N*,4-dimethylbenzamide **112**, 0.038 g, 0.215 mmol, b) complex **138**, 0.005 g, 0.006 mmol, 3 mol%, c) DCM, 2.5 ml, d) 0.5 h, and e) 38% at δ 7.30 and 3% at δ 2.98.

Table 100, Entry 9, Run 2

a) *N*-ethyl-*N*,4-dimethylbenzamide **112**, 0.038 g, 0.215 mmol, b) complex **138**, 0.005 g, 0.006 mmol, 3 mol%, c) DCM, 2.5 ml, d) 0.5 h, and e) 31% at δ 7.30 and 4% at δ 2.98.

Table 100, Entry 10, Run 1

a) *N*-ethyl-*N*,4-dimethylbenzamide **112**, 0.038 g, 0.215 mmol, b) complex **138**, 0.0083 g, 0.01 mmol, 5 mol%, c) DCM, 2.5 ml, d) 16 h, and e) 78% at δ 7.30 and 4% at δ 2.98.

Table 100, Entry 10, Run 2

a) *N*-ethyl-*N*,4-dimethylbenzamide **112**, 0.038 g, 0.215 mmol, b) complex **138**, 0.0083 g, 0.01 mmol, 5 mol%, c) DCM, 2.5 ml, d) 16 h, and e) 87% at δ 7.30 and 7% at δ 2.98.

Deuteration of N,N-*Diethyl-4-methylbenzamide* ***113***

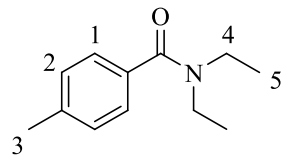

^{1}H NMR (400 MHz, d_6-acetone): δ 7.27-7.22 (m, 4H, ^{1}CH and ^{2}CH), 3.38 (br s, 4H, ^{4}CH), 2.36 (s, 3H, ^{3}CH), 1.14 (s, 6H, ^{5}CH).

Incorporation expected at δ 7.27-7.22. Determined against integral at δ 2.36.

Following *General Procedure C*, results are reported as a) amount of substrate, b) amount of catalyst, c) solvent, volume of solvent, d) reaction time, and e) level of incorporation.

Table 101, Entry 1, Run 1

a) *N*,*N*-diethyl-4-methylbenzamide **113**, 0.041 g, 0.215 mmol, b) complex **135**, 0.001 g, 0.001 mmol, 0.5 mol%, c) DCM, 2.5 ml, d) 2 h, and e) 29%.

Table 101, Entry 1, Run 2

a) *N*,*N*-diethyl-4-methylbenzamide **113**, 0.041 g, 0.215 mmol, b) complex **135**, 0.001 g, 0.001 mmol, 0.5 mol%, c) DCM, 2.5 ml, d) 2 h, and e) 37%.

Table 101, Entry 2, Run 1

a) *N*,*N*-diethyl-4-methylbenzamide **113**, 0.041 g, 0.215 mmol, b) complex **135**, 0.0098 g, 0.01 mmol, 5 mol%, c) DCM, 2.5 ml, d) 16 h, and e) 99%.

Table 101, Entry 2, Run 2

a) *N*,*N*-diethyl-4-methylbenzamide **113**, 0.041 g, 0.215 mmol, b) complex **135**, 0.0098 g, 0.01 mmol, 5 mol%, c) DCM, 2.5 ml, d) 16 h, and e) 99%.

Table 101, Entry 3, Run 1

a) *N*,*N*-diethyl-4-methylbenzamide **113**, 0.041 g, 0.215 mmol, b) complex **124**, 0.002 g, 0.002 mmol, 1 mol%, c) DCM, 2.5 ml, d) 1 h, and e) 85%.

Table 101, Entry 3, Run 2

a) *N*,*N*-diethyl-4-methylbenzamide **113**, 0.041 g, 0.215 mmol, b) complex **124**, 0.002 g, 0.002 mmol, 1 mol%, c) DCM, 2.5 ml, d) 1 h, and e) 85%.

Table 101, Entry 4, Run 1

a) *N*,*N*-diethyl-4-methylbenzamide **113**, 0.041 g, 0.215 mmol, b) complex **136**, 0.0049 g, 0.006 mmol, 3 mol%, c) DCM, 2.5 ml, d) 2 h, and e) 16%.

Table 101, Entry 4, Run 2

a) *N*,*N*-diethyl-4-methylbenzamide **113**, 0.041 g, 0.215 mmol, b) complex **136**, 0.0049 g, 0.006 mmol, 3 mol%, c) DCM, 2.5 ml, d) 2 h, and e) 18%.

Table 101, Entry 5, Run 1

a) *N*,*N*-diethyl-4-methylbenzamide **113**, 0.041 g, 0.215 mmol, b) complex **136**, 0.0082 g, 0.01 mmol, 5 mol%, c) DCM, 2.5 ml, d) 16 h, and e) 93%.

Table 101, Entry 5, Run 2

a) *N*,*N*-diethyl-4-methylbenzamide **113**, 0.041 g, 0.215 mmol, b) complex **136**, 0.0082 g, 0.01 mmol, 5 mol%, c) DCM, 2.5 ml, d) 16 h, and e) 91%.

Table 101, Entry 6, Run 1

a) *N*,*N*-diethyl-4-methylbenzamide **113**, 0.041 g, 0.215 mmol, b) complex **125**, 0.0021 g, 0.002 mmol, 1 mol%, c) DCM, 2.5 ml, d) 2 h, and e) 99%.

Table 101, Entry 6, Run 2

a) *N*,*N*-diethyl-4-methylbenzamide **113**, 0.041 g, 0.215 mmol, b) complex **125**, 0.0021 g, 0.002 mmol, 1 mol%, c) DCM, 2.5 ml, d) 2 h, and e) 97%.

Table 101, Entry 7, Run 1

a) *N*,*N*-diethyl-4-methylbenzamide **113**, 0.041 g, 0.215 mmol, b) complex **138**, 0.005 g, 0.006 mmol, 3 mol%, c) DCM, 2.5 ml, d) 0.5 h, and e) 58%.

Table 101, Entry 7, Run 2

a) *N*,*N*-diethyl-4-methylbenzamide **113**, 0.041 g, 0.215 mmol, b) complex **138**, 0.005 g, 0.006 mmol, 3 mol%, c) DCM, 2.5 ml, d) 0.5 h, and e) 58%.

Table 101, Entry 8, Run 1

a) *N*,*N*-diethyl-4-methylbenzamide **113**, 0.041 g, 0.215 mmol, b) complex **138**, 0.0083 g, 0.01 mmol, 5 mol%, c) DCM, 2.5 ml, d) 16 h, and e) 78%.

Table 101, Entry 8, Run 2

a) *N*,*N*-diethyl-4-methylbenzamide **113**, 0.041 g, 0.215 mmol, b) complex **138**, 0.0083 g, 0.01 mmol, 5 mol%, c) DCM, 2.5 ml, d) 16 h, and e) 79%.

*Deuteration of Acetanilide **73***

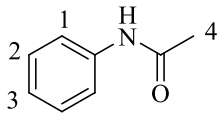

^{1}H NMR (400 MHz, MeOD): δ 7.50 (d, *J* = 7.9 Hz, 2H, ^{1}CH), 7.32 (t, *J* = 7.9 Hz, 2H, ^{2}CH), 7.11 (t, *J* = 7.4 Hz, 1H, ^{3}CH), 2.12 (s, 3H, ^{4}CH).

Incorporation expected at δ 7.50. Determined against integral at δ 2.12.

Following *General Procedure C*, results are reported as a) amount of substrate, b) amount of catalyst, c) solvent, volume of solvent, d) reaction time, and e) level of incorporation.

Table 102, Entry 1, Run 1

a) acetanilide **73**, 0.029 g, 0.215 mmol, b) complex **135**, 0.001 g, 0.001 mmol, 0.5 mol%, c) DCM, 2.5 ml, d) 2 h, and e) 18%.

Table 102, Entry 1, Run 2

a) acetanilide **73**, 0.029 g, 0.215 mmol, b) complex **135**, 0.001 g, 0.001 mmol, 0.5 mol%, c) DCM, 2.5 ml, d) 2 h, and e) 10%.

Table 102, Entry 2, Run 1

a) acetanilide **73**, 0.029 g, 0.215 mmol, b) complex **135**, 0.0098 g, 0.01 mmol, 5 mol%, c) DCM, 2.5 ml, d) 16 h, and e) 94%.

Table 102, Entry 2, Run 2

a) acetanilide **73**, 0.029 g, 0.215 mmol, b) complex **135**, 0.0098 g, 0.01 mmol, 5 mol%, c) DCM, 2.5 ml, d) 16 h, and e) 95%.

Table 102, Entry 3, Run 1

a) acetanilide **73**, 0.029 g, 0.215 mmol, b) complex **124**, 0.002 g, 0.002 mmol, 1 mol%, c) DCM, 2.5 ml, d) 1 h, and e) 15%.

Table 102, Entry 3, Run 2

a) acetanilide **73**, 0.029 g, 0.215 mmol, b) complex **124**, 0.002 g, 0.002 mmol, 1 mol%, c) DCM, 2.5 ml, d) 1 h, and e) 16%.

Table 102, Entry 4, Run 1

a) acetanilide **73**, 0.029 g, 0.215 mmol, b) complex **124**, 0.0094 g, 0.01 mmol, 5 mol%, c) DCM, 2.5 ml, d) 16 h, and e) 90%.

Table 102, Entry 4, Run 2

a) acetanilide **73**, 0.029 g, 0.215 mmol, b) complex **124**, 0.0094 g, 0.01 mmol, 5 mol%, c) DCM, 2.5 ml, d) 16 h, and e) 94%.

Table 102, Entry 5, Run 1

a) acetanilide **73**, 0.029 g, 0.215 mmol, b) complex **136**, 0.0049 g, 0.006 mmol, 3 mol%, c) DCM, 2.5 ml, d) 2 h, and e) 21%.

Table 102, Entry 5, Run 2

a) acetanilide **73**, 0.029 g, 0.215 mmol, b) complex **136**, 0.0049 g, 0.006 mmol, 3 mol%, c) DCM, 2.5 ml, d) 2 h, and e) 17%.

Table 102, Entry 6, Run 1

a) acetanilide **73**, 0.029 g, 0.215 mmol, b) complex **136**, 0.0082 g, 0.01 mmol, 5 mol%, c) DCM, 2.5 ml, d) 16 h, and e) 60%.

Table 102, Entry 6, Run 2

a) acetanilide **73**, 0.029 g, 0.215 mmol, b) complex **136**, 0.0082 g, 0.01 mmol, 5 mol%, c) DCM, 2.5 ml, d) 16 h, and e) 62%.

Table 102, Entry 7, Run 1

a) acetanilide **73**, 0.029 g, 0.215 mmol, b) complex **125**, 0.0021 g, 0.002 mmol, 1 mol%, c) DCM, 2.5 ml, d) 2 h, and e) 6%.

Table 102, Entry 7, Run 2

a) acetanilide **73**, 0.029 g, 0.215 mmol, b) complex **125**, 0.0021 g, 0.002 mmol, 1 mol%, c) DCM, 2.5 ml, d) 2 h, and e) 7%.

Table 102, Entry 8, Run 1

a) acetanilide **73**, 0.029 g, 0.215 mmol, b) complex **125**, 0.0096 g, 0.01 mmol, 5 mol%, c) DCM, 2.5 ml, d) 16 h, and e) 42%.

Table 102, Entry 8, Run 2

a) acetanilide **73**, 0.029 g, 0.215 mmol, b) complex **125**, 0.0096 g, 0.01 mmol, 5 mol%, c) DCM, 2.5 ml, d) 16 h, and e) 38%.

Table 102, Entry 9, Run 1

a) acetanilide **73**, 0.029 g, 0.215 mmol, b) complex **138**, 0.005 g, 0.006 mmol, 3 mol%, c) DCM, 2.5 ml, d) 0.5 h, and e) 12%.

Table 102, Entry 9, Run 2

a) acetanilide **73**, 0.029 g, 0.215 mmol, b) complex **138**, 0.005 g, 0.006 mmol, 3 mol%, c) DCM, 2.5 ml, d) 0.5 h, and e) 13%.

Table 102, Entry 10, Run 1

a) acetanilide **73**, 0.029 g, 0.215 mmol, b) complex **138**, 0.0083 g, 0.01 mmol, 5 mol%, c) DCM, 2.5 ml, d) 16 h, and e) 66%.

Table 102, Entry 10, Run 2

a) acetanilide **73**, 0.029 g, 0.215 mmol, b) complex **138**, 0.0083 g, 0.01 mmol, 5 mol%, c) DCM, 2.5 ml, d) 16 h, and e) 70%.

*Deuteration of Benzanilide **83***

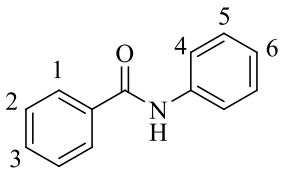

^{1}H NMR (400 MHz, d_6-acetone): δ 9.50 (s, 1H, NH), 7.99 (dd, *J* = 7.0 Hz, ^{4}J = 1.5 Hz, 2H, ^{1}CH), 7.86 (d, *J* = 8.0 Hz, 2H, ^{4}CH), 7.60-7.50 (m, 3H, ^{2}CH and ^{3}CH), 7.36 (t, *J* = 7.0 Hz, 2H, ^{5}CH), 7.11 (t, *J* = 7.3 Hz, 1H, ^{6}CH).

Incorporation expected at δ 7.99 and 7.86. Determined against integral at δ 7.11.

Following *General Procedure C*, results are reported as a) amount of substrate, b) amount of catalyst, c) solvent, volume of solvent, d) reaction time, and e) level of incorporation.

Table 103, Entry 1, Run 1

a) benzanilide **83**, 0.042 g, 0.215 mmol, b) complex **135**, 0.001 g, 0.001 mmol, 0.5 mol%, c) DCM, 2.5 ml, d) 2 h, and e) 95% at δ 7.99 and 16% at δ 7.86.

Table 103, Entry 1, Run 2

a) benzanilide **83**, 0.042 g, 0.215 mmol, b) complex **135**, 0.001 g, 0.001 mmol, 0.5 mol%, c) DCM, 2.5 ml, d) 2 h, and e) 91% at δ 7.99 and 12% at δ 7.86.

Table 103, Entry 2, Run 1

a) benzanilide **83**, 0.042 g, 0.215 mmol, b) complex **135**, 0.001 g, 0.001 mmol, 0.5 mol%, c) DCM, 2.5 ml, d) 1 h, and e) 91% at δ 7.99 and 2% at δ 7.86.

Table 103, Entry 2, Run 2

a) benzanilide **83**, 0.042 g, 0.215 mmol, b) complex **135**, 0.001 g, 0.001 mmol, 0.5 mol%, c) DCM, 2.5 ml, d) 1 h, and e) 87% at δ 7.99 and 3% at δ 7.86.

Table 103, Entry 3, Run 1

a) benzanilide **83**, 0.042 g, 0.215 mmol, b) complex **124**, 0.002 g, 0.002 mmol, 1 mol%, c) DCM, 2.5 ml, d) 1 h, and e) 87% at δ 7.99 and 34% at δ 7.86.

Table 103, Entry 3, Run 2

a) benzanilide **83**, 0.042 g, 0.215 mmol, b) complex **124**, 0.002 g, 0.002 mmol, 1 mol%, c) DCM, 2.5 ml, d) 1 h, and e) 93% at δ 7.99 and 38% at δ 7.86.

Table 103, Entry 4, Run 1

a) benzanilide **83**, 0.042 g, 0.215 mmol, b) complex **124**, 0.001 g, 0.001 mmol, 0.5 mol%, c) DCM, 2.5 ml, d) 1 h, and e) 65% at δ 7.99 and 11% at δ 7.86.

Table 103, Entry 4, Run 2

a) benzanilide **83**, 0.042 g, 0.215 mmol, b) complex **124**, 0.001 g, 0.001 mmol, 0.5 mol%, c) DCM, 2.5 ml, d) 1 h, and e) 68% at δ 7.99 and 10% at δ 7.86.

Table 103, Entry 5, Run 1

a) benzanilide **83**, 0.042 g, 0.215 mmol, b) complex **136**, 0.0049 g, 0.006 mmol, 3 mol%, c) DCM, 2.5 ml, d) 2 h, and e) 88% at δ 7.99 and 30% at δ 7.86.

Table 103, Entry 5, Run 2

a) benzanilide **83**, 0.042 g, 0.215 mmol, b) complex **136**, 0.0049 g, 0.006 mmol, 3 mol%, c) DCM, 2.5 ml, d) 2 h, and e) 94% at δ 7.99 and 32% at δ 7.86.

Table 103, Entry 6, Run 1

a) benzanilide **83**, 0.042 g, 0.215 mmol, b) complex **136**, 0.0016 g, 0.002 mmol, 1 mol%, c) DCM, 2.5 ml, d) 1 h, and e) 73% at δ 7.99 and 9% at δ 7.86.

Table 103, Entry 6, Run 2

a) benzanilide **83**, 0.042 g, 0.215 mmol, b) complex **136**, 0.0016 g, 0.002 mmol, 1 mol%, c) DCM, 2.5 ml, d) 1 h, and e) 80% at δ 7.99 and 9% at δ 7.86.

Table 103, Entry 7, Run 1

a) benzanilide **83**, 0.042 g, 0.215 mmol, b) complex **125**, 0.0021 g, 0.002 mmol, 1 mol%, c) DCM, 2.5 ml, d) 2 h, and e) 96% at δ 7.99 and 17% at δ 7.86.

Table 103, Entry 7, Run 2

a) benzanilide **83**, 0.042 g, 0.215 mmol, b) complex **125**, 0.0021 g, 0.002 mmol, 1 mol%, c) DCM, 2.5 ml, d) 2 h, and e) 96% at δ 7.99 and 14% at δ 7.86.

Table 103, Entry 8, Run 1

a) benzanilide **83**, 0.042 g, 0.215 mmol, b) complex **125**, 0.0021 g, 0.002 mmol, 1 mol%, c) DCM, 2.5 ml, d) 1 h, and e) 82% at δ 7.99 and 9% at δ 7.86.

Table 103, Entry 8, Run 2

a) benzanilide **83**, 0.042 g, 0.215 mmol, b) complex **125**, 0.0021 g, 0.002 mmol, 1 mol%, c) DCM, 2.5 ml, d) 1 h, and e) 88% at δ 7.99 and 8% at δ 7.86.

Table 103, Entry 9, Run 1

a) benzanilide **83**, 0.042 g, 0.215 mmol, b) complex **138**, 0.005 g, 0.006 mmol, 3 mol%, c) DCM, 2.5 ml, d) 0.5 h, and e) 67% at δ 7.99 and 16% at δ 7.86.

Table 103, Entry 9, Run 2

a) benzanilide **83**, 0.042 g, 0.215 mmol, b) complex **138**, 0.005 g, 0.006 mmol, 3 mol%, c) DCM, 2.5 ml, d) 0.5 h, and e) 74% at δ 7.99 and 15% at δ 7.86.

*Deuteration of Niclosamide **117***

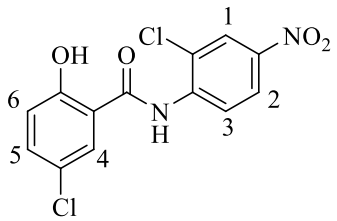

^{1}H NMR (400 MHz, d_6-DMSO): δ 11.37 (br s, 1H, OH), 8.81 (d, *J* = 9.2 Hz, 1H, ^{3}CH), 8.41 (d, ^{4}J = 2.8 Hz, 1H, ^{1}CH), 8.29 (dd, *J* = 9.2 Hz, ^{4}J = 2.8 Hz, 1H, ^{2}CH), 7.95 (d, ^{4}J = 2.8 Hz, 1H, ^{4}CH), 7.53 (dd, *J* = 8.8 Hz, ^{4}J = 2.8 Hz, 1H, ^{5}CH), 7.08 (d, *J* = 8.4 Hz, 1H, ^{6}CH).

Incorporation expected at δ 8.81, 8.41, 8.29, and 7.95. Determined against integral at δ 7.08.

Following *General Procedure C*, results are reported as a) amount of substrate, b) amount of catalyst, c) solvent, volume of solvent, d) reaction time, and e) level of incorporation.

Table 104, Entry 1, Run 1

a) Niclosamide **117**, 0.033 g, 0.1 mmol, b) complex **135**, 0.0047 g, 0.005 mmol, 5 mol%, c) DCM, 2.5 ml, d) 1 h, and e) 3% at δ 8.81, 55% at δ 8.41, 34% at δ 8.29, and 68% at δ 7.95.

Table 104, Entry 1, Run 2

a) Niclosamide **117**, 0.033 g, 0.1 mmol, b) complex **135**, 0.0047 g, 0.005 mmol, 5 mol%, c) DCM, 2.5 ml, d) 1 h, and e) 4% at δ 8.81, 54% at δ 8.41, 34% at δ 8.29, and 60% at δ 7.95.

Table 104, Entry 2, Run 1

a) Niclosamide **117**, 0.033 g, 0.1 mmol, b) complex **124**, 0.0047 g, 0.005 mmol, 5 mol%, c) DCM, 2.5 ml, d) 1 h, and e) 14% at δ 8.81, 32% at δ 8.41, 16% at δ 8.29, and 30% at δ 7.95.

Table 104, Entry 2, Run 2

a) Niclosamide **117**, 0.033 g, 0.1 mmol, b) complex **124**, 0.0047 g, 0.005 mmol, 5 mol%, c) DCM, 2.5 ml, d) 1 h, and e) 12% at δ 8.81, 29% at δ 8.41, 12% at δ 8.29, and 31% at δ 7.95.

Table 104, Entry 3, Run 1

a) Niclosamide **117**, 0.033 g, 0.1 mmol, b) complex **136**, 0.0041 g, 0.005 mmol, 5 mol%, c) DCM, 2.5 ml, d) 1 h, and e) 4% at δ 8.81, 20% at δ 8.41, 4% at δ 8.29, and 17% at δ 7.95.

Table 104, Entry 3, Run 2

a) Niclosamide **117**, 0.033 g, 0.1 mmol, b) complex **136**, 0.0041 g, 0.005 mmol, 5 mol%, c) DCM, 2.5 ml, d) 1 h, and e) 2% at δ 8.81, 18% at δ 8.41, 1% at δ 8.29, and 15% at δ 7.95.

Table 104, Entry 4, Run 1

a) Niclosamide **117**, 0.033 g, 0.1 mmol, b) complex **125**, 0.0048 g, 0.005 mmol, 5 mol%, c) DCM, 2.5 ml, d) 1 h, and e) 5% at δ 8.81, 22% at δ 8.41, 5% at δ 8.29, and 20% at δ 7.95.

Table 104, Entry 4, Run 2

a) Niclosamide **117**, 0.033 g, 0.1 mmol, b) complex **125**, 0.0048 g, 0.005 mmol, 5 mol%, c) DCM, 2.5 ml, d) 1 h, and e) 11% at δ 8.81, 26% at δ 8.41, 12% at δ 8.29, and 28% at δ 7.95.

Table 104, Entry 5, Run 1

a) Niclosamide **117**, 0.033 g, 0.1 mmol, b) complex **138**, 0.0042 g, 0.005 mmol, 5 mol%, c) DCM, 2.5 ml, d) 1 h, and e) 1% at δ 8.81, 10% at δ 8.41, 1% at δ 8.29, and 11% at δ 7.95.

Table 104, Entry 5, Run 2

a) Niclosamide **117**, 0.033 g, 0.1 mmol, b) complex **138**, 0.0042 g, 0.005 mmol, 5 mol%, c) DCM, 2.5 ml, d) 1 h, and e) 1% at δ 8.81, 12% at δ 8.41, 1% at δ 8.29, and 10% at δ 7.95.

*Deuteration of Celecoxib **119***

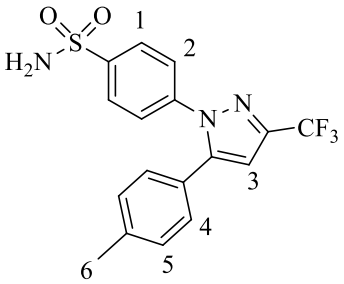

^{1}H NMR (400 MHz, MeOD): δ 7.93 (d, *J* = 8.8 Hz, 2H, ^{1}CH), 7.49 (d, *J* = 8.8 Hz, 2H, ^{2}CH), 7.21-7.16 (m, 4H, ^{4}CH and ^{5}CH), 6.90 (s, 1H, ^{3}CH), 2.35 (s, 3H, ^{6}CH).

Incorporation expected at δ 7.93 and δ 7.49. Determined against integral at δ 2.35.

Following *General Procedure C*, results are reported as a) amount of substrate, b) amount of catalyst, c) solvent, volume of solvent, d) reaction time, and e) level of incorporation.

Table 105, Entry 1, Run 1

a) Celecoxib **119**, 0.019 g, 0.05 mmol, b) complex **135**, 0.0025 g, 0.0025 mmol, 5 mol%, c) DCM, 2.5 ml, d) 1 h, and e) 11% at δ 7.93 and 98% at δ 7.49.

Table 105, Entry 1, Run 2

a) Celecoxib **119**, 0.019 g, 0.05 mmol, b) complex **135**, 0.0025 g, 0.0025 mmol, 5 mol%, c) DCM, 2.5 ml, d) 1 h, and e) 9% at δ 7.93 and 99% at δ 7.49.

Table 105, Entry 2, Run 1

a) Celecoxib **119**, 0.019 g, 0.05 mmol, b) complex **135**, 0.0049 g, 0.005 mmol, 10 mol%, c) DCM, 2.5 ml, d) 1 h, and e) 25% at δ 7.93 and 97% at δ 7.49.

Table 105, Entry 2, Run 2

a) Celecoxib **119**, 0.019 g, 0.05 mmol, b) complex **135**, 0.0049 g, 0.005 mmol, 10 mol%, c) DCM, 2.5 ml, d) 1 h, and e) 18% at δ 7.93 and 95% at δ 7.49.

Table 105, Entry 3, Run 1

a) Celecoxib **119**, 0.019 g, 0.05 mmol, b) complex **124**, 0.0024 g, 0.0025 mmol, 5 mol%, c) DCM, 2.5 ml, d) 1 h, and e) 10% at δ 7.93 and 98% at δ 7.49.

Table 105, Entry 3, Run 2

a) Celecoxib **119**, 0.019 g, 0.05 mmol, b) complex **124**, 0.0024 g, 0.0025 mmol, 5 mol%, c) DCM, 2.5 ml, d) 1 h, and e) 11% at δ 7.93 and 98% at δ 7.49.

Table 105, Entry 4, Run 1

a) Celecoxib **119**, 0.019 g, 0.05 mmol, b) complex **124**, 0.0047 g, 0.005 mmol, 10 mol%, c) DCM, 2.5 ml, d) 1 h, and e) 13% at δ 7.93 and 96% at δ 7.49.

Table 105, Entry 4, Run 2

a) Celecoxib **119**, 0.019 g, 0.05 mmol, b) complex **124**, 0.0047 g, 0.005 mmol, 10 mol%, c) DCM, 2.5 ml, d) 1 h, and e) 12% at δ 7.93 and 97% at δ 7.49.

Table 105, Entry 5, Run 1

a) Celecoxib **119**, 0.019 g, 0.05 mmol, b) complex **136**, 0.002 g, 0.0025 mmol, 5 mol%, c) DCM, 2.5 ml, d) 1 h, and e) 12% at δ 7.93 and 98% at δ 7.49.

Table 105, Entry 5, Run 2

a) Celecoxib **119**, 0.019 g, 0.05 mmol, b) complex **136**, 0.002 g, 0.0025 mmol, 5 mol%, c) DCM, 2.5 ml, d) 1 h, and e) 13% at δ 7.93 and 97% at δ 7.49.

Table 105, Entry 6, Run 1

a) Celecoxib **119**, 0.019 g, 0.05 mmol, b) complex **136**, 0.0041 g, 0.005 mmol, 10 mol%, c) DCM, 2.5 ml, d) 1 h, and e) 12% at δ 7.93 and 93% at δ 7.49.

Table 105, Entry 6, Run 2

a) Celecoxib **119**, 0.019 g, 0.05 mmol, b) complex **136**, 0.0041 g, 0.005 mmol, 10 mol%, c) DCM, 2.5 ml, d) 1 h, and e) 13% at δ 7.93 and 95% at δ 7.49.

Table 105, Entry 7, Run 1

a) Celecoxib **119**, 0.019 g, 0.05 mmol, b) complex **125**, 0.0024 g, 0.0025 mmol, 5 mol%, c) DCM, 2.5 ml, d) 1 h, and e) 12% at δ 7.93 and 89% at δ 7.49.

Table 105, Entry 7, Run 2

a) Celecoxib **119**, 0.019 g, 0.05 mmol, b) complex **125**, 0.0024 g, 0.0025 mmol, 5 mol%, c) DCM, 2.5 ml, d) 1 h, and e) 12% at δ 7.93 and 94% at δ 7.49.

Table 105, Entry 8, Run 1

a) Celecoxib **119**, 0.019 g, 0.05 mmol, b) complex **125**, 0.0048 g, 0.005 mmol, 10 mol%, c) DCM, 2.5 ml, d) 1 h, and e) 12% at δ 7.93 and 86% at δ 7.49.

Table 105, Entry 8, Run 2

a) Celecoxib **119**, 0.019 g, 0.05 mmol, b) complex **125**, 0.0048 g, 0.005 mmol, 10 mol%, c) DCM, 2.5 ml, d) 1 h, and e) 10% at δ 7.93 and 95% at δ 7.49.

Table 105, Entry 9, Run 1

a) Celecoxib **119**, 0.019 g, 0.05 mmol, b) complex **138**, 0.0021 g, 0.0025 mmol, 5 mol%, c) DCM, 2.5 ml, d) 1 h, and e) 10% at δ 7.93 and 99% at δ 7.49.

Table 105, Entry 9, Run 2

a) Celecoxib **119**, 0.019 g, 0.05 mmol, b) complex **138**, 0.0021 g, 0.0025 mmol, 5 mol%, c) DCM, 2.5 ml, d) 1 h, and e) 9% at δ 7.93 and 98% at δ 7.49.

Table 105, Entry 10, Run 1

a) Celecoxib **119**, 0.019 g, 0.05 mmol, b) complex **138**, 0.0042 g, 0.005 mmol, 10 mol%, c) DCM, 2.5 ml, d) 1 h, and e) 13% at δ 7.93 and 99% at δ 7.49.

Table 105, Entry 10, Run 2

a) Celecoxib **119**, 0.019 g, 0.05 mmol, b) complex **138**, 0.0042 g, 0.005 mmol, 10 mol%, c) DCM, 2.5 ml, d) 1 h, and e) 10% at δ 7.93 and 98% at δ 7.49.

6.9 Application of Novel Ir(I) Complexes in HIE Reactions Conducted in Alternative Solvents

*Deuteration of Acetophenone **54***

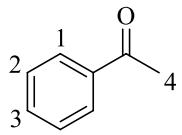

^{1}H NMR (400 MHz, $CDCl_3$): δ 7.93 (d, *J* = 7.5 Hz, 2H ^{1}CH), 7.54 (t, *J* = 7.4 Hz, 1H, ^{3}CH), 7.40 (t, *J* = 7.4 Hz, 2H ^{2}CH), 2.58 (s, 3H, ^{4}CH).

Incorporation expected at δ 7.93. Determined against integral at δ 2.58.

Following *General Procedure C*, results are reported as a) amount of substrate, b) amount of catalyst, c) solvent, volume of solvent, d) reaction time, and e) level of incorporation.

Table 106, Entry 1, Run 1

a) acetophenone **54**, 0.026 g, 0.215 mmol, b) complex **135**, 0.0098 g, 0.01 mmol, 5 mol%, c) Et_2O, 4 ml, d) 16 h, and e) 5%.

Table 106, Entry 1, Run 2

a) acetophenone **54**, 0.026 g, 0.215 mmol, b) complex **135**, 0.0098 g, 0.01 mmol, 5 mol%, c) Et_2O, 4 ml, d) 16 h, and e) 5%.

Table 106, Entry 2, Run 1

a) acetophenone **54**, 0.026 g, 0.215 mmol, b) complex **124**, 0.0094 g, 0.01 mmol, 5 mol%, c) Et_2O, 4 ml, d) 16 h, and e) 38%.

Table 106, Entry 2, Run 2

a) acetophenone **54**, 0.026 g, 0.215 mmol, b) complex **124**, 0.0094 g, 0.01 mmol, 5 mol%, c) Et_2O, 4 ml, d) 16 h, and e) 41%.

Table 106, Entry 3, Run 1

a) acetophenone **54**, 0.026 g, 0.215 mmol, b) complex **136**, 0.0082 g, 0.01 mmol, 5 mol%, c) Et_2O, 4 ml, d) 16 h, and e) 75%.

Table 106, Entry 3, Run 2

a) acetophenone **54**, 0.026 g, 0.215 mmol, b) complex **136**, 0.0082 g, 0.01 mmol, 5 mol%, c) Et_2O, 4 ml, d) 16 h, and e) 84%.

Table 106, Entry 4, Run 1

a) acetophenone **54**, 0.026 g, 0.215 mmol, b) complex **125**, 0.0096 g, 0.01 mmol, 5 mol%, c) Et_2O, 4 ml, d) 16 h, and e) 48%.

Table 106, Entry 4, Run 2

a) acetophenone **54**, 0.026 g, 0.215 mmol, b) complex **125**, 0.0096 g, 0.01 mmol, 5 mol%, c) Et_2O, 4 ml, d) 16 h, and e) 56%.

Table 106, Entry 5, Run 1

a) acetophenone **54**, 0.026 g, 0.215 mmol, b) complex **138**, 0.0083 g, 0.01 mmol, 5 mol%, c) Et_2O, 4 ml, d) 16 h, and e) 8%.

Table 106, Entry 5, Run 2

a) acetophenone **54**, 0.026 g, 0.215 mmol, b) complex **138**, 0.0083 g, 0.01 mmol, 5 mol%, c) Et_2O, 4 ml, d) 16 h, and e) 9%.

Table 107, Entry 1, Run 1

a) acetophenone **54**, 0.026 g, 0.215 mmol, b) complex **135**, 0.0098 g, 0.01 mmol, 5 mol%, c) ^{t}BuOMe, 4 ml, d) 16 h, and e) 35%.

Table 107, Entry 1, Run 2

a) acetophenone **54**, 0.026 g, 0.215 mmol, b) complex **135**, 0.0098 g, 0.01 mmol, 5 mol%, c) ^{t}BuOMe, 4 ml, d) 16 h, and e) 38%.

Table 107, Entry 2, Run 1

a) acetophenone **54**, 0.026 g, 0.215 mmol, b) complex **124**, 0.0094 g, 0.01 mmol, 5 mol%, c) ^{t}BuOMe, 4 ml, d) 16 h, and e) 29%.

Table 107, Entry 2, Run 2

a) acetophenone **54**, 0.026 g, 0.215 mmol, b) complex **124**, 0.0094 g, 0.01 mmol, 5 mol%, c) ^{t}BuOMe, 4 ml, d) 16 h, and e) 28%.

Table 107, Entry 3, Run 1

a) acetophenone **54**, 0.026 g, 0.215 mmol, b) complex **136**, 0.0082 g, 0.01 mmol, 5 mol%, c) ^{t}BuOMe, 4 ml, d) 16 h, and e) 24%.

Table 107, Entry 3, Run 2

a) acetophenone **54**, 0.026 g, 0.215 mmol, b) complex **136**, 0.0082 g, 0.01 mmol, 5 mol%, c) ^{t}BuOMe, 4 ml, d) 16 h, and e) 32%.

Table 107, Entry 4, Run 1

a) acetophenone **54**, 0.026 g, 0.215 mmol, b) complex **125**, 0.0096 g, 0.01 mmol, 5 mol%, c) ^{t}BuOMe, 4 ml, d) 16 h, and e) 46%.

Table 107, Entry 4, Run 2

a) acetophenone **54**, 0.026 g, 0.215 mmol, b) complex **125**, 0.0096 g, 0.01 mmol, 5 mol%, c) ^{t}BuOMe, 4 ml, d) 16 h, and e) 42%.

Table 107, Entry 5, Run 1

a) acetophenone **54**, 0.026 g, 0.215 mmol, b) complex **138**, 0.0083 g, 0.01 mmol, 5 mol%, c) ^{t}BuOMe, 4 ml, d) 16 h, and e) 7%.

Table 107, Entry 5, Run 2

a) acetophenone **54**, 0.026 g, 0.215 mmol, b) complex **138**, 0.0083 g, 0.01 mmol, 5 mol%, c) ^{t}BuOMe, 4 ml, d) 16 h, and e) 12%.

Table 108, Entry 1, Run 1

a) acetophenone **54**, 0.026 g, 0.215 mmol, b) complex **135**, 0.0098 g, 0.01 mmol, 5 mol%, c) 2-MeTHF, 2.5 ml, d) 16 h, and e) 33%.

Table 108, Entry 1, Run 2

a) acetophenone **54**, 0.026 g, 0.215 mmol, b) complex **135**, 0.0098 g, 0.01 mmol, 5 mol%, c) 2-MeTHF, 2.5 ml, d) 16 h, and e) 39%.

Table 108, Entry 2, Run 1

a) acetophenone **54**, 0.026 g, 0.215 mmol, b) complex **124**, 0.0094 g, 0.01 mmol, 5 mol%, c) 2-MeTHF, 2.5 ml, d) 16 h, and e) 20%.

Table 108, Entry 2, Run 2

a) acetophenone **54**, 0.026 g, 0.215 mmol, b) complex **124**, 0.0094 g, 0.01 mmol, 5 mol%, c) 2-MeTHF, 2.5 ml, d) 16 h, and e) 18%.

Table 108, Entry 3, Run 1

a) acetophenone **54**, 0.026 g, 0.215 mmol, b) complex **136**, 0.0082 g, 0.01 mmol, 5 mol%, c) 2-MeTHF, 2.5 ml, d) 16 h, and e) 67%.

Table 108, Entry 3, Run 2

a) acetophenone **54**, 0.026 g, 0.215 mmol, b) complex **136**, 0.0082 g, 0.01 mmol, 5 mol%, c) 2-MeTHF, 2.5 ml, d) 16 h, and e) 60%.

Table 108, Entry 4, Run 1

a) acetophenone **54**, 0.026 g, 0.215 mmol, b) complex **125**, 0.0096 g, 0.01 mmol, 5 mol%, c) 2-MeTHF, 2.5 ml, d) 16 h, and e) 17%.

Table 108, Entry 4, Run 2

a) acetophenone **54**, 0.026 g, 0.215 mmol, b) complex **125**, 0.0096 g, 0.01 mmol, 5 mol%, c) 2-MeTHF, 2.5 ml, d) 16 h, and e) 15%.

Table 108, Entry 5, Run 1

a) acetophenone **54**, 0.026 g, 0.215 mmol, b) complex **138**, 0.0083 g, 0.01 mmol, 5 mol%, c) 2-MeTHF, 2.5 ml, d) 16 h, and e) 32%.

Table 108, Entry 5, Run 2

a) acetophenone **54**, 0.026 g, 0.215 mmol, b) complex **138**, 0.0083 g, 0.01 mmol, 5 mol%, c) 2-MeTHF, 2.5 ml, d) 16 h, and e) 27%.

6.10 Application of Ir(COD)(NHC)Cl in Hydrogen Isotope Exchange

*Deuteration of Acetophenone **54** using Ir(COD)(NHC)Cl*

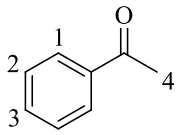

^{1}H NMR (400 MHz, $CDCl_3$): δ 7.93 (d, *J* = 7.5 Hz, 2H ^{1}CH), 7.54 (t, *J* = 7.4 Hz, 1H, ^{3}CH), 7.40 (t, *J* = 7.4 Hz, 2H ^{2}CH), 2.58 (s, 3H, ^{4}CH).

Incorporation expected at δ 7.93. Determined against integral at δ 2.58.

Following *General Procedure C*, results are reported as a) amount of substrate, b) amount of catalyst, c) solvent, volume of solvent, d) reaction time, and e) level of incorporation.

Table 113, Entry 1, Run 1

a) acetophenone **54**, 0.026 g, 0.215 mmol, b) complex **131**, 0.0055 g, 0.01 mmol, 5 mol%, c) DCM, 2.5 ml, d) 16 h, and e) 7%.

Table 113, Entry 1, Run 2

a) acetophenone **54**, 0.026 g, 0.215 mmol, b) complex **131**, 0.0055 g, 0.01 mmol, 5 mol%, c) DCM, 2.5 ml, d) 16 h, and e) 6%.

Table 113, Entry 2, Run 1

a) acetophenone **54**, 0.026 g, 0.215 mmol, b) complex **132**, 0.0058 g, 0.01 mmol, 5 mol%, c) DCM, 2.5 ml, d) 16 h, and e) 6%.

Table 113, Entry 2, Run 2

a) acetophenone **54**, 0.026 g, 0.215 mmol, b) complex **132**, 0.0058 g, 0.01 mmol, 5 mol%, c) DCM, 2.5 ml, d) 16 h, and e) 3%.

Table 113, Entry 3, Run 1

a) acetophenone **54**, 0.026 g, 0.215 mmol, b) complex **130**, 0.0073 g, 0.01 mmol, 5 mol%, c) DCM, 2.5 ml, d) 16 h, and e) 91%.

Table 113, Entry 3, Run 2

a) acetophenone **54**, 0.026 g, 0.215 mmol, b) complex **130**, 0.0073 g, 0.01 mmol, 5 mol%, c) DCM, 2.5 ml, d) 16 h, and e) 83%.

7 References

1. C. P. Adams and V. V. Brantner, *Health Econ.*, **2010**, *19*, 130.
2. *Clinical Drug Trials and Tribulations*; A. Cato, L. Sutton, A. Cato III (Eds.), Marcel Dekker Inc., New York, **2002**, 1.
3. A. Mullard, *Nature Rev. Drug Discov.*, **2011**, *10*, 82.
4. L. Lang, *Gastroenterology*, **2004**, *127*, 1026.
5. J. McMurray and R. C. Fay, *Chemistry, Fourth Edition*; Prentice Hall, New Jersey, **2004**.
6. R. R. Wolfe and D. L. Chinkes, *Isotope Tracers in Metabolic Research, Second Edition*; Wiley, New York, **2004**, 1.
7. P. H. Allen, M. J. Hickey, L. P. Kingston and D. J. Wilkinson, *J. Labelled Compd. Radiopharm.*, **2010**, *53*, 731.
8. W. J. S. Lockley and J. R. Heys, *J. Labelled Compd. Radiopharm.*, **2010**, *53*, 635.
9. J. L. Garnett and R. J. Hodges, *J. Am. Chem. Soc.*, **1967**, *89*, 4546.
10. J. L. Garnett, M. A. Long, A. B. McLaren and K. B. Peterson, *J. Chem. Soc., Chem. Commun.*, **1973**, 749.
11. M. R. Blake, J. L. Garnett, I. K. Gregor, W. Hannan, K. Hoa and M. A. Long, *J. Chem. Soc., Chem. Commun.*, **1975**, 930.
12. W. J. S. Lockley, *Tetrahedron Lett.*, **1982**, *23*, 3819.
13. W. J. S. Lockley, *J. Labelled Compd. Radiopharm.*, **1984**, *21*, 45.
14. W. J. S. Lockley, *J. Labelled Compd. Radiopharm.*, **1985**, *22*, 623.
15. D. Hesk, J. R. Jones and W. J. S. Lockley, *J. Labelled Compd. Radiopharm.*, **1990**, *28*, 1427.
16. R. Heys, *J. Chem. Soc., Chem. Commun.*, **1992**, 680.

17. R. H. Crabtree, E. M. Holt, M. Lavin and S. M. Morehouse, *Inorg. Chem.*, **1985**, *24*, 1986.

18. a) R. H. Crabtree, H. Felkin and G. E. Morris, *J. Organomet. Chem.*, **1977**, *141*, 205; b) R. H. Crabtree, *Acc. Chem. Res.*, **1979**, *12*, 331.

19. D. Hesk, P. R. Das and B. Evans, *J. Labelled Compd. Radiopharm.*, **1995**, *36*, 497.

20. A. Y. L. Shu, W. Chen and J. R. Heys, *J. Organomet. Chem.*, **1996**, *524*, 87.

21. R. Salter, M. Chapelle, A. Morgan, P. Ackermann, T. Moenius, M. Studer, F. Spindler and A. Togni, *Synthesis and Applications of Isotopically Labelled Compounds*; U. Pleiss and R. Voges (Eds.), Wiley, New York, **2001**, 63.

22. G. J. Ellames, J. S. Gibson, J. M. Herbert, W. J. Kerr and A. H. McNeill, *Tetrahedron Lett.*, **2001**, *42*, 6413.

23. P. W. C. Cross, G. J. Ellames, J. S. Gibson, J. M. Herbert, W. J. Kerr, A. H. McNeill and T. W. Mathers, *Tetrahedron*, **2003**, *59*, 3349.

24. G. J. Ellames, J. S. Gibson, J. M. Herbert and A. H. McNeill, *Tetrahedron*, **2001**, *57*, 9487.

25. H. M. Lee, T. Jiang, E. D. Stevens and S. P. Nolan, *Organometallics*, **2001**, *20*, 1255.

26. J. Huang, E. D. Stevens, S. P. Nolan and J. L. Peterson, *J. Am. Chem. Soc.*, **1999**, *121*, 2674.

27. A. C. Chen, L. Ren, A. Decken and C. M. Crudden, *Organometallics*, **2000**, *19*, 3459.

28. C. Zhang, J. Huang, M. L. Trudell and S. P. Nolan, *J. Org. Chem.*, **1999**, *64*, 3804.

29. P. W. C. Cross, *PhD Thesis*, University of Strathclyde, **2004**.

30. L. D. Vázquez-Serrano, B. T. Owens and J. M. Buriak, *Chem. Commun.*, **2002**, 2518.

31. L. D. Vázquez-Serrano, B. T. Owens and J. M. Buriak, *Inorganica Chimica Acta*, **2006**, *359*, 2786.

32. J. A. Brown, *PhD Thesis*, University of Strathclyde, **2007**.

33. C. Köcher and W. A. Herrmann, *J. Organomet. Chem.*, **1997**, *532*, 261.

34. S. Irvine, *PhD Thesis*, University of Strathclyde, **2009**.

35. J. A. Brown, S. Irvine, A. R. Kennedy, W. J. Kerr, S. Andersson and G. N. Nilsson, *Chem. Commun.*, **2008**, 1115.

36. C. A. Tolman, *Chem. Rev.*, **1977**, *77*, 313.

37. http://www.sigmaaldrich.com/MSDS/MSDS/DisplayMSDSPage.do?country=GB&language=en&productNumber=443484&brand=SIAL&PageToGoToURL=%2Fsafety-center.html accessed on 15 August, 2011.

38. R. K. Henderson, C. Jiménez-González, D. J. C. Constable, S. R. Alston, G. G. A. Inglis, G. Fisher, J. Sherwood, S. P. Binks and A. D. Curzons, *Green Chem.*, **2011**, *13*, 854.

39. R. Salter and I. Bosser, *J. Labelled Compd. Radiopharm.*, **2003**, *46*, 489.

40. S. C. Schou, *J. Labelled Compd. Radiopharm.*, **2009**, *52*, 376.

41. R. H. Crabtree, *The Organometallic Chemistry of the Transition Metals*; Wiley, Toronto, **1998**.

42. H. W. Wanzlick and H. J. Schönherr, *Angew. Chem. Int. Ed.*, **1968**, *7*, 141.

43. K. Öfele, *J. Organomet. Chem.*, **1968**, *12*, 42.

44. For reviews, see: a) W. A. Herrmann, *Angew. Chem. Int. Ed.*, **2002**, 41, 1291; b) S. Díez-González, N. Marion and S. P. Nolan, *Chem. Rev.*, **2009**, *109*, 3612.

45. *N-Heterocyclic Carbenes in Synthesis*; S. P. Nolan (Ed.), Wiley, Weinheim, **2006**.

46. R. A. Kelly III, H. Clavier, S. Giudice, N. M. Scott, E. D. Stevens, J. Bordner, I. Samardjiev, C. D. Hoff, L. Cavallo and S. P. Nolan, *Organometallics*, **2008**, *27*, 202.

47. V. C. Vargas, R. J. Rubio, T. K. Hollis and M. E. Salcido, *Org. Lett.*, **2003**, *5*, 4847.

48. M. A. Taige, A. Zeller, S. Ahrens, S. Goutal, E. Herdtweck and T. Strasner, *J. Organomet. Chem.*, **2007**, *692*, 1519.

49. R. H. Grubbs, *Tetrahedron*, **2004**, *60*, 7117.

50. M. Scholl, S. Ding, C. W. Lee and R. H. Grubbs, *Org. Lett.*, **1999**, *1*, 953.

51. A. J. Arduengo III, R. L. Harlow and M. Kline, *J. Am. Chem. Soc.*, **1991**, *113*, 361.

52. W. A. Herrmann and C. Köcher, *Angew. Chem. Int. Ed.*, **1997**, *36*, 2162.

53. R. Dorta, E. D. Stevens, N. M. Scott, C. Costabile, L. Cavallo, C. D. Hoff and S. P. Nolan, *J. Am. Chem. Soc.*, **2005**, *127*, 2485.

54. a) A. C. Hilier, W. J. Sommer, B. S. Yong, J. L. Petersen, L. Cavallo and S. P. Nolan, *Organometallics*, **2003**, *22*, 4322; b) H. Clavier and S. P. Nolan, *Chem. Commun.*, **2010**, *46*, 841.

55. a) L. S. Bennie, *MSci Thesis*, University of Strathclyde, **2008**; b) L. S. Bennie, C. J. Fraser, S. Irvine, W. J. Kerr, S. Andersson and G. N. Nilsson, *Chem. Commun.*, **2011**, *47*, 11653.

56. K. Alfonsi, J. Colberg, P. J. Dunn, T. Fevig, S. Jennings, T. A. Johnson, H. P. Kleine, C. Knight, M. A. Nagy, D. A. Perry and M. Stefaniak, *Green Chem.*, **2008**, *10*, 31.

57. D. H. Brown Ripin and M. Vetelino, *Synlett*, **2003**, 2353.

58. http://www.drugs.com/cons/niclosamide.html accessed on 15 August, 2011.

59. http://celecoxib.org/ accessed on 15 August, 2011.

60. F. Liu, W. Chen and X. You, *J. Chem. Crystallogr.*, **2002**, *32*, 27.

61. J. Clayden, N. Greeves, S. Warren, P. Wothers, *Organic Chemistry*; Oxford University Press, Oxford, **2001**.

62. a) M. Brookhart, M. L. H. Green and G. Parkin, *Proc. Natl. Acad. Sci. U. S. A.*, **2007**, *104*, 6908; b) M. Lein, *Coord. Chem. Rev.*, **2009**, *253*, 625.

63. M. Reid, *MSci Thesis*, University of Strathclyde, **2011**.

64. For reviews, see: a) B. E. Moulton, *Organometallic Chemistry*; I. J. S. Fairlamb and J. M. Lynam (Eds.), Manchester, U.K., **2010**, *36*, 93; b) H.-W. Lee and F.-Y. Kwong,

Eur. J. Org. Chem., **2010**, 789; c) *The Pauson-Khand Reaction: Scope, Variations and Applications*; R. R. Torres (Ed.), Wiley, Chichester, U.K., **2012**.

65. T. Shibata, N. Toshida, M. Yamasaki, S. Maekawa and K. Takagi, *Tetrahedron*, **2005**, *61*, 9974.

66. D. D. Perrin and W. L. F. Amarego, *Purification of Laboratory Chemicals*; Pergamon Press: Oxford, 3rd Edition, **1998**.

67. W. Kohn and L. J. Sham, *Phys. Rev.*, **1965**, *140*, 1133.

68. R. G. Parr and W. T. Yang, *Density Functional Theory of Atoms and Molecules*; Oxford University Press, New York, **1989**.

69. a) A. D. Becke, *Phys. Rev. A*, **1988**, *38*, 3098; b) J. P. Perdew, *Phys. Rev. B*, **1986**, *33*, 8822; c) S. H. Vosko, L. Wil and M. Nusair, *Can. J. Phys.*, **1980**, *58*, 1200.

70. K. Eichkorn, O. Treutler, H. Ohm, M. Häser and R. Ahlrichs, *Chem. Phys. Lett.*, **1995**, *240*, 283.

71. a) *TURBOMOLE*, v.5.10.1, cosmologic g.M.B.h & Co. KG, Leverkusen, Germany, **2008**; b) R. Ahlrichs, M. Bär, M. Häser, H. Horn and C. Kölmel, *Chem. Phys. Lett.*, **1989**, *162*, 165; c) K. Eichkorn, O. Treutler, H. Ohm, M. Häser, R. Ahlrichs, *Chem. Phys. Lett.*, **1995**, *242*, 652; d) O. Treutler and R. Ahlrichs, *J. Chem. Phys.*, **1995**, *102*, 346.

72. D. Andrae, U. Haussermann, M. Dolg, H. Stoll and H. Preuss, *Theoretica Chimica Acta*, **1990**, *77*, 123.

73. F. Weigend and R. Ahlrichs, *Phys. Chem. Chem. Phys.*, **2005**, *7*, 3297.

74. M. J. Frisch, G. W. Trucks, H. B Schlegel, G. E. Scuseria, M. A. Robb, J. R. Cheeseman, G. Scalmani, V. Barone, B. Mennucci, G. A. Petersson, H. Nakatsuji, M. Caricato, X. Li, H. P. Hratchian, A. F. Izmaylov, J. Bloino, G. Zheng, J. L. Sonnenberg, M. Hada, M. Ehara, K. Toyota, R. Fukuda, J. Hasegawa, M. Ishida, T. Nakajima, Y. Honda, O. Kitao, H. Nakai, T. Vreven, J. A. Jr. Montgomery, J. E. Peralta, F. Ogliaro, M. Bearpark, J. J. Heyd, E. Brothers, K. N. Kudin, V. N. Staroverov, R. Kobayashi, J. Normand, K. Raghavachari, A. Rendell, J. C. Burant, S. S. Iyengar, J. Tomasi,

M. Cossi, N. Rega, J. M. Millam, M. Klene, J. E. Knox, J. B. Cross, V. Bakken, C. Adamo, J. Jaramillo, R. Gomperts, R. E. Stratmann, O. Yazyev, A. J. Austin, R. Cammi, C. Pomelli, J. W. Ochterski, R. L. Martin, K. Morokuma, V. G. Zakrzewski, G. A. Voth, P. Salvador, J. J. Dannenberg, S. Dapprich, A. D. Daniels, O. Farkas, J. B. Foresman, J. V. Ortiz, J. Cioslowski, and D. J. Fox, *Gaussian 09*, revision A.02; Gaussian, Inc.: Wallingford, CT, **2009**.

75. Y. Zhao and D. G. Truhlar, *Theor. Chem. Acc.*, **2008**, *120*, 215.

76. a) W. J. Hehre, R. Ditchfield and J. A. Pople, *J. Chem. Phys.* **1972**, *56*, 2257; b) M. M. Francl, W. J. Petro, W. J. Hehre, J. S. Binkley, M. S. Gordon, D. J. DeFrees and J. A. Pople, *J. Chem. Phys.* **1982**, *77*, 3654.

77. a) D. Andrae, U. Häussermann, M. Dolg, H. Stoll and H. Preuss, *Theor. Chim. Acta* **1990**, *77*, 123; b) A. Bergner, M. Dolg, W. Küchle, H. Stoll and H. Preuss, *Mol. Phys.* **1993**, *80*, 1431.

78. To view the optimised structures as intended in 3D, access is required to either the Gaussview or Avogadro computer program. The latter may be downloaded free of charge at http://avogadro.en.softonic.com/ accessed on 8 January, 2013.

79. K. Hosoi, K. Nozaki and T. Hiyama, *Org. Lett.*, **2002**, *4*, 2849.

80. E. T. McCabe, W. F. Barthel, S. I. Gertler and S. A. Hall, *J. Org. Chem.*, **1954**, *19*, 493.

81. Y.-H. Chang, C.-F. Fu, Y.-H. Liu, S.-M. Peng, J.-T. Chen and S.-T. Liu, *Dalton Trans.*, **2009**, 861.